Metabolic regulation of tissue destruction in tuberculosis

Radha Mukul Asher

Department of Infectious Disease

Imperial College London

July 2020

Thesis submitted for the degree of Doctor of Philosophy

Declaration of authenticity

I confirm that this thesis is entirely my own work. All referenced studies have been appropriately cited and included in the reference list.

Radha Mukul Asher

Copyright declaration

The copyright of this thesis rests with the author and its contents are licensed under a Creative Commons Attribution Non-Commercial No Derivatives 4.0 International Licence. Researchers may copy and redistribute the material in any medium or format on the condition that; you credit the author, do not use it for commercial purposes and do not distribute modified versions of the work. If this work is reused or redistributed, the licence terms should be made clear to others by naming the licence and linking to the licence text.

Abstract

Background: Tuberculosis (TB), the deadliest infection worldwide, causes severe tissue destruction associated with excess inflammation. This process is driven by matrix metalloproteinase (MMP) enzymes regulated by the innate immune response. Patients also experience profound metabolic changes, such as weight loss. TB-infected macrophages show the Warburg effect, a metabolic shift from oxidative phosphorylation to aerobic glycolysis. However, the relationship between innate inflammation and cellular metabolism in TB is unclear.

Materials/methods: Primary monocyte-derived macrophages (MDMs) or normal human bronchial epithelial cells (NHBEs) were incubated with specific metabolic inhibitors or transfected with siRNA. Glycolysis was blocked with the hexokinase (HK) inhibitor, 2-deoxyglucose (2DG). Cells were then directly infected with live, virulent *Mycobacterium tuberculosis* (*M.tb*) H37Rv or stimulated with TB cytokine networks. Protein secretion and expression, gene expression and functional tissue damage were measured by ELISA, luminex, zymography, Western blot, real-time PCR and DQ collagen assay. HK2 immunohistochemistry was performed in samples from a murine TB model and TB patients.

Results: HK2 was highly expressed in murine and human tissue sites of TB inflammation. *In vitro,* 2DG downregulated gene expression and secretion of MMP-1 and the proinflammatory cytokine IL-1β; expression of the hypoxic transcription factor HIF-1α; functional matrix degradation and intracellular bacillary growth. The metabolic regulator AMPK upregulated MMP-1 secretion in TB, while MMP-1 was downregulated by the Pi3-kinase-Akt-mTORC1 signal transduction pathway.

Conclusions: MMP-1, HIF-1α and pro-inflammatory cytokines are modulated by glycolysis, AMPK and the Pi3-kinase-Akt-mTORC1 pathway in TB. Immunometabolic regulation of tissue destruction in TB might provide new avenues for host-directed therapies.

Table of contents

Declarations……..…….....2

Abstract……..3

Table of contents……..4

List of figures……..……11

List of tables……16

Acknowledgements..…...……17

CHAPTER 1: INTRODUCTION……..18

1.1 Tuberculosis……..19

1.1.1 The tuberculosis epidemic……..……..19

1.1.2. Clinical features and diagnosis of tuberculosis……20

1.1.3 Tuberculosis treatment and the rise of drug resistance…….……22

1.2. Pathogenesis of tuberculosis ……24

1.3 The innate immune response in tuberculosis……...27

1.3.1. Macrophages……28

1.3.2 Airway epithelial cells…….……33

1.3.3 Cytokines……36

1.4. Tissue destruction in tuberculosis……..……..39

1.4.1 Tissue destruction and cavitation in tuberculosis…….……..39

1.4.2 Structure and classification of matrix metalloproteinases…….……40

1.4.3 Function of matrix metalloproteinases……..…42

1.4.4 Control of matrix metalloproteinases……..…..43

1.4.5 Matrix metalloproteinases in tuberculosis……..…….45

1.4.6 Matrix metalloproteinases and host-directed therapies in tuberculosis…….……51

1.5 Metabolic regulation of tuberculosis……...……52

1.5.1 Cellular metabolic reprogramming…….……..52

1.5.2 Hypoxia-inducible factor-1α…….……..……61

1.5.3 AMP-activated protein kinase ……..…….……...63

1.5.4 The Pi3-kinase-Akt-mTOR pathway……..……..……66

1.5.5 Summary……..…68

1.6 Hypothesis and aims……69

1.6.1 Hypothesis……..……...…….69

1.6.2 Aims…….……...…….69

CHAPTER 2: MATERIALS AND METHODS……..71

2.1 *M.tb* culture……..……72

2.2 Monocyte and macrophage culture……72

2.3 Sterilisation of cell culture supernatants……..…73

2.4 Conditioned medium from *M.tb*-infected monocytes……..…..73

2.5 *M.tb* killing……75

2.6 Normal human bronchial epithelial cell culture……..……76

2.7 ELISA……..……76

2.8 Gelatin zymography……78

2.9 Western blotting……78

2.10 Chemical reagents……81

2.11 Lactate dehydrogenase assay……82

2.12 RNA extraction, cDNA synthesis and RT-PCR……82

2.13 Luminex……85

2.14 Lactate assay……85

2.15 RNA interference using siRNA……86

2.16 DQ collagen and DQ gelatin matrix assay……88

2.17 Live cell confocal imaging……88

2.18 Immunohistochemistry……89

2.19 Statistical analysis ……90

CHAPTER 3: METABOLIC PATHWAYS REGULATE MMPs IN TB-INFECTED HUMAN MACROPHAGES……91

3.1 Introduction……92

3.2 Results……94

3.2.1 Extracellular lactate secretion is upregulated in *M.tb*-infected MDMs……94

3.2.2 HK2 expression is upregulated in *M.tb*-infected MDMs……95

3.2.3 Glycolysis upregulates MMP-1 secretion and gene expression in *M.tb*-infected MDMs……96

3.2.4 Glycolysis upregulates MMP-2, MMP-3, MMP-7, MMP-8 and MMP-10 secretion in *M.tb*-infected MDMs……...98

3.2.5 Glycolysis upregulates TIMP-1 and TIMP-2 secretion from *M.tb*-infected MDMs……..100

3.2.6 Glycolysis regulates cytokine secretion from *M.tb*-infected MDMs..……101

3.2.7 Glycolysis upregulates EMMPRIN secretion from *M.tb*-infected MDMs……102

3.2.8 Stabilisation of HIF-1α expression in *M.tb*-infected MDMs is enhanced by glycolysis……103

3.2.9 Glycolysis reduces intracellular bacillary killing in *M.tb*-infected MDMs……..104

3.2.10 HK2 is expressed in human TB lymphadenitis……....105

3.2.11 Diethylsuccinate does not affect MMP-1 or TIMP secretion from *M.tb*-infected MDMs….107

3.2.12 Diethylsuccinate regulates cytokine secretion from *M.tb*-infected MDMs……...109

3.2.13 AMPK increases HIF-1α and HK2 protein expression……..……...111

3.2.14 AMPK upregulates MMP-1 secretion and gene expression in *M.tb*-infected MDMs…...113

3.2.15 AMPK upregulates IL-1β, TNF-α and IL-10 secretion in *M.tb*-infected MDMs…….115

3.2.16 Metformin has a biphasic effect on MMP-1 secretion from *M.tb*-infected MDMs……..117

3.2.17 Metformin regulates cytokine secretion from *M.tb*-infected MDMs……..118

3.2.18 pS670K is upregulated in *M.tb*-infected MDMs…….……..……119

3.2.19 The Pi3-kinase-Akt-mTORC1 pathway has a biphasic effect on MMP-1 regulation in *M.tb*-infected MDMs……..……..120

3.2.20 The Pi3-kinase-Akt-mTORC1 pathway regulates cytokine secretion in *M.tb*-infected MDMs……...122

3.3 Discussion……..…….125

CHAPTER 4: METABOLIC PATHWAYS REGULATE MMPs IN TB NETWORK-STIMULATED HUMAN AIRWAY EPITHELIAL CELLS……130

4.1 Introduction……..……131

4.2 Results……..133

4.2.1 HK2 is expressed in a murine model of pulmonary TB……..133

4.2.2 HK2 gene and protein expression is upregulated in CoMTB-stimulated NHBEs……135

4.2.3 Glycolysis upregulates MMP-1 secretion and gene expression in CoMTB-stimulated NHBEs……..136

4.2.4 Glycolysis upregulates MMP-9 secretion, functional activity and gene expression in CoMTB-stimulated NHBEs……..……138

4.2.5 Glycolysis upregulates MMP-2, MMP-3, MMP-8 and MMP-10 secretion in CoMTB-stimulated NHBEs…….……140

4.2.6 Glycolysis upregulates TIMP secretion in CoMTB-stimulated NHBEs…….142

4.2.7 Glycolysis upregulates a functional increase in collagenase and gelatinase activity in CoMTB-stimulated NHBEs.……..……144

4.2.8 siRNA interference of HK2 downregulates MMP-9 gene expression in CoMTB-stimulated NHBEs..……..……..145

4.2.9 Diethylsuccinate increase MMP-1 and MMP-9 secretion and gene expression in CoMTB-stimulated NHBEs……..147

4.2.10 Diethylsuccinate downregulates MMP-3 but upregulates MMP-10 secretion in CoMTB-stimulated NHBEs……..149

4.2.11 Diethylsuccinate does not regulate TIMP secretion in CoMTB-stimulated NHBEs……...150

4.2.12 Diethylsuccinate upregulates a functional increase in collagenase and gelatinase activity in CoMTB-stimulated NHBEs……151

4.2.13 Diethylsuccinate upregulates HIF-1α expression in CoMTB-stimulated NHBEs…….152

4.2.14 AMPK upregulates MMP-1 and MMP-9 secretion and gene expression in CoMTB-stimulated NHBEs……153

4.2.15 AMPK upregulates MMP-3 and MMP-10 secretion in CoMTB-stimulated NHBEs…..155

4.2.16 AMPK upregulates a functional increase in collagenase and gelatinase activity in CoMTB-stimulated NHBEs……..157

4.2.17 Metformin upregulates MMP-1 and MMP-9 secretion in CoMTB stimulated NHBEs….158

4.2.18 The Pi3-kinase-Akt-mTORC1 pathway downregulates MMP-1 and MMP-9 secretion in CoMTB-stimulated NHBEs…….....160

4.2.19 The Pi3-kinase-Akt-mTORC1 pathway upregulates MMP-3 and MMP-10 secretion in CoMTB-stimulated NHBEs……162

4.2.20 The Pi3-kinase-Akt-mTORC1 pathway downregulates a functional increase in collagenase and gelatinase activity in CoMTB-stimulated NHBEs……..164

4.3 Discussion……...168

CHAPTER 5: CONCLUSIONS AND FUTURE PERSPECTIVES……..……172

5.1 Summary of findings…..……..173

5.2 Therapeutic implications……177

5.3 Future work……..178

5.4 Final conclusions……..……183

References……184

Appendix 1: List of abbreviations……226

Appendix 2: Conference proceedings……231

List of figures

Figure 1: Thoracic CT scan of TB patient……..….40

Figure 2: Schematic representation of glycolysis……..…54

Figure 3: Schematic representation of the tricarboxylic acid (Kreb's) cycle…….54

Figure 4: Schematic representation of the Warburg effect……..55

Figure 5: Simplified schematic representation of metabolic signalling pathways in TB……...69

Figure 6: Testing the effectiveness of conditioned medium from *M.tb*-infected monocytes (CoMTB)…….74

Figure 7: Extracellular lactate secretion is upregulated in *M.tb*-infected MDMs ……..94

Figure 8: HK2 gene and protein expression are upregulated in *M.tb*-infected MDMs……95

Figure 9: Glycolysis upregulates MMP-1 secretion and gene expression from *M.tb*-infected MDMs…….97

Figure 10: Glycolysis upregulates MMP-2, MMP-3, MMP-7, MMP-8 and MMP-10 secretion from *M.tb*-infected MDMs……..99

Figure 11: Glycolysis upregulates TIMP-1 and TIMP-2 secretion from *M.tb*-infected MDMs….100

Figure 12: Glycolysis upregulates IL-1β and IL-10, but downregulates TNF-α secretion from *M.tb*-infected MDMs…….101

Figure 13: Glycolysis upregulates EMMPRIN secretion from *M.tb*-infected MDMs……..102

Figure 14: 2DG attenuates *M.tb*-induced HIF-1α stabilisation in MDMs……..103

Figure 15: Glycolysis reduces intracellular bacillary killing in *M.tb*-infected MDMs……...104

Figure 16: HK2 is expressed in granulomas of patients with TB lymphadenitis……106

Figure 17: Diethylsuccinate does not affect MMP-1 or TIMP secretion in *M.tb*-infected MDMs...108

Figure 18: Diethylsuccinate upregulates IL-1β and downregulates TNF-α and IL-10 cytokine secretion from *M.tb*-infected MDMs……110

Figure 19: p-AMPK protein expression and the effect of AMPK inhibition on HIF-1α and HK2 expression in *M.tb*-infected MDMs…….,,,.……112

Figure 20: AMPK upregulates MMP-1 gene expression and secretion in *M.tb*-infected MDMs...114

Figure 21: AMPK upregulates IL-1β, TNF-α and IL-10 cytokine secretion from *M.tb*-infected MDMs……...116

Figure 22: Metformin has a biphasic effect on MMP-1 secretion from *M.tb*-infected MDMs……117

Figure 23: Metformin regulates cytokine secretion from *M.tb*-infected MDMs……118

Figure 24: pS670K protein expression is upregulated in *M.tb*-infected MDMs…….……..119

Figure 25: The Pi3-kinase-Akt-mTORC1 pathway has a biphasic effect on MMP-1 in *M.tb*-infected MDMs……...……121

Figure 26: The Pi3-kinase-Akt-mTORC1 pathway downregulates IL-1β secretion in *M.tb*-infected MDMs……...122

Figure 27: The Pi3-kinase-Akt-mTORC1 pathway downregulates TNF-α secretion in *M.tb*-infected MDMs……...123

Figure 28: The Pi3-kinase-Akt-mTORC1 pathway has a biphasic effect on IL-10 secretion in *M.tb*-infected MDMs……124

Figure 29: Summary of key findings from *in vitro* metabolic signalling experiments in *M.tb*-infected MDMs……125

Figure 30: HK2 is expressed in lung tissue in a mouse model of pulmonary TB ……134

Figure 31: HK2 gene and protein expression is upregulated in CoMTB-stimulated NHBEs…..135

Figure 32: Glycolysis upregulates MMP-1 gene expression and secretion in CoMTB-stimulated NHBEs……137

Figure 33: Glycolysis upregulates MMP-9 secretion, functional activity and gene expression in CoMTB-stimulated NHBEs……139

Figure 34: Glycolysis upregulates MMP-2, MMP-3, MMP-8 and MMP-10 secretion in CoMTB-stimulated NHBEs……141

Figure 35: Glycolysis upregulates TIMP secretion in CoMTB-stimulated NHBEs……143

Figure 36: Glycolysis upregulates functional collagenase and gelatinase activity in CoMTB-stimulated NHBEs……144

Figure 37: siRNA interference of HK2 downregulates MMP-9 gene expression in CoMTB-stimulated NHBEs……146

Figure 38: Diethylsuccinate upregulates MMP-1 and MMP-9 secretion and gene expression CoMTB-stimulated NHBEs……148

Figure 39: Diethylsuccinate regulates MMP-3 and MMP-10 secretion in CoMTB-stimulated NHBEs……..……149

Figure 40: Diethylsuccinate does not regulate TIMP secretion CoMTB-stimulated NHBEs…....150

Figure 41: Diethylsuccinate upregulates functional collagenase and gelatinase activity in CoMTB-stimulated NHBEs…….……151

Figure 42: Diethylsuccinate stabilizes HIF-1α protein expression in CoMTB-stimulated NHBEs..……152

Figure 43: AMPK upregulates MMP-1 and MMP-9 secretion and gene expression in CoMTB-stimulated NHBEs……..…….154

Figure 44: AMPK upregulates MMP-3 and MMP-10 secretion in CoMTB-stimulated NHBEs….156

Figure 45: AMPK upregulates functional collagenase and gelatinase activity in CoMTB-stimulated NHBEs……..157

Figure 46: Metformin upregulates MMP-1 and MMP-9 secretion in CoMTB-stimulated NHBEs……..159

Figure 47: The Pi3-kinase-Akt-mTORC1 pathway downregulates MMP-1 and MMP-9 secretion in CoMTB-stimulated
NHBEs……..161

Figure 48: The Pi3-kinase-Akt-mTORC1 pathway upregulates MMP-3 and MMP-10 secretion in CoMTB-stimulated NHBEs……..……..163

Figure 49: The Pi3-kinase-Akt-mTORC1 pathway downregulates functional collagenase and gelatinase activity in CoMTB-stimulated NHBEs……..…….165

Figure 50: Pi3-kinase downregulates gelatinase activity in live-cell confocal imaging of CoMTB-stimulated NHBEs……..……167

Figure 51: Summary of key findings from the *in vitro* metabolic signalling experiments in CoMTB-stimulated NHBEs……..168

List of tables

Table 1: Classification and substrates of MMPs in TB……41

Table 2: Components of conditioned medium from *M.tb*-infected monocytes (CoMTB)……75

Table 3: Specifications of ELISA antibodies……77

Table 4: Western blot antibodies and dilutions……..80

Table 5: Chemical metabolic inhibitors and activators……81

Table 6: RT-PCR primers and probes……84

Table 7: Demographic and clinico-pathological characteristics of patients with TB lymphadenitis samples immunostained for HK2……..105

Table 8: Table 8: Comparison of the key immunometabolic effects of glycolysis and succinate shown in *M.tb*-infected MDMs and CoMTB-stimulated NHBEs…….……..174

Table 9: Comparison of the key immunometabolic effects of AMPK and the Pi3-kinase-Akt-mTORC1 pathway shown in *M.tb*-infected MDMs and CoMTB-stimulated NHBEs…..…….176

Acknowledgements

First of all, I owe a great debt of gratitude to my PhD supervisor, Professor Jon Friedland, whose counsel, encouragement and insight has been invaluable throughout this project. I would like to thank him for his unwavering faith in me over the last 8 years. I would also like to give a special mention to Dr Sara Brilha, who taught me the techniques of cell culture at the start of my PhD and was always a fount of knowledge and source of reassurance. I am deeply grateful for the friendship and assistance of everyone in the Friedland group, with particular appreciation for Dr Ashley Whittington, Dr Daniela Kirwan, Dr Cristina Loader, Dr Sajeel Shah, Dr Sally Hargreaves and Dr Laura Nellums. I would also like to thank my Masters degree students, Mr Daniel Zaki and Dr Yunisa Pamela, for their enthusiasm and skilful laboratory assistance.

I would like to extend my sincerest gratitude to my funding bodies, the Medical Research Council and the Mason Medical Research Trust, for their flexible and generous support. I received human lymph node tissue samples from Dr Daniela Kirwan and Dr Robert Gilman and mouse lung tissue samples as a kind gift from Dr Nitya Krishnan and Dr Brian Robertson. I am extremely grateful for both of these donations. I would like to offer my thanks to Mrs Sandra Ashton of the Image Resource Facility, St George's, University of London for performing the immunohistochemistry and to Dr Deborah Chong for helping me to interpret the results. I would also like to thank Mr Gregory Perry of the Image Resource Facility for his patience and expertise in helping me to perform the confocal microscopy experiments.

I am very grateful to my lovely parents, who have always supported me in all my endeavours and encouraged me to aim high. Finally, I would like to thank my husband, without whose love and support this project would have been impossible, and my beautiful children for the joy they bring to my life.

Chapter 1: Introduction

1.1 Tuberculosis

1.1.1 The tuberculosis epidemic

Tuberculosis (TB) was declared a global emergency by the World Health Organisation (WHO) in 1993, but continues to be the leading infectious cause of mortality worldwide (1). In 2018, *Mycobacterium tuberculosis* (*M.tb*), the aetiological agent of TB, infected 10 million people and caused an estimated 1.5 million deaths (1).

TB is an ancient scourge and has plagued humans throughout our history. Early progenitors of *M.tb* might have infected hominids in East Africa up to 3 million years ago (2), though population genomics studies suggest that modern *M.tb* strains originated 70,000 years ago (3). Exploration of the world, along with increases in human population density 10,000 years ago, contributed to global TB expansion and dissemination (3). TB surged across Europe and North America and became epidemic in the 18th and 19th centuries, contributing to around 25% of all deaths (4). The French physician, René Théophile Hyacinthe Laennec, first elucidated the pathogenesis of TB in 1819 and the German scientist Robert Koch identified the tubercle bacillus in 1882 (5). However, before the era of modern TB chemotherapy, sanatorium care for rest and fresh air was the mainstay of treatment.

Despite introduction of the Bacille Calmette-Guérin (BCG) vaccine in 1921 (6) and the discovery of streptomycin in 1943, followed by several more antimycobacterial drugs (7), initial optimism regarding TB control was not sustained. *M.tb* is a highly successful pathogen because of its remarkable ability to persist and survive in humans; over time, it has evolved sophisticated techniques to subvert host defences (8). Conquest of the TB epidemic has been impaired by

several factors, including low BCG vaccine efficacy, lack of rapid diagnostics, prolonged and dated treatments and the concerning rise of *M.tb* drug resistance (8).

As a result, TB continues to pose an urgent and daunting public health challenge. 25% of the global population, comprising 1.7 billion people, is infected with *M.tb* and at risk of progression to active TB (9). The highest TB burden is predominantly in low-resource countries in Asia and Africa (1) and illness is also associated with substantial economic costs (10). The Sustainable Development Goals and the WHO's End TB strategy have affirmed targets to control the global TB epidemic by 2030. However, these milestones cannot be achieved without intensified research and development. Advances in TB therapeutics have been constrained by limited understanding of the complex host-pathogen interactions in TB; hence, greater insight into TB immunopathogenesis is vital for future progress.

1.1.2 Clinical features and diagnosis of tuberculosis

M.tb is transmitted through the aerosol route, by close proximity to a coughing infected contact.

Following infection with *M.tb*, 10% of patients develop progressive primary disease; this occurs rapidly after exposure and is more common in children (11). Primary TB results from haematogenous dissemination of bacilli and has a characteristic miliary pattern on chest radiograph. The remaining 90% of patients control the initial infection and remain asymptomatic (11). These individuals are presumed to have latent infection, in which *M.tb* survives in a quiescent form.

The lifetime risk of developing post-primary TB is 5-10% (11); reactivation of latent TB is often triggered by immunosuppression, particularly HIV co-infection (12). Pulmonary TB is the most common form of active TB, comprising 70% of cases (11). Extrapulmonary TB can affect virtually

any organ; frequently affected sites are lymph nodes, bone, the pleura, the central nervous system, the genitourinary tract and the peritoneal cavity. The symptoms of pulmonary TB reflect host response to the pathogen; localised symptoms of tissue destruction are predominantly cough, sputum production and haemoptysis, while systemic symptoms include fever, night sweats, and weight loss (13). Cachexia can be profound and debilitating; hence, TB was known as 'consumption' in Victorian times. If left untreated, sputum smear-positive pulmonary TB has a 10-year case fatality rate of 70% in immunocompetent patients (14).

Latent TB can be diagnosed by demonstrating host reactivity to *M.tb* antigens, either with a tuberculin skin test (TST) or with an IFN-γ release assay (IGRA). In the TST, a delayed-type hypersensitivity reaction is detected following intradermal challenge with purified protein derivative (PPD) of limited specificity (15). IGRA tests have subsequently been developed to measure reactivity to more *M.tb*-specific antigens, such as early secretory antigen target-6 (ESAT-6) and culture filtrate protein-10 (CFP-10) (15). However, positive TST or IGRA tests merely confirm prior *M.tb* exposure and cannot distinguish latent from active TB, nor identify those with latent TB at highest risk of progressing to active TB (11).

Confirming the diagnosis of active TB can be difficult, but is essential for optimal clinical management. The symptoms of TB are often insidious and may mimic other conditions, hence late clinical presentation and delays in diagnosis are not uncommon (16), which impacts on disease control (17). The main diagnostic tools for pulmonary TB are chest imaging and sputum microscopy and culture. Frequently observed abnormalities on chest radiograph include consolidation, linear or nodular opacities and cavitation in an upper zone distribution (18). Sputum smear microscopy with auramine or Ziehl-Neelson staining is in widespread use, as it is rapid, simple and inexpensive. However, it does not distinguish between *M.tb* and non-tuberculous mycobacteria and has a variable sensitivity of 32-97%, depending on technique (19). The gold

standard of diagnosis remains *M.tb* culture (20), which has the additional benefit of permitting drug susceptibility testing. However, isolation and confirmation of *M.tb* by culture can often take 6-8 weeks, contributing to diagnostic delays, though automated liquid culture systems can be swifter than the conventional Löwenstein-Jensen slope (21). More recently, the WHO has endorsed the Xpert MTB/RIF and the more sensitive Xpert MTB/RIF Ultra assays; these are rapid nucleic acid amplification tests (NAATs) for *M.tb* detection and rifampicin resistance that provide a result within hours (22).

1.1.3 Tuberculosis treatment and the rise of drug resistance

In the last century, two milestones raised hopes that TB could be conquered; the first was the introduction of the Bacillus Calmette Guérin (BCG) vaccine in 1921 and the second was the discovery of streptomycin, the first effective antituberculosis agent, in 1943.

BCG is a live strain of *Mycobacterium bovis (M. bovis)* developed by Calmette and Guérin as an attenuated vaccine to prevent TB (6). BCG has been administered to over 3 billion people worldwide and is recommended for all infants in high TB incidence countries by the WHO (23). Neonatal BCG vaccination confers 60-80% protective efficacy against severe forms of TB in children, such as disseminated TB and TB meningitis (24). However, in adults, BCG has limited efficacy against pulmonary TB (24); this protection also varies depending on geographical latitude, which has been attributed to sensitisation by environmental mycobacteria (25).

Streptomycin was followed by development of the first-line antituberculous agents in the 1950s and 1960s (7). The 6-month therapeutic regimen for drug-sensitive pulmonary TB comprises rifampicin, isoniazid, pyrazinamide and ethambutol for 2 months (the intensive phase), followed by rifampicin and isoniazid for 4 months (the continuation phase) (1). Treatment coverage was 69% in 2018, with a treatment success rate for new and relapsed cases of 85% worldwide (1).

This standard TB treatment has remained unchanged for more than 35 years; this can be attributed, in part, to a lack of research innovation and investment in TB since the 1980s.

This dated TB regimen, coupled with the neglect of public health infrastructure, presents several obstacles to robust disease control. The treatment period is protracted and multiple drugs are required to prevent selection of drug-resistant bacterial mutants (11). Major and minor drug-related adverse events are common; hepatotoxicity, which occurs in 3-25% of cases (26), can be severe enough to require hospitalisation and treatment interruption. These factors beget poor adherence which, in conjunction with inappropriate drug use, is fuelling an epidemic of TB drug resistance, increasing the risks of disease transmission, treatment failure and death (27). *M.tb* can be rifampicin resistant (RR) or multi-drug resistant (MDR), defined as resistant to rifampicin and isoniazid. In 2018, there were 484,000 incident cases of MDR/RR-TB worldwide (1). However, this may not reflect the real burden, as many laboratories in high-burden TB countries have limited capacity for drug susceptibility testing (28). Some cases of MDR-TB, known as extensively drug-resistant (XDR) TB, are also resistant to the fluoroquinolones and at least one of three injectable second-line drugs, amikacin, capreomycin or kanamycin. Cases of XDR-TB had been reported in 131 countries by 2018 (1). There have also been occasional reports of virtually untreatable totally drug-resistant (TDR) TB (28). Drug regimens for MDR/RR-TB and XDR-TB are complicated and prolonged, requiring toxic and often injectable agents. Cure rates are low; just 56% of MDR/RR-TB patients and 39% of XDR-TB patients successfully completed treatment in 2018 (1). The WHO released updated guidance in 2019 recommending that most MDR/RR-TB patients could be treated with fully oral regimens, including the new or repurposed drugs bedaquiline, delamanid and linezolid; however, the specified treatment duration remains 18-20 months (1).

Hence, reducing the global TB burden remains a daunting challenge and novel treatment strategies are urgently required. In particular, shorter, simpler and better-tolerated drug regimens are critical to combat drug resistance and enhance patient outcomes. This has fostered substantial interest in developing adjunctive host-directed therapies (HDTs) which modulate the host immune response to control TB pathogenesis; these can be used in conjunction with current and future antituberculous agents (29). *M.tb* has co-evolved with the human immune system and deploys several strategies to persist within infected cells; this delays treatment efficacy and contributes to the evolution of drug-resistant strains (30). HDTs have the potential to contain *M.tb* infection and ameliorate inflammation, as well as enhance antibiotic effects, shorten treatment duration, and promote immunological memory to protect against relapse (30–32). However, research into HDTs in TB has been hampered by limited understanding of the pathogenesis of early infection and factors influencing host susceptibility, protection and progression to active disease (29). Further studies elucidating these complex immune mechanisms in TB are essential to inform new strategies for development of HDTs.

1.2 Pathogenesis of tuberculosis

M.tb is a slow-growing, facultative, intracellular pathogen with an immunoregulatory cell wall rich in mycolic acids. Its evolutionary survival depends on its ability to persist and replicate within the human host, hijack immune mechanisms and, ultimately, facilitate onward transmission of infection (8).

Following inhalation of infected droplets into the distal lung alveoli, the innate immune system is critical for the initial host defence against *M.tb* infection. *M.tb* is rapidly phagocytosed by resident alveolar macrophages (AMs) via pattern recognition receptors (PRRs) (33–35). For the first 10 days, intracellular bacilli replicate exponentially within the phagosome, suggesting that AMs

provide an early niche for proliferation (33–35). *M.tb* deploys numerous strategies to avoid elimination by AMs, including inhibition of normal phagosome maturation (36). Infected AMs recruit additional circulating AMs, monocytes, and neutrophils to the site of infection via expression of chemokines such as CCL2 and CXCL10 (37). Airway epithelial cells (AEC) might amplify this response by intercellular communication with infected AMs, mediated by cytokines such as IL-1β (38). *M.tb*-infected AMs then transmigrate across the alveolar barrier into the lung interstitial tissue by diapedesis via the 'Trojan horse' mechanism (39). This process is mediated by the host adaptor protein myeloid differentiation primary response 88 (MyD88) / Interleukin -1 receptor (IL-1R) and the mycobacterial ESAT-6 secretion system 1 (ESX-1) (34). These *M.tb*-infected AMs release chemokines and cytokines to drive a localised inflammatory response, with massive infiltration of myeloid cells into the lung dominated by monocytes, interstitial macrophages (IMs), neutrophils and dendritic cells (35,40). Dissemination and transfer of *M.tb* to these recruited cells results in a rapid increase in the bacterial burden, prior to the induction of the adaptive immune response (41).

Following the onset of adaptive host defence, specific CD4+ Th1 type cells secrete IFN-γ to cause potent macrophage activation, resulting in enhanced mycobacterial control and killing to facilitate granuloma formation (42). CD8+ T-cells are also important cells for controlling *M.tb* during the chronic phase of infection. Infected cells coalesce to form a granuloma, a compact and organized aggregate of mature macrophages which is the histopathological hallmark of TB (43). Mature granuloma macrophages can be transformed into specialised epithelioid cells, fused into multinucleated Langhans giant cells or differentiated into lipid-rich foamy macrophages. Several other cells including neutrophils, dendritic cells, fibroblasts, B and T lymphocytes and natural killer (NK) cells also populate the granuloma. Surrounding AEC, though not incorporated into the structure of the granuloma, participate in its formation by ESX-1-mediated chemotaxis of new macrophages (44).

The granuloma exists in a state of complex and dynamic equilibrium (43). It has historically been considered to be a host-protective structure which walls off and restricts mycobacterial proliferation (45–47). However, there is increasing evidence that *M.tb* exploits the host response to allow a favourable niche for replication and dissemination (43,44,48,49). Early granuloma formation can benefit *M.tb* by recruiting macrophages that serve as additional sanctuaries for bacterial growth and population expansion (50). Long-term, the granuloma provides a safe environment to establish bacterial latency that facilitates host-controlled persistence of the organism in the granuloma (43,51).

90% of *M.tb*-infected individuals contain the infection at the latent stage and remain asymptomatic. However, in 5-10% of patients with latent infection, post-primary TB develops following reactivation of bacilli (52). Molecular epidemiological studies suggest this can occur up to 30 years after the initial infection (53). Reactivation of TB is associated with immunosuppression, with HIV co-infection being the most common risk factor (12). Caseating granulomas, resulting from necrotic breakdown of macrophages, are a signature of active TB (43). Histopathological studies show that a highly enhanced bacterial load is associated with areas of soft caseation in early granulomas (54). Liquefaction of the caseous region is crucial to enabling extracellular bacterial proliferation and subsequent cavity formation (43,55). *M.tb* can also adapt to specific microenviromental features of caseation such as hypoxia and lipid abundance; this may facilitate persistance and affect treatment susceptibility (56). Once TB cavities form in the lung apex and connect with an airway, there is exponential proliferation of *M.tb*. This ultimately results in the release of large quantities of viable infectious bacilli, which can be transmitted to a new human host, completing the cycle (52). Cavitating disease in TB is also associated with treatment failure, higher relapse rates and the development of drug resistance (56).

Studies in cynomolgus macaques show that the evolution of granulomas is often highly nuanced (57). Clinically latent macaques can have necrotic granulomas, while those with active TB can

have quiescent and calcified granulomas; furthermore, discrete granulomas in the same host can also be heterogenous (57). The specific factors determining the behaviour of each granuloma are still unclear, but the local balance of pro- and anti-inflammatory cytokines appears to be critical (58).

Hence, the immunopathological trajectory of TB is complex and heterogenous; further understanding of its mechanisms is crucial to formulating new host-directed strategies to combat this disease.

1.3 The innate immune response in tuberculosis

The complex host defence to *M.tb* includes both the innate and adaptive immune response. Early innate immune interactions are crucial and predictive of the eventual outcome of *M.tb* infection, but remain poorly understood due to a historic emphasis on later adaptive immunity in TB pathogenesis (59).

The adaptive immune response, orchestrated by CD4+ T helper 1 (Th-1) cells, is crucial for containment of *M.tb* infection in the lung (11). CD4+ Th-1 cells activate macrophages via IFN-γ secretion, leading to increased elimination of mycobacteria and formation of granulomas (42). However, the onset of adaptive immunity is considerably delayed in TB relative to other bacterial pathogens. It can take up to 6 weeks for adaptive immunity to be induced after *M.tb* infection, as assessed by a positive TST or IGRA result; this offers an opportunistic window for mycobacterial expansion (60).

Hence, following *M.tb* inhalation, the innate immune response is critical for first-line host protection; this needs to be balanced to induce sufficient *M.tb* control, while limiting lung tissue damage (61,62). Studies demonstrate that innate processes alone might facilitate early bacterial

clearance (63); case contact studies in TB show that approximately 50% of exposed individuals are TST negative (64). If *M.tb* infection is established, several phagocytes, such as monocytes, macrophages, neutrophils and DC, as well as non-traditional immune cells, such as AEC and platelets, participate in the innate inflammatory response, mediated by a network of cytokines and chemokines. However, *M.tb* can manipulate innate immune effector mechanisms to persist and replicate within cells and disrupt the onset of adaptive immunity (65).

Evidence suggests that the initial host-pathogen interaction in TB is shaped by the two predominant cell varieties in the lung: macrophages and AEC (38). These central players in the TB innate immune response, as well as selected regulatory cytokines, will be discussed in more detail below.

1.3.1 Macrophages

Macrophages are the primary targets of *M.tb* infection and regulate the balance between pro- and anti-inflammatory immune responses to control bacterial replication and tissue damage (66).

Macrophages can have different roles, phenotypes and metabolic profiles depending on their ontogeny. During the first 10-14 days after infection, *M.tb* resides almost exclusively in AMs; intracellular bacteria replicate exponentially, suggesting that AMs are an early niche for mycobacterial replication (33–35). Following translocation of *M.tb*-infected AMs into the lung tissue, *M.tb* is phagocytosed by recruited interstitial macrophages (IMs) and DCs derived from monocyte precursors, as well as neutrophils. Macrophages also initiate the adaptive immune response via CD4+ Th1 antigen presentation and are the predominant cells in TB granulomas. Hence, macrophages also act as a reservoir of infection.

Macrophages can be polarised by different stimuli to acquire M1 (classically activated) and M2 (alternatively activated) phenotypes. M1 macrophages are stimulated by microbial products and have high expression of pro-inflammatory IL-1β, IL-6, IL-12, TNF-α and ROS/RNS (67). M2 macrophages help maintain tissue homeostasis and suppress inflammation by secreting high levels of IL-4, IL-10 and TGF-β (67). There is increasing evidence for an intimate connection between the polarisation states of macrophages and their metabolic dynamics in *M.tb* infection (68,69).

Macrophages internalise *M.tb* by non-specific pinocytosis or receptor-mediated phagocytosis; the latter can be opsonic or non-opsonic (8). Opsonic uptake of *M.tb* involves recognition of bacteria coated with antibodies, complement factors or surfactant by the Fcγ receptor (FcγR) or complement receptor (CR) 3 (70). Non-opsonic ingestion of *M.tb* by macrophages, which predominates in the early stages of infection, occurs when macrophage pattern recognition receptors (PRRs) recognise highly conserved pathogen-associated molecular patterns (PAMPs) (70). These include C-type lectin receptors (CLRs), scavenger receptors (SRs), Toll-like receptors (TLRs), CD14 and nucleotide-binding-oligomerisation-domain (NOD)-like receptors (71). Non-opsonic uptake facilitates greater intracellular survival of *M.tb* (72).

TLRs, in particular TLR2 (alone or as a heterodimer with TLR1 or TLR6), as well as TLR4 and TLR9, play a critical role in innate resistance to TB. (73,74). TLR2, TLR4 and TLR9 signalling in TB is triggered via the adaptor protein MyD88, which activates the transcription factor NF-κB; this leads to increased transcription of pro-inflammatory cytokines and chemokines, such as IL-1β and TNF-α, which mediate immune cell recruitment to the site of infection (75). MyD88 knockout mice are highly susceptible to *M.tb* infection and succumb early (76,77). Of note, TLR4 can also induce an intracellular response via a MyD88-independent cascade (75). TLR2 is important in TB innate host defence via stimulation of IL-1β and TNF-α production in *M.tb*-infected macrophages

(75,78). TLR2 knockout mice infected with *M.tb* display reduced bacterial clearance and defective granuloma formation, eventually developing fatal pulmonary disease (79). *In vitro* studies demonstrate TLR4 recognition of *M.tb* (80); however, different models of TLR4 knockout mice show conflicting *M.tb* susceptibilities, hence further studies are required (81,82). Although impaired production of IL-12 and IFN-γ occurs in *M.tb*-infected TLR9-deficient mice, greater susceptibility to *M.tb* infection is seen in TLR2/9 double knockout mice than in TLR9-deficient mice alone (83).

Depending on activation status, macrophages kill intracellular pathogens such as *M.tb* by employing myriad immune effector functions; these include phagosome-lysosome fusion, apoptosis, autophagy and production of reactive nitrogen species (RNS) and reactive oxygen species (ROS) (8). However, *M.tb* can harness several complex strategies to circumvent these antimicrobial mechanisms, allowing persistence and replication within macrophages; this is fundamental to its success as a pathogen (8). Some of these functions and the immunoevasive tactics of *M.tb* will be discussed in more detail below.

1.3.1.1 Phagosome maturation

Following phagocytosis, *M.tb* killing relies on the process of phagosome maturation. This involves fusion of phagosomes with endosomes and lysosomes, with subsequent acidification of phagosomes by the actions of vesicular ATPase (V-ATPase) pumps and proteolytic lysosomal hydrolases, as well as the production of ROS (36). *M.tb* inhibition of normal phagosome maturation is crucial to its survival in macrophages; up to 70% of *M.tb*-containing phagosomes do not fuse with lysosomes (84). Binding of the mannose receptor (MR), a type of CLR, to *M.tb* surface mannosylated lipoarabinomannan (manLAM) strongly inhibits phagosome-lysosome fusion, generating an early phagosomal niche for *M.tb* (85). *M.tb* also secretes macromolecules that interfere with phagosome maturation, such as the phosphatases PtpA (86) and SapM (87).

PtpA dephosphorylates and inhibits a vesicle trafficking protein VPS33B resulting in maturational arrest (86) and also disrupts the V-ATPase pump to inhibit phagosome acidification (88). The inhibition of phagolysosome biogenesis by *M.tb* also impairs the processing of mycobacterial proteins for antigen presentation, required to initiate an adaptive immune response (8). Hence, *M.tb* can evade proteolytic degradation to persist in macrophages.

1.3.1.2 Apoptosis

Following phagocytosis, *M.tb* infection of macrophages can induce cell death in the form of either apoptosis or necrosis. In apoptosis, macrophages maintain an intact plasma membrane; this process is associated with reduced *M.tb* viability and enhanced host immunity (89). Efferocytosis of apoptotic *M.tb*-infected macrophages facilitates their rapid clearance by phagocytes and limits mycobacterial growth (90). In contrast, necrosis is defined by plasma membrane lysis, which allows *M.tb* to exit from macrophages, infect surrounding macrophages and disseminate. Necrosis is crucial for the formation of TB granulomas and subsequent caseation, liquefaction and exponential *M.tb* proliferation (91). Infection with attenuated *M.tb* strains results in macrophage apoptosis (92). However, virulent *M.tb* strains inhibit apoptosis in favour of necrosis, thus realigning the balance of cell death to foil innate host defences (93). Strategies utilised by virulent *M.tb* strains to evade apoptosis include perturbation of eicosanoid regulation to induce pro-necrotic lipoxin A_4 (LXA_4) and inhibit pro-apoptotic prostaglandin E_2 (PGE_2) production (89); impairment of cholesterol homeostasis (94); and interference with TNF-α signalling (95).

1.3.1.3 Autophagy

The fate of *M.tb* can be influenced by autophagy, a homeostatic process in which cytoplasmic components, including organelles and intracellular pathogens, are degraded in the lysosome (96). Stimulation of autophagy increases *M.tb* killing in macrophages, while inhibition enhances *M.tb* survival (97,98). Impaired autophagy is associated with severe disease and poor treatment

outcomes in TB patients (99). Increased *M.tb*-stimulated production of IFN-γ activates macrophages to induce autophagy (100). This ubiquitin-dependent process requires several key proteins including LC3, lysosomal marker lysosomal associated membrane protein-1 (LAMP1) and Smurf1 (96). The nuclear receptor peroxisome proliferator-activated receptor-α (PPARα), mediated by the upregulation of *Lamp2, Rab7*, and *Tfeb* genes, plays a key role in autophagy (101). Autophagy is also regulated by metabolic signalling cascades; adenosine monophosphate (AMP)-activated protein kinase (AMPK) promotes autophagy, while mechanistic target of rapamycin (mTOR) is inhibitory (102). *M.tb* has evolved numerous strategies to exploit the host autophagy response in macrophages. *M.tb* possesses the enhanced intracellular survival (*Eis*) gene, which inhibits autophagy by increasing IL-10 and upregulating mTOR signalling (103,104). In addition, *M.tb* can produce IL-6 to inhibit IFN-γ (100), inhibit Ras-related protein Rab-7a-dependent maturation of autophagosomes to autolysosomes (105) and upregulate microRNAs to inhibit TLR signalling and autophagy (106).

1.3.1.4 Production of Reactive Nitrogen Species and Reactive Oxygen Species

M.tb-infected macrophages produce antibacterial RNS and ROS via activation of the enzymes inducible nitric oxide synthase (iNOS) and NADPH oxidase (NOX2) respectively (107). RNS have a more potent direct bactericidal effect on *M.tb* than ROS *in vitro* (107,108). Several studies confirm that iNOS-deficient mice are highly susceptible to TB; treatment of *M.tb*-infected mice with iNOS inhibitors results in mice rapidly succumbing to the disease (108). However, the role of ROS in TB *in vivo* is less well-defined. There is limited and transient inhibition of the ability to control *M.tb* growth in NOX2-deficient mice in early infection (109). Patients with the primary immunodeficiency Chronic Granulomatous Disease (CGD), who have a genetic NOX2 deficiency, are more prone to TB, but the mechanism is unclear (110,111). The evidence suggests that ROS-dependent signalling might be more important for host defence that direct *M.tb* killing by ROS

(110). *M.tb* evasion strategies include the scavenging of oxygen radicals by the *M.tb* cell wall components LAM and phenolic glycolipid 1 (PGL-1) (112); production of enzymes such as catalases and superoxide dismutases (113) and synthesis of the reducing agents ergothioneine and mycothiol (114,115). The ability of *M.tb* to maintain reduction-oxidation (redox) homeostasis and the redox environment of the granuloma contribute to virulence and drug susceptibility in TB (114,116).

1.3.2 Airway epithelial cells

Airway epithelial cells (AECs) are the predominant cells lining the airways as part of the respiratory mucosa and form an interface between the external milieu and the lung. The continuous, pseudostratified epithelial layer creates a tight barrier and comprises several cell types, including basal cells, club cells, ciliated cells, mucus-producing goblet cell and neuroendocrine cells (117). AECs are likely to be the initial point of contact in the host for inhaled pathogens such as *M.tb*; hence, their traditional functions were considered to be structural barrier protection against infection and mucociliary clearance. However, AECs are increasingly recognised as crucial, active players in the innate immunopathogenesis of TB (118).

AMs are thought to be the first cells to phagocytose *M.tb* to provide a niche for intracellular growth. However, several studies demonstrate that *M.tb* can also invade and proliferate within AECs (119–122); in fact, *M.tb* replication is 50-fold higher in human and mouse AECs compared to macrophages *in vitro* (122). The resulting high *M.tb* burden can overwhelm AECs and induce cell necrosis (122) or, less commonly, apoptosis (123). Hence, early invasion may benefit *M.tb* by providing a protected intracellular site conducive to bacterial growth (124). It may also facilitate alteration of the *M.tb* envelope surface and gene expression to evade recognition by phagocytes and enhance virulence (120,125). It has been postulated that necrosis of AECs could result in

increased *M.tb* burden in the alveolar space, leading to enhanced infection of adjacent AECs or phagocytes (124). The *M.tb*-secreted adhesin ESAT-6 can also act as a cytolytic toxin for AECs and contribute to cell-to-cell spread and bacterial dissemination via the alveolar wall (126).

AECs express numerous PRRs, such as TLRs, RIG-1-like receptors, NOD-like receptors, mannose receptor and C-type lectins, which sense *M.tb*-specific PAMPs on the bacterial surface to drive mucosal immune responses to TB (117,127,128). Recognition of *M.tb* by AECs results in activation of these signalling pathways, with subsequent production of pro-inflammatory cytokines and chemokines, including IL-1β, IL-6, TNF-α, IFN-γ and granulocyte macrophage colony-stimulating factor (GM-CSF) (118). This leads to recruitment, activation and enhanced survival of immune cells, including monocytes, macrophages, neutrophils and T cells, to facilitate bacterial clearance at the site of infection (128). Of note, differences in responsiveness to pro-inflammatory mediators between upper and lower AECs have been reported (129). In addition, AEC secretion of TGF-β plays an important immunoregulatory role in safeguarding epithelial integrity and preventing immune-mediated destruction by limiting inflammation (74).

Of note, a recent cellular and transcriptomic s*tudy found that* AECs were relatively inert to direct *M.tb* infection, but potent responders to an *M.tb*-activated immune network; this was mediated by the cytokines IL-1β and type 1 interferon, released by infected alveolar macrophages (38). The epithelial response induced by this intercellular cross-talk promotes early neutrophil influx to the initial site of infection, as well as creating an extracellular antimicrobial milieu (38). This is consistent with data from a murine model showing that, 48 hours after intratracheal *M.tb* infection, 90% of bacilli are found in macrophages or neutrophils and only 10% in AECs (121). Hence, given that few aerosolised mycobacteria are required for infection, amplification of the AM response to infection by surrounding uninfected AECs has been postulated to be a key determinant of the host response in TB pathogenesis (38). *In vivo*, in a zebrafish model of

Mycobacterium marinum (*M. marinum*) infection, ESAT-6-induced macrophage recruitment by epithelial cells is essential for nascent granuloma formation and bacterial growth in TB (44).

AECs can also secrete inducible antimicrobial peptides (AMP), such as cathelicidin (LL-37), human β-defensin-2 and hepcidin, which are critical for innate immunity against mycobacteria (128). LL-37, the only human cathelicidin, is produced by AECs and alveolar macrophages in early *M.tb* infection. LL-37 activates AECs and acts as a chemoattractant for immune cells at the site of infection (130). LL-37 is upregulated by A549 AECs infected with *M.tb* or stimulated with BCG; the latter is mediated by NADPH/ROS, MEK 1/2 and p38 MAPK signalling pathways (131,132). Human β-defensin (HBD) -2 and -3 play an important role in growth control and chemotactic activity of *M.tb* in AECs (133,134). In a murine model of progressive pulmonary TB, early rapid expression of HBD-3 by AECs correlates with bacillary control; however, HBD-3 expression declines in later disease (134). Interestingly the antidiabetic drug metformin has been found to increase HBD-2 and -3 production and promote *M.tb* killing in both AECs and macrophages (135). In children with pulmonary TB, LL-37 and HBD-2 levels are increased in bronchoalveolar lavage fluid (BALF) (136), while circulating HBD-3 levels are elevated in adults with severe disease (137). Hepcidin is a key regulator of iron homeostasis. *In vitro*, hepcidin inhibits *M.tb* proliferation and HBD-2 expression in *M.tb*-infected AECs (133,138). However, the role of hepcidin in TB immune defences *in vivo* is uncertain; although elevated hepcidin is associated with increased TB susceptibility in humans (139,140), this is not corroborated by recent studies in hepcidin knockout mice (141,142). Hence, AEC-derived AMP are important in early host defence against *M.tb* infection.

Surfactant proteins (SP) -A and -D are also highly expressed by AECs and genetic polymorphisms are associated with increased susceptibility to TB (143). SP-A and SP-D bind to a variety of

PAMPs to mediate opsonisation and phagocytosis of *M.tb* by macrophages (144), hence contributing to the innate immune response in TB.

Taken together, several lines of evidence show that, in addition to their barrier function, AECs are critical frontline players in the orchestration of TB innate immunopathogenesis and inflammation in the lung.

1.3.3 Cytokines

Several cytokines are crucial to the regulation of host immune defences in *M.tb* infection and their interactions are complex and intertwined. *M.tb* proliferates within macrophages and DC and stimulates the release of pro-inflammatory cytokines, including IL-1β, TNF-α and IL-6, which in turn activate macrophages to induce *M.tb* elimination (145). The anti-inflammatory cytokine, IL-10, is also produced by immune cells (145). In addition, IL-12 and IL-18 bridge innate and adaptive immunity to induce production of IFNγ by T-cells (146). Although IFN-γ can also be secreted by innate immune cells, its production largely by CD4+ Th1 cells is critical to the initiation of adaptive immunity and control of *M.tb* infection (112). I will discuss selected cytokines key to the innate immune response in more detail below.

1.3.3.1 Interleukin-1 beta

Interleukin-1 beta (IL-1β) is a classic pro-inflammatory cytokine critical to host immune response to *M.tb* infection (147). It upregulates key mediators required for TB control, including NO production, phagosomal acidification and maturation and adhesion molecules (74). It mediates differentiation of monocytes into macrophages with enhanced phagocytic and antigen-presenting functions in TB (148). Several studies of mice deficient in IL-1β signalling have confirmed that they are highly susceptible to TB, with increased mortality, greater bacterial burden and more

extensive pulmonary necrosis (76,149–153). Similar features of TB susceptibility were demonstrated in MyD88 knockout mice, suggesting that IL-1β induction is dependent on the MyD88 pathway (76,149). It has recently been shown that *M.tb*-infected macrophages show a metabolic shift towards aerobic glycolysis, resulting in increased bacterial killing via succinate-mediated induction of IL-1β (154). The role of IL-1β in containing *M.tb* replication in macrophages is also associated with its ability to trigger prostaglandin E2 (PGE2) synthesis and COX-2 activation (155). Cross-talk between Type 1 interferons, which can inhibit IL-1β, in part by inducing anti-inflammatory IL-10, could help to balance the innate inflammatory equilibrium in *M.tb* infection in macrophages (156,157). In AECs, IL-1β, enhanced by TNF-α, can induce the antimicrobial peptide (AMP) HBD-2 to control *M.tb* growth and chemotaxis (38). IL-1β overproduction can be detrimental; hence, its expression is tightly regulated at several levels. For example, IL-1β is secreted as a precursor and requires proteolytic cleavage for maturation; this is accomplished by inflammasome-mediated caspase-1 activation *in vitro* (158,159). However, in *M.tb*-infected mice deficient in caspase-1, it was shown that IL-1β production was not impaired and TB susceptibility was reduced compared to wild-type mice (149). Further studies have implicated caspase-1-independent mechanisms, such as the serine proteases proteinase 3, elastase and cathepsin-G, in *in vivo* processing of pro-IL-1β (160,161). Human polymorphisms of IL-1β and its antagonist, IL-1 receptor antagonist (IL-1Ra) genes are also associated with susceptibility to TB (162).

1.3.3.2 Tumour Necrosis Factor-alpha

The pro-inflammatory cytokine, tumour necrosis factor alpha (TNF-α), is a highly potent modulator of early inflammatory responses in *M.tb* infection and plays an important role in host protection. However, excessive production can mediate tissue damage and promote transmission, requiring TNF-α activity to be finely balanced; hence, along with IL-1β, it has been termed a “Goldilocks” cytokine (147). Numerous studies have demonstrated that mice deficient in either TNF-α or TNF

receptor 1 are profoundly susceptible to pulmonary TB and succumb more rapidly to infection; these mice show decreased recruitment of macrophages and T-cells into the lung, high bacterial loads, progressive necrosis and disorganised granuloma formation (163–167). The zebrafish model of *M. marinum* infection shows that TNF-α is critical for high microbicidal activity in macrophages (168). TNF-α also plays significant roles in regulation of macrophage apoptosis (92,169,170), autophagy (171), upregulation of adhesion molecules (172) and generation of mitochondrial ROS (173). TNF-α also supports IFN-γ-mediated phagosome maturation and acidification in macrophages and this effect is abrogated by treatment with TNF-α inhibitors (174). TNF-α increases expression of the chemokines CCL5, CXCL9 and CXCL10, which mediate macrophage and T cell recruitment to the granuloma; hence, it is essential for communication between innate and adaptive immunity in TB (147). Patients with latent TB treated with anti-TNF-α therapies, such as infliximab and adalimumab, have a higher rate of TB reactivation, a more aggressive disease course and an increased rate of extrapulmonary TB (175–177). Hence, these patients are routinely screened and treated for latent TB prior to commencing anti-TNF-α treatment. Similarly, TNF-α is needed to prevent active disease in murine models of latent TB, suggesting that it is required for control of both active and latent TB (169,178). Hence, TNF-α is a key effector in TB immunopathogenesis.

1.3.3.3 Interleukin-10

IL-10 is an anti-inflammatory cytokine that regulates the innate and adaptive immune response in TB (179). IL-10 gene polymorphisms, specifically -1082G/A and -592A/C, are associated with TB susceptibility (180). In TB patients, IL-10 expression correlates with higher bacterial burden and greater disease severity (181,182), as well as TB recurrence (183). Following *M.tb* infection, IL-10 is produced by macrophages, dendritic cells, neutrophils and B and T cells. In macrophages, IL-10, mediated by STAT3, can inhibit phagosome maturation and macrophage activation to

generate a niche for *M.tb* to survive and replicate within the phagosome (184). IL-10 can also inhibit IFNγ- and TNF-α-mediated macrophage activation in *M.tb* infection and suppresses apoptosis (95) and autophagy (104). There is, however, conflicting data on the immunomodulatory effect of IL-10 in TB *in vivo*. Some studies have shown decreased bacterial loads in the lungs of *M.tb*-infected IL-10-knockout mice (185,186), but others demonstrate no difference (187–189). Hence, the significance of IL-10 in TB *in vivo* requires further elucidation.

1.4 Tissue destruction in tuberculosis

1.4.1 Tissue destruction and cavitation in tuberculosis

Morbidity and mortality in TB relates to progressive, severe inflammatory tissue destruction triggered by *M.tb* infection (190). This results in pulmonary cavitation, the classic hallmark of established disease, which is fundamental to the global success of this pathogen (Figure 1). Cavities provide an immunoprivileged niche, which drive exponential growth and transmission of the pathogen via the aerosol route (52,191,192). Cavities are also poorly penetrated by antituberculous drugs, leading to greater risk of treatment failure, relapse and resistance (193). Formation of cavities requires destruction of the lung parenchyma. The tissue architecture of the lung is determined by the pulmonary extracellular matrix (ECM), which consists of several macromolecules that support physiological lung function. The most abundant macromolecules in the lung scaffolding are fibrillar collagens which determine tensile strength; in addition, elastin confers resilience, while fibronectin and laminins are crucial adhesion proteins (194).

Pulmonary cavitation was classically attributed to cell necrosis and lipid accumulation in the caseous granuloma (195). However, there is now considerable evidence that cavity formation requires active, proteolytic destruction of the ECM (196,197). Collectively, only the matrix

metalloproteinase (MMP) enzymes can degrade all components of the ECM at neutral pH (198), implicating them as critical mediators in TB pathogenesis.

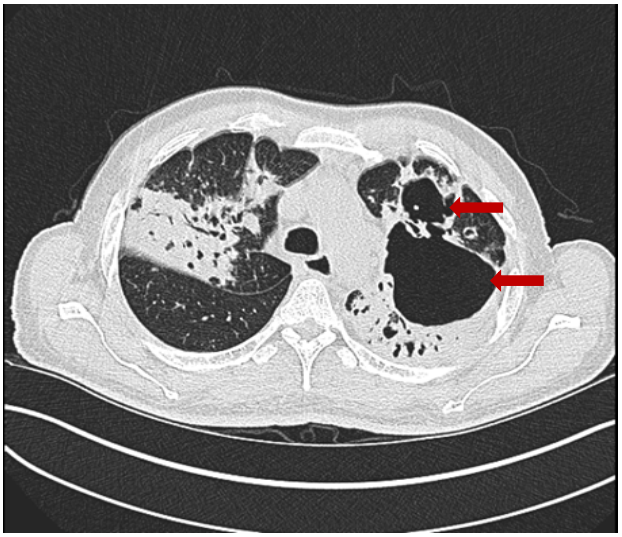


Figure 1: Thoracic CT scan of TB patient. ECM degradation leads to severe tissue damage and marked cavitation (arrows) in the lungs of a patient with pulmonary TB. Computerised tomography (CT) image courtesy of Professor Jon Friedland and reproduced with patient consent.

1.4.2 Structure and classification of matrix metalloproteinases

MMPs are a family of calcium- and zinc-dependent endopeptidases within the metzincin superfamily. The first MMP, described by Gross and Lapiere in 1962, was a collagenase facilitating tail resorption in tadpole metamorphosis (199). Subsequent identification of a similar collagenase in human skin was termed MMP-1. Since then, a total of 23 MMPs have been described in humans, which are expressed in almost all organs and tissues (200).

Most MMPs share a homologous structure comprising 4 distinct functional regions: an N-terminal signal peptide, an inhibitory pro-domain, a catalytic domain, and a C-terminal hemopexin domain (201,202). The N-terminal signal peptide targets MMPs for secretion. The catalytic domain, which

contains two zinc ions, is responsible for proteolytic activity. The covalent “cysteine switch” interaction between a thiol of the conserved cysteine residue in the inhibitory pro-domain and a zinc ion in the catalytic domain maintains MMPs in their latent state (203). Functional MMP activation occurs when the inhibitory pro-domain is destabilised. The catalytic domain is connected to the C-terminal hemopexin domain by a flexible, proline-rich hinge region. The C-terminal hemopexin domain plays a role in substrate recognition and confers MMP substrate specificity. It is arranged in a four-bladed propeller structure and has been shown to be crucial for the degradation of triple-helical collagens (204).

MMP	Classification	Substrates
MMP-1	Collagenase	Collagens I, II and III, gelatin, α2-macroglobulin, proteoglycans, L-selectin, pro-TNF-α
MMP-2	Gelatinase	Gelatin, collagen IV and V, laminin, fibronectin, elastin, proteoglycans, pro-TNF-α, pro-IL-1β
MMP-3	Stromelysin	Pro-MMP-1, pro-MMP-8 and pro-MMP-9, collagen III, IV and V, laminin, E-cadherin, fibronectin, proteoglycans, pro-IL-1β
MMP-7	Matrilysin	Collagen IV, elastin, pro-MMP-2, laminin, fibronectin, pro-TNF-α
MMP-8	Collagenase	Collagens I, II and III, laminin, fibronectin, α2-macroglobulin, serpins
MMP-9	Gelatinase	Gelatin, collagen IV and V, fibronectin, elastin, pro-TNF-α, pro-IL-1β, latent VEGF
MMP-10	Stromelysin	Pro-MMP-1, pro-MMP-7, pro-MMP-8 and pro-MMP-9, proteoglycans, collagen III and IV, laminin, fibronectin, elastin
MMP-14	Membrane-type	Collagens I, II and III, gelatin, laminin, fibronectin, syndecan-1, pro-MMP-2

Table 1: Classification and substrates of MMPs in TB. Modified from Parks, *et al* (208); Nagase, *et al* (205) and Ong, *et al* (240).

MMPs are often classified according to substrate specificity and whether they are secreted or membrane-bound (205). MMPs target a wide range of extracellular matrix (ECM) substrates and, collectively, they can degrade all the components of the ECM (198). MMPs include collagenases (MMP-1, -8 and -13), gelatinases (MMP-2 and -9), stromelysins (MMP-3 and -10), matrilysins (MMP-7), elastases (MMP-12) and membrane-type MMPs (MMP-14, -15, -16, -17, -24 and -25) (205,206). Table 1 outlines the key MMPs upregulated in TB together with a selection of their main substrates.

1.4.3 Function of matrix metalloproteinases

MMPs are responsible for the degradation and remodelling of the ECM (198) and play important roles in both physiological and pathological processes. MMP function is complex and has been described as a “double-edged sword” (207). MMPs are essential for maintenance of homeostasis in normal circumstances, in which they are expressed at a low level and their activity is strictly controlled. However, profligate or unrestrained MMP expression can be detrimental and result in tissue damage (207,208).

Physiologically, MMPs are crucial in cell migration; embryonic development; reproduction; and tissue homeostasis, including wound healing and tissue repair, bone and organ remodelling, neuroplasticity and angiogenesis. (200,209–212) For example, the repair of skin wounds requires the collagenase MMP-1, which facilitates keratinocyte migration and directionality to remodel damaged ECM collagen (213). In the lung, MMP-7 is expressed by injured epithelial cells and mediates healing of the lung tissue (214).

MMPs are also implicated in the pathogenesis of numerous diseases, in which they mediate ECM remodelling and immunomodulation. In cancer, MMP-mediated ECM degradation is necessary for metastatic spread. Excessive MMP activity also contributes to tissue damage in chronic

inflammatory conditions, including atherosclerosis, chronic obstructive pulmonary disease, pulmonary fibrosis, rheumatoid arthritis, inflammatory bowel disease, Parkinson's disease and multiple sclerosis (202,215).

In addition to ECM matrix degradation, MMPs can also contribute to inflammation by regulating immunomodulatory activity. MMPs can proteolytically modulate cytokines and chemokines to regulate signal transduction cascades and leucocyte recruitment to sites of inflammation. (208). Hence, MMPs can either promote or suppress inflammation, leading to complex interactions (216). For example, MMP-1, -2, -3 and -9 can degrade and inactivate IL-1β (217), but MMPs -2, -3 and -9 can also activate pro-IL-1β (218). Several MMPs, including MMP-1, -2, -3 and -9, can cleave latent TNF-α to its active form by proteolysis (219). In addition, MMPs can regulate chemokine gradients to mediate inflammatory cell recruitment. In a model of allergic lung inflammation, MMP-2 and -9 cleave the eosinophil chemoattractant, CCL11, to increase eosinophil airway accumulation (220). In contrast, MMP-1 and -2 cleave MCP-1 and CCL7 respectively, generating antagonistic peptides which inhibit the inflammatory response (221).

1.4.4 Control of matrix metalloproteinases

MMPs are ubiquitously expressed and integrated as regulators for tissue homeostasis and immune function. However, due to the destructive nature of excessive MMP activity, these enzymes are tightly controlled at 4 levels: gene expression with transcriptional and post-transcriptional regulation, secretion as inactive zymogens, discrete pericellular compartmentalisation and specific inhibition of active enzymes by Tissue Inhibitors of Metalloproteinases (TIMPs) (210,222).

MMPs are predominantly regulated at the transcriptional level, resulting in minimal basal MMP expression in physiological conditions (210,223). Transcriptional induction of MMP genes occurs

several hours after initial exposure to stimuli such as cytokines, chemokines, growth factors and cell–cell or cell–ECM interactions (224). Each of these triggers may activate specific signalling cascades of early response genes, which encode signalling proteins such as the mitogen activated protein kinases (MAPK) and phosphatidylinositol-3 kinase (Pi3-kinase). These proteins phosphorylate transcription factors such as activator protein 1 (AP-1), nuclear factor kappa B (NF-κB), and the signal transducers and activators of transcription (STAT), which then bind to the promoters of MMP genes (223). This suggests that MMP promoters are downstream targets of these early response genes. Most MMPs share common cis-acting elements in their promoters; hence, they are often co-expressed in response to various stimuli (225). In turn, inhibition of these signalling pathways blocks transactivation, with subsequent silencing of gene expression (225). The transcriptional regulation of MMPs may also be influenced by epigenetic mechanisms, such as DNA methylation or chromatin remodelling with histone acetylation (226). Post-transcriptional gene regulation of MMPs occurs by modulating cytosolic mRNA stability. This is mediated via untranslated regions (UTR)-binding proteins, which bind to specific sequences in MMP 5' or 3' UTR transcripts (210). Modulation of translational efficiency may also be another post-transcriptional mechanism for controlling MMP expression (227).

MMPs are then controlled at the post-translational stage. Secreted MMPs are initially released as inactive pro-enzymes, termed zymogens. The interaction between a thiol of the conserved cysteine residue in the pro-domain and a zinc ion in the catalytic domain maintains the enzyme in its latent state. MMP activation occurs when this "cysteine switch" motif is disrupted by conformational change in the pro-domain (228). This can occur via 3 mechanisms: cleavage of the prodomain by itself (autolysis) or by serine proteases such as plasmin (proteolysis); allosteric reconfiguration of the prodomain; or chemical modification of the cysteine thiol group by ROS (210,222,229). In addition to serine proteases, the stromelysins MMP-3 and -10 can also activate the collagenases MMP-1 and -8 and the gelatinase MMP-9 (230–232). Further, there is a potent

synergistic interaction between the stromelysins and plasmin to generate an activate form of MMP-1 that is 10-fold more efficient than the enzyme produced by serine proteases alone (233). In contrast, MT-MMPs are activated intracellularly by pro-protein convertases or furins before insertion into the cell membrane (210).

The activity and specificity of MMPs is also regulated by pericellular compartmentalisation, possibly through their interaction with glycosaminoglycans (234).

Finally, once activated, MMPs can be inhibited by specific Tissue Inhibitors of Metalloproteinases (TIMPs). The TIMP family comprises 4 members (TIMP-1, -2, -3 and -4), which all inhibit MMPs, binding them in a 1:1 stoichiometric ratio (235). TIMP-3 is bound to the ECM, whereas the other TIMPs are present in soluble form (236). In general, TIMPs are broad-spectrum MMP inhibitors, but can show a preference for specific MMPs. For example, TIMP-2 -3 and -4, but not TIMP-1, can effectively inhibit MT-MMPs and MMP-19 (237). However, TIMP-1 is more potent for MMP-3 and -7 than TIMP-2 and -3 (237). TIMPs can also inhibit MMPs at the pro-enzyme level. For example, both the catalytic domain of MT-MMP MMP-14 and the hemopexin domain of secreted pro-MMP-2 interact with TIMP-2 to form a ternary complex that regulates the activation of pro-MMP-2 (238,239).The MMP/TIMP balance is an important factor in regulating overall proteolytic activity *in vivo* (202).

1.4.5 Matrix metalloproteinases in tuberculosis

There is considerable evidence from cellular, animal and clinical studies that MMPs play a crucial role in TB immunopathogenesis (197,240). MMPs are produced by several key cells involved in the TB host response, including monocytes, macrophages, neutrophils, airway epithelial cells, T cells and fibroblasts. Our group developed the concept of an inflammatory matrix-degrading phenotype in TB, in which MMP activity is relatively unopposed by a compensatory increase in

TIMP concentrations (190,241). MMPs degrade the intricate ECM scaffolding in the lung, including highly resilient triple-helical fibrillar collagens and other components, to drive tissue reconfiguration and pulmonary cavitation in TB (197,240). This ECM degradation is strongly correlated with mycobacterial replication, transmission and resistance, with profound implications for TB morbidity and mortality (197,240).

1.4.5.1 Cellular studies

MMP gene expression and secretion in TB *in vitro* is regulated by direct *M.tb* infection, as well as intercellular cytokine network effects (197). *M.tb* has a low infectious dose, with few aerosolised mycobacteria required for infection. Immunohistochemistry of granulomas from *M.tb*-infected patients demonstrates widespread MMP staining with minimal TIMP expression, despite the presence of low numbers of bacilli (242). Hence, excessive tissue destruction occurs in TB despite a modest bacterial load, suggesting that the majority of cells involved in TB host responses are not in direct contact with *M.tb*. Signals from *M.tb*-infected immune cells may amplify host immune responses by potent stimulation of uninfected surrounding cells. These communications can occur by secretion of pro-inflammatory cytokines, local growth factors and microbial products. For instance, AECs are relatively resistant to direct *M.tb* infection, but respond to IL-1β and Type 1 interferon cytokine release by *M.tb*-infected macrophages to permit cellular cross talk (38,121). Hence, the elaborate intercellular networks driving MMP secretion are crucial to development of the matrix-degrading phenotype in TB (197).

Direct *M.tb* infection potently upregulated MMP-1 gene expression and secretion in human macrophages; in contrast, the BCG vaccine, which does not cause pulmonary cavitation in immunocompetent hosts, did not induce MMP-1 (243). Ro32-3555, a collagenase inhibitor of proven safety in humans, was shown to completely suppress MMP-1 in *M.tb*-infected human macrophages (190). *M.tb* also drives human macrophages to secrete MMP-10, an important

activator of MMP-1; this process is driven in part by the virulence factor ESAT-6 (244). *M.tb* infection also increased MMP-1, 3, -7, -8, -10, -12 and -14 gene expression and secretion from primary human monocytes, with MMP-1 the most highly expressed (190).

Cell-cell network communications have been assessed *in vitro* using conditioned media from *M.tb*-infected monocytes (CoMTB); this contains secreted bacterial factors such as ESAT-6 and secreted cytokines, chemokines, growth factors from *M.tb*-infected monocytes (245). CoMTB, though not direct *M.tb* infection, upregulates MMP-1, -3 and -9 gene expression and secretion from human AECs (246–248). Similar *M.tb*-induced network effects modulate MMP-1, -2 and -3 gene expression and secretion from microglia (249,250); MMP-1 from fibroblasts (251); and MMP-9 from monocytes (242) and astrocytes (252). Recent studies have shown that platelet-monocyte interactions also drive MMP-1 and -10 gene expression and secretion (253).

Monocyte secretion of MMP-14 (254) and neutrophil secretion of MMP-8 and -9 (255,256) are regulated by both direct *M.tb* infection and CoMTB stimulation. Concurrent incubation of neutrophils with both *M.tb* and CoMTB had an additive effect on neutrophil MMP-9 secretion (256).

Several intracellular signalling pathways regulate MMPs in TB. The upregulation of MMPs in TB is dependent on the p38 MAPK signalling pathway in *M.tb*-infected macrophages (246), as well as in CoMTB-stimulated AECs, monocytes (254), neutrophils (256), fibroblasts (251) and microglia (257). There is evidence of MMP regulation by the Pi3-kinase pathway in *M.tb*-infected macrophages (258) and in CoMTB-stimulated AECs (248) and neutrophils (256); and by AMPK in both *M.tb*-infected and CoMTB-stimulated neutrophils (255). The transcription factor NF-κB has been implicated in MMP regulation in *M.tb*-infected neutrophils (255,256) and CoMTB-stimulated fibroblasts (251), astrocytes (252) and microglia (249). Intracellular accumulation of a second transcription factor, HIF-1α upregulates MMP-1 secretion in *M.tb*-infected macrophages

(259) and MMP-8 and -9 in *M.tb*-infected neutrophils (260). The cytokines TNF-α and IL1β have been found to be important in regulating MMPs production from *M.tb*-stimulated macrophages (244) and CoMTB-stimulated monocytes (242), fibroblasts (251) and microglia (249).

1.4.5.2 Animal studies

Numerous animal models have implicated MMPs in TB pathogenesis, including zebrafish, mice, rabbits and non-human primates. However, none entirely replicates the immunopathology of TB in humans (261). Hence, although these models offer valuable insights, they might not precisely reflect the mechanisms of tissue destruction in human TB. In *M. marinum*-infected zebrafish, the bacterial virulence factor ESAT-6 selectively induced MMP-9 from epithelial cells adjacent to infected macrophages (44). MMP-9 enhanced macrophage recruitment to granulomas and was crucial for bacterial proliferation and nascent granuloma maturation (44). In addition to being a gelatinase, the ability of MMP-9 to degrade Type IV collagen, a key component of the lung basement membrane (262) and the blood brain barrier, may facilitate its role in granuloma development. Murine TB studies have also implicated MMPs in TB immunopathology. Mice do not express an orthologue of human MMP-1 in the lung. Hence, caseating necrosis or cavitation reflective of human disease is not seen in mice following *M.tb* infection (263). However, in transgenic mice expressing human MMP-1 under control of the scavenger receptor A promoter/enhancer, *M.tb* infection enhanced collagen breakdown and alveolar wall destruction in lung granulomas. This preceded the onset of caseous necrosis, suggesting that direct collagenase activity of MMP-1 drives tissue destruction in TB (190,264). In another murine model of pulmonary TB, MMP-9 expression in the lung was associated with macrophage recruitment and tissue remodelling to form well-organised granulomas (265). In this model, MMPs were also associated with early *M.tb* dissemination; haematogenous spread of bacilli was reduced by the broad-spectrum MMP inhibitor batimastat (BB-94) (265). This is consistent with the findings of the

M. marinum zebrafish model (44). Raised serum MMP-9 levels were also observed in a murine model of tuberculous meningitis; adjuvant treatment with the specific MMP-9 inhibitor, SB-3CT, potentiated bacillary clearance (266). Guinea pigs show mature TB granuloma formation, though rarely cavitate (267); these models have been used to investigate the effects of the MMP inhibitor doxycycline *in vivo* (268). Rabbits are naturally resistant to *M.tb* infection; however, pulmonary cavitation, similar to that in humans, is observed in established disease. In a rabbit model of cavitatory TB, several MMPs, including MMP-1 and -9, were upregulated in the lungs of *M.tb*-infected rabbits with destructive pathology (269). In another rabbit model, an MMP-1/TIMP imbalance was associated with progression of consolidated tissue to cavities with high bacillary burdens (192). Non-human primates demonstrate TB pathology that most closely mirrors human disease, with the presence of caseating granulomatous inflammation and pulmonary cavitation. Microarray studies in *M.tb*-infected rhesus macaques showed upregulation of multiple MMPs in early TB lesions. Though MMP-1 was the most highly expressed, MMP-2, -7, -9 and -14 were also increased (270). However, as TB is a disease of humans, patient studies are essential to fully elucidate the immunopathology of tissue destruction.

1.4.5.3 Patient studies

Finally, several clinical studies support the importance of MMPs in the pathophysiology of TB.

MMP-1 and -3 concentrations are increased in sputum and BALF of TB patients compared to symptomatic controls (190), while MMP-1, -2, -3 -8 and -9 levels are raised in sputum of TB patients at diagnosis compared to healthy controls (271). MMP sputum concentrations decrease rapidly in the first 2 weeks of antituberculous treatment, resulting in resolution of the matrix-degrading phenotype (271). Higher MMP concentrations at diagnosis also predict delay to sputum culture negativity following treatment initiation (271).

Plasma and sputum from TB patients show higher concentrations of matrix degradation products such as procollagen III N-terminal peptide (PIIINP) and desmosine, released during collagen and elastin degradation respectively (272). MMP-1, -8 and -9 are also increased in the pleural fluid of TB patients compared with other aetiologies (273). Sputum MMP-1 concentrations in TB patients show a positive correlation with clinical severity score (271); plasma PIIINP levels (272) and the degree of chest radiograph cavitation and infiltration (268). In addition, immunohistochemical staining of TB lung biopsies demonstrated that MMP-1 is expressed in the necrotic centre of granulomas adjacent to tissue destruction (243,264). MMP-1 immunoreactivity is also present in CNS TB granulomas (249). This suggests that MMP-1 is a key collagenase driving tissue destruction and the development of pulmonary cavitation in TB (190).

Neutrophil-derived MMP-8 has recently been characterised as the second most important collagenase in TB (255). MMP-8-containing neutrophils were found in the walls of TB cavities and in central areas of caseous necrosis. Raised sputum MMP-8 concentrations from pulmonary TB patients is associated with elevated neutrophil activation markers, radiographic pulmonary cavitation and greater disease severity (255). MMP-8 is also correlated with *M.tb*-triggered NETs in TB patient sputum (255).

MMP-9 concentrations are upregulated in the cerebrospinal fluid (CSF) of patients with TB meningitis without a concurrent increase in TIMP-1 concentrations (241). CSF MMP-9 concentrations correlated with signs of cerebral tissue injury, such as reduced consciousness and focal neurological deficit, and with death (241). In brain biopsies of CNS TB patients, raised concentrations of MMP-9 have also been demonstrated in astrocytes (252) and neutrophils (256) in TB granulomas. Similarly, patients with TB lymphadenitis also show enhanced granulomatous MMP-9 expression (242).

Identification of MMP promoter polymorphisms in diverse patient populations further implicate MMPs in TB pathogenesis (240). The 1G MMP-1 genotype, which upregulates MMP-1 activity, predisposes to endobronchial TB (274); the G-1607GG polymorphism increases fibrotic risk after TB treatment (275); and the MMP-1 2G/2G genotype increases the likelihood of developing pulmonary TB in BCG-vaccinated individuals (276). The MMP-9 (-1562C/T) polymorphism, which reduces MMP-9 activity, has been associated with disseminated disease (277).

Increased concentrations of multiple MMPs indicate that several proteases may collectively remodel the ECM in TB. It is possible that various MMPs contribute to the degradation of specific ECM structural components and predominate at different temporal stages of TB immunopathogenesis. Overall, there is substantial evidence that MMPs are critical immunopathological mediators in TB. Enhanced understanding of MMP signalling and regulation could identify switch points for future pharmacological intervention.

1.4.6 MMPs and host-directed therapy in tuberculosis

There is considerable evidence for the critical role of MMPs in TB immunopathology. MMPs, regulated by the innate immune response, drive tissue destruction in TB, suggesting a potential role for adjuvant, host-directed immunomodulatory therapies. Dexamethasone is an established adjuvant treatment for CNS TB that reduces mortality in TB meningitis (278) and causes a fall in CSF MMP-9 concentrations (279). Doxycycline, a tetracycline antibiotic, is the only currently licensed MMP inhibitor by the United States Food and Drug Administration. The main therapeutic indication of doxycycline is to reduce the concentration of collagenases in periodontal disease in sub-antimicrobial doses (280). It also enhances pulmonary function in patients with asthma (281) and chronic obstructive pulmonary disease (282) in conjunction with standard treatments. Doxycycline suppresses MMP-1 and -9 secretion in human macrophages and epithelial cells and

also inhibited *M.tb* proliferation *in vitro* and in a guinea pig model (268); it may, therefore, hold therapeutic promise in TB.

In addition, there are several broad-spectrum MMP inhibitors such as marimastat and batimastat, which were developed for cancer treatment (283), or Ro32-3555, first trialed in rheumatoid arthritis (284). However, clinical trials of marimastat in cancer demonstrated no survival benefit; patients also exhibited severe musculoskeletal toxicity attributed to non-specific inhibition and off-target effects (283). These agents may still hold promise as potential adjuvant therapies in TB, especially for shorter durations of drug administration which might be better tolerated (240). Adjuvant treatment of *M.tb*-infected mice with marimastat significantly increased bacterial killing by the first-line antituberculous drugs rifampicin and isoniazid; marimastat impacted granuloma formation and enhanced blood vessel health in infected tissues to enhance drug penetration and retention (285). Similarly, targeting MMP-9 with a specific antibody in conjunction with standard antituberculous treatment reduced pulmonary bacterial load and decreased relapse rates in a cavitary murine model of TB (286). Hence, MMP inhibition in tandem with existing antituberculous chemotherapy may be beneficial; however, further translational studies are required. Enhanced understanding of TB immunopathogenesis is crucial to developing novel, host-directed therapies for TB. Dissecting the complex pathways that regulate MMP expression in TB might permit targeted treatment strategies that limit ECM destruction without the risk of adverse effects.

1.5 Metabolic regulation of TB

1.5.1 Cellular metabolic reprogramming

In TB, once called “consumption”, profound weight loss is common, suggesting a role for cellular metabolism in TB immunopathogenesis. Recent insights in the exciting new field of

immunometabolism suggest that innate immune cells are closely coupled to bioenergetic pathways and metabolic perturbations strongly influence cell fate and effector functions (287). Metabolic reprogramming of the cell is mediated, among other factors, by the transcription factor (TF) HIF-1α, the metabolic sensor, AMPK and the signal transduction pathway Pi3-kinase-Akt-mTORC1, which are also emerging as cellular regulators of inflammation in TB. However, the effect of rewiring cellular energy metabolism on ECM degradation and tissue destruction in TB has not yet been studied. I will discuss these pathways in more detail below though, to provide context, they operate within a cellular metabolic network that is highly dynamic, complex and intertwined.

1.5.1.1 Normal cellular energy metabolism

In a normal resting cell, glucose enters the cell and is metabolised to pyruvate by the process of glycolysis (Figure 2). Glycolysis comprises 10 enzyme-catalysed steps, with the first step being the conversion of glucose to glucose-6-phosphate by hexokinase (HK). In normoxia, each glucose molecule produces 2 molecules of pyruvate, which enter the mitochondria. Pyruvate is then decarboxylated by pyruvate dehydrogenase (PDH) into acetyl coenzyme A (CoA), which undergoes oxidative phosphorylation (OXPHOS) in the TCA cycle (Figure 3). The total energy gain in these conditions is approximately 32 molecules of ATP for each glucose molecule. However, in hypoxia, pyruvate is diverted away from the TCA cycle and converted to lactate by lactate dehydrogenase (LDH) in the cytosol. This process of aerobic glycolysis only generates 2 molecules of ATP, but allows regeneration of NAD+ required for glycolysis to proceed.

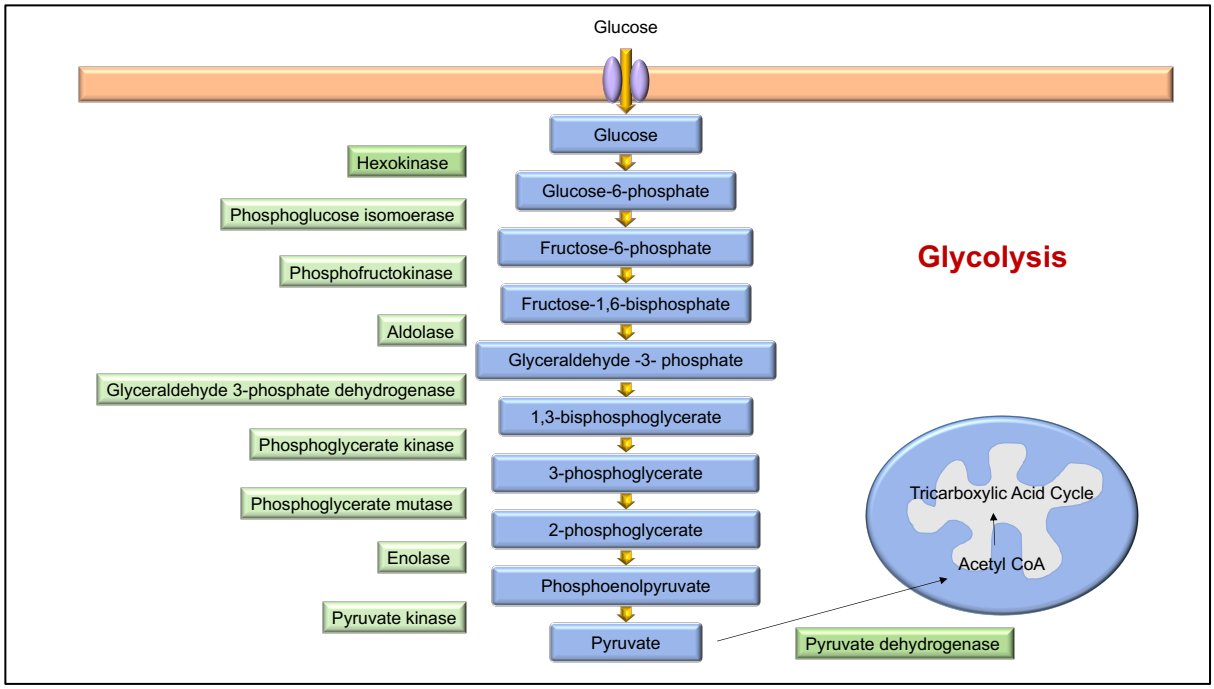


Figure 2: Schematic representation of glycolysis

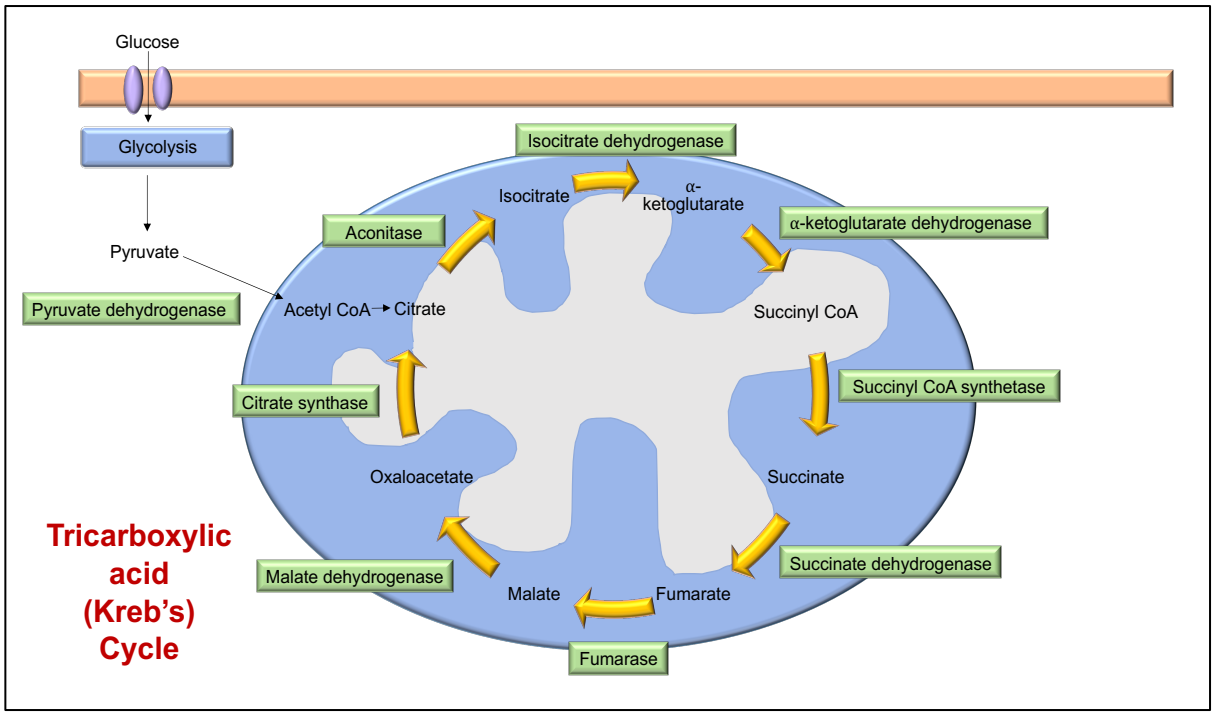


Figure 3: Schematic representation of the tricarboxylic acid (Kreb's) cycle

1.5.1.2 The Warburg effect

Otto Warburg first described the Warburg effect in cancer cells in 1927 (288). This phenomenon occurs when rapidly proliferating tumour cells switch their metabolic profile from OXPHOS to aerobic glycolysis (Figure 4). The high glycolytic rate and lactate production allow the cells to generate energy faster in the form of ATP and provide the necessary biosynthetic precursors required for cell growth (289).

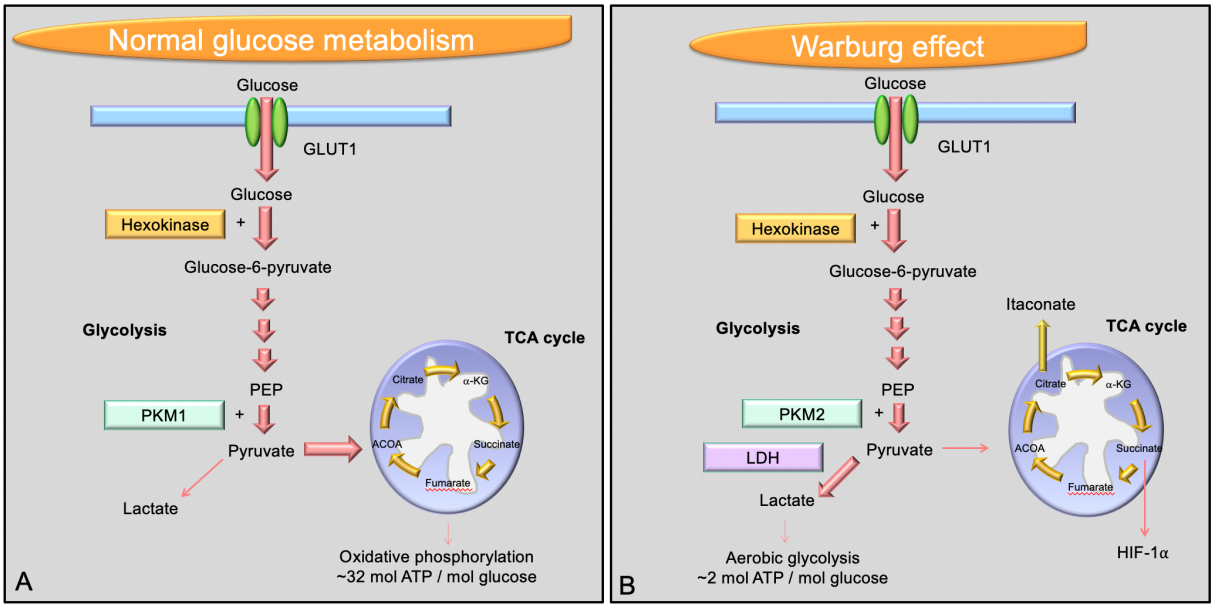


Figure 4: Schematic representation of the Warburg effect The Warburg effect is a metabolic switch from oxidative phosphorylation to aerobic glycolysis, first described in cancer cells by Otto Warburg in 1927 (286).

1.5.1.3 Cellular metabolic reprogramming in innate immune cells

Nearly a century later, there is considerable evidence that the Warburg effect regulates inflammation in activated innate immune cells. Metabolic reprogramming similar to neoplastic cells has recently been reported in a diverse array of bacterial and viral and parasitic infections,

including *Legionella pneumophila* (290), *Listeria monocytogenes* (291), *Salmonella typhimurium* (292), human adenovirus (293) and *Schistosoma japonicum* (294).

The bioenergetic rewiring of innate immune cells was first demonstrated by stimulation of murine macrophages (295,296) and dendritic cells (297) with lipopolysaccharide (LPS), a Gram-negative bacterial product. LPS activates TLR4 to induce the Warburg effect, as evidenced by increased rates of glycolysis and reduced OXPHOS via the TCA cycle (295–297). In addition, glycolysis in LPS-stimulated murine macrophages can also be directed towards the pentose phosphate pathway (PPP) and the malate-aspartate shuttle to support NADPH synthesis for ROS production (298)

The metabolic profile of macrophages can induce differential polarisation along M1 or M2 lines to define their functional phenotype (299,300). Classically activated, pro-inflammatory M1 macrophages display enhanced glycolysis and increased oxygen consumption and offer protection against bacterial infection. This response is mediated by HIF-1α and mTOR and involves multiple cytokines, RNS and ROS (301–303). In contrast, alternatively activated M2 macrophages are associated with OXPHOS and have a pro-resolution phenotype, primarily mediated by AMPK (304). OXPHOS also promotes immune cell longevity; switching cellular metabolism from glycolysis to OXPHOS facilitates a shift from short-lived M1 macrophages to longer-lived M2 macrophages (305). However, the M1 and M2 macrophage paradigm *in vitro* represents a continuum of activation states *in vivo* (306); in addition, M1 and M2 macrophages can undergo reversible functional changes depending on the cytokine milieu (307). Hence, macrophage plasticity plays an important dynamic role during inflammation and its resolution.

The rewired TCA cycle has recently emerged as a central immunometabolic hub that regulates signalling cascades to impact key effectors in activated immune cells (308). It has been postulated that 2 metabolic breakpoints occur in the TCA cycle in response to pro-inflammatory LPS

activation of macrophages (309); these are at the levels of succinate dehydrogenase (SDH) and isocitrate dehydrogenase (IDH), leading to transient accumulation of succinate and citrate respectively (298,310). Succinate-mediated upregulation of the key transcription factor HIF-1α occurs in LPS-stimulated murine macrophages, leading to increased pro-inflammatory IL-1β secretion; this process is largely dependent on glutamine anaplerosis (296). The balance between succinate and α-ketoglutarate can also regulate members of the α-ketoglutarate -dependent dioxygenases (α-KGDDs) involved in epigenome remodelling and innate immune memory (311). Citrate effluxes from mitochondria to the cytosol and is converted to acetyl-CoA and oxaloacetate by ATP citrate lyase (ACL). Acetyl-CoA is essential for fatty acid synthesis and histone acetylation, which can regulate inflammation *in vitro* (312,313). In addition, citrate accumulation leads to production of the anti-bacterial metabolite itaconate (314). Citrate is acted on by the mitochondrial aconitase 2 (ACO2) to produce cis-aconitate, which is then decarboxylated by cis-aconitate decarboxylase (CAD), also known as immunoresponsive gene 1 (IRG1), to produce itaconate (315). Itaconate also has immunoregulatory functions and can temper the inflammatory response in macrophages; following LPS stimulation, itaconate can inhibit pro-inflammatory cytokine production, such as IL-1β and IL-6 (316). Itaconate can also inhibit SDH-mediated succinate oxidation to reduce ROS production and promote succinate accumulation (316,317), activate the master antioxidant regulator NRF2 (318) and induce the anti-inflammatory transcription factor ATF3 (319). There is early evidence that itaconate can also inhibit aerobic glycolysis enzymes, including lactate dehydrogenase A (LDHA), by the cysteine-modifying process of 2,3-dicarboxypropylation (318,320).

Hence, cellular metabolism is closely coupled to the function of activated immune cells; this potentially has profound implications for TB immunopathogenesis.

1.5.1.4 Cellular metabolic reprogramming in TB

The metabolic profile of innate immune cells in TB need to be functionally committed to controlling *M.tb* infection; hence, it is essential that their metabolic profile meets the bioenergetic and biosynthetic requirements needed for efficient containment of the pathogen (287). There is increasing evidence that *M.tb*-induced metabolic reprogramming in immune cells regulates their effector functions and, ultimately, determine the outcome of the host-pathogen interaction in TB (321).

Transcriptomic analysis of murine (322) and human (323–325) models of pulmonary TB demonstrate significant upregulation of genes involved in glycolysis, with downregulation of genes encoding TCA cycle and oxidative phosphorylation (OXPHOS) enzymes, suggesting the presence of the Warburg effect. In *M.tb*-infected murine and human lungs, upregulated glycolysis genes include those encoding glucose transporters (GLUT) 1, 3 and 6, as well as enzymes such as hexokinase (HK) 2 and 3, phosphofructokinase (PFK) 1 and 2, glyceraldehyde 3-phosphate dehydrogenase (GAPDH), phosphoglycerate kinase (PGK) 1, enolase (ENO) 1 and lactate dehydrogenase (LDH) A (322,323). There is also heightened induction of the H^+ V-ATPase and lactate monocarboxylate transporters (MCT) 1,2 and 4, which are involved in cytosolic pH homeostasis (322,323). There is a simultaneous upregulation of the PPP, consistent with the metabolic state of activated immune cells (322). Finally, the Warburg effect correlates with increased levels of mRNA and protein of HIF-1α in macrophages (322).

This metabolic switch in TB is further demonstrated in targeted ^{1}H-nuclear magnetic resonance (NMR) spectroscopy-based metabolomic profiling studies (325–328). In *M.tb*-infected mice, enhanced lactate concentrations are shown in granulomas (326) and *M.tb*-infected human macrophages and monocytes also display raised intracellular lactate to glucose ratios (325). Lactate is utilised as a carbon substrate for growth of *M.tb* and is also required for intracellular

replication in human macrophages (329). Interestingly, the extracellular matrix metalloproteinase inducer (EMMPRIN), which is an upstream inducer of several MMPs, also regulates expression of the lactate MCTs 1 and 4 (330).

Several studies have described increased aerobic glycolysis in *M.tb*-infected human monocytes and macrophages (154,324,331–335). Extracellular flux analysis confirms *M.tb*-induced metabolic reprogramming from oxidative phosphorylation to aerobic glycolysis in human alveolar macrophages and monocyte-derived macrophages (MDMs) (154), as well as in human monocytes (324). Metabolic rewiring in human macrophages results in enhanced pro-inflammatory IL-1β production and suppression of anti-inflammatory IL-10 (154). This IL-1β-dependent host resistance to *M.tb* infection is associated with eicosanoid production by inducing the *PTGS2* gene, which encodes the cyclooxygenase (COX)-2 enzyme (154). In human monocytes, the increase in aerobic glycolysis is accompanied by enhanced expression of HK2 and PFKB3 (324).

The mechanisms that regulate glycolysis in TB are poorly understood. Glycolysis in *M.tb*-infected macrophages is suppressed by upregulation of microRNA-21 (miR-21) by proliferating mycobacteria (332). This is mediated through targeting of the PFK-M isoform at the committed step of glycolysis, which facilitates bacterial growth by limiting pro-inflammatory mediators, chiefly IL-1β. IFN-γ, which is key for *M.tb* control, inhibits miR-21 expression to augment PFK-M expression and macrophage glycolysis (332). Recent data suggests that the iron chelator desferrioxamine (DFX) enhances glycolysis and boosts immune responses in *M.tb*-infected macrophages via HIF-1α stabilisation (333).

Evidence from a murine model of TB showed that *M.tb* infection induced accumulation of interstitial macrophages (IM) that were distinct from tissue-resident alveolar macrophages (AM) (331). IMs were highly glycolytically active, whereas AMs were reliant on fatty acid oxidation and

fatty acid uptake (331); intracellular *M.tb* can use host fatty acids and cholesterol as nutrients, which confers a metabolic advantage on bacteria in AMs (336). Depletion of interstitial macrophages increases the bacterial burden, while depletion of alveolar macrophages reduces the bacterial burden, suggesting that the latter permit a favourable niche for bacterial growth in the lung (331). Inhibition of glycolysis with 2DG *in vivo* reduces the number of interstitial macrophages, with a corresponding rise in bacterial burden, thereby linking metabolism and cellular function (331). *M.tb*-infected murine bone-marrow derived macrophages (BMDM) treated with 2DG also resulted in enhanced bacterial growth *in vitro*. (331). This is consistent with studies implicating this pathway in controlling intracellular *M.tb* replication, potentially mediated by IL-1β (154,322). In addition, *ex vivo* secretion of TNF-α and IL-1β in response to *M.tb* infection is diminished with 2DG treatment in IMs (331). In another TB granuloma model M1 macrophages promote granuloma formation and bactericidal activity *in vitro*, while M2 macrophages inhibit these effects (337). In TB patients, M2 macrophages predominate in necrotic and non-necrotic granulomas (337).

Finally, the TCA cycle-derived metabolite itaconate has also been detected in the lungs of *M.tb*-infected mice (326). Itaconate inhibits *M.tb* growth *in vitro* (315) and has been shown to protect mice from pulmonary inflammation and lethality following *M.tb* infection (338).

Although there has been considerable recent interest in the role of *M.tb*-induced metabolic rewiring in macrophages and other traditional immune cells, this phenomenon remains understudied in AECs. In addition, the metabolic regulation of MMPs, which are crucial drivers of ECM degradation and tissue damage in TB, has not yet been investigated.

1.5.2 Hypoxia Inducible Factor-1α

HIF-1 is a highly conserved, helix-loop-helix transcription factor which co-ordinates the cellular response to hypoxia. However, more recently, it has been implicated in the regulation of the Warburg effect, infection and inflammation.

HIF-1 forms a heterodimeric complex comprising oxygen-responsive HIF-1α and constitutively expressed HIF-1β subunits (339). In normoxia, HIF-1α is continually hydroxylated by prolyl hydroxylases (PHDs); this allows binding of the von Hippel–Lindau E3 ubiquitin ligase and targets HIF-1α for rapid proteosomal degradation (340). Hence, basal HIF-1α levels are low in resting cells. However, under hypoxic conditions, PHD inhibition results in HIF-1α accumulation and nuclear translocation to bind HIF-1β and form HIF-1 (339). The HIF-1 complex binds to the promoters of target genes containing hypoxia response elements (HREs), leading to transcription of several genes involved in cellular adaptation to hypoxia, metabolism and immunity (341).

1.5.2.1 HIF-1α, the Warburg effect and innate immunity

In addition to its role in hypoxia, HIF-1α also modulates the Warburg effect and the innate immune response in normoxia. HIF-1 stabilisation in normoxia has been demonstrated *in vitro* and *in vivo* with LPS stimulation (296,342–344), as well as Gram-positive bacterial infection (345,346). Mice with myeloid cell-specific HIF-1α deletion show decreased bactericidal activity to Group A *Streptococcus* and *Pseudomonas aeruginosa* and a failure to restrict systemic spread of infection (346). HIF-1α stabilisation is essential for cellular metabolic reprogramming to glycolysis, which in turn regulates myeloid cell infiltration and activation, phagocytosis and bacterial killing (343,345,347).

Several signalling molecules influence HIF-1α stabilisation upon infection, including NF-κB, PKM2, PHDs and iNOS/ROS. IKK-β-responsive NF-κB, a central regulator of the innate immune response, upregulates HIF-1α mRNA transcription; bacteria-infected macrophages or mice subjected to hypoxia show a profound HIF-1α induction defect upon IKK-β deletion (348). In addition to boosting HIF-1α, NF-κB can modulate the expression of cytokines, chemokines and antimicrobial peptides and enhance glycolysis, facilitating a co-ordinated host defence response (348). This reflects a close, synergistic relationship between hypoxia and innate host defence (349). Enhanced HIF-1α expression is also associated with pyruvate kinase M2 (PKM2), an enzyme that catalyses the final step of glycolysis. In LPS-activated of macrophages, PKM2 dimers stabilise HIF-1α, upregulating glycolysis and IL-1β production and reprogramming macrophages to an M1 phenotype (350). PHD3 has been shown to increase glucose uptake and lactate production by facilitating the binding of PKM2 to HIF-1α, which activates HIF-1α-mediated gene expression (351). LPS-induced succinate, a TCA cycle intermediate, inhibits PHDs to stabilise HIF-1α and induce IL-1β in macrophages (296). HIF-1α stabilisation also depends on iNOS (352) and ROS (353).

1.5.2.2 HIF-1α in TB

Recent studies suggest that HIF-1α regulates the Warburg effect and host defence in *M.tb* infection. Transcriptomic profiling shows upregulation of genes involved in both the Warburg effect and HIF-1α regulation in murine and rabbit models of pulmonary TB, as well as in TB patients (322,323,354). Macrophages from *M.tb*-infected murine lungs show increased levels of HIF-1α mRNA and protein (322). HIF-1α co-ordinates metabolic reprogramming to aerobic glycolysis in *M.tb* infection in human macrophages activated by IFN-γ; this enhanced glycolytic flux is crucial for infection control (335). Macrophage activation is amplified by a positive feedback loop between

HIF-1α and aerobic glycolysis (335). Expression of the *Ikbkb*/*IKBKB* and *Pkm2/PKM2* genes is also upregulated in TB (322,323,354), suggesting that NF-κB and PKM2 regulate this process.

Metabolic rewiring via HIF-1α may constitute a bioenergetic requirement to mount effective host antimicrobial and immune responses to *M.tb* infection (299). This is consistent with data that, in early *M. marinum* infection in zebrafish, pharmacological and genetic stabilisation of HIF-1α is associated with reduced bacterial burden (355). HIF-1α-deficient mice have increased susceptibility to *M.tb* infection and exhibit defective production of inflammatory cytokines and microbicidal effectors (335). It has been postulated that HIF-1α performs a dual role in TB, with an early protective function and a later detrimental effect (356). The HIF-1α-mediated Warburg effect likely contributes to protective immune responses at the site of infection early in disease but may lead to detrimental necrosis and pathology during a prolonged infection (356).

HIF-1α also regulates MMPs in TB. Pulmonary lesions are severely hypoxic in TB patients (259). In human TB lung biopsies, macrophages within TB granulomas are immunoreactive for HIF-1α (259). Hypoxia synergistically upregulates HIF-1α-dependent MMP-1 gene expression and secretion in TB *in vitro* (259). However, *M.tb* can also stabilise HIF-1α in normoxia in human macrophages and AECs to drive MMP-1 upregulation (259). However, the immunopathological association between glucose metabolism, HIF-1α and MMP-induced tissue destruction in TB is not well understood.

1.5.3 AMP-activated protein kinase

AMPK, a master metabolic regulator, plays a fundamental role in energy homeostasis in response to metabolic, infectious or inflammatory stress (357).

AMPK is a serine-threonine (Ser/Thr) protein kinase, existing in eukaryotic cells in the form of a heterotrimeric complex comprising a catalytic α-subunit and regulatory β and γ subunits (Hardie and Alessi, 2013). Phosphorylation of a conserved threonine residue Thr 172 on the α-subunit by the protein kinase LKB1 results in AMPK activation. Binding of cellular adenosine triphosphate (ATP) (which signifies adequate energy status) to the γ subunit reduces Thr 172 phosphorylation, whereas binding of adenosine diphosphate (ADP) or AMP (which signifies impaired energy status) increases Thr 172 phosphorylation to enhance AMPK activity (358). Following activation, AMPK attempts to restore energy homeostasis by promoting catabolic pathways, such as fatty acid β-oxidation, mitochondrial OXPHOS, mitochondrial biogenesis and autophagy and inhibiting anabolic pathways such as gluconeogenesis (358).

AMPK is considered to be an essential regulator of immunometabolism in innate immune cells and its activation drives an anti-inflammatory M2 macrophage profile (359). AMPK can also inhibit NF-κB signalling (357); in addition, macrophages and dendritic cells from AMPKα1 knockout mice increase production of the pro-inflammatory cytokines TNF-α and IL-6 and reduce production of IL-10 in response to LPS (360).

Emerging data suggests that AMPK is a crucial modulator of metabolic reprogramming and inflammation in *M.tb* infection (357). AMPK activation enhances mitochondrial biogenesis via peroxisome, proliferator-activated receptor-γ co-activator (PGC)-1α, which is a regulator of *M.tb* antimicrobial immune defence and phagosomal maturation (361). AMPK and sirtuin 1 (SIRT1) activation also upregulate estrogen-related receptor (ERR)-α, which mediates autophagy and innate antimicrobial defence in *M.tb* infection (362). AMPK promotes the induction and maturation of autophagy in response to infection and activates the transcriptional factor transcription factor EB (TFEB), which targets specific signalling modules for lysosomal function and fatty acid β-oxidation (106). The activation of peroxisome proliferator-activated receptor (PPAR)-α, which

interacts with AMPK during metabolism (363), enhances TFEB-mediated lysosomal biogenesis and function, as well as host responses against *M.tb* (101). The GTPase IRGM, an autophagy protein, is crucial for phagosomal maturation and *M.tb* killing in macrophages; IGRM-mediated stabilisation of AMPK preserves the autophagy-initiating kinase ULK1 and has been implicated in innate immunity (364).

Diabetes mellitus increases TB susceptibility (365) and worsens TB outcome (366). Metformin, the AMPK-activating antidiabetic drug, has attracted interest as an adjunctive treatment for TB and may improve clinical outcomes. In TB patients, adjunctive metformin therapy has been associated with lower TB mortality rates (367,368), increased treatment success and decreased relapse rates (369) and enhanced sputum culture conversion (369,370). In human TB studies *in vitro* and *in vivo*, metformin upregulates glycolysis and downregulates OXPHOS; decreases pro-inflammatory cytokine production and mTOR signalling; and enhances phagocytosis and ROS production (371). In a murine model of TB, metformin treatment also decreases lung bacillary load, ameliorates inflammation and tissue destruction and enhances the efficacy of conventional antituberculous drugs (367). However, another murine study of adjunctive metformin showed no significant effect on *M.tb* bacillary burden, though a different murine model and antituberculous regimen was used (372).

AMPK can also induce MMP-8 secretion in *M.tb*-infected human neutrophils to drive innate-immune mediated matrix destruction and cavitation (255) In human TB lung specimens, AMPKα is phosphorylated within the nuclei of neutrophils in pulmonary cavities, indicating a state of energy depletion (373).

Hence, AMPK is likely to have complex and divergent effects in TB, meriting further investigation into its immunoregulatory role.

1.5.4 The Pi3-kinase-Akt-mTOR pathway

The Pi3-kinase-Akt-mTORC1 pathway is an important signal transduction pathway that regulates core cellular processes such as proliferation, apoptosis, cell morphology and migration, protein synthesis, and metabolism (374).

Pi3-kinase is a family of lipid kinases that phosphorylates the 3-hydroxyl group of the inositol ring of phosphatidylinositol. Class 1 Pi3-kinases comprise 2 domains: a p110 catalytic domain and a p85 regulatory domain. Pi3-kinase binds to phosphorylated tyrosines on a range of receptor tyrosine kinases, leading to activation. Pi3-kinase catalyses the phosphorylation of the membrane lipid phosphatidylinositol-4,5-bisphosphonate (PIP2) to phosphatidylinositol-3,4,5-trisphosphonate (PIP3); this reaction is inhibited by the lipid phosphatase and tensin homologue (PTEN). PIP3 activates the phosphoinositide-dependent kinase PDK1, which phosphorylates threonine 308 to activate Akt. Akt is a family of 3 closely related serine-threonine protein kinases that are crucial to multiple cellular processes, including proliferation, apoptosis, differentiation and metabolism.

mTOR is a key downstream target of Akt can be activated via growth factors, TLR ligands or cytokines. It exists in 2 distinct complexes: mTORC1 and mTORC2. mTORC1 regulates protein synthesis and cellular metabolism through 2 major substrates: p70 ribosomal protein S6-kinase ($p70^{S6K}$) and eukaryotic initiation factor 4E binding protein 1 (EIF4EBP1). The mTORC2 complex phosphorylates Akt on serine 473 upstream, which is essential for Akt activation. The control of cellular energy metabolism by mTORC1 is central to innate effector responses. mTORC1 mediates metabolic reprogramming towards aerobic glycolysis via HIF-1a and MYC, which increases glucose influx by promoting expression and surface translocation of glucose transporter 1 (GLUT1) and increased expression of glycolytic genes (374). mTORC1-dependent induction of

glycolysis is also critical for activation of the NLRP3 inflammasome and maturation of pro-IL-1b in macrophages (375).

M.tb infection of monocytes and macrophages induces strong activation of the mTORC1/p70^{S6K} and Akt signalling cascades via TLR2 to modulate host autophagy and metabolism (324,361,376). These pathways play an essential role in the HIF-1a-mediated immunometabolic shift to the Warburg effect in immune cells following *M.tb* infection (324). mTOR upregulation of PKM2 expression is also crucial to this process (377).

The role of the Pi3-kinase-Akt-mTORC1 pathway in the control of MMP gene expression and secretion in TB appears to be complex and MMP- and cell-specific (248,258). Chemical inhibition of the proximal catalytic Pi3-kinase p110α subunit augments MMP-1 and -9 in a dose-dependent manner, but suppresses MMP-3 in CoMTB-stimulated human bronchial epithelial cells (248). However, blockade of p70^{S6K} by rapamycin reduces MMP-1 and -3 secretion (248). In *M.tb*-infected macrophages, the Pi3-kinase-Akt-mTORC1 pathway exerts a negative regulatory effect on MMP-1 gene expression and secretion and pro-inflammatory cytokine profiling; in addition, cross-talk between the Pi3-kinase and MAPK-interacting kinase (MNK) pathways occurs at the level of eIF4e phosphorylation (258). Pi3-kinaseδ expression is suppressed within infected granulomas in TB patients (258). However, the effects of the PI3-kinase-Akt-mTORC1 pathway on functional matrix destruction in TB have not yet been ascertained.

Hence, in summary, the balance of the reciprocal interactions between AMPK and mTORC1 is a crucial axis for the immunometabolic modulation of cellular innate host defence (357). AMPK can inhibit mTORC1 by phosphorylating tuberous sclerosis complex (TSC) 2 and regulatory-associated protein of mTORC1 (RAPTOR), while AMPK suppresses mTORC1 activation through p70^{S6K}-mediated inhibition of TAK1 (374). In the early phase of infection, mTORC1 activation leads to the immunometabolic shift to M1 macrophages that stimulates aerobic glycolysis, pro-

inflammatory cytokines and *de novo* lipid synthesis through the HIF-1α and NF-kB pathways. In the later stage, AMPK senses the energy status of the inflammatory cells and its activation drives catabolic processes and enhances mitochondrial OXPHOS to generate M2 macrophages. AMPK also increases PGC1a and ERRa activity to promote autophagy regulation and increases fatty acid oxidation. Although the mTORC1-HIF-1α pathway is essential for initial control of *M.tb* growth, excessive induction of inflammation appears to be harmful to the host; similarly, prolonged AMPK activation may result in immunosuppression that is detrimental to the control of *M.tb* infection (259,361).

1.5.5 Summary

These interdependent intracellular pathways in TB are shown in a simplified diagram in Figure 5. The regulation of tissue destruction and pulmonary cavitation in TB by these intricate metabolic signalling networks is not yet well characterised. Hence, greater understanding of the immunometabolic switch points in TB pathogenesis is essential to further the development of novel therapeutic options in TB.

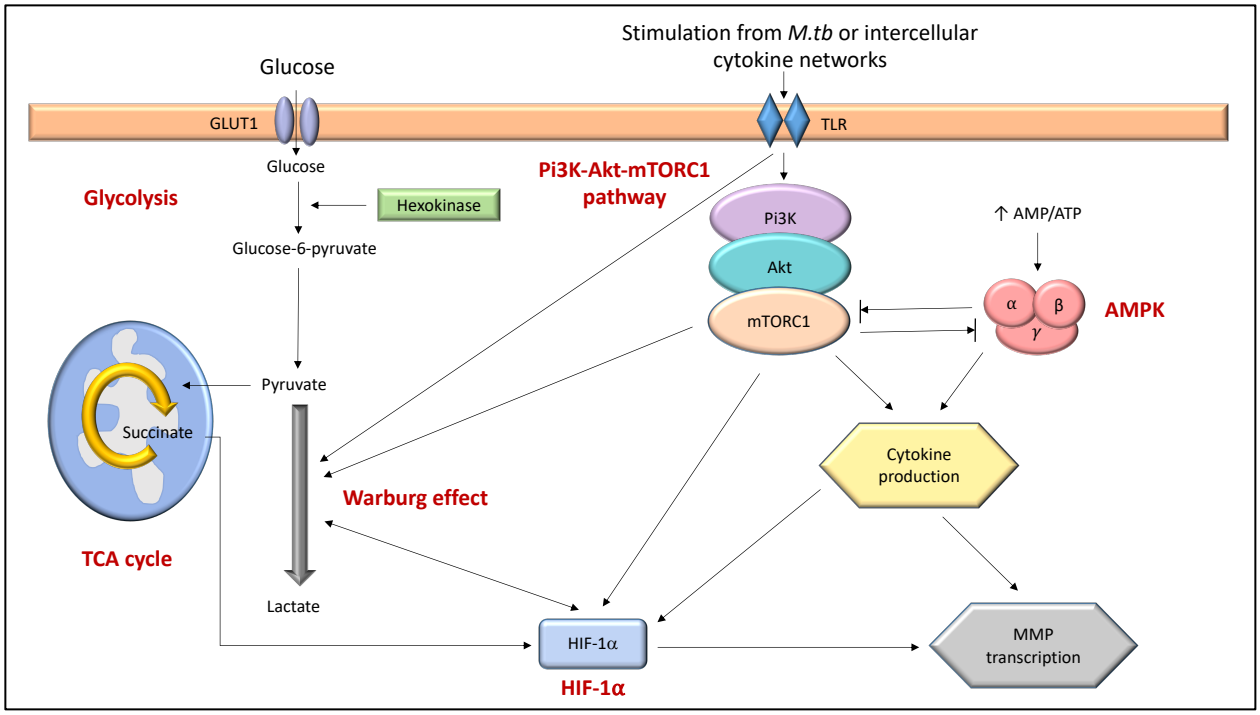


Figure 5: Simplified schematic representation of metabolic signalling pathways in TB

1.6 Hypothesis and aims

1.6.1 Hypothesis

My hypothesis is that metabolic pathways regulate the gene expression and secretion of MMPs to drive immunopathology in TB.

1.6.2 Aims

In Chapter 3, I aim to investigate:

1. The presence of the key glycolytic enzyme, HK2, in the tissue of human lymph node TB.

2. The interaction between cellular glucose metabolism and MMP gene expression and secretion in macrophages in TB.
3. The role of HIF-1α, intracellular AMPK and the Pi3-kinase-Akt-mTORC1 pathways in the regulation of MMPs in macrophages in TB.
4. Cytokine regulation by metabolic pathways in macrophages in TB.

In Chapter 4, I aim to investigate:

1. The presence of the key glycolytic enzyme, HK2, in the tissue of murine pulmonary TB.
2. The interaction between cellular glucose metabolism, MMP gene expression and secretion and functional tissue destruction in AECs in TB.
3. The role of HIF-1α, intracellular AMPK and the Pi3-kinase-Akt-mTORC1 pathways in the regulation of MMPs in AECs in TB.

Chapter 2: Materials and methods

2.1 *M.tb* culture

Mycobacterium tuberculosis (*M.tb*) H37Rv Pasteur was defrosted from stock stored in 30-50% v/v glycerol at -80ºC. It was cultured in Middlebrook 7H9 medium (BD Diagnostics, UK) supplemented with 10% v/v ADC enrichment medium (BD Diagnostics, UK), 0.2% v/v glycerol (Sigma Aldrich, UK) and 0.02% v/v Tween 80 (Sigma Aldrich, UK) at 37ºC, with circular agitation at 10 rotations per minute (rpm). Subculture was performed when the optical density (OD) reached 1.0, as measured by a Biowave Cell Density meter (WPA, UK). For cell culture experiments, *M.tb* was grown to mid-log phase, corresponding to an OD of 0.6, then used at predetermined volumes representing a multiplicity of infection (MOI) of 1. Equivalent volumes of Middlebrook 7H9 medium were used as controls.

2.2 Monocyte and macrophage culture

Peripheral blood mononuclear cells (PBMC) were isolated from single-donor buffy coats (National Blood Transfusion Service, Colindale, UK) by density gradient centrifugation and adhesion purification. Leucocytes were diluted 1:2 with Hanks Balanced Salt Solution (HBSS) (Gibco, UK), layered on Histopaque (Sigma Aldrich, UK) and centrifuged at 500g for 30 minutes. The PBMC layer between the 2 phases was aspirated, diluted with HBSS to 50ml and centrifuged at 300g for 5 minutes. HBSS was discarded and the PBMC pellet resuspended in 50ml of fresh HBSS and centrifuged again; this process was repeated for a total of 5 washes. After the 4^{th} wash, the total number of monocytes was counted in the PBMC fraction, following adhesion to a haemocytometer slide incubated for 5 minutes at 37°C / 5% v/v CO_2. After the 5^{th} wash, PBMCs were resuspended in RPMI 1640 medium (Life Technologies, UK) supplemented with 2mM glutamine (Sigma Aldrich, UK) and 10µg/ml ampicillin (Sigma Aldrich, UK) and seeded at 2.5 x 10^5 monocytes / cm^2.

The cell culture plates were incubated for 1 hour at 37°C / 5% v/v CO_2; non-adherent cells were removed by washing 3 times with HBSS.

Monocyte-derived macrophages (MDMs) were generated by culturing monocytes in RPMI 1640 medium supplemented with 2mM glutamine, 10µg/ml ampicillin, 10% v/v heat-inactivated foetal calf serum (FCS) (Labtech, UK) and 100ng/ml macrophage colony stimulating factor (M-CSF) (Invitrogen, UK) for 4 days at 37°C / 5% v/v CO_2. Macrophages were washed in HBSS to remove non-adherent cells, then cultured in fresh RPMI 1640 with 2mM glutamine, 10µg/ml ampicillin and 10% v/v FCS for a further 24 hours at 37°C / 5% v/v CO_2. The medium was changed to macrophage serum-free medium (M-SFM) (Gibco, Life Technologies, UK) at the start of the experiment.

2.3 Sterilisation of cell culture supernatants

M.tb-infected MDM culture supernatants required removal of *M.tb* by sterile filtration before safe analysis outside the Category 3 facility. Supernatants were transferred to 0.22µm Durapore PVDF centrifugal filter units (Merck Millipore, UK), which remove *M.tb* without MMP binding (378), and centrifuged at 12,000g for 1 minute before storage at -20°C.

2.4 Conditioned medium from *M.tb*-infected monocytes

Conditioned medium from *M.tb*-infected monocytes (CoMTB) and uninfected monocytes (ConCont) were used to assess intercellular network interactions. PBMC isolation was performed as described in 5.3 and the cells were seeded at 2.5 x 10^5 monocytes / cm^2 in 60mm petri dishes. After washing with HBSS to remove non-adherent cells, fresh RPMI 1640 supplemented with 2mM glutamine and 10µg/ml ampicillin was added. Monocytes were infected with *M.tb* H37Rv at

an MOI of 1 to generate CoMTB, or with 7H9 medium for ConCont, then then incubated for 24 hours at 37°C / 5% v/v CO_2. Supernatants were collected, filtered through an Whatman Anotop 25 0.2μM polypropylene filter (GE Healthcare, UK) to remove both *M.tb* and MMPs (378), aliquoted and stored at -20^{0}C. The constituents of CoMTB are listed in Table 2. Each batch of CoMTB and ConCont was tested by stimulation of normal human bronchial epithelial cells (NHBEs), with measurement of MMP-1 secretion after 72 hours (Figure 6). Previously tested CoMTB was used as a positive control; CoMTB that elicited significant MMP-1 secretion in NHBEs comparable to the positive control was used in cell culture experiments in a 1:5 concentration with culture medium. Effective CoMTB upregulated MMP-1 secretion at least 2-fold compared to ConCont.

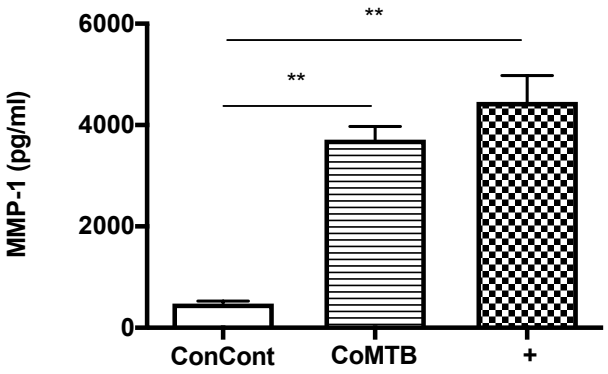


Figure 6: Testing the effectiveness of conditioned medium from *M.tb*-infected monocytes (CoMTB).

Secreted MMP-1 concentrations from NHBEs stimulated with ConCont or CoMTB were measured by ELISA. Previously tested CoMTB served as a positive control (+). Bars show mean ± SD. Statistical analysis was performed using an ordinary one-way ANOVA with Tukey's post-test correction. **p<0.01

Cytokines	Chemokines	Growth Factors
IL-1β	CCL2 (MCP-1)	GM-CSF
TNF-α	CCL3 (MIP-1α)	G-CSF
IL-6	CCL4 (MIP-1β)	VEGF
IL-12	CXCL8 (IL-8)	FGF
IFN-α	CXCL9 (MIG)	
IL-1 receptor antagonist		
IL-2 receptor		

Table 2: Components of conditioned medium from *M.tb*-infected monocytes (CoMTB). Adapted from Sathyamoorthy, 2013 (245).

2.5 *M.tb* killing

MDM killing of *M.tb* was measured using colony forming units (CFU) on Middlebrook 7H11 agar, supplemented with 10% v/v OADC enrichment medium (BD Diagnostics, UK) and 0.2% v/v glycerol. MDMs were cultured in M-SFM in 12-well plates and infected with *M.tb* at MOI 1. After 24 hours, supernatants were discarded and adherent MDMs washed with phosphate buffered saline (PBS), before lysis in 500µl sterile water. Cell lysates were diluted further in sterile water and plated in duplicate on 7H11 agar. Plates were incubated for 2 to 4 weeks at 37ºC / 5% v/v CO_2, then individual colonies counted to assess the number of colony forming units (CFU).

2.6 Normal human bronchial epithelial cell culture

Cryopreserved primary normal human bronchial epithelial cells (NHBEs) (Lonza, Switzerland) were selected from non-smokers with no co-morbidities. NHBEs were cultured in bronchial epithelial growth medium (BEGM), with added growth factors and supplements as per manufacturer's instructions (Lonza, Switzerland). The cells were subcultured at 70-80% confluence; adherent cells were detached with Trypsin-EDTA (Lonza, Switzerland) for 2 minutes, then neutralised with Trypsin Neutralizing Solution (Lonza, Switzerland). After 3 passages, the cells were resuspended in 10% v/v DMSO (Sigma Aldrich, UK) / 90% v/v FCS (Labtech, UK) and cryopreserved in liquid nitrogen. For experiments, performed at passage 4, the cells were defrosted, resuspended in BEGM, seeded at 50,000 cells/cm2 and rested for 24 hours at 37°C / 5% v/v CO_2.

2.7 ELISA

Concentrations of MMP-1 and -9, TIMP-1 and -2, IL-1β, TNF-α, IL-6 and IL-10 in cell supernatants were measured by Duoset ELISA Development System (R&D Systems, UK) according to the manufacturer's protocol. 96-well ELISA plates (Costar, Sigma Aldrich, UK) were coated with 100µl of primary (capture) antibody overnight at room temperature, them washed 3 times with PBS / 0.05% v/v Tween. Free binding sites were saturated with PBS / 1% w/v BSA for 1 hour at room temperature. A standard curve was produced with 1 in 2 serial dilutions. The ELISA plate was loaded with standards and samples in the appropriate wells and incubated for 2 hours at room temperature. 3 washes were performed, then 100µl of secondary (detection) antibody was added per well for 2 hours at room temperature. Following another 3 washes, each well was incubated with 100µl streptavidin-HRP and protected from light for 20 minutes. After a final 3 washes, 100µl

tetramethylbenzidine (TMB) (Sigma Aldrich, UK) substrate solution was added to each well to stimulate colour change; the reaction was terminated with 50µl per well of 2M sulphuric acid. The plate was read at an absorbance of 450nm with a reference wavelength of 540 nm on a colorimetric µQuant microplate reader (BioTek Instruments Inc, UK). Table 3 shows the ranges of the standard, capture and detection antibody concentrations for the proteins analysed.

Protein	1st standard (pg/ml)	1° (capture) antibody(µg/ml)	2° (detection) antibody (ng/ml)
MMP-1	10000	2	50
MMP-9	2000	1	150
TIMP-1	2000	2	50
TIMP-2	2000	2	12.5
IL-1β	250	4	150
TNF-α	1000	4	250
IL-6	600	2	50
IL-10	2000	2	50

Table 3: Specifications of ELISA antibodies

2.8 Gelatin zymography

Gelatin zymography was performed to assess the amount of functionally active MMP-9 in samples. Cell culture medium was diluted 1:50 in RPMI. 20µl aliquots with 5x loading buffer,

comprising 0.25M Tris (pH 6.8), 50% v/v glycerol, 5% w/v SDS and 0.01% w/v Bromophenol blue, were electrophoresed on 11% acrylamide gels impregnated with 0.1% gelatin at 180V for 3.5 hours. Gels were incubated in 2.5% v/v Triton X for 1 hour with agitation and washed twice in collagenase buffer, consisting of 55mM Tris, 200mM sodium chloride, 5mM calcium chloride and 0.02% w/v Brij 35 (pH 7.6). Gels were then incubated overnight in collagenase buffer at 37ºC. Gelatinolytic activity was detected by a single step stain and destain method with 0.02% w/v Coomassie Brilliant Blue in 1:3:6 acetic acid:methanol:water. Samples were run in parallel with 2ng recombinant human MMP-9 standards (Calbiochem, Merck Biosciences, UK). Densitometric analysis was performed by digital image acquisition (UVP) with subsequent proteolytic band quantification with NIH image version 1.61.

2.9 Western blotting

Protein expression was assessed by Western blotting. NHBEs or MDMs were washed with sterile PBS (GE Healthcare, UK) and lysed in 300μl sodium dodecyl sulfate (SDS) sample buffer, comprising 62.5mM Tris (pH 6.8), 2% w/v SDS, 50mM dithiothreitol (DTT), 10% v/v glycerol, and 0.01% w/v Bromophenol blue, at defined time points. The lysed cells were aliquoted and stored at -80°C. For analysis of protein expression, samples were defrosted and heat-denatured at 70ºC for 10 minutes, then centrifuged for 1 minute prior to loading onto a NuPAGE Novex 10% Bis-Tris protein gel (Life Technologies, UK). Proteins were then separated by electrophoresis at 200 volts (V) for 50 minutes using the Sure-Lock MiniCell system (Life Technologies, UK), with MES running buffer for small proteins <60kDA and MOPS running buffer for large proteins >60kDA (Life Technologies, UK). 500µl NuPAGE Antioxidant (Life Technologies, UK) was added to the cassette. Full range recombinant Amersham™ ECL™ Rainbow™ molecular weight markers (Sigma Aldrich, UK) were run concurrently to assess protein size. Proteins were then electro-

transferred to a nitrocellulose membrane (Amersham Biosciences, UK) at 30V for 90 minutes using an X-Cell Blot Module (Life Technologies, UK) with transfer buffer (Life Technologies, UK). The membrane was washed 3 times with wash buffer composed of 0.1% v/v Tween-20 (Sigma Aldrich, UK) in Tris buffered saline. The membrane was subsequently blocked for 1 hour in blocking buffer comprising 5% w/v dry milk protein (Marvel, Premier Foods Group Ltd, UK) dissolved in wash buffer. Following another triple wash, the membrane was probed with primary antibody overnight at 4°C. The next day, the membrane was washed 3 times and incubated with HRP-linked anti-rabbit secondary antibody or HRP-linked anti-mouse secondary antibody (both Sigma Aldrich, UK) for 1 hour, followed by a further 3 washes. Chemiluminescence was then detected with Luminata Classico or Crescendo substrate (Merck Millipore, UK) for 1 minute. The blot was then imaged using the Chemidoc Touch Imaging System (BioRad Laboratories, UK). Image Lab version 6.1 was used for post-acquisition image processing. Table 4 shows the antibodies used and their dilutions.

Western blot antibody	1° or 2°	Dilution	Manufacturer (Catalogue number)
Anti-hexokinase II rabbit monoclonal	1°	1:1000	Cell Signaling Technology, Netherlands (2867)
Anti-HIF-1α rabbit monoclonal	1°	1:1000	Abcam, UK (ab51608)
Anti-PFKFB3 rabbit monoclonal	1°	1:1000	Cell Signaling Technology, Netherlands (13123)
Anti-GLUT1 rabbit polyclonal	1°	1:1000	Abcam, UK (ab15309)
Phospho-/total-AMPKα rabbit polyclonal	1°	1:1000	Cell Signaling Technology, Netherlands (2531/2532)
Phospho-/total-mTOR rabbit monoclonal	1°	1:1000	Cell Signaling Technology, Netherlands (5536/2983)
Phospho-/total Akt rabbit monoclonal	1°	1:000	Cell Signaling Technology, Netherlands (4058/9272)
Phospho-/total-p70 S6 kinase rabbit monoclonal	1°	1:1000	Cell Signaling Technology, Netherlands (9234/2708)
Anti-PHD1 rabbit monoclonal	1°	1:1000	Abcam, UK (ab108980)
Anti-β-actin mouse monoclonal	1°	1:10000	Sigma Aldrich, UK (A2228)
Goat anti-rabbit IgG HRP-linked conjugate	2°	1:1000	Cell Signaling Technology, Netherlands (7074S)
Goat anti-mouse IgG HRP-linked conjugate	2°	1:10000	Sigma Aldrich, UK (12-349)

Table 4: Western blot antibodies and dilutions

2.10 Chemical reagents

The chemical inhibitors and activators used in this project and their targets are listed in Table 5. NHBEs or MDMs were incubated with these metabolic inhibitors or activators at a range of concentrations for 2 or 1 hours respectively, before stimulation with CoMTB or infection with *M.tb*. Cell viability was assessed using a LDH cytotoxicity assay.

Reagent	Target action	Manufacturer
2-deoxyglucose (2DG)	Glycolysis (HK) inhibition	Sigma Aldrich, UK
Diethylsuccinate	Cell-permeable TCA cycle intermediate succinate	Sigma Aldrich, UK
Compound C	AMPK inhibition	Sigma Aldrich, UK
Metformin	AMPK activation	Sigma Aldrich, UK
LY94002	Pi3-kinase p110 subunit inhibition	Sigma Aldrich, UK
VIII	Akt inhibition	Sigma Aldrich, UK
Rapamycin	mTORC1 inhibition	Sigma Aldrich, UK
Tepp-46	PKM2 activation	Sigma Aldrich, UK
Shikonin	PKM2 inhibition	Cayman Chemical, USA
Octyl α-ketoglutarate	Cell-permeable TCA cycle intermediate α-ketoglutarate	Cayman Chemical, USA
Sodium oxamate	Glycolysis (LDH) inhibition	Sigma Aldrich, UK

Table 5: Chemical metabolic inhibitors and activators

2.11 Lactate dehydrogenase assay

Cell cytotoxicity was measured using an LDH Assay Activity Kit (Sigma Aldrich, UK), as per manufacturer's instructions. To prepare the reaction mixture, 2.5μl of reconstituted catalysis solution was mixed with 112.5μl dye solution for each sample. 100μl of controls or cell culture supernatants were pipetted into a 96-well plate. 100μl of the reaction mixture was added to each well and incubated in the dark for 5-30 minutes at room temperature. 50μl of stop solution was added to each well to terminate the reaction and the plate agitated for 10 seconds. The assay was read at 490 or 492nm, with a reference wavelength over 600nm on a colorimetric μQuant microplate reader (BioTek Instruments Inc, UK). The background control was experimental medium, which was subtracted from all readings. The low control was supernatant of untreated normal cells and the high control was supernatant of cells killed with lysis solution. Cytotoxicity was calculated as a percentage using the equation:

$$Cytotoxicity\ (\%) = \frac{Expected\ value - Low\ control}{High\ control - Low\ control}\ x\ 100$$

2.12 RNA extraction, cDNA synthesis and RT-PCR

Cultured NHBEs or MDMs were washed with PBS and lysed with Tri-Reagent® RNA isolation reagent (Sigma Aldrich, UK).

RNA extraction was performed by spin purification using the Direct-zol™ RNA Miniprep Kit (ZymoResearch, USA) as per manufacturer's instructions. Cell lysates were mixed with equal volumes of 100% ethanol and vortexed to mix. This mixture was transferred to ZymoSpin™ columns and centrifuged for 1 minute. The column was washed twice with 400μl of RNA pre-wash

and once with 700μl of RNA wash buffer. The column was then centrifuged for 1 minute to dry the membrane. Finally, RNA was eluted with 30μl of DNAase/RNAase-free water and stored at -80°C. The amount and purity of the resulting RNA was quantified by spectrophotometry (Nanodrop ND 1000, ThermoScientific, UK).

cDNA was synthesized from RNA using the Quantitect® Reverse Transcription Kit (Qiagen, UK). For each sample, 500ng RNA was diluted up to 12μl with DNAase/RNAase-free water. 2μl of gDNA wipeout buffer was added, prior to heating at 42°C for 2 minutes. 6μl of reverse transcription mastermix, comprising 1μl Quantiscript® reverse transcriptase, 1μl random primers and 4μl Quantiscript® RT buffer 5x, was made up and added. The samples were heated at 42°C for 15 minutes to facilitate primer annealing and strand extension, before heating at 95°C for 3 minutes to stop the reaction. Synthesised cDNA was stored at -20ºC.

Real-time polymerase chain reaction (RT-PCR) was performed in a low-profile plate (ThermoFisher Scientific, UK) on a CFX Connect Real-Time System instrument (Bio-Rad Laboratories, UK). cDNA was diluted and amplified using a mastermix comprising Brilliant II (Agilent Technologies, USA) and the primer and probes for the gene of interest and housekeeping gene. The housekeeping gene used was β-actin for NHBEs and 18S rRNA for MDMs. The RT-PCR thermal profile was 95ºC for 10 minutes, followed by 40 cycles at 95ºC for 30 seconds, then 60ºC for 1 minute. MMP-1 and -9 primer and probes were used at 1μM and the sequences are shown in Table 6.

MMP-1 and -9 copy numbers were calculated using plasmid standards, kindly synthesised by Dr Catherine Ong (379). Serial dilutions were performed to generate a standard curve with a known number of gene copies. The cycle threshold for the gene of interest and housekeeping gene was extrapolated from the standard curve to give an amount and the gene of interest normalised to

the housekeeping gene. There was no plasmid standard available for HK2, hence the delta-delta-CT (Pfaffl) method (380) was used for comparison by applying the equation:

$$Gene\ expression\ ratio\ = \frac{(E_{GOI})^{\Delta Ct\ GOI}}{(E_{HKG})^{\Delta Ct\ HKG}}$$

where E = primer efficiency, GOI = gene of interest, HKG = housekeeping gene and Ct = cycle threshold.

PCR data was presented as fold changes. The mean of each loading triplicate was calculated and normalised to the mean of the unstimulated control sample to generate fold changes.

MMP-1 (Sigma Aldrich, UK)	
Forward primer	5'-AAGATGAAAGGTGGACCAACAATT-3'
Reverse primer	5'-CCAAGAGAATGGCCGAGTTC-3'
Probe	5'-FAM-CAGAGAGTACAACTTACATGCTGTTGCGGCTC-TAMRA-3'
MMP-9 (Sigma Aldrich, UK)	
Forward primer	5'-AGGCGCTCATGTACCCTATGT-3'
Reverse primer	5'-GCCGTGGCTCAGGTTCA-3'
Probe	5'-FAM-CATCCGGCACCTCTATGGTCCTCG-TAMRA-3'
Hexokinase 2 (Applied Biosystems, UK)	
20x mix	
β-actin/18S Housekeeping (Applied Biosystems, UK)	
20x mix	

Table 6: RT-PCR primers and probes

2.13 Luminex

Luminex® bead-based multiplex immunoassay allows simultaneous profiling of several target analytes in small volumes of a sample. Colour-coded beads are pre-coated with analyte-specific capture antibodies which bind to the analytes of interest. Luminex panels were used to quantify multiple MMPs (MMP-1, -2, -3, -7, -8, -9 and -10) and cytokines (IL-1β, IL-2, IL-4, IL-5, IL-6, IL-10, TNF-α, GM-CSF, IFN-γ and EMMPRIN) in cell supernatants (R&D Systems, UK), as per manufacturer's instructions. The beads were prepared by adding 17μl of each bead to 5.2ml of diluent in a mixing bottle. 50μl of beads and 50μl of standards or samples per well were pipetted into the Luminex plate and agitated at 500rpm for 2 hours. 50μl of biotinylated secondary antibodies were then added to each well and agitated at 500rpm for 1 hour. Next, 50μl of streptavidin-PE was added per well with agitation for a further 30 minutes to generate a signal. The beads were then resuspended in 100μl of wash buffer per well. The plate was washed 3 times with 100μl of wash buffer between each of these steps, using a magnetic plate washer (Bio-Plex®, Bio-Rad Laboratories, UK). The plate was then read using a dual laser Luminex system (Bio-Plex™200, Bio-Rad Laboratories, UK).

2.14 Lactate assay

Extracellular lactate concentration was measured using a Lactate Assay Kit (Sigma Aldrich, UK), according to manufacturer's instructions. 10μl of Lactate Standard was diluted with 990μl of Lactate Assay Buffer to generate a 1nmole/μl standard solution and 0, 2, 4, 6, 8 and 10μl loaded on a 96-well plate (Costar, Sigma Aldrich, UK) to generate a standard curve. Cell culture supernatant samples were deproteinised with a 10kDA MWCO spin filter (Amicon®Ultra, Merck

Millipore, Ireland) to remove lactate dehydrogenase and 1μl of sample loaded on the plate. Standard and sample wells were made up to 50μl with lactate assay buffer. 50μl of master reaction mix, comprising 46μl lactate assay buffer, 2μl lactate enzyme mix and 2μl lactate probe, was then added to each well. The reaction was protected from light and incubated for 30 minutes at room temperature. Absorbance was measured at 570nm on a colorimetric μQuant microplate reader (BioTek Instruments Inc, UK). Baseline absorbance was subtracted from each reading and the lactate concentration was determined using the equation:

$$S_a/S_v = C$$

where S_a = amount of lactate (nmole) in unknown sample from standard curve, S_v = sample volume (μl) added into the wells and C = concentration.

2.15 RNA interference using siRNA

ON-TARGETplus SMARTPool human HK2 siRNAs (Horizon Discovery, UK) and ON-TARGETplus Non-targeting Control Pool siRNAs (Horizon Discovery, UK) were resuspended in 1x siRNA buffer (ThermoScientific, UK) to a stock concentration of 20μM. The concentration was verified by spectrophotometry (Nanodrop ND 1000, ThermoScientific, UK) and the stock aliquoted and stored at -80°C.

NHBEs were cultured in 12-well plates to 70% confluence and transfected using the Lipofectamine® 2000 transfection reagent (Invitrogen, UK). For each well, 2.5μl of Lipofectamine® 2000 was diluted in 97.5μl of OptiMEM® reduced serum medium (Gibco, Life Technologies, UK). HK2 and non-targeting siRNAs were diluted in OptiMEM® to achieve a final transfection concentration of 25nM per well. For each well to be transfected, 100μl of diluted

Lipofectamine® was mixed with 100µl of diluted siRNA, vortexed for 1 minute, then allowed to complex for 20 minutes at room temperature. 800µl of non-supplemented BEGM and 200µl of the complex were added to each well and the plate incubated for 4 hours at 37°C / 5% v/v CO_2. The cells were washed with sterile PBS and rested overnight in partially-supplemented BEGM at 37°C / 5% v/v CO_2; bovine pituitary extract and epidermal growth factor were omitted from the medium to minimise NHBE division and siRNA dilution.

MDMs were seeded in 12-well plates at a lower density of 105,000 cells/cm^2 to facilitate differentiation and transfected using the DharmaFECT 3 transfection reagent (ThermoScientific, UK). For each well, 5µl DharmaFECT 3 was diluted in 95µl antibiotic- and serum-free RPMI 1640 supplemented with 2mM glutamine. HK2 and non-targeting siRNAs were suspended in siRNA buffer in a 1:5 ratio, then diluted in serum-free RPMI 1640 to achieve a final transfection concentration of 25nM per well. The diluted transfection reagent and siRNA were combined and allowed to complex for 20 minutes at room temperature. 200 µl of this complex was added to each well, along with 800µl of antibiotic-free RPMI 1640 supplemented with 10% v/v heat-inactivated FCS and 2mM glutamine. The plates were incubated for 6-8 hours at 37°C / 5% v/v CO_2, then washed with sterile PBS and rested overnight in antibiotic-free RPMI 1640 at 37°C / 5% v/v CO_2.

Transfection efficiency was assessed by measuring the uptake of 25nM fluorescent (FAM)-labelled siRNA (Dharmacon, UK) by flow cytometry (BD FACSCalibur™, Becton Dickinson, UK). Gene and protein knockdown were confirmed by HK2 qPCR and Western blot respectively. For the experiments, transfected cells were stimulated with CoMTB or infected with *M.tb* for 24 hours prior to qPCR analysis.

2.16 DQ collagen and DQ gelatin matrix degradation assay

Type 1 collagenase and gelatinase activity was assessed using the EnzChek™ Gelatinase/Collagenase Assay Kit (ThermoFisher Scientific, UK) according to the manufacturer's protocol. DQ collagen and DQ gelatin, fluorescein conjugate, were diluted with reaction buffer (RB) to achieve a final working concentration of 25μg/ml. Serial dilutions of *Clostridium* collagenase in RB were used to create a standard curve, with a maximum concentration of 0.5U/ml. Samples were activating by adding 2mM of 4-amino-phenyl mercuric acetate (APMA) and incubating at 37°C / 5% v/v CO_2 for 1 hour. 80μl of 1x RB and 20μl of DQ collagen or DQ gelatin per well were added to black 96-well plates (ThermoFisher Scientific, UK), followed by 100μl of standards or activated samples. The plate was protected from light and incubated at 37°C / 5% v/v CO_2 for 24 or 48 hours, then fluorescence measured on a microplate reader (FLUOstar Omega, BMG Labtech, UK). The increase in fluorescence with DQ collagen and DQ gelatin degradation was proportional to proteolytic enzyme activity. Background fluorescence was subtracted from each reading.

2.17 Live cell confocal microscopy

Type 1 collagenase and gelatinase activity was assessed using the EnzChek™ Gelatinase/Collagenase Assay Kit (ThermoFisher Scientific, UK) according to the manufacturer's protocol. DQ collagen and DQ gelatin, fluorescein conjugate, were diluted with reaction buffer (RB) to achieve a final working concentration of 25μg/ml. 8 well glass chamber μ slides (Ibidi, UK) were pre-coated with DQ collagen or DQ gelatin at 150ng/ml for 2 hours, then washed with PBS. NHBEs were seeded into wells at 25,000/cm^2 and incubated at 37°C / 5% v/v CO_2 for 4 hours to

adhere to the plate. The cells were washed again with PBS and incubated with Cell Tracker™ Deep Red Dye (ThermoFisher Scientific, UK) at a concentration of 10μM for 30 minutes, as per the manufacturer's protocol. Following another wash, the cells were pretreated with the Pi3-kinase inhibitor LY294002 for 2 hours, then stimulated with CoMTB or ConCont just prior to confocal imaging.

Confocal microscopy was performed in the Image Resource Facility, St George's, University of London using a Nikon A1R confocal microscope. Images were acquired using a 20X CFI Plan Apochromat VC objective; a 488nm laser was used for the green fluorescent protein (GFP) channel and a 561nm laser was used to image the Cell Tracker™ Deep Red Dye**.** Emissions were acquired in series on separate GaAsp detectors using a 525/50 and 595/50 bandpass filter for GFP and the Deep Red dye respectively. Laser power and gain for the GFP channel were kept the same across wells and replicates. The prepared 8-well plate was placed in the confocal chamber at 37°C / 5% v/v CO_2 and live-cell time-lapse imaging was performed over a period of 72 hours. Images were obtained every 30 minutes.

2.18 Immunohistochemistry

Paraffin-embedded lung samples from 5 Balb/C *M.tb*-infected mice, harvested 56 days post infection, were a kind gift from Dr Brian Robertson's laboratory at Imperial College London, UK. Paraffin-embedded lymph node biopsy samples from 5 patients with TB lymphadenitis were kindly provided by Dr Daniela Kirwan in our group. These samples were collected in Peru as part of a joint study conducted by Imperial College London, UK, Johns Hopkins University, Baltimore, USA and Universidad Peruana Cayetano Heredia, Lima, Peru (381). The study was approved by the Institutional Ethics Committee of Universidad Peruana Cayetano Heredia, Asociación Benéfica

PRISMA, and local ethics committees. Written informed consent was obtained from all patients for their tissue samples to be stored and used for TB research.

Immunohistochemistry of mouse and human tissue samples was performed by the Image Resource Facility, St George's, University of London. Heat induced antigen retrieval was performed in a microwave using 10mM Tris-HCL buffer at pH 10. HK2 primary antibody (Bio-Techne, UK) incubation was for 12 hours at 4°C using a 1 in 500 dilution. Samples were then incubated with ready to use (RTU) biotinylated goat anti-rabbit IgG secondary antibody (Vector Laboratories, UK) for 30 minutes at room temperature. This was followed by incubation with RTU streptavidin-HRP (Vector Laboratories, UK) detection reagent for 30 minutes at room temperature. Slides were counterstained with Harris haematoxylin (Sigma Aldrich, UK), dehydrated and mounted using DPX mounting medium (Agilent Dako, UK). For each patient slide stained with HK2 primary antibody, a sequential selection from the same patient was stained with a matched IgG isotype control antibody as a control for non-specific staining.

2.19 Statistical analysis

GraphPad Prism 8 (GraphPad Software) was used for data analysis. Multiple intervention experiments were compared by an ordinary one-way Anova followed by a Tukey's post-test correction. Graphs display mean ± standard deviation of 3 technical replicates of a single independent experiment, unless otherwise stated. Each graph is representative of at least 3 independent experiments performed on separate occasions. The response to 7H9 controls or ConCont controls is represented by white bars and the response to *M.tb* infection or CoMTB stimulation by black bars in all graphs, unless otherwise indicated. P values of less than 0.05 were considered statistically significant. Significance was represented on graphs as ns (not significant), *p<0.05, **p<0.01, ***p<0.001 or ****p<0.0001.

Chapter 3: Metabolic pathways regulate MMPs in human TB macrophages

3.1 Introduction

Macrophages are crucial in TB immunopathogenesis as they are often the first cells to encounter and phagocytose *M.tb* following infection. Macrophages have a critical role in pro-inflammatory control of *M.tb* infection and can deploy several immune effector strategies for bacterial eradication, including phagosome-lysosome fusion, apoptosis and autophagy (8). However, *M.tb* can subvert these antimicrobial mechanisms and can, in fact, exploit the host response to allow a favourable niche for persistence (8). Hence, macrophages can also act as a reservoir in TB granulomas and encourage bacterial replication (43).

Macrophage plasticity is, therefore, an important aspect of host inflammatory responses. It has been postulated that the metabolic profile of macrophages can induce differential M1 or M2 polarisation to define their functional phenotype (299,300). Proinflammatory M1 macrophages have enhanced glycolytic metabolism and protect the host; this response is modulated by HIF-1α, mTORC1 and ROS/RNS. M2 macrophages are pro-resolution and survive longer; this response is AMPK-dependent. AMPK and mTORC1 have reciprocal functions and are also both crucial regulators of macrophage innate immune functions (357).

I was interested to explore the role of these signalling pathways in the control of MMP gene expression, secretion and function in TB, in order to determine whether cellular metabolic rewiring was, therefore, a determinant of tissue destruction and pulmonary cavitation in TB.

In this chapter, I performed *in vitro* experiments using representative human MDMs infected with live, virulent *M.tb* H37RV. I first sought to interrogate the role of glycolysis and the TCA cycle intermediate, succinate, in the regulation of MMPs and cytokines in *M.tb*-infected MDMs. I then aimed to assess the effect of glycolysis on *M.tb* modulation of the key transcription factor, HIF-

1α. Next, I aimed to investigate the functional effect of glycolysis on intracellular *M.tb* killing. I then attempted to determine the role of the master metabolic regulator, AMPK, and the key Pi3-kinase-Akt-mTORC1 signal transduction pathway on MMP and cytokine secretion in *M.tb*-infected MDMs. I also aimed to evaluate the effect of AMPK on *M.tb* regulation of HIF-1α and HK2 expression. Finally, I sought to investigate the expression of HK2 in lymph node tissue of patients with TB lymphadenitis.

3.2 Results

3.2.1 Extracellular lactate secretion is upregulated in *M.tb*-infected MDMs

First, I assessed the effect of *M.tb* on macrophage glycolysis *in vitro* in a human MDM cell culture model. Lactate, the final product of aerobic glycolysis, is generated from the reduction of pyruvate by the LDH enzyme. The secreted lactate concentration is an indicator of intracellular glycolytic activity, as lactate removal from the cell is catalysed by MCTs. There was a significant increase in extracellular lactate concentration to 576.3 ± 6.3 ng/μl in *M.tb*-infected MDMs at 24 hours compared to 337.4 ± 30.55 ng/μl from control cells ($p<0.0001$), which was partially abrogated by 2DG, the hexokinase (HK) inhibitor which blocks glycolysis ($p<0.0001$) (Figure 7).

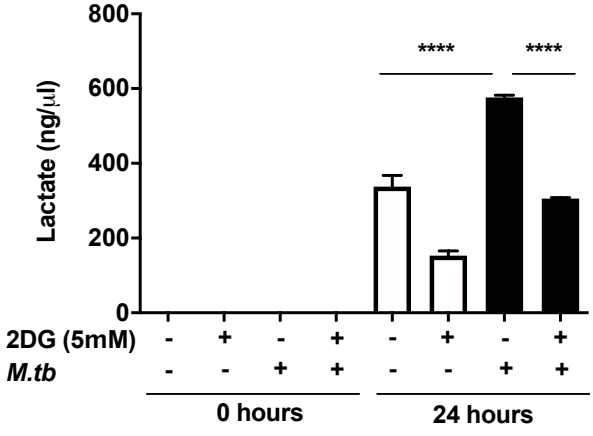


Figure 7: Extracellular lactate secretion is upregulated in *M.tb*-infected MDMs. MDMs were infected with live, virulent *M.tb* H37Rv with or without pre-treatment with 2DG for 1 hour. Supernatants were collected and filtered with a 10kDA MWCO spin filter to remove LDH at 0 and 24 hours. Secreted lactate concentration was significantly upregulated in *M.tb*-infected MDMs at 24 hours and this was partially decreased by 2DG. Bars show mean ± SD of 3 technical replicates of a single independent experiment and are representative of 3 independent experiments. Statistical analysis was performed using an ordinary one-way ANOVA with Tukey's post-test correction. ****$p<0.0001$.

3.2.2 HK2 expression is upregulated in *M.tb*-infected MDMs

In order to analyse the metabolic regulation of MMPs in human MDMs. I first ascertained whether, the *M.tb*-induced extracellular lactate increase was accompanied by an increase in glycolytic enzymes. I performed an RT-PCR analysis and Western blot which confirmed upregulation of gene and protein expression of HK2, an isoform of the first enzyme in glycolysis, in *M.tb*-infected MDMs. There was a significant 8.8-fold upregulation of HK2 mRNA at 24 hours (Figure 8A) compared to controls, while there was increased protein expression of HK2 at 8, 24 and 48 hours (Figure 8B). The phenomenon of an *M.tb*-induced metabolic shift to cellular glycolysis is supported by MDM upregulation of both lactate and HK2 following *M.tb* infection.

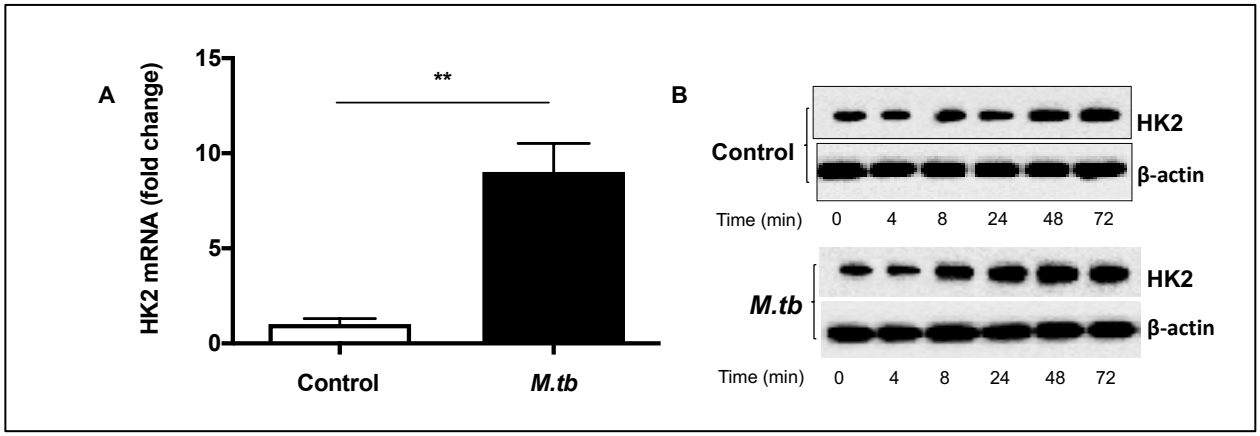


Figure 8: HK2 gene and protein expression are upregulated in *M.tb*-infected MDMs. MDMs were cultured and infected with *M.tb* or 7H9 medium as a control. HK2 was detected by (A) RT-PCR and (B) Western blot. (A) HK2 gene expression was upregulated at 24 hours in *M.tb*-infected MDMs on RT-PCR. Bars show mean ± SD of 3 technical replicates of a single independent experiment and are representative of 2 independent experiments. Statistical analysis was performed using an ordinary one-way ANOVA with Tukey's post-test correction. **p<0.01. (B) HK2 protein expression was upregulated at 8, 24 and 48 hours *M.tb*-infected MDMs on Western blot. The blot image shows a single independent experiment and is representative of 2 independent experiments.

3.2.3 Glycolysis upregulates MMP-1 secretion and gene expression in *M.tb*-infected MDMs

I was then interested in analysing the effect of glycolysis on the gene expression and secretion of the key collagenase, MMP-1 in TB. In order to do so, I used the chemical glycolysis inhibitor 2DG, which blocks HK, the first enzyme in glycolysis. 2DG is a synthetic glucose analogue which is phosphorylated by HK to 2-deoxy-D-glucose-6-phosphate (2-DG-6-P), which cannot be used in subsequent steps of glycolysis. Hence, 2-DG-6-P accumulates intracellularly to cause product inhibition of HK. The doses of 2DG were ascertained by a preliminary dose-response study in MDMs using a wide concentration range. The optimal 2DG doses chosen were those that elicited MMP and cytokine production without evidence of cytotoxicity. MMP-1 secretion from MDMs was upregulated by both direct *M.tb* infection (Figure 9A) and cytokine-dependent network effects (Figure 9B), though the former had a 5-fold more potent effect. Glycolysis inhibition with 2DG then downregulated secretion of the key collagenase, MMP-1, in a dose-dependent manner. There was a 5-fold drop in MMP-1 secretion from 34733 ± 2911 pg/ml in *M.tb*-infected MDMs alone to 6709 ± 876.7 pg/ml in *M.tb*-infected MDMs treated with 2DG ($p \leq 0.0001$) at 24 hours (Figure 9A). Stimulation of MDMs with CoMTB resulted in a similar 4.4-fold decrease in MMP-1 secretion following 2DG treatment (Figure 9B). This was reflected intracellularly at the level of gene expression, with a 4-fold reduction in MMP-1 mRNA with 2DG-induced glycolysis inhibition in *M.tb*-infected MDMs, compared to *M.tb*-infected MDMs alone (Figure 9C). In order to ascertain that these findings were not confounded by MDM cytotoxicity, an LDH release assay was performed. This confirmed that there was no loss of MDM viability with *M.tb* infection or 2DG treatment compared with control cells (Figure 9D).

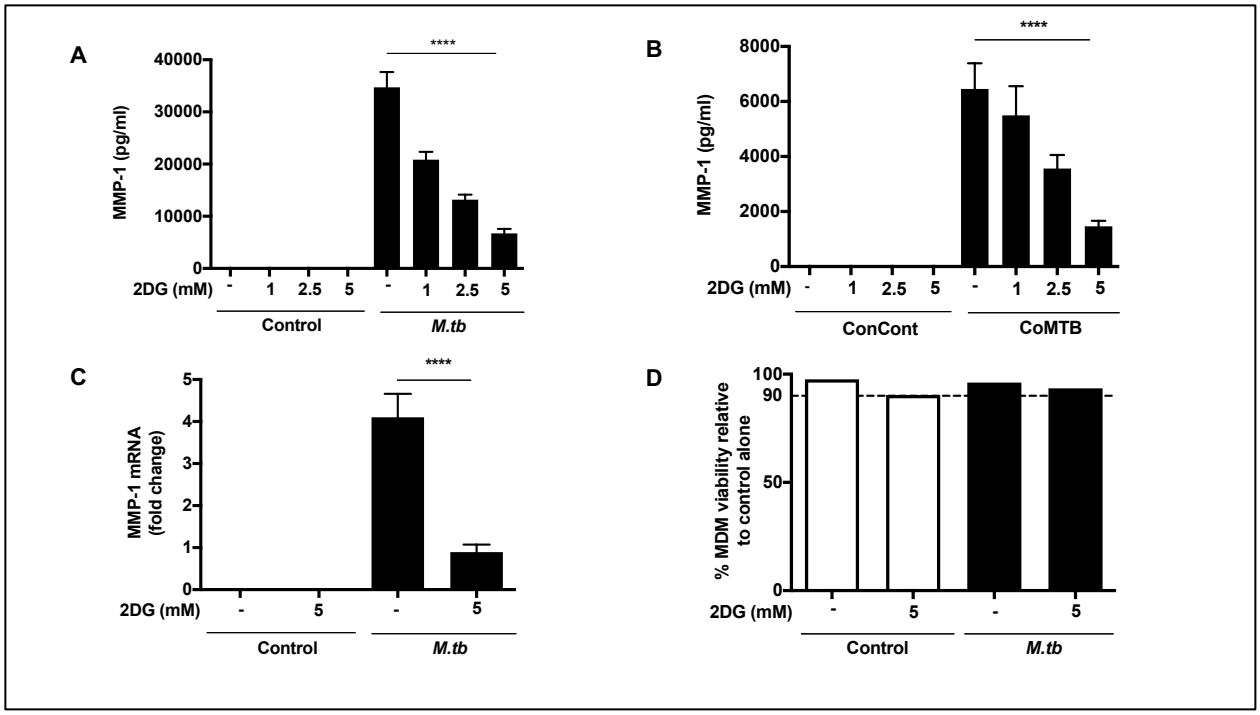


Figure 9: Glycolysis upregulates MMP-1 secretion and gene expression in *M.tb*-infected MDMs. MDMs were infected with virulent *M.tb* H37Rv or stimulated with CoMTB, with or without pre-treatment with 2DG for 1 hour. MMP-1 was detected by (A,B) ELISA or (C) RT-PCR. 2DG downregulated MMP-1 secretion in a dose-dependent manner in both (A) *M.tb*-infected and (B) CoMTB-stimulated MDMs at 24 hours. (C) 2DG downregulated MMP-1 gene expression in *M.tb*-infected MDMs at 24 hours. (D) MDM viability was not affected by *M.tb* infection or 2DG treatment compared to control cells in an LDH release assay. Bars show mean ± SD of 3 technical replicates of a single independent experiment and are representative of 5 independent experiments. Statistical analysis was performed using an ordinary one-way ANOVA with Tukey's post-test correction. ****$p<0.0001$.

3.2.4 Glycolysis upregulates MMP-2, MMP-3, MMP-7, MMP-8 and MMP-10 secretion from *M.tb*-infected MDMs

I then performed a Luminex assay to ascertain the role of glycolysis in regulating the secretion of other MMPs important in TB pathogenesis. 2DG induced a global reduction in the secretion of MMPs, including the gelatinase, MMP-2, the collagenase, MMP-8, the matrilysin, MMP-7 and the stromelysins, MMP-3 and -10 from *M.tb*-infected MDMs in comparison to *M.tb* infection alone. The greatest effect was on MMP-2 secretion, which was downregulated 11-fold, from 25947 ± 1667 pg/ml to 2224 ± 224.3 pg/ml ($p<0.0001$) (Figure 10A). MMP-3 secretion was decreased 3.5-fold, from 178.7 ± 21 pg/ml to 51.3 ± 9.5 pg/ml ($p<0.0001$) (Figure 10B); MMP-7 secretion 5.5-fold, from 354232 ± 22918 pg/ml to 64459 ± 5527 pg/ml ($p<0.0001$) (Figure 10C); MMP-8 secretion 5.5-fold, from 235.1 ± 22.9 pg/ml to 79 ± 0.8 pg/ml ($p<0.0001$) (Figure 10D); and MMP-10 secretion 2.5-fold, from 438.6 ± 24.9 pg/ml to 177.6 ± 27 pg/ml ($p<0.0001$) (Figure 10E).

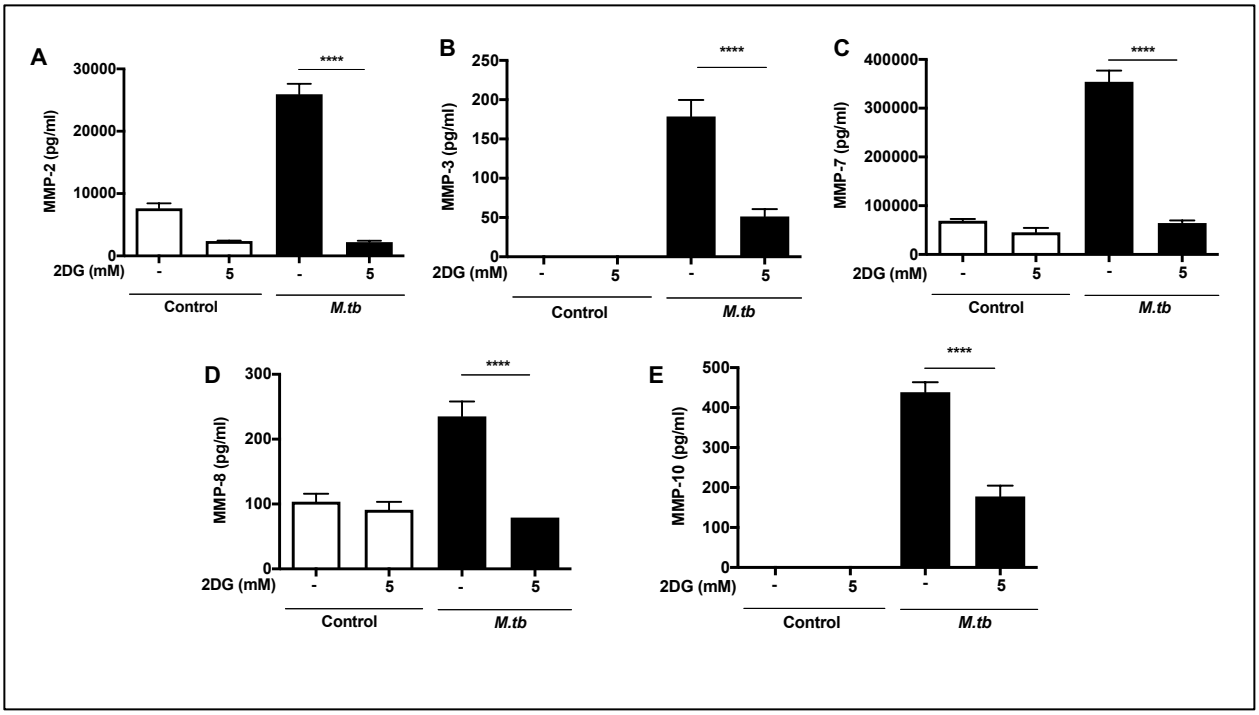


Figure 10: Glycolysis upregulates MMP-2, MMP-3, MMP-7, MMP-8 and MMP-10 secretion from *M.tb*-infected MDMs. MDMs were infected with virulent *M.tb* H37Rv, with or without pre-treatment with 2DG for 1 hour. MMPs were detected by Luminex assay. 2DG downregulated (A) MMP-2 (B) MMP-3 (C) MMP-7 (D) MMP-8 and (E) MMP-10 secretion from *M.tb*-infected MDMs at 24 hours compared to *M.tb* infection alone. Bars show mean ± SD of 3 technical replicates of a single independent experiment and are representative of 3 independent experiments. Statistical analysis was performed using an ordinary one-way ANOVA with Tukey's post-correction test. ****p<0.0001.

3.2.5 Glycolysis upregulates TIMP-1 and TIMP-2 secretion from *M.tb*-infected MDMs

I also measured the secretion of TIMPs.TIMP-1 secretion was increased 2-fold with *M.tb* infection compared with uninfected cells; treatment with 2DG in the presence of *M.tb* downregulated TIMP-1 secretion 5-fold ($p<0.0002$) (Figure 11A). TIMP-2 secretion was not induced by *M.tb*, but was downregulated 1.5-fold by 2DG ($p<0.05$) in infected cells (Figure 11B).

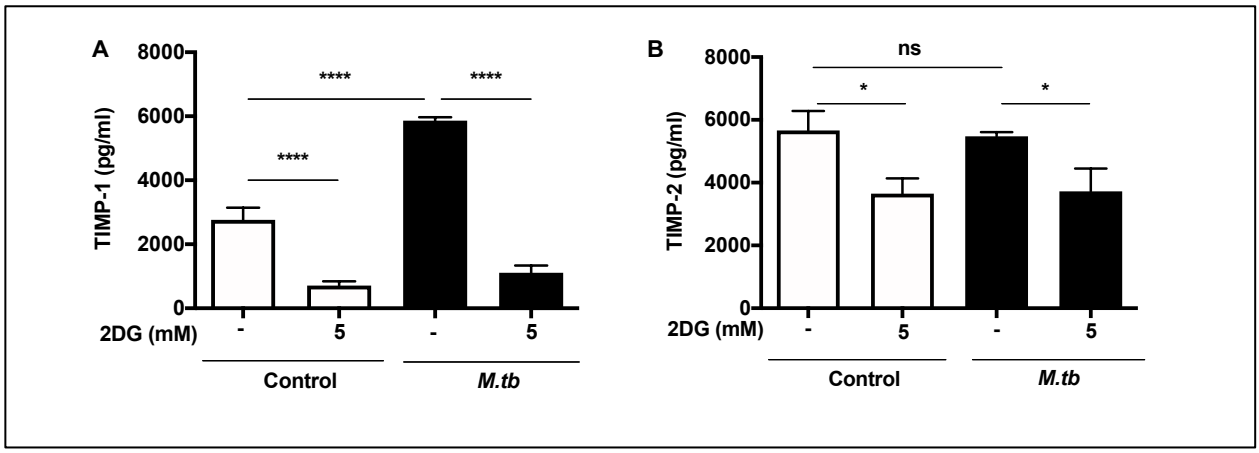


Figure 11: Glycolysis upregulates TIMP-1 and TIMP-2 secretion from *M.tb*-infected MDMs. MDMs were infected with virulent *M.tb* H37Rv, with or without pre-treatment with 2DG for 1 hour. TIMPs were detected by ELISA. (A) TIMP-1 secretion was upregulated in *M.tb*-infected MDMs at 24 hours, then reduced with 2DG treatment. (B) TIMP-2 secretion was not upregulated by *M.tb* infection, but was suppressed by 2DG. Bars show mean ± SD of 3 technical replicates of a single independent experiment and are representative of 3 independent experiments. Statistical analysis was performed using an ordinary one-way ANOVA with Tukey's post-test correction. ns not significant *$p<0.05$ ***$p<0.001$.

3.2.6 Glycolysis regulates cytokine secretion from *M.tb*-infected MDMs

I then queried whether glycolysis inhibition with 2DG regulates cytokine secretion in TB. In *M.tb*-infected MDMs, pro-inflammatory IL-1β secretion was downregulated 4-fold, from 268.3 ± 12.27 pg/ml to 66.20 ± 21.13 pg/ml ($p<0.001$) following 2DG treatment (Figure 12A). However, pro-inflammatory TNF-α secretion was increased 4-fold, from 3130 ± 463.1 pg/ml in *M.tb*-infected MDMs alone to 12624 ± 884.4 pg/ml ($p<0.0001$) in *M.tb*-infected MDMs treated with 2DG (Figure 12B). IL-10 secretion followed a similar pattern to IL-1β, with a 2DG-induced fall of 3.5-fold, from 1511 ± 108.2 pg/ml to 406.4 ± 53.05 pg/ml ($p<0.0001$) in *M.tb*-infected MDMs (Figure 12C).

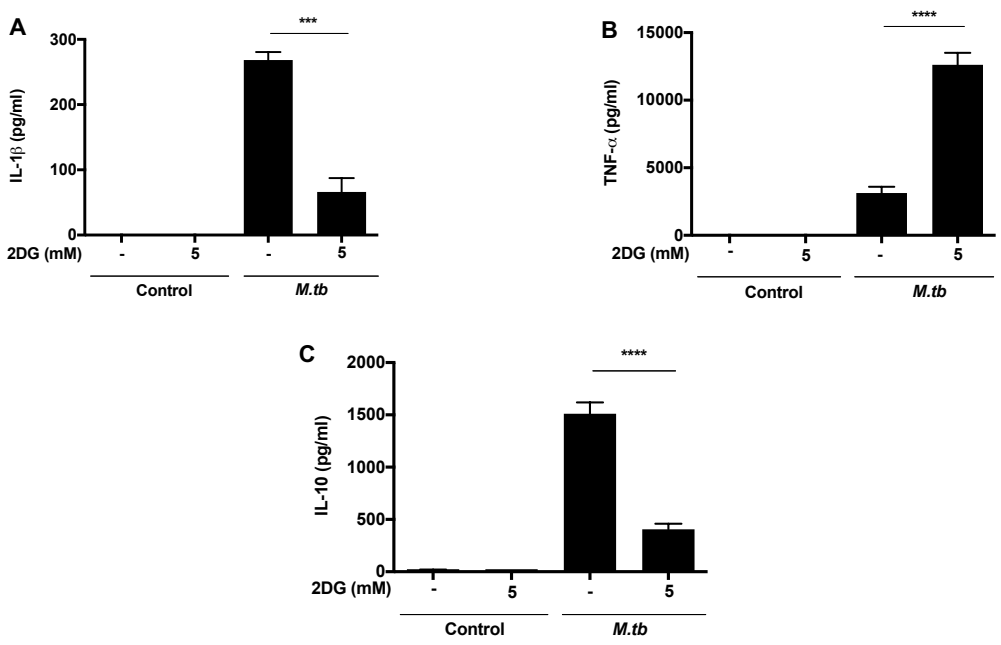


Figure 12: Glycolysis upregulates IL-1β and downregulates TNF-α and IL-10 cytokine secretion from *M.tb*-infected MDMs. MDMs were infected with virulent *M.tb* H37Rv with or without pre-treatment with 2DG for 1 hour. Cytokines were detected by Luminex assay or ELISA. 2DG significantly decreased (A) IL-1β and (C) IL-10 secretion from *M.tb*-infected MDMs. (B) 2DG significantly upregulated TNF-α secretion from *M.tb*-infected MDMs. Bars show mean ± SD of 3 technical replicates of a single independent experiment and are representative of 3 independent experiments. Statistical analysis was performed using an ordinary one-way ANOVA with Tukey's post-test correction. ***$p<0.001$ ***$p<0.0001$.

3.2.7 Glycolysis upregulates EMMPRIN secretion from *M.tb*-infected MDMs

I was also interested in measuring soluble EMMPRIN secretion in TB as, in addition to its MMP inducing function, EMMPRIN is known to be a regulator of lactate MCTs. *M.tb* upregulates EMMPRIN secretion from MDMs compared to uninfected cells ($P<0.001$) at 24 hours. This increase is partially abrogated by HK inhibition with 2DG ($p<0.05$). EMMPRIN secretion was increased 1.9-fold from baseline, then decreased 1.4-fold, from 4021 ± 494.8 pg/ml to 2914 ± 284.1 pg/ml ($p<0.001$) (Figure 13).

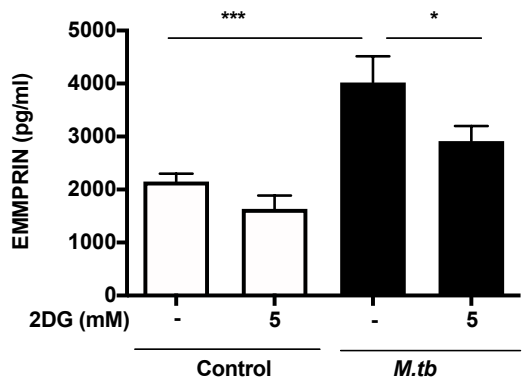


Figure 13: Glycolysis upregulates EMMPRIN secretion from *M.tb*-infected MDMs. MDMs were infected with virulent *M.tb* H37Rv with or without pre-treatment with 2DG for 1 hour. Secreted EMMPRIN concentration was upregulated from *M.tb*-infected MDMs at 24 hours and this effect was partially reduced by 2DG treatment. Bars show mean ± SD of 3 technical replicates of a single independent experiment and are representative of 3 independent experiments. Statistical analysis was performed using an ordinary one-way ANOVA with Tukey's post-test correction. *$p<0.05$ ***$p<0.001$.

3.2.8 Stabilisation of HIF-1α expression in M.tb-infected MDMs is enhanced by glycolysis

The transcription factor, HIF-1α, plays a key role in glycolysis and metabolic reprogramming in innate immune cells (296). It also regulates MMP-1 secretion in normoxia and hypoxia (259). *M.tb*-enhanced stabilisation of HIF-1α expression at 8 and 24 hours was completely abrogated by 2DG treatment, suggesting that glycolysis upregulates HIF-1α expression (Figure 14).

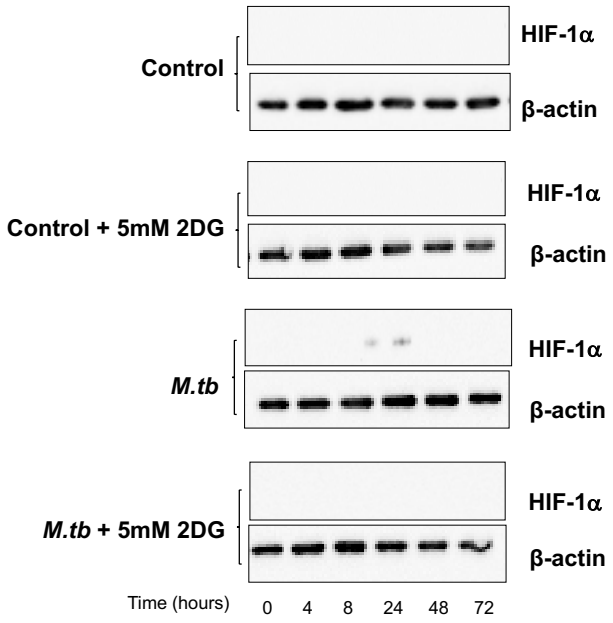


Figure 14: 2DG attenuates *M.tb*-induced HIF-1α stabilisation in MDMs.

MDMs were infected with virulent *M.tb* H37Rv, with or without pre-treatment with 2DG for 1 hour. Lysates were collected at 0, 4, 8, 24, 48 and 72 hours and HIF-1α and β-actin protein detected by Western blot. *M.tb* alone upregulated HIF-1α expression at 8 and 24 hours, but this was completely attenuated by 2DG. The blot image shows a single independent experiment and is representative of 2 independent experiments.

3.2.9 Glycolysis inhibition reduces intracellular bacillary killing in *M.tb*-infected MDMs

In order to investigate if glycolysis regulation has a functional effect on MDM bacillary killing, MDMs were infected with *M.tb* alone and in the presence of 2DG for 24 hours. Cells were then washed and lysates plated onto 7H11 agar at various dilutions for *M.tb* growth. Colony forming units (CFU) were counted to measure viable intracellular bacteria after 2 weeks of incubation. In MDM lysates infected with *M.tb* alone, there were 3.5-fold fewer CFU that in *M.tb*-infected MDMs treated with 2DG, demonstrating significantly curtailed bacterial killing with glycolysis inhibition (Figure 15).

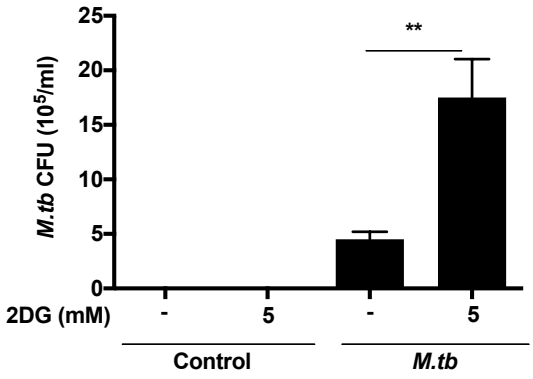


Figure 15: Glycolysis inhibition reduces intracellular bacillary killing in *M.tb*-infected MDMs. MDMs were infected with live, virulent *M.tb* H37Rv or 7H9 medium with or without pre-treatment with 2DG for 1 hour and incubated for 24 hours. Cell lysates were plated on 7H11 medium and colony forming units (CFU) counted after 2 weeks. Significantly more CFU were seen in *M.tb*-infected MDMs treated with 2DG. Bars show mean ± SD of 3 technical replicates of a single independent experiment and are representative of 3 independent experiments. Statistical analysis was performed using an ordinary one-way ANOVA with Tukey's post-test correction. **p<0.01.

3.2.10 HK2 is expressed in human TB lymphadenitis

Immunohistochemistry (IHC) was performed on human TB lymph node biopsies to investigate the expression of the HK2 isoform of the first enzyme in glycolysis (Figure 16). These samples were collected from TB patients in Peru as part of a previous study (381) and were kindly provided by Dr Daniela Kirwan. Table 7 details the demographic and clinico-pathological characteristics of the 5 patients whose biopsies were immunostained for HK2 expression. All patients were HIV-negative and had a diagnosis of culture-positive TB. The biopsies were scored by 3 independent pathologists to ascertain the presence of the classic features of TB lymphadenitis; all 5 patients had caseating granulomatous necrosis, though only 1 had visible acid and alcohol fast bacilli (AAFB).

Patient	**Age (years)**	**Sex**	**HIV status**	**Lymph node microbiology**			**Lymph node histopathology**	
				Auramine smear	MODS assay	L-J culture	AAFB	Caseating granulomas
1	45	M	-	-	+	+	No	Yes
2	26	M	-	+	+	+	Yes	Yes
3	58	F	-	-	+	+	No	Yes
4	22	M	-	-	+	+	No	Yes
5	43	F	-	-	-	+	No	Yes

Table 7: Demographic and clinico-pathological characteristics of patients with TB lymphadenitis samples immunostained for HK2. Abbreviations: M = Male; F = Female; HIV = Human immunodeficiency virus; MODS = Microscopic observation drug susceptibility; L-J = Löwenstein-Jensen; AAFB = Acid and alcohol fast bacilli.

The images in Figure 3 are from a single patient and representative of all 5 patients. Haematoxylin and eosin (H&E) staining confirmed features of tuberculous granulomatous inflammation in the lymph node biopsies (Figure 15A). There was prominent HK2 expression in areas of central granulomatous necrosis (Figure 15B), compared to no background staining with an IgG isotype control antibody (Figure 15C). In particular, HK2 expression was seen in epithelioid macrophages (Figure 15D) and Langhans giant cells (Figure 15E).

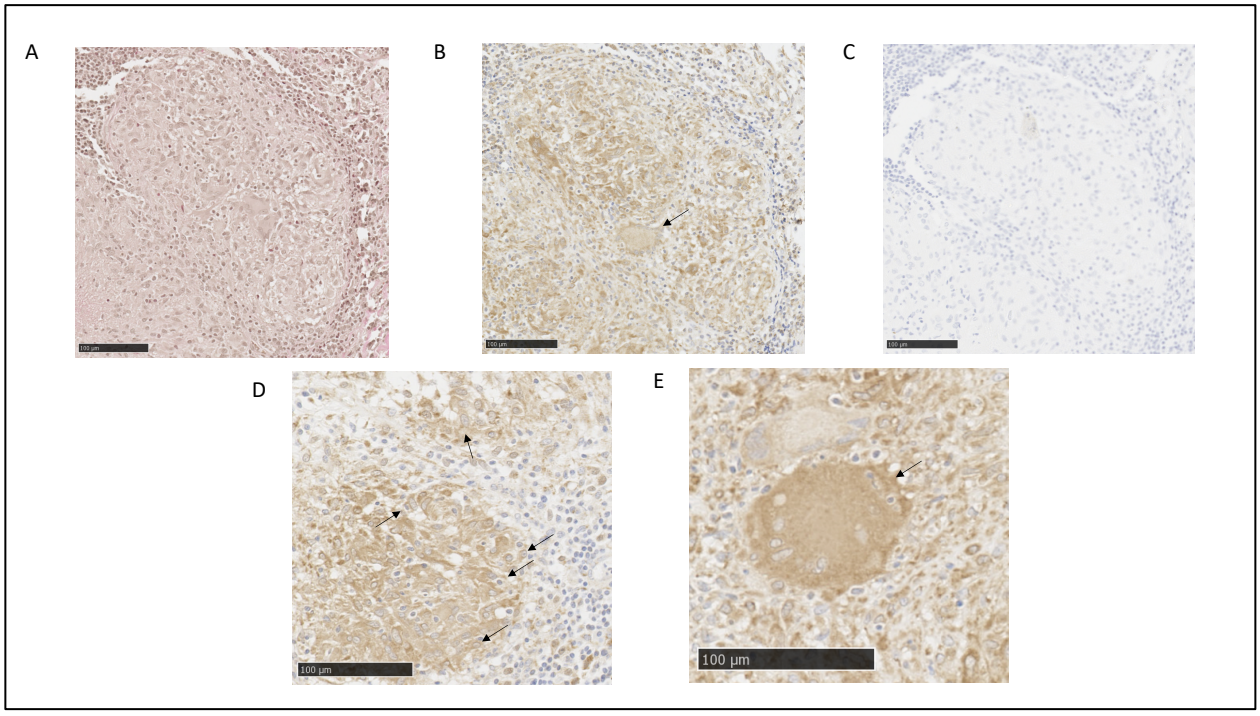


Figure 16: HK2 is expressed in granulomas of patients with TB lymphadenitis. HK2 staining was performed in tuberculous lymphadenitis samples (A-E). (A) Representative H&E staining showing tuberculous granulomatous inflammation and tissue remodelling. (B) HK2 staining seen in the necrotic centre of the tuberculous granuloma, with a Langhans giant cell (arrow) surrounded by epithelioid macrophages. (C) IgG control antibody staining showed no background staining. (D) HK2 staining in an area of macrophages (arrows) (E) HK2 staining in a characteristic Langhans giant cell (arrow). Images are from a single patient and representative of the 5 patients in Table 7. Magnification 20x (A-C) and 30x (D, E). Scale 100µm.

3.2.11 Diethylsuccinate does not affect MMP-1 or TIMP secretion from *M.tb*-infected MDMs

I then proceeded to analyse the regulation of MMP and cytokine secretion by the TCA cycle intermediate, succinate. MDMs were treated with exogenous diethylsuccinate, the doses of which were chosen by a preliminary dose-response study using a wide concentration range. The optimal diethylsuccinate doses selected were those that elicited MMP and cytokine production without evidence of cytotoxicity. MDMs were infected with *M.tb* in the presence or absence of cell-permeable diethylsuccinate and supernatants were assessed for MMP-1 secretion after 24 hours. Diethylsuccinate had no effect on MMP-1 secretion in *M.tb*-infected MDMs (Figure 17A). I also investigated whether diethylsuccinate had an effect on TIMP secretion. TIMP-1 secretion was upregulated in MDMs with *M.tb* infection, but was not affected by diethylsuccinate (Figure 17B). TIMP-2 concentrations were neither upregulated in TB nor altered by diethylsuccinate (Figure 17C).

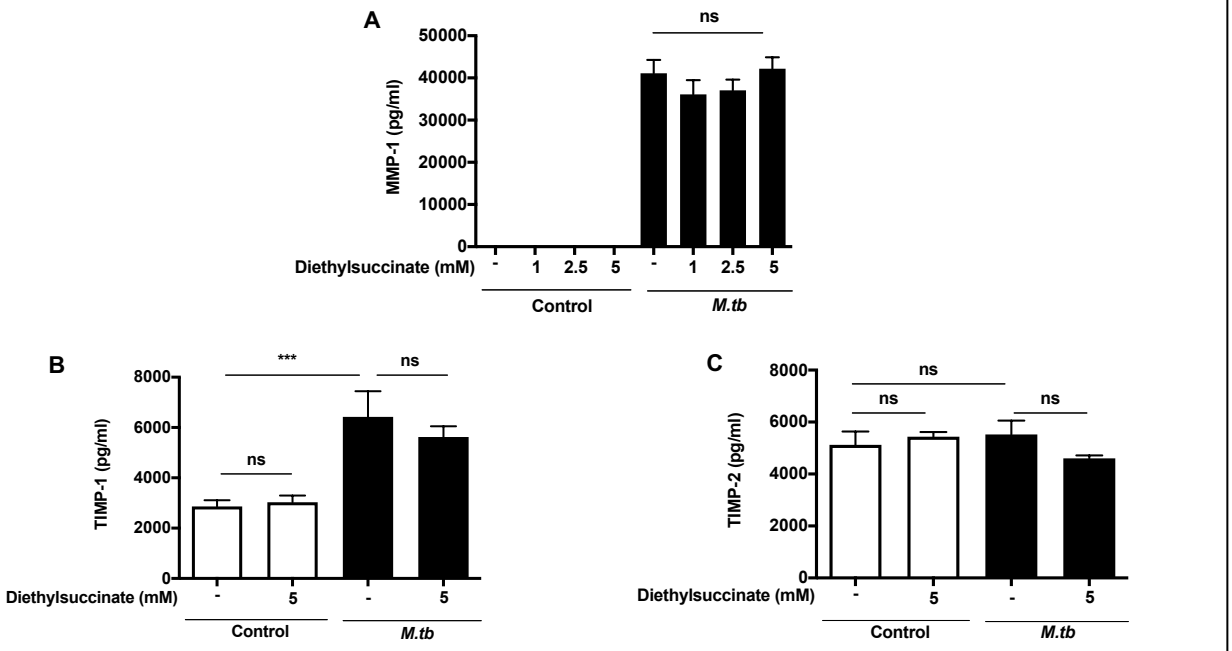


Figure 17: Diethylsuccinate does not affect MMP-1 or TIMP secretion from *M.tb*-infected MDMs. MDMs were infected with virulent *M.tb* H37Rv, with or without pre-treatment with diethylsuccinate for 1 hour. MMP-1 and TIMPs were detected by ELISA. (A) MMP-1 and (B) TIMP-1secretion are upregulated in *M.tb*-infected MDMs at 24 hours. However, diethylsuccinate did not affect (A) MMP-1 (B) TIMP-1 or (C) TIMP-2 secretion. Bars show mean ± SD of 3 technical replicates of a single independent experiment and are representative of 3 independent experiments. Statistical analysis was performed using an ordinary one-way ANOVA with Tukey's multiple comparison test. ns not significant ***p<0.001.

3.2.12 Diethylsuccinate regulates cytokine secretion from *M.tb*-infected MDMs

Although diethylsuccinate did not regulate MMP-1 secretion, I was interested to assess its effect on cytokines involved in the inflammatory response to TB. *M.tb*-infected MDMs secretion of pro-inflammatory IL-1β and TNF-α and anti-inflammatory IL-10 in the presence of diethylsuccinate were evaluated by Luminex assay or ELISA. Diethylsuccinate upregulated IL-1β secretion 1.5-fold to 185.8 ± 8.9 pg/ml from 121.2 ± 2.9 pg/ml ($p<0.0001$) with *M.tb* infection alone (Figure 18A). However, TNF-α and IL-10 secretion were both significantly downregulated by diethylsuccinate. *M.tb* induced TNF-α secretion of 7349 ± 201.5 pg/ml, which decreased to 1767 ± 115.7 pg/ml with diethylsuccinate treatment (Figure 18B). IL-10 secretion fell from 2069 ± 102.1 pg/ml with *M.tb* infection alone to 1454 ± 144.3 pg/ml ($p<0.001$) with the addition of diethylsuccinate (Figure 18C).

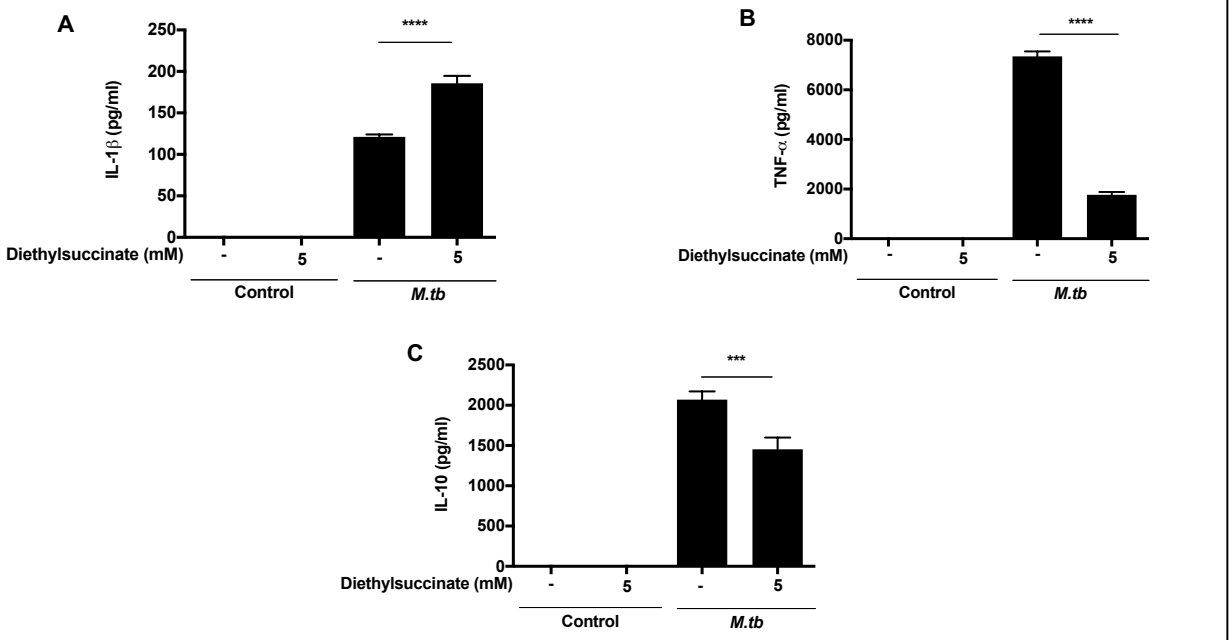
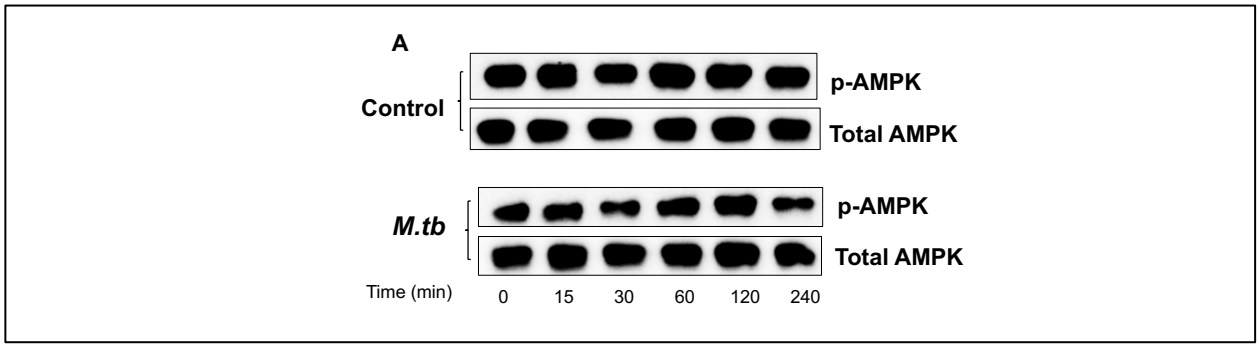


Figure 18: Diethylsuccinate upregulates IL-1β and downregulates TNF-α and IL-10 cytokine secretion from *M.tb*-infected MDMs. MDMs were infected with virulent *M.tb* H37Rv with or without pre-treatment with diethylsuccinate for 1 hour. Cytokines were detected by Luminex assay or ELISA. (A) Diethylsuccinate significantly upregulated IL-1β secretion from *M.tb*-infected MDMs. Diethylsuccinate downregulated (B) TNF-α and (C) IL-10 secretion from *M.tb*-infected MDMs. Bars show mean ± SD of 3 technical replicates of a single independent experiment and are representative of 3 independent experiments. Statistical analysis was performed using an ordinary one-way ANOVA with Tukey's multiple comparison test. ***p<0.001 ***p<0.0001.

3.2.13 p-AMPK protein expression and the effect of AMPK inhibition on HIF-1α and HK2 protein expression

I was then interested in analysing the role of the essential metabolic sensor, AMPK, in the regulation of MMP gene expression and secretion in TB. First, I performed Western blot analysis to ascertain whether p-AMPK protein expression in MDMs is modulated by *M.tb* infection. There was a partial downregulation of p-AMPK protein expression following *M.tb* infection (Figure 19A).

Next, I assessed the impact of AMPK blockade on HIF-1α and HK2 protein expression in *M.tb* infection using the chemical inhibitor, Compound C. Compound C, a pyrazolopyrimidine derivative, is an ATP-competitive inhibitor which binds to the highly conserved active site of AMPK (382). *M.tb*-induced protein expression of both HIF-1α (Figure 19B) and HK2 (Figure 19C) was attenuated from 24 hours in the presence of Compound C. Hence, this suggests that AMPK stabilises both HIF-1α and HK2 protein expression in *M.tb*-infected MDMs.



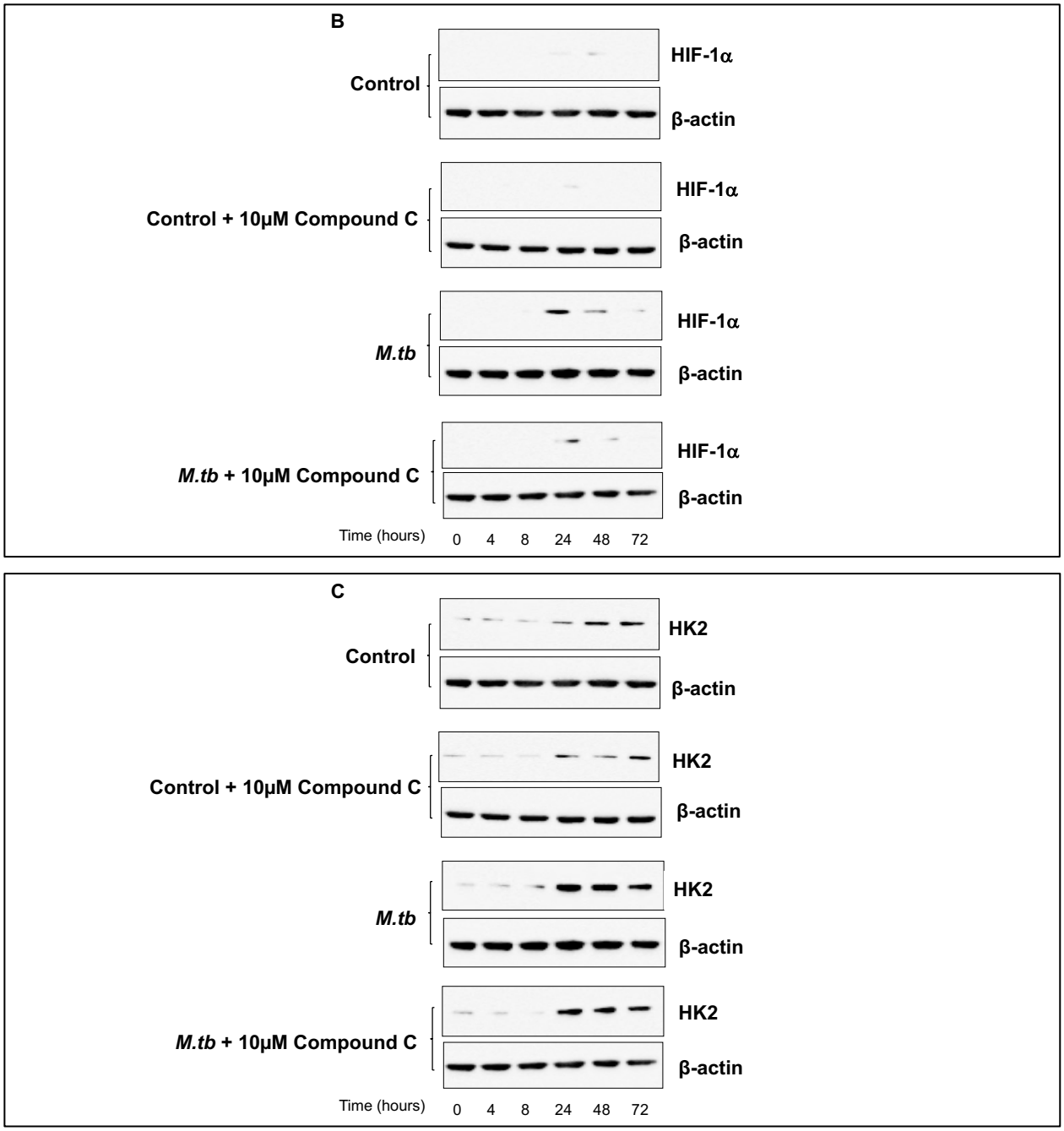


Figure 19: p-AMPK protein expression and the effect of Compound C on HIF-1α and HK2 expression in *M.tb*-infected MDMs. (A) MDMs were cultured and infected with *M.tb* or 7H9 medium and lysates collected at 0, 15, 30, 60, 120 and 240 minutes for Western blot. p-AMPK protein expression was partially downregulated from 15 minutes following *M.tb* infection. (B, C) MDMs were cultured and infected with *M.tb* or 7H9 medium, in the presence or absence of Compound C and lysates collected at 0, 4, 8, 24, 48 and 72 minutes for Western blot. *M.tb*-induced expression of (B) HIF-1α and (C) HK2 was attenuated by Compound C from 24 hours. All blot images are from single independent experiments and representative of 3 independent experiments.

3.2.14 AMPK upregulates MMP-1 secretion and gene expression in *M.tb*-infected MDMs

Although pAMPK is generally downregulated in *M.tb*-infected MDMs, I was interested in analysing whether specific inhibition of AMPK affects MMP gene expression and secretion. I incubated MDMs with Compound C for 1 hour, prior to infection with virulent *M.tb* H37Rv. At 24 hours, Compound C downregulated MMP-1 secretion 2-fold from 4644 ± 608 pg/ml ($p<0.0001$) with *M.tb* alone to 2203 ± 249.1 pg/ml ($p<0.0001$) with Compound C and *M.tb* (Figure 20A). There was a similar fold decrease in MMP secretion at 72 hours with Compound C, though the *M.tb*-induced baseline secretion was higher at 16226 ± 1795 pg/ml (Figure 20B). There was also evidence of intracellular regulation of MMP-1 secretion, as Compound C induced a 6.9-fold drop in MMP-1 mRNA in *M.tb*-infected MDMs compared to *M.tb* infection alone (Figure 20C). In light of these findings, I performed an LDH release assay for reassurance that Compound C did not adversely impact MDM viability. This showed that MDM viability was >90% for all experimental conditions relative to unstimulated control cells and that it was unlikely that MMP downregulation could be attributed to chemical cytoxicity (Figure 20D).

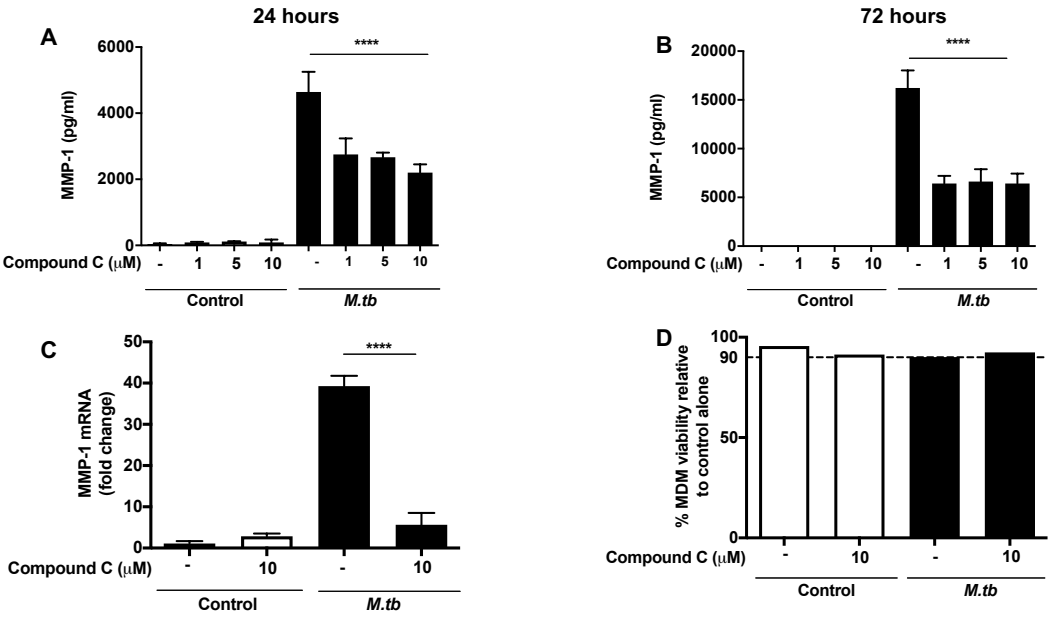


Figure 20: AMPK upregulates MMP-1 secretion and gene expression in *M.tb*-infected MDMs. MDMs were infected with virulent *M.tb* H37Rv, with or without pre-treatment with Compound C for 1 hour. MMP-1 was detected by (A, B) ELISA and (C) RT-PCR. MMP-1 secretion was downregulated by Compound C inhibition of AMPK at (A) 24 and (B) 72 hours in *M.tb*-infected MDMs. (C) MMP-1 mRNA was downregulated at 24 hours with Compound C in *M.tb*-infected MDMs. (D) LDH release assay showing no cytotoxicity with Compound C. Bars show mean ± SD of 3 technical replicates of a single independent experiment and are representative of 3 independent experiments. Statistical analysis was performed using an ordinary one-way ANOVA with Tukey's post-test correction. ****p<0.0001.

3.2.15 AMPK upregulates IL-1β, TNF-α and IL-10 secretion from *M.tb*-infected MDMs

Compound C inhibition of AMPK upregulated both the pro-inflammatory cytokines, IL-1β and TNF-α, as well as the anti-inflammatory cytokine, IL-10, at 24 and 72 hours in *M.tb*-infected MDMs. IL-1β was downregulated 6.1-fold by Compound C at 24 hours, from 314.3 ± 67.8 pg/ml to 51 ± 7.995 pg/ml ($p<0.001$) (Figure 21A). At 72 hours, the *M.tb*-induced concentration of IL-1β was higher at 5972 ± 45.7 pg/ml, but Compound C generated only a 2.6-fold fall in secretion to 2308 ± 572.5 pg/ml ($p<0.0001$) (Figure 21B). TNF-α secretion at 24 hours fell 7.6-fold from 6248 ± 376.5 pg/ml with M.tb alone to 814.2 ± 57.8 pg/ml with Compound C treatment in the presence of *M.tb* infection ($p<0.0001$) (Figure 21C), while TNF-α secretion at 72 hours fell 4.7-fold from 9805 ± 629pg/ml to 2081 ± 403.5pg/ml ($p<0.0001$) (Figure 21D). IL-10 secretion decreased 7.5-fold at 24 hours from 633.5 ± 138.2pg/ml to 84.4 ± 5.6pg/ml ($p<0.0001$) (Figure 21E) and 6.9-fold 72 hours from 625 ± 7.1 pg/ml to 90.6 ± 8.0 pg/ml ($p<0.0001$) (Figure 21F) with Compound C in *M.tb*-infected MDMs.

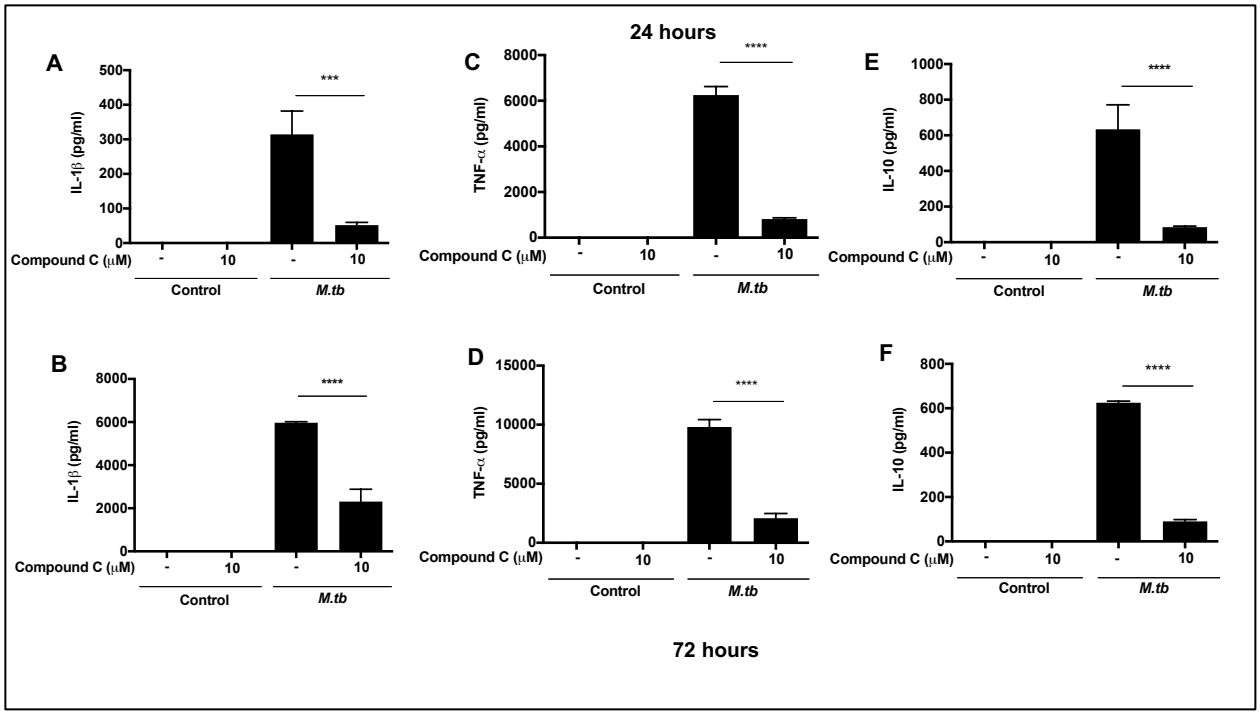


Figure 21: AMPK upregulates IL-1β, TNF-α and IL-10 cytokine secretion from *M.tb*-infected MDMs. MDMs were infected with virulent *M.tb* H37Rv with or without pre-treatment with Compound C for 1 hour. Cytokines were detected by Luminex assay or ELISA. Compound C significantly downregulated IL-1β secretion at (A) 24 and (B) 72 hours; TNF-α secretion at (B) 24 and (72) hours; and IL-10 secretion at (A) 24 and (B) 72 hours. Bars show mean ± SD of 3 technical replicates of a single independent experiment and are representative of 3 independent experiments. Statistical analysis was performed using an ordinary one-way ANOVA with Tukey's post-test correction. ***p<0.001 ***p<0.0001.

3.2.16 Metformin has a biphasic effect on MMP-1 secretion in *M.tb*-infected MDMs

Metformin has recently been proposed as an adjuvant treatment for tuberculosis due to its AMPK activation role. I was interested to assess its effect on MMP and cytokine secretion. Metformin increased MMP-1 secretion 1-3-fold at 24 hours in *M.tb*-infected MDMs (Figure 22A), while MMP-1 secretion was downregulated 2.2-fold at 72 hours ($p<0.0001$) (Figure 22B)

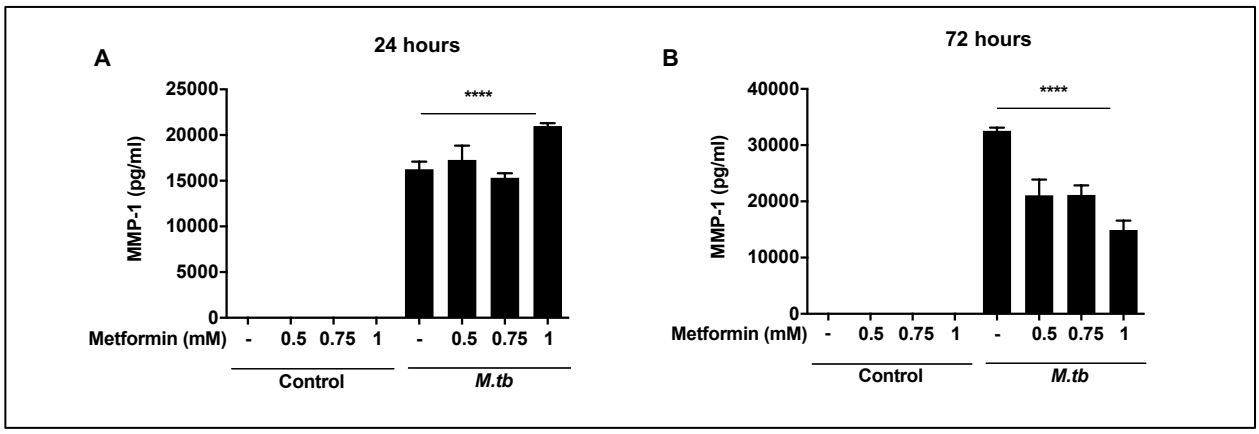


Figure 22: Metformin has a biphasic effect on MMP-1 secretion from *M.tb*-infected MDMs. MDMs were infected with virulent *M.tb* H37Rv with or without pre-treatment with metformin for 1 hour. MMPs were detected by ELISA. (A) MMP-1 was increased by metformin at 24 hours. (B) MMP-1 was decreased by metformin at 72 hours. Bars show mean ± SD of 3 technical replicates of a single independent experiment and are representative of 3 independent experiments. Statistical analysis was performed using an ordinary one-way ANOVA with Tukey's post-test correction. ***$p<0.0001$.

3.2.17 Metformin regulates cytokine secretion from *M.tb*-infected MDMs

Metformin has diverse effects on cytokine secretion from *M.tb*-infected MDMs at both 24 and 72 hours, with an increase in IL-1β secretion at both timepoints (Figures 23A and 23D); an increase in TNF-α secretion at 24 hours (Figure 23B), but a decrease at 72 hours (Figure 23E); and no effect on IL-10 at 24 hours (Figure 23C), but a decrease at 72 hours (Figure 23F) in *M.tb*-infected MDMs.

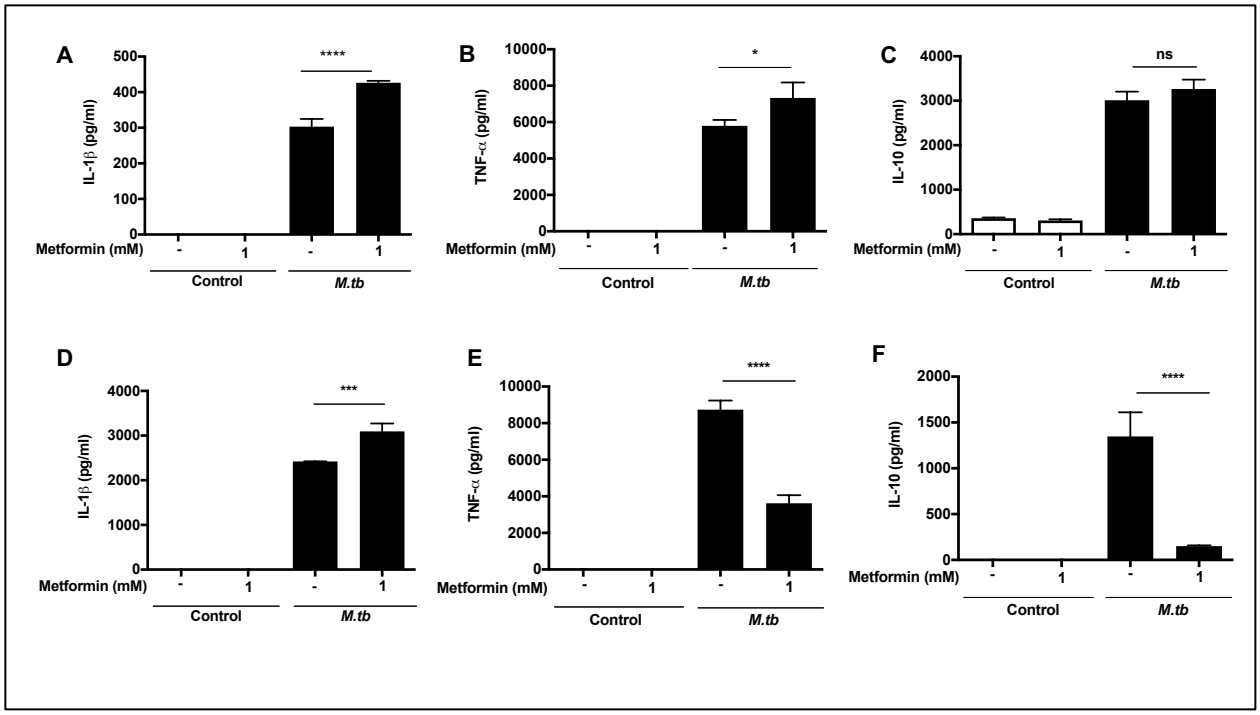


Figure 23: Metformin regulates cytokine secretion from *M.tb*-infected MDMs. MDMs were infected with virulent *M.tb* H37Rv with or without pre-treatment with metformin for 1 hour. Cytokines were detected by Luminex assay or ELISA. Metformin significantly downregulated IL-1β secretion at (A) 24 and (B) 72 hours; TNF-α secretion at (B) 24 and (72) hours; and IL-10 secretion at (A) 24 and (B) 72 hours. Bars show mean ± SD of 3 technical replicates of a single independent experiment and are representative of 3 independent experiments. Statistical analysis was performed using an ordinary one-way ANOVA with Tukey's post-test correction. ***p<0.001 ***p<0.0001.

3.2.18 p70^{S6K} protein expression is upregulated in *M.tb*-infected MDMs

Prior to investigating the role of the Pi3-kinase/Akt/mTOR pathway on MMP and cytokine secretion, I measured the protein expression of p-p70^{S6K}, a downstream target of mTOR, in response to *M.tb* infection of MDMs. *M.tb* infection resulted in a clear upregulation of p-p70^{S6K} expression from 15 minutes on Western blot analysis (Figure 24). Though upregulation of p-p70^{S6K} expression over time was also noted in the controls, *M.tb*-induced p-p70^{S6K} expression was comparatively greater at all time points relative to the controls.

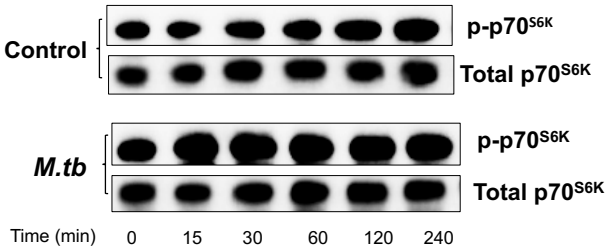


Figure 24: Phosphorylated p70^{S6K} protein expression is upregulated in *M.tb*-infected MDMs. MDMs were infected with *M.tb* or 7H9 medium as a control for 0, 15, 30 60, 120 and 240 minutes. Cell lysates were collected and phosphorylated p70^{S6K} (p-p70^{S6K}) and total p70^{S6K} protein detected by Western blot. *M.tb* infection increased the expression of p-p70^{S6K} from 15 minutes relative to controls. The blot image is from a single independent experiment and representative of 2 independent experiments.

3.2.19 The Pi3-kinase-Akt-mTORC1 pathway has a biphasic effect on MMP-1 regulation in *M.tb*-infected MDMs

Finally, I investigated the temporal effect of the Pi3-kinase/Akt/mTOR pathway on the regulation of MMP and cytokine secretion, using the chemical inhibitors LY294002, VIII and rapamycin. LY294002 inhibits Pi3-kinase, VIII inhibits Akt and rapamycin inhibits mTORC1. These inhibitors had a biphasic effect on MMP-1 secretion, with a general downregulation of MMP-1 secretion at 24 hours and an upregulation at 72 hours in *M.tb*-infected MDMs (Figure 25). The fold change increases in inhibitor-induced secretion at 72 hours ranged between 1.6 and 2.5 compared to *M.tb* alone.

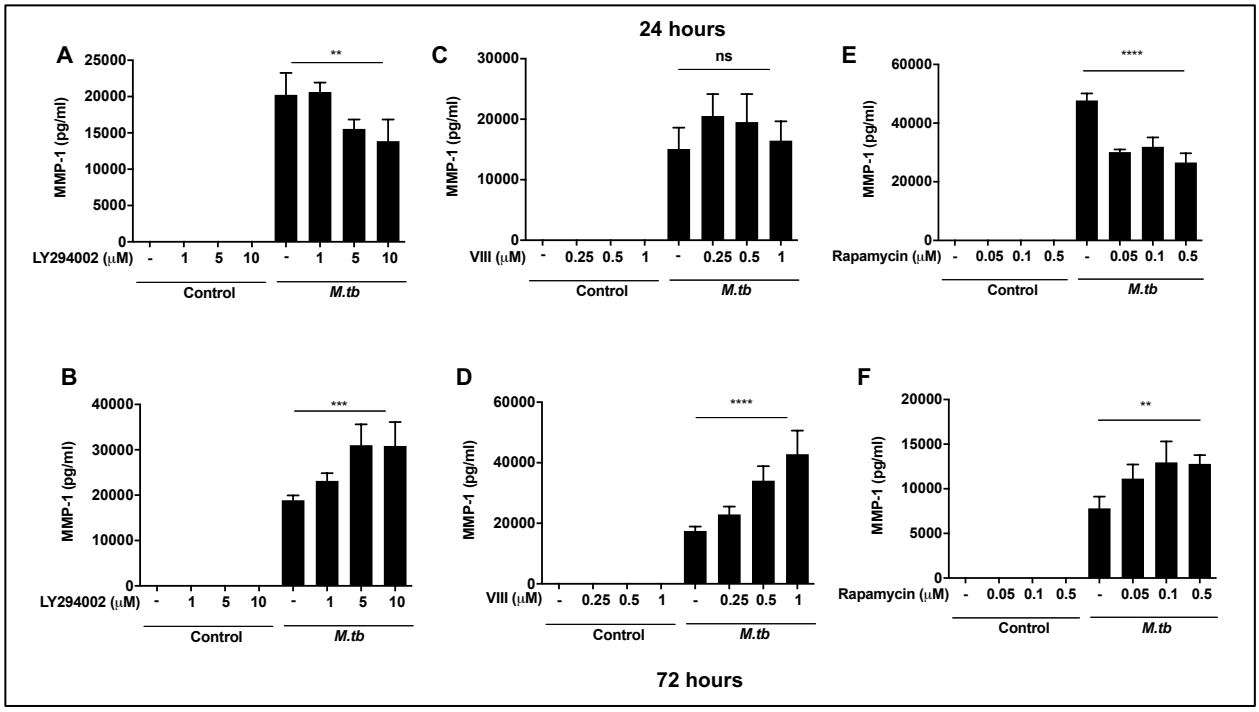


Figure 25: The Pi3-kinase/Akt/mTORC1 pathway has a biphasic effect on MMP-1 secretion in *M.tb*-infected MDMs. MDMs were infected with virulent *M.tb* H37Rv with or without pre-treatment with LY294002, VIII or rapamycin for 1 hour. MMP-1 was detected by ELISA. MMP-1 secretion at 24 hours was significantly downregulated by (A) LY294002 and (E) rapamycin, though it was not affected by (C) VIII. MMP-1 secretion at 72 hours was significantly upregulated by (B) LY294002 (D) VIII and (F) rapamycin. Bars show mean ± SD of 3 technical replicates of a single independent experiment and are representative of 3 independent experiments. Statistical analysis was performed using an ordinary one-way ANOVA with Tukey's post-test correction. ns not significant **p<0.01 ***p<0.001 ***p<0.0001.

3.2.20 The Pi3-kinase-Akt-mTORC1 pathway regulates cytokine secretion in *M.tb*-infected MDMs

3.2.20.1 The Pi3-kinase-Akt-mTORC1 pathway upregulates IL-1β secretion in TB

LY294002, VIII and rapamycin all upregulated IL-1β at both 24 and 72 hours in *M.tb*-infected MDMs (Figure 26). The greatest effect was with rapamycin at 72 hours, with a 5-fold rise in IL-1β secretion from 1247 ± 86.98 pg/ml to 6393 ± 913.8 pg/ml ($p<0.0001$) compared with TB alone (Figure 26F).

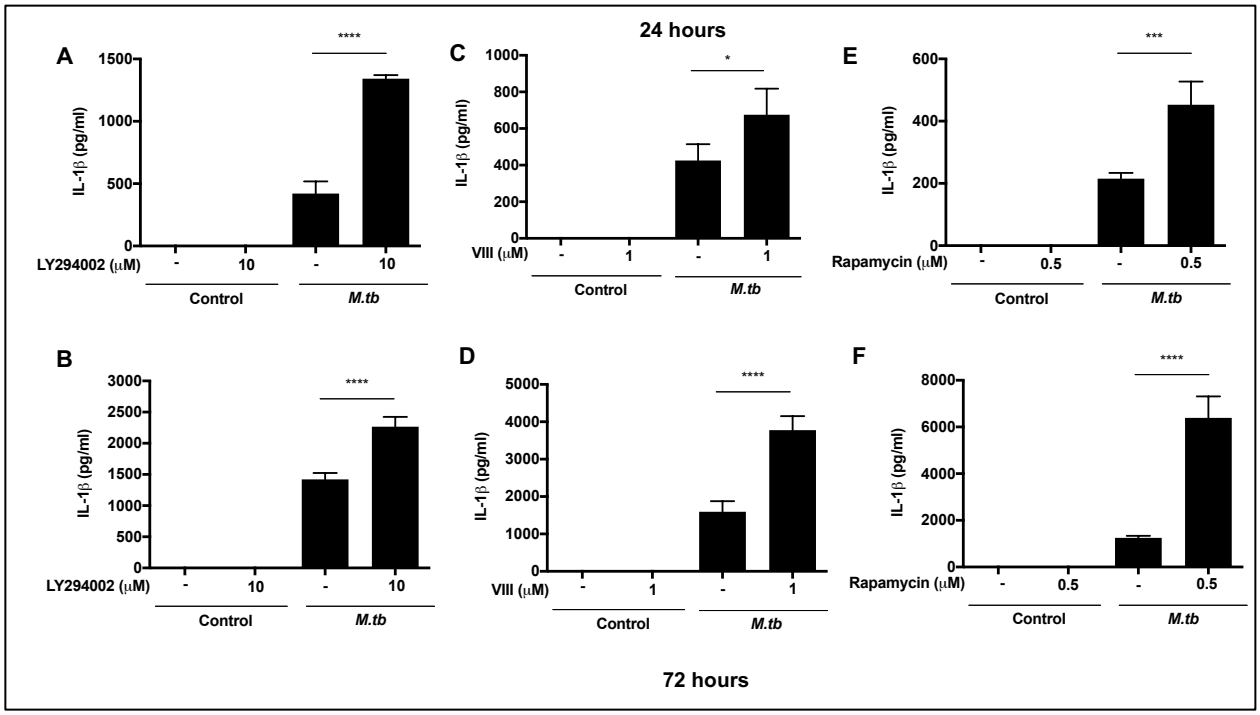


Figure 26: The Pi3-kinase/Akt/mTORC1 pathway downregulates IL-1β secretion. MDMs were infected with virulent *M.tb* H37Rv with or without pre-treatment with LY294002, VIII or rapamycin for 1 hour. Cytokines were detected by Luminex assay or ELISA. LY294002 upregulated IL-1β secretion at (A) 24 hours and (B) 72 hours. VIII upregulated IL-1β secretion at (C) 24 hours and (D) 72 hours. Rapamycin upregulated IL-1β secretion at (E) 24 hours and (F) 72 hours. Bars show mean ± SD of 3 technical replicates of a single independent experiment and are representative of 3 independent experiments. Statistical analysis was performed using an ordinary one-way ANOVA with Tukey's post-test correction. *$p<0.05$ ***$p<0.001$ ***$p<0.0001$.

3.2.20.2 The Pi3-kinase-Akt-mTORC1 pathway downregulates TNF-α secretion in TB

LY294002, VIII and rapamycin upregulated IL-1β, TNF-α and IL-10 at both 24 and 72 hours in *M.tb*-infected MDMs (Figure 27). These inhibitors all induced modest rises in cytokine secretion at 24 hours, with fold changes of around 2.5. At 72 hours, however, rapamycin had a highly potent effect on TNF-α secretion, with a 27-fold upregulation from 514.7 ± 292.4 pg/ml to 14224 ± 777 pg/ml ($p<0.0001$) compared to *M.tb* infection alone (Figure 27F). LY294002 also upregulated TNF-α secretion 5.5-fold at 72 hours compared to TB alone, from 704.2 ± 255.8 pg/ml to 3840 ± 630.2 pg/ml ($p<0.0001$) (Figure 27B)

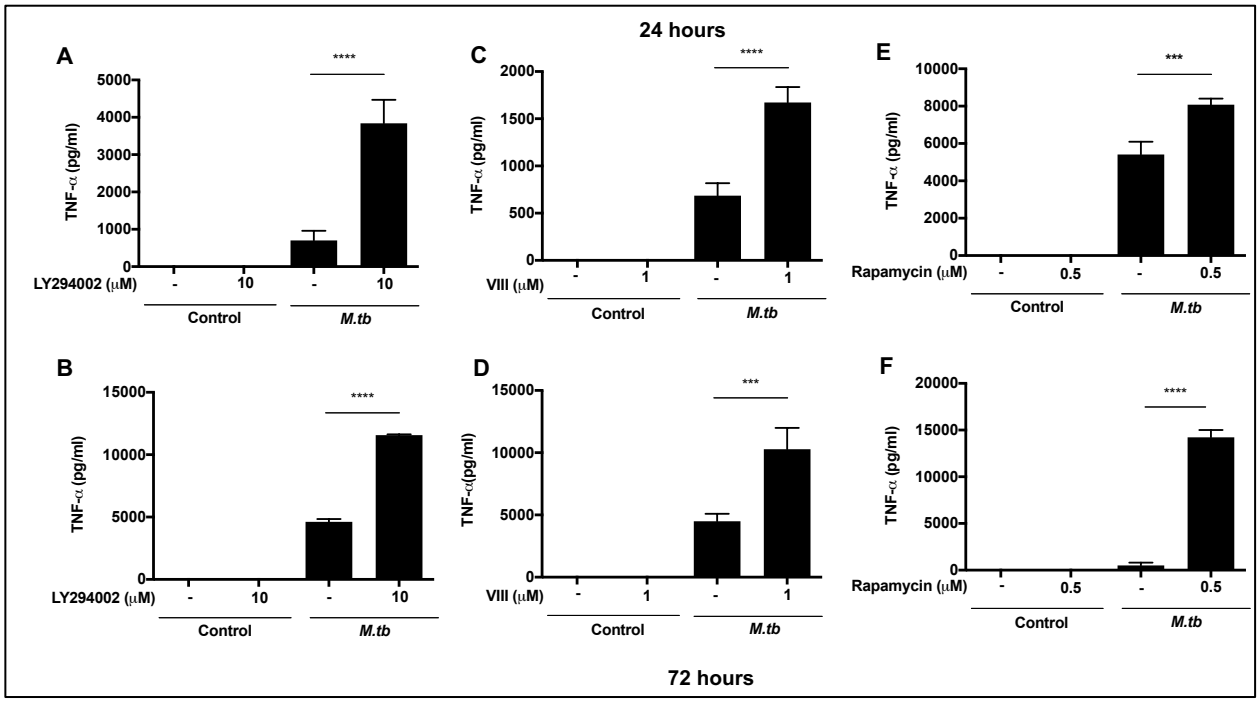


Figure 27: The Pi3-kinase/Akt/mTORC1 pathway downregulates TNF-α secretion. MDMs were infected with virulent *M.tb* H37Rv with or without pre-treatment with LY294002, VIII or rapamycin for 1 hour. Cytokines were detected by Luminex assay or ELISA. LY294002 upregulated TNF-α secretion at (A) 24 hours and (B) 72 hours. VIII upregulated TNF-α secretion at (C) 24 hours and (D) 72 hours. Rapamycin upregulated TNF-α secretion at (E) 24 hours and (F) 72 hours. Bars show mean ± SD of 3 technical replicates of a single independent experiment and are representative of 3 independent experiments. Statistical analysis was performed using an ordinary one-way ANOVA with Tukey's post-test correction. ***$p<0.001$ ***$p<0.0001$.

3.2.20.3 The Pi3-kinase-Akt-mTORC1 pathway has a biphasic effect on IL-10 secretion in TB

LY294002, VIII and rapamycin had a biphasic effect on IL-10 secretion, with a downregulation of IL-10 at 24 hours and an upregulation at 72 hours in *M.tb*-infected MDMs (Figure 28). The fold changes in both directions were between 1 and 2 in almost all cases, though rapamycin induced a higher fold change upregulation of 3.6 at 72 hours compared to *M.tb*-infection alone (Figure 28F). *M.tb* alone induced higher secretion of all 3 cytokines at 24 hours than at 72 hours. Hence, the Pi3-kinase/Akt/mTOR pathway increases IL-10 secretion at 24 hours and decreases it at 72 hours after infection.

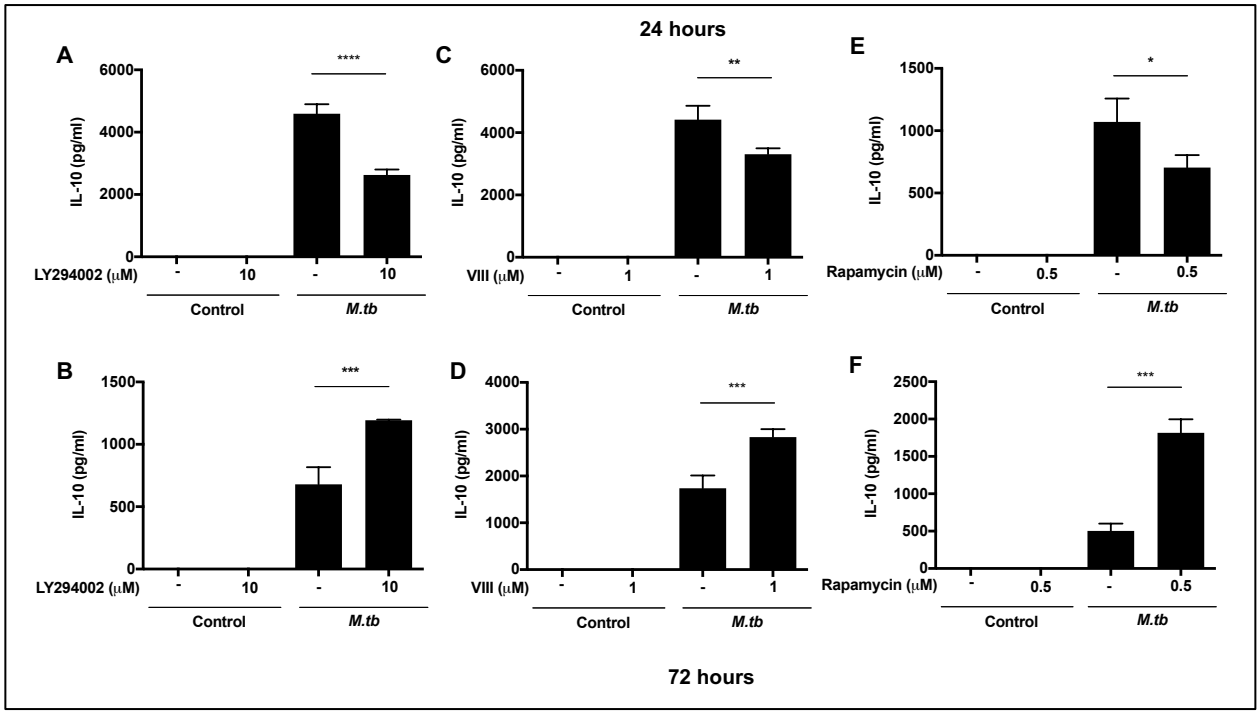


Figure 28: The Pi3-kinase/Akt/mTORC1 pathway has a biphasic effect on IL-10 secretion MDMs were infected with virulent *M.tb* H37Rv with or without pre-treatment with LY294002, VIII or rapamycin for 1 hour. Cytokines were detected by Luminex assay or ELISA. IL-10 secretion at 24 hours was significantly downregulated by (A) LY294002 (C) VIII and (E) rapamycin. IL-10 secretion at 72 hours was significantly upregulated by (B) LY294002 (D) VIII and (F) rapamycin. Bars show mean ± SD of 3 technical replicates of a single independent experiment and are representative of 3 independent experiments. Statistical analysis was performed using an ordinary one-way ANOVA with Tukey's post-test correction. *p<0.05 **p<0.01 ***p<0.001 ***p<0.0001.

3.3 Discussion

This project investigated the effect of cellular metabolic signalling on the innate inflammatory response in TB using *in vitro* experiments with primary human MDMs, as well as immunohistochemical analysis of lymph nodes from TB patients. The key findings from the cellular TB experiments are summarised in Figure 29.

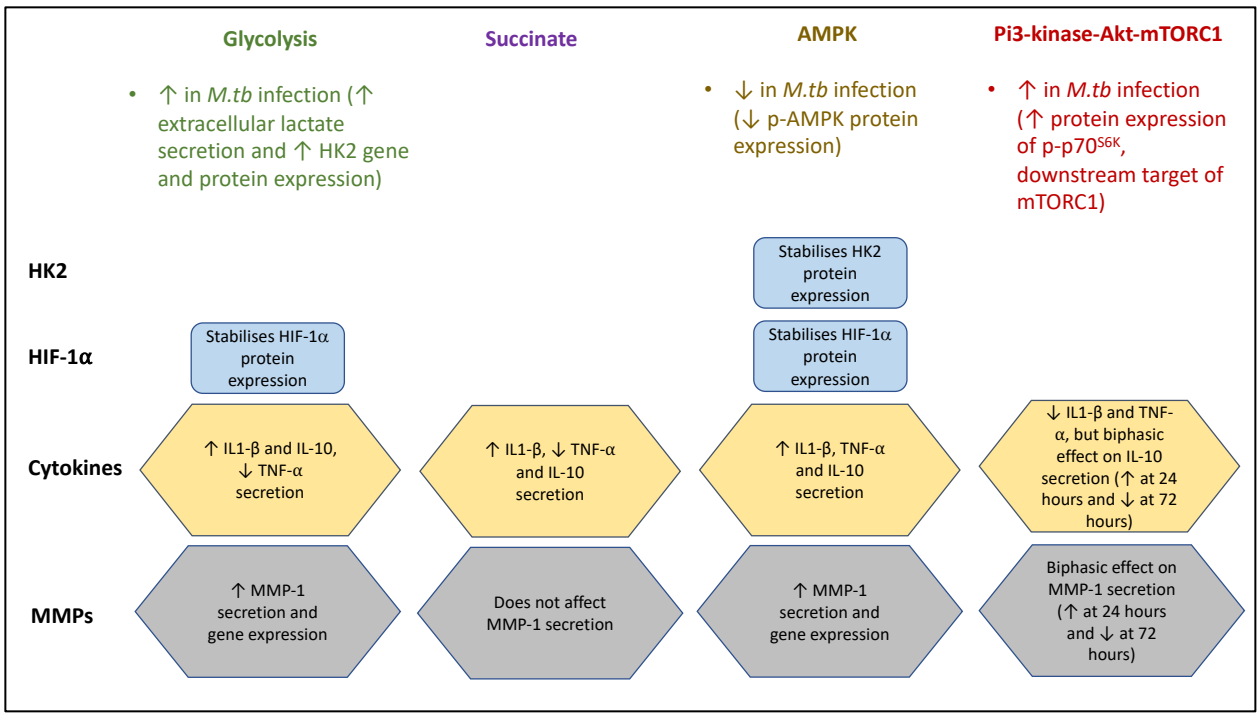


Figure 29: Summary of key findings from *in vitro* metabolic signalling experiments in *M.tb*-infected MDMs

First, I showed that *M.tb* favours a glycolytic profile in MDMs by demonstrating the upregulation of extracellular lactate secretion and HK2 gene and protein expression. Secreted lactate concentration is an indicator of intracellular glycolytic activity, as lactate MCTs are also upregulated in the Warburg effect in TB (322). These finding are consistent with data from detailed

Seahorse analysis of MDMs in TB showing metabolic reprogramming towards glycolysis (154,324,335)

I then demonstrated for the first time that glycolysis enhances mRNA accumulation and secretion of the key collagenase, MMP-1, which drives a tissue-destructive phenotype in TB (190). Sputum MMP-1 concentrations in TB patients correlate positively with clinical severity score (271), plasma PIIINP levels (272) and the degree of chest radiograph cavitation and infiltration (268). There is concurrent upregulation of the MMP-1 activators, MMP-3 and -10, as well as MMP-8, another vital collagenase in TB (383). Glycolysis, but not diethylsuccinate, also modulated TIMP -1 and -2 secretion, but only TIMP-1 secretion was upregulated in TB.

Glycolysis also stabilises the protein expression of the transcription factor HIF-1α, which is a crucial regulator of MMP-1 (259), as well as of pro-inflammatory glycolytic reprogramming (296) in TB. This finding supports the concept of an *M.tb*-induced positive feedback loop between HIF-1α and glycolysis which amplifies macrophage activation (335). Previous studies also showed that HIF-1α regulated IFN-γ-dependent control of bacterial growth and production of the pro-inflammatory cytokine IL-1β, NO and PGE2 in TB macrophages, while HIF-1α-deficient mice were highly susceptible to TB infection *in vivo* (335). Hence, HIF-1α may function as an immunometabolic co-ordinator in TB.

Secretion of IL-1β, though not TNF-α, is increased by glycolysis and cell-permeable diethylsuccinate, which is also consistent with previous studies (154,384). IL-1β plays a vital role in macrophage immune responses and is crucial for nitric oxide production, phagosomal acidification and maturation, and adhesion molecule expression (74). In murine models, IL-1β also regulates the granuloma formation, impairs *M.tb* proliferation, and induces other cytokines (150,151). Interestingly, IL-10 was downregulated by glycolysis in *M.tb*-infected MDMs in a

previous study (154), whereas it was upregulated in my cellular model. This difference may be attributable to the different pharmacological methods used for induction of glycolysis and perhaps a difference in dynamic polarisation state of the macrophages used. However, IL-10 was downregulated by diethylsuccinate in this study. Of note, glycolysis also upregulates EMMPRIN, which modulates lactate MCTs in addition to its role in MMP induction (330). I also showed that glycolysis impairs intracellular survival of *M.tb*, which corroborates previous studies (154,322,331).

Finally, I showed that HK2 is highly expressed in areas of granulomatous inflammation and tissue remodelling in human TB lymph nodes, with potent immunostaining of characteristic epithelioid macrophages and Langhans giant cells.

One limitation of these *in vitro* experiments was the reliance on chemical inhibition with 2DG, which has been reported to have off-target metabolic effects (385). In order to mitigate this, I attempted siRNA transfection of HK2 in MDMs, but, despite a high transfection efficiency, was technically unable to achieve HK2 gene knockdown. However, successful HK2 CRISPR-Cas9 knockout has recently been reported and might be an avenue for future research (386). I also attempted to use chemical inhibitors to investigate some of the other mediators in glycolysis and the TCA cycle, such as PFKB3, GLUT1, PKM2 and α-ketoglutarate, but the results were inconclusive. One interesting TCA cycle mediator to evaluate in future research is itaconate, which is currently showing novel immunomodulatory promise in *M.tb* infection (308).

I then proceeded to analyse MMP regulation by the master metabolic regulator AMPK and the key Pi3-kinase-Akt-mTOR signal transduction pathway in *M.tb*-infected MDMs. Protein expression of p-AMPK is partially downregulated in *M.tb*-infected MDMs. I showed that AMPK increases MMP-1 secretion at both 24 hours and 72 hours in *M.tb*-infected MDMs; MMP-1 gene expression is also upregulated at 24 hours. This is accompanied by an increase in secretion of

the pro-inflammatory cytokines IL-1β and TNF-α, as well as IL-10 at both 24 hours and 72 hours. In addition, AMPK stabilises HIF-1α and HK2 protein expression, suggesting that AMPK promotes glycolysis in *M.tb*-infected MDMs. Hence, AMPK fosters a pro-inflammatory milieu in *M.tb*-infected MDMs. These findings are consistent with previous data from our group, which showed that AMPK increases MMP-8 secretion from neutrophils, is present in human TB lung cavities and correlates with clinical and chest radiographic severity scores in TB patients (240). However, the AMPK inhibitor used, Compound C, has been shown to cause AMPK-independent effects *in vitro*, including inhibition of other kinases (387). Hence, it would be beneficial to confirm these findings with AMPK gene knockdown using siRNA or CRISPR-Cas9 gene editing techniques. Genetic inactivation of AMPK α1/α2 catalytic subunits by CRISPR-Cas9 has recently been described in human cell lines (388) and this could be adapted for TB immunometabolism studies. Metformin treatment of *M.tb*-infected MDMs results in a biphasic effect on MMP-1 secretion, with an increase at 24 hours and a decrease at 72 hours. Metformin also upregulates IL-1β at 24 hours and 72 hours, while TNF-α and IL-10 are upregulated at 24 hours and downregulated at 72 hours. These diverse findings might be related to AMPK-independent effects; metformin acts through several pathways including increased AMPK signalling; mitochondrial complex I inhibition; and decreased glucagon and mTORC1 signalling (104). Interestingly, my data is divergent from several murine and human studies, which have shown that metformin may improve clinical outcomes in TB (367,368). This anti-inflammatory effect of metformin was supported by a recent study in which metformin dampened pro-inflammatory cytokine production while promoting antimycobacterial processes such as phagocytosis and ROS production in TB; this was associated with an inhibition of the type 1 IFN pathway, a decrease in p-AKT and p-P38 signalling, and an increase in AMPK signalling (371). Another study showed that AMPK activation resulted in increased mitochondrial biogenesis and autophagy through peroxisome proliferator-activated receptor-γ coactivator (PGC)-1α, a downstream molecule of AMPK signalling involved in the antimicrobial immune

defence and phagosomal maturation against *M.tb* (361). Further research is required to elucidate the balance of AMPK-induced effector pathways in TB host immune responses.

Protein expression of $p70^{S6K}$, a downstream target of mTORC1, is upregulated in *M.tb*-infected MDMs. The Pi3-kinase-Akt-mTORC1 pathway has a biphasic effect on MMP-1 secretion in *M.tb*-infected MDMs, with an initial increase at 24 hours, followed by downregulation at 72 hours. This is consistent with previous data from our group showing that the Pi3-kinase-Akt-mTORC1 pathway negatively regulates MMP-1 in *M.tb*-infected MDMs at 72 hours (258). The Pi3-kinase-Akt-mTORC1 pathway downregulates secretion of the pro-inflammatory cytokines IL-1β and TNF-α at both 24 hours and 72 hours. mTORC1 is thought to inhibit pro-inflammatory cytokine production via its effect on NF-κB (374). However, it has a biphasic effect on the anti-inflammatory cytokine IL-10, with a downregulation at 24 hours and an upregulation at 72 hours.

Hence, in *M.tb*-infected MDMs, there is downregulation of p-AMPK, but upregulation of $p70^{S6K}$ protein expression. In addition, AMPK has a broadly positive and mTORC1 a broadly negative regulatory effect on MMP-1 and pro-inflammatory cytokines in *M.tb*-infected MDMs. This is consistent with the paradigm that AMPK and mTORC1 have elaborate reciprocal effects and the dynamic balance of activation of these metabolic mediators is linked to cellular immune effector functions.

To summarise, I demonstrated that cellular metabolic signalling regulates MMPs, pro-inflammatory cytokines and HIF-1α in *M.tb*-infected MDMs. HK2, the first and rate-limiting enzyme in glycolysis, was also expressed in areas of granulomatous necrosis in human TB lymph nodes. Hence, metabolic reprogramming is a fundamental regulatory strategy driving destructive immunopathology in TB. Greater understanding of immunometabolic mechanisms in TB is key to identifying new host-directed therapeutic targets.

Chapter 4. Metabolic pathways regulate MMPs in CoMTB-stimulated NHBEs

4.1 Introduction

In the previous chapter, I sought to elucidate the role of metabolic pathways in the regulation of MMPs in MDMs. I was then interested in investigating the effect of metabolic signalling on tissue destruction in airway epithelial cells (AECs), which play a crucial role in early host-pathogen interactions.

AECs are the most abundant cells in the respiratory tract and, are likely to be one of the first cells encountered by *M.tb* following aerosol inhalation. In addition to their well-established role in host barrier protection, there is increasing evidence that AECs are critical, active players in the innate immune response to *M.tb* infection. However, the interaction between *M.tb* and AECs is less well defined than the role of macrophages in *M.tb* infection.

Recognition of *M.tb* by PRRs on AECs triggers secretion of numerous cytokines, chemokines and AMPs leading to recruitment and activation of immune cells to facilitate bacterial clearance. TB is a paucibacillary disease in which the majority of *M.tb*-infected immune cells are macrophages. Global transcriptomic profiling shows that AEC are highly responsive to cytokine signals, such as IL-1β, from *M.tb*-infected macrophages, but relatively inert to direct *M.tb* infection (38). Hence, amplification of the innate immune response by facilitating efficient cross-talk with uninfected AECs is an important aspect of host defence.

Several *in vitro* studies have demonstrated that MMP-1, -3, -9 and -10 secretion from AECs is triggered by monocyte-dependent cytokine networks, though not direct *M.tb* infection (246–248). In patients, AECs adjacent to pulmonary TB granulomas show high expression of MMP-1, in contrast to uninfected lung tissue (246). In zebrafish model of *M. marinum*, ESAT-6 induces MMP-

9 secretion from epithelial cells adjacent to infected macrophages; this enhances macrophage recruitment, contributing to nascent granuloma maturation and bacterial growth (44).

There are limited data for the effect of cellular glucose metabolism on innate immune responses in AECs following infection. Recent studies have shown that certain respiratory viruses trigger metabolic reprogramming in AECs, including influenza A virus (IAV), respiratory syncytial virus, human metapneumovirus and human adenovirus (293,389–391). In IAV, HIF-1α knockdown promotes IAV replication in AECs by reducing glycolysis and augmenting AMPK-mediated autophagy (389). *Pseudomonas aeruginosa* also perturbs cellular bioenergetics and mitochondrial biogenesis in AECs (392). However, little is known about the role of glycolysis in AECs in regulating tissue destruction in TB. There is preliminary evidence that other signalling pathways such as p38 MAPK (246) and the Pi3-kinase pathway (248) regulate MMPs in CoMTB-stimulated AECs but, again, the mechanisms are not well understood.

In this chapter, I first aimed to investigate the presence of the key glycolysis enzyme, HK2, in lung tissue of a murine model of pulmonary TB. I then sought to analyse the *in vitro* effect of glycolysis and the TCA cycle intermediate, succinate, on MMP gene expression, secretion and functional matrix destruction in CoMTB-stimulated NHBEs. I also aimed to evaluate whether the key transcription factor, HIF-1α, is regulated by cellular glucose metabolism. Finally, I sought to assess the effect of the master metabolic regulator, AMPK, and the key Pi3-kinase signal transduction pathway on MMP production and function. For my *in vitro* experiments, I used primary NHBE cells (Lonza, Switzerland) stimulated with CoMTB to assess intercellular cytokine networks.

4.2 Results

4.2.1 HK2 is expressed in a murine model of pulmonary TB

I investigated the presence of HK2 in paraffin-embedded murine lung samples from Balb/C mice using immunohistochemistry (IHC). The murine samples were a kind gift from Dr Brian Robertson and Dr Nitya Krishnan. Scant HK2 expression was seen in peripheral lung tissue with limited *M.tb*-induced inflammation and preservation of normal alveolar structures (Figure 30A). In contrast, there was marked HK2 staining in areas of active inflammation, necrosis and immune cell infiltration, loss of normal alveolar architecture and destruction of alveolar walls (Figure 30B). HK2 staining in characteristic foam cells was especially prominent (arrows) (Figure 30C). HK2 was also expressed in bronchial airway epithelial cells in murine lung (arrows) (Figure 30D and 30E).

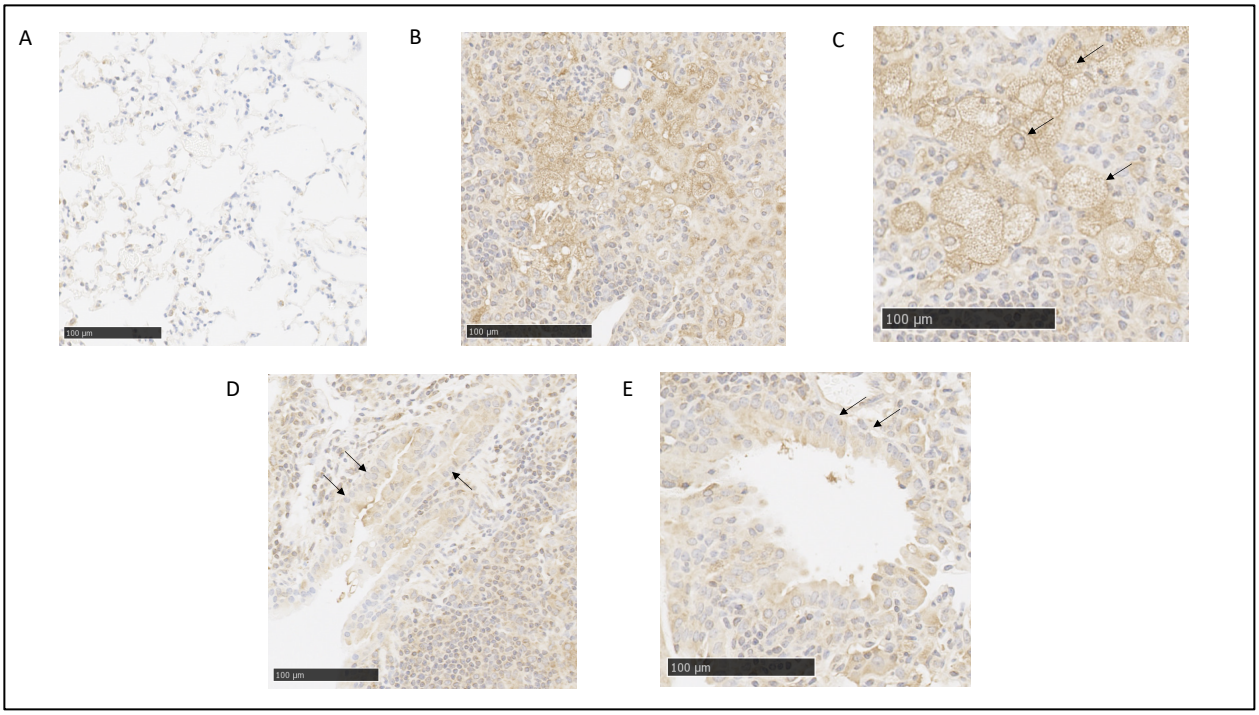


Figure 30: HK2 is expressed in lung tissue in a mouse model of pulmonary TB. HK2 IHC staining was performed on paraffin-embedded Balb/C murine lung samples harvested 56 days after *M.tb* infection. (A-E). (A) Weak HK2 staining was present in normal, peripheral lung tissue with limited *M.tb*-induced inflammation and tissue remodelling (B) Strong HK2 staining was seen in areas of active *M.tb*-induced inflammation, tissue remodelling and cell infiltration, with loss of normal alveolar architecture (C) HK2 staining was prominent in foamy macrophages (arrows). (D, E) HK2 expression was detected in bronchial epithelial cells (arrows). Images are from a single mouse and representative of 5 mice. Magnification 20x (A-C) and 30x (D, E). Scale 100µm.

4.2.2 HK2 gene and protein expression is upregulated in CoMTB-stimulated NHBEs

I was then interested in studying the metabolic regulation of MMPs in a human cellular model of primary NHBEs. In order to proceed, I was first keen to ascertain whether the enhanced expression of HK2 in mouse lung tissue was reflected *in vitro*. I performed a RT-PCR analysis and Western blot showing that HK2 gene and protein expression respectively is upregulated in CoMTB-stimulated NHBEs compared to unstimulated cells. HK2 gene expression was upregulated 0.6-fold ($p<0.05$) at 24 hours in CoMTB-stimulated NHBEs (Figure 31A), while there was increased protein expression of HK2 at 4, 8, 24 and 48 hours (Figure 31B). The phenomenon of an *M.tb*-induced metabolic shift to cellular glycolysis in NHBEs is supported by upregulation of this key glycolytic enzyme.

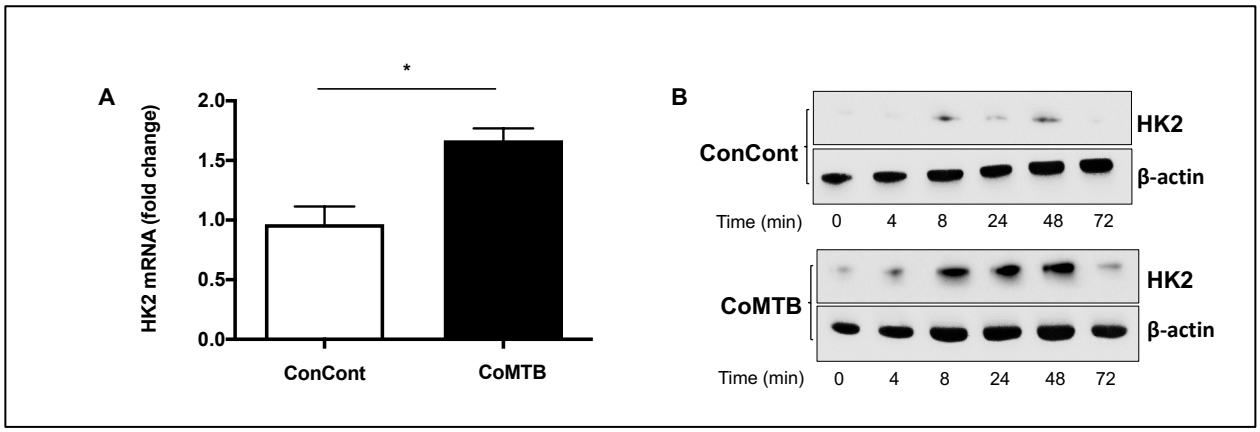


Figure 31: HK2 gene and protein expression are upregulated in CoMTB-stimulated NHBEs. NHBEs were stimulated with CoMTB and HK2 was detected by (A) RT-PCR and (B) Western blot. (A) HK2 gene expression was upregulated at 24 hours in CoMTB-stimulated NHBEs on RT-PCR. Bars show mean ± SD of 3 technical replicates of a single independent experiment and are representative of 3 independent experiments. Statistical analysis was performed using an ordinary one-way ANOVA with Tukey's post-test correction. *$p<0.05$. (B) HK2 protein expression was upregulated at 4, 8, 24 and 48 hours in CoMTB-stimulated NHBEs on Western blot. The blot image shows a single independent experiment and is representative of 2 independent experiments.

4.2.3 Glycolysis upregulates MMP-1 secretion and gene expression in CoMTB-stimulated NHBEs

NHBEs were pre-treated with the glycolysis inhibitor 2DG for 2 hours prior to stimulation with CoMTB or ConCont and secretion and matrix degradation analysis was performed at 72 hours post-stimulation. Kinetic data showed that CoMTB only induced a 1.7-fold increase in MMP-1 secretion at 48 hours, whereas CoMTB stimulated a 6-fold increase in MMP-1 secretion at 72 hours compared to ConCont (Figure 32A). In CoMTB-treated NHBEs, 2DG significantly downregulated MMP-1 secretion at 72 hours in a dose-dependent manner ($p \leq 0.0001$) (Figure 32B). There was a 7-fold reduction in MMP-1 secretion from 5852 ± 1090 pg/ml to to 774 ± 17.36 pg/ml ($p<0.0001$). I then assessed if the 2DG-mediated downregulation of MMP-1 was reflected at the level of gene expression (Figure 32C). 2DG induced a significant 4-fold decrease in MMP-1 gene expression in CoMTB-stimulated NHBEs at 24 hours ($p<0.001$). In order to ensure that the decrease in MMP-1 secretion and gene expression was not artefactual due to 2DG-induced cell death, an LDH cytotoxicity assay was performed. This confirmed that NHBE viability was >90% in all experimental conditions relative to unstimulated cells at 72 hours (Figure 32D). Having established that glycolysis upregulates gene expression and secretion of MMP-1, the key collagenase in TB, I was then assessed its effect on the major gelatinase, MMP-9.

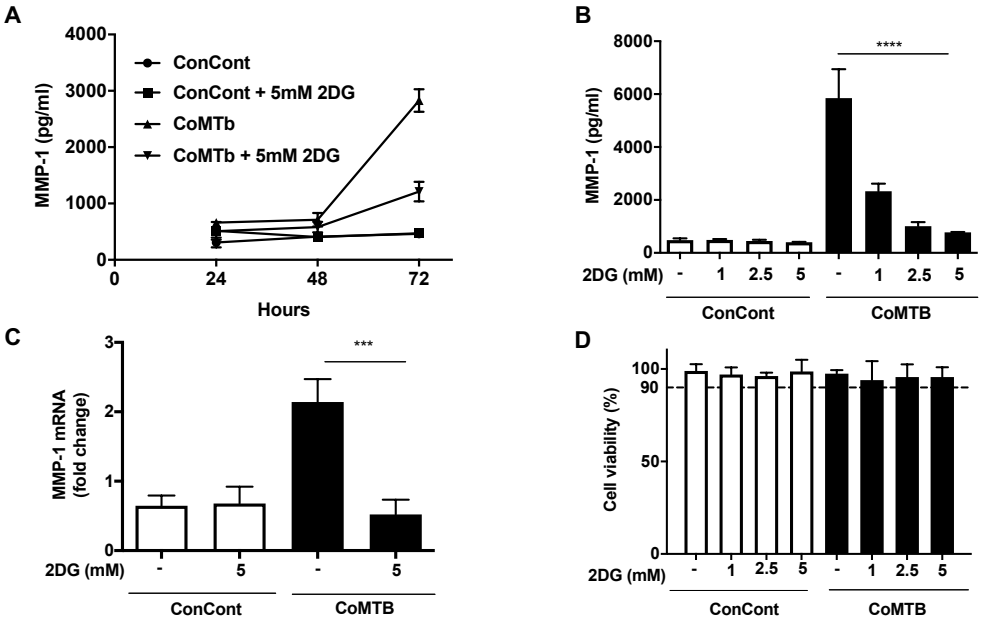


Figure 32: Glycolysis upregulates MMP-1 gene expression and secretion in CoMTB-stimulated NHBEs. NHBEs were stimulated with CoMTB or ConCont, with or without pre-treatment with 2DG for 2 hours. MMP-1 was detected by (A, B) ELISA and (C) RT-PCR. (A) MMP-1 secretion from CoMTB-stimulated NHBEs compared to ConCont-stimulated NHBEs was greater at 72 hours than at 24 or 48 hours. (B) 2DG significantly downregulated MMP-1 secretion in a dose-dependent manner in CoMTB-stimulated NHBEs at 72 hours. (C) 2DG significantly decreased MMP-1 gene expression in CoMTB-stimulated NHBEs at 24 hours. (D) LDH cytotoxicity assay shows that cell viability was >90% relative to unstimulated cells in all experimental conditions at 72 hours. Data points and bars show mean ± SD of 3 technical replicates of a single independent experiment and are representative of 3 independent experiments. Statistical analysis was performed using an ordinary one-way ANOVA with Tukey's post-test correction. ***$p<0.001$ ****$p<0.0001$.

4.2.4 Glycolysis upregulates MMP-9 secretion, functional activity and gene expression in CoMTB-stimulated NHBEs

I proceeded to analyse the effect of 2DG on MMP-9 secretion at 72 hours in CoMTB-stimulated NHBEs. There was a marked 7-fold, dose-dependent fall in MMP-9 secretion from 601698 ± 88006 pg/ml to 82676 ± 11995 pg/ml ($p<0.0001$) in 2DG-treated, CoMTB-stimulated NHBEs compared to CoMTB alone (Figure 33A). Gelatin zymography confirmed a 2DG-induced reduction in the amount of functionally active MMP-9 in CoMTB-stimulated NHBEs (Figure 33B). 2DG and COMTB stimulation also decreased MMP-9 gene expression by 2.7-fold in in NHBEs, compared to CoMTB alone (Figure 33C). Hence, glycolysis also potently upregulates the gene expression and secretion of MMP-9.

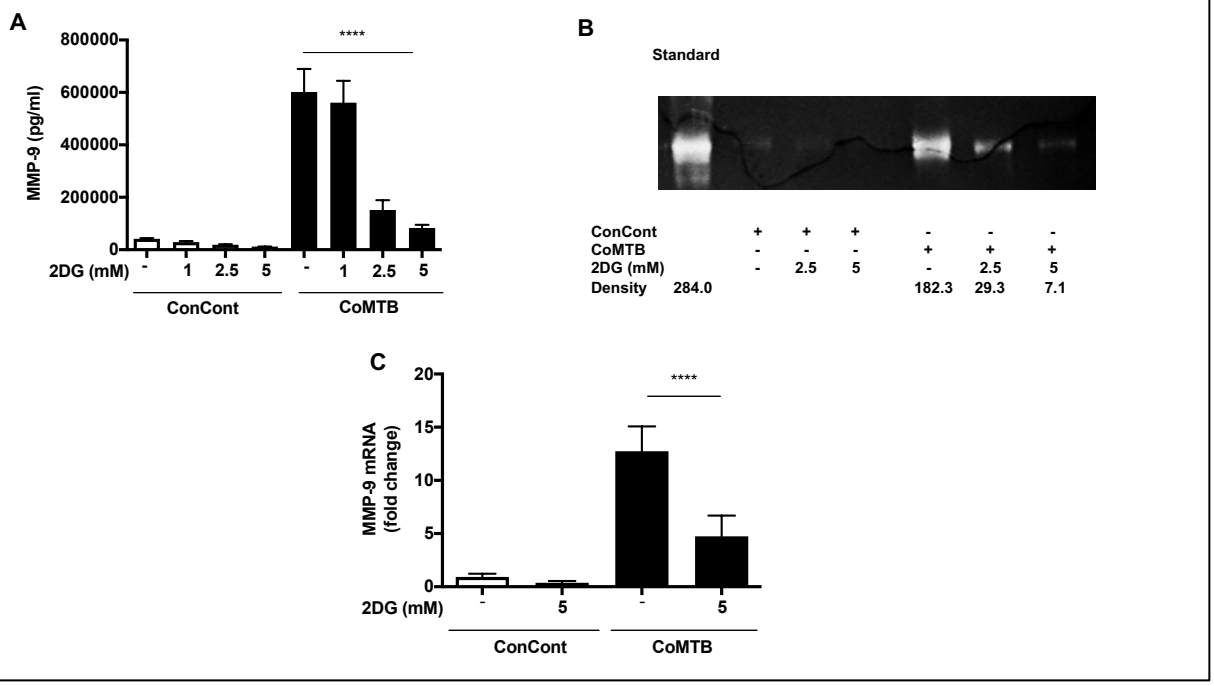


Figure 33: Glycolysis upregulates MMP-9 secretion, functional activity and gene expression in CoMTB-stimulated NHBEs. NHBEs were stimulated with CoMTB or ConCont, with or without pre-treatment with 2DG for 2 hours. MMP-9 was detected by (A) ELISA, (B) gelatin zymography or (C) RT-PCR. (A) 2DG significantly downregulated MMP-9 secretion in a dose-dependent manner in CoMTB-stimulated NHBEs at 72 hours. (B) 2DG decreased the amount of functionally active MMP-9 in CoMTB-stimulated NHBEs at 72 hours. (C) 2DG significantly decreased MMP-9 gene expression in CoMTB-stimulated NHBEs at 24 hours. Bars show mean ± SD of 3 technical replicates of a single independent experiment and are representative of 3 independent experiments. Statistical analysis was performed using an ordinary one-way ANOVA with Tukey's multiple comparison test. ****$p<0.0001$. The gelatin zymogram image shows a single independent experiment and is representative of 2 independent experiments.

4.2.5 Glycolysis upregulates MMP-2, MMP-3, MMP-8 and MMP-10 secretion in CoMTB-stimulated NHBEs

I then went on to evaluate the role of glycolysis in the secretion of additional MMPs that are upregulated in TB and contribute to its pathogenesis. Of particular interest were MMP-3 and -10, which can regulate MMP-1. HK inhibition with 2DG resulted in downregulation of the gelatinase MMP-2, the collagenase, MMP-8, and the stromelysins MMP-3 and -10 in CoMTB-stimulated NHBEs. Hence, MMP secretion in TB is widely and significantly upregulated by glycolysis. MMP-2 secretion was reduced 2.3-fold, from 3777 ± 138.8 pg/ml to 1675 ± 101.6 pg/ml ($p<0.0001$) (Figure 34A), MMP-3 secretion 10.5-fold, from 3596 ± 251.3 pg/ml to 345 ± 10.7 pg/ml ($P<0.0001$) (Figure 34B), MMP-8 secretion 2.3-fold, from 631.8 ± 64.9 pg/ml to 280.6 ± 23.4 pg/ml ($p<0.0001$) (Figure 34C) and MMP-10 secretion 3.9-fold, from 7499 ± 269.8 pg/ml to 1932 ± 101 pg/ml ($p<0.0001$) (Figure 34D).

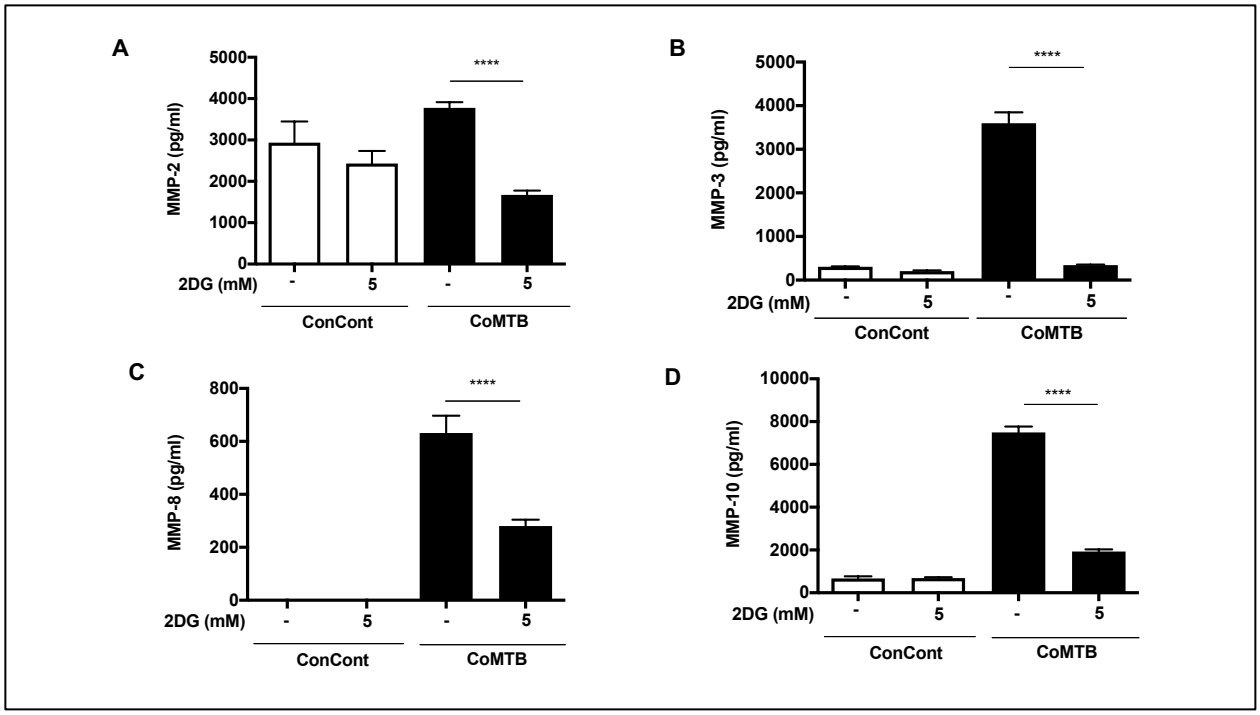


Figure 34: Glycolysis upregulates MMP-2, MMP-3, MMP-8 and MMP-10 secretion in CoMTB-stimulated NHBEs. NHBEs were stimulated with CoMTB or ConCont, with or without pre-treatment with 2DG for 2 hours. MMPs were detected by Luminex array. In CoMTB-stimulated NHBEs (A) MMP-2, (B) MMP-3, (C) MMP-8 and (D) MMP-10 secretion was significantly downregulated by 2DG at 72 hours. Bars show mean ± SD of 3 technical replicates of a single independent experiment and are representative of 3 independent experiments. Statistical analysis was performed using an ordinary one-way ANOVA with Tukey's post-test correction. ****$p<0.0001$.

4.2.6 Glycolysis upregulates TIMP secretion in CoMTB-stimulated NHBEs

I was then interested in the effect of glycolysis on TIMPs, which inhibit MMPs. CoMTB stimulation and HK inhibition with 2DG had divergent effects on TIMP-1 and TIMP-2 secretion. TIMP-1 baseline secretion was 4642 ± 660.7 pg/ml in ConCont-stimulated NHBEs, with no significant difference in CoMTB-stimulated NHBEs (Figure 35A). However, 2DG treatment reduced TIMP-1 secretion in both ConCont and CoMTB-stimulated NHBEs 2.7-fold ($p<0.0001$) and 1.5-fold ($p<0.05$) respectively (Figure 35A). TIMP-2 secretion, however, was significantly upregulated 4-fold ($p<0.001$) in CoMTB-stimulated NHBEs compared to baseline, then reduced 15-fold ($p<0.001$) by 2DG treatment (Figure 35B). However, despite this potent decrease, the TIMP-2 secretion concentrations were low, at 390 ± 69.46 pg/ml with CoMTB stimulation, decreased to 25.56 ± 11.34 pg/ml after 2DG treatment. Of note, TIMP-1 was secreted at higher concentrations than TIMP-2. Hence, although only TIMP-2 secretion was upregulated in CoMTB-stimulated NHBEs, glycolysis increased both TIMP-1 and TIMP-2 secretion.

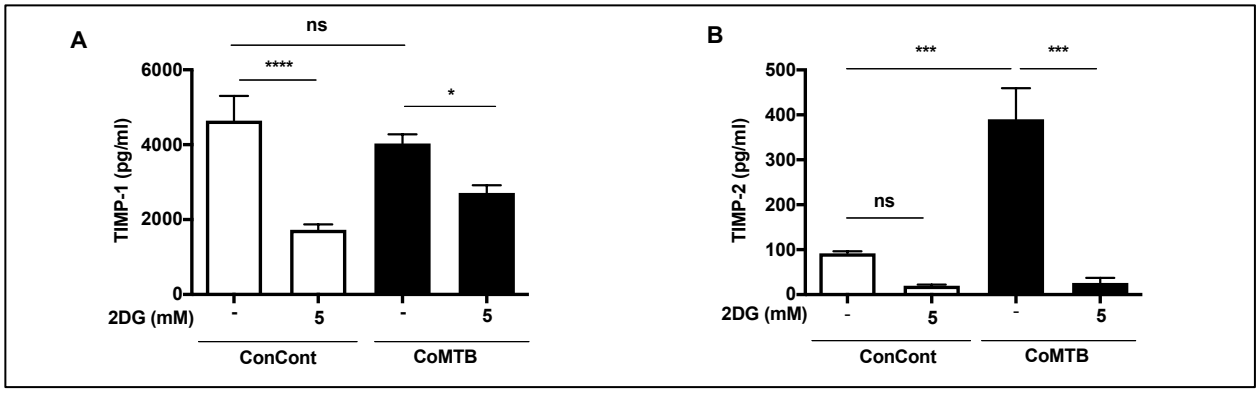


Figure 35: Glycolysis upregulates TIMP secretion in CoMTB-stimulated NHBEs. NHBEs were stimulated with CoMTB or ConCont, with or without pre-treatment with 2DG for 2 hours. TIMP-1 and TIMP-2 were detected by ELISA. (A) There was no significant difference in TIMP-1 secretion in NHBEs stimulated with CoMTB or ConCont. 2DG reduced TIMP-1 concentrations in both conditions. (B) There was significant upregulation of TIMP-2 secretion in CoMTB-stimulated NHBEs, which was decreased by 2DG. Bars show mean ± SD of 3 technical replicates of a single independent experiment and are representative of 3 independent experiments. Statistical analysis was performed using an ordinary one-way ANOVA with Tukey's post-test correction. ns not significant, *p<0.05, ***p<0.001, ****p<0.0001

4.2.7 Glycolysis upregulates a functional increase in collagenase and gelatinase activity in CoMTB-stimulated NHBEs

ECM degradation in TB is driven by the collagenase, MMP-1 and the gelatinase, MMP-9. In light of the glycolysis-induced increase in MMP-1 and -9 secretion and gene expression, I then evaluated whether glycolysis regulated functional matrix degradation activity in CoMTB-stimulated NHBEs. To determine this, I performed assays using DQ collagen and DQ gelatin, which gain fluorescence on degradation, measured in relative fluorescent units (RFU). 2DG downregulated Type 1 collagenase activity 3-fold from 74132 ± 3005 RFU to 24775 ± 322.5 RFU ($p<0.0001$) in CoMTB-stimulated NHBEs at 72 hours (Figure 36A). 2DG significantly downregulated gelatinase activity 7.8-fold from 133545 ± 3250 RFU to 17027 ± 2227 RFU ($p<0.0001$) in CoMTB-stimulated NHBEs at 72 hours (Figure 36B). Hence the upregulation of MMP-1 and -9 by glycolysis is reflected at a functional level of tissue destruction.

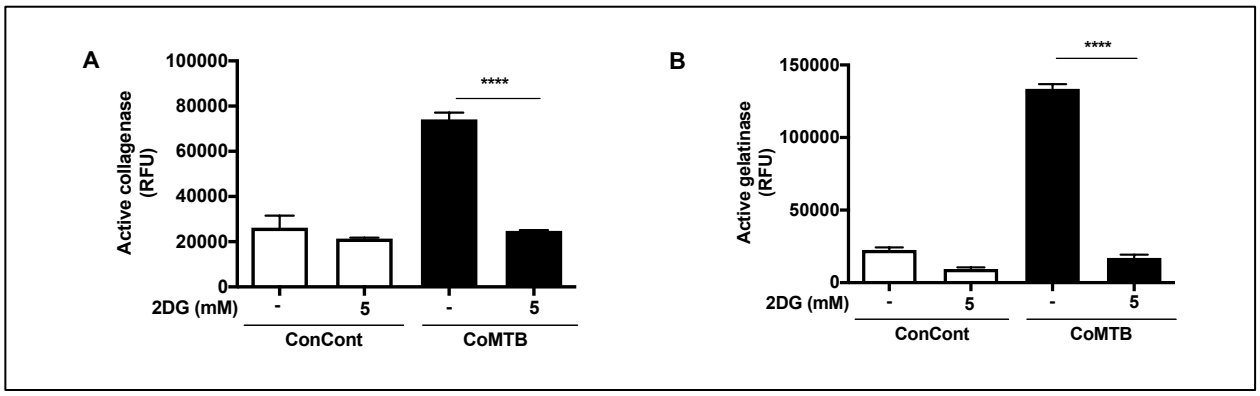


Figure 36: Glycolysis upregulates functional collagenase and gelatinase activity in CoMTB-stimulated NHBEs. NHBEs were stimulated with CoMTB or ConCont, with or without pre-treatment with 2DG for 2 hours. Type 1 collagenase and gelatinase activity was detected by fluorescent degradation of DQ collagen and DQ gelatin respectively and quantified in relative fluorescent units (RFU). 2DG downregulated (A) Type 1 collagenase activity and (B) gelatinase activity in CoMTB-stimulated NHBEs. Bars show mean ± SD of 3 technical replicates of a single independent experiment and are representative of 3 independent experiments. Statistical analysis was performed using an ordinary one-way ANOVA with Tukey's post-test correction. ****$p<0.0001$.

4.2.8 siRNA interference of HK2 downregulates MMP-9 gene expression in CoMTB-stimulated NHBEs

Although 2DG has been extensively used as a specific and competitive HK inhibitor, it can also have off-target metabolic effects. Hence, it was important to confirm the effect of glycolysis inhibition on MMPs in CoMTB-stimulated NHBEs by HK siRNA gene knockdown. The HK2 isoenzyme has been shown to be key modulator of aerobic glycolysis in transcriptomic analysis of murine and human models of TB (322,325). In addition to HK2 siRNA, I used a non-targeting (NT) siRNA as a control. The transfection efficiency achieved was 94.3% using Lipofectamine® 2000 (Invitrogen, UK) transfection reagent, as measured by flow cytometry (BD FACSCalibur™, Becton Dickinson, UK) using fluorescent (FAM)-labelled siRNA (Dharmacon, UK) (Figures 37A and 37B). HK2 siRNA knockdown decreased the protein expression of HK2 on Western blot (Figure 37C) and downregulated HK2 mRNA to 17% of that seen in control cells (Figure 37D). siRNA knockdown reduced the gene expression of MMP-9 2.6-fold ($p<0.0001$) (Figure 37F) compared to unstimulated cells in CoMTB-stimulated NHBEs, similar to the results seen following chemical inhibition with 2DG. However, I was unable to replicate the pattern of 2DG-induced downregulation with MMP-1 with HK2 siRNA transfection (Figure 37E).

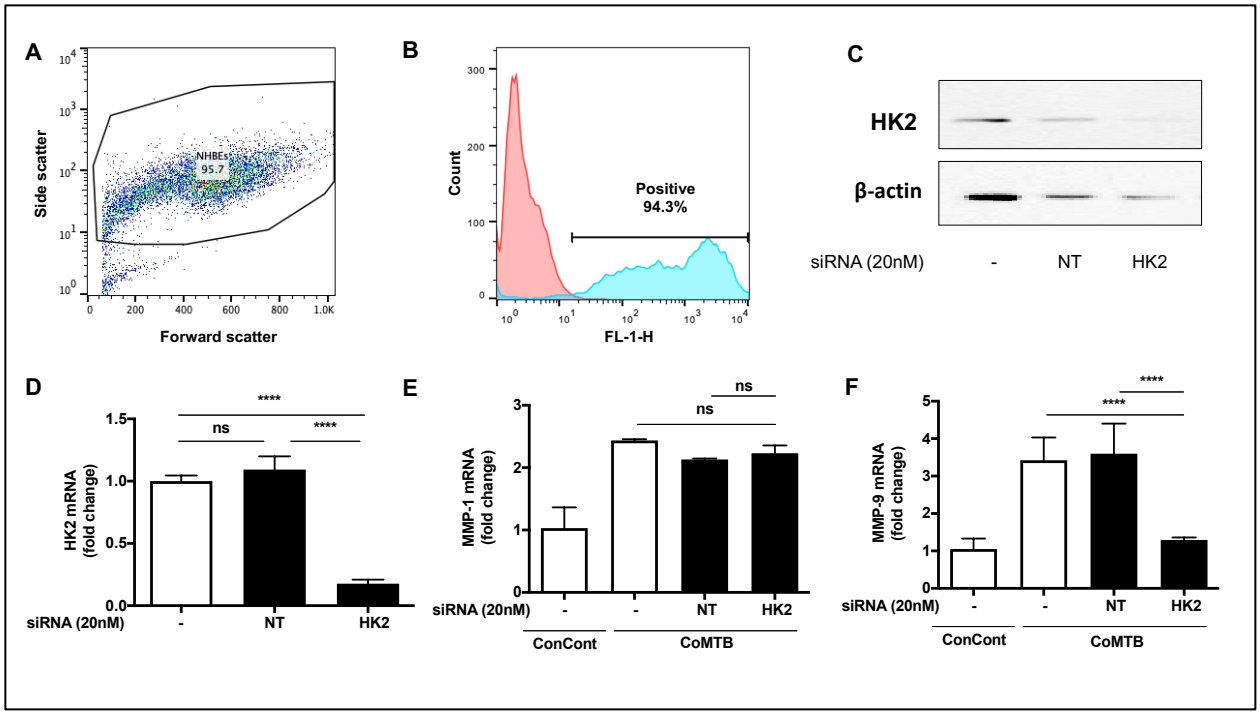


Figure 37: siRNA interference of HK2 downregulates MMP-9 gene expression in ComTB-stimulated NHBEs. NHBEs were treated with 20nm non-targeting (NT) or HK2 siRNA prior to treatment with CoMTB or ConCont. (A, B) siRNA transfection efficiency was measured to be 94.3% by FACS. Following siRNA treatment, (C) Western blot confirmed knockdown of HK2 protein expression and (D) PCR confirmed knockdown of HK2 gene expression. (E) There was no reduction in MMP-1 gene expression with siRNA interference of HK2 in CoMTB-stimulated NHBEs. (F) MMP-9 gene expression was significantly downregulated in CoMTB-stimulated NHBEs. Bars show mean ± SD of 3 technical replicates of a single independent experiment and are representative of 3 independent experiments. Statistical analysis was performed using an ordinary one-way ANOVA with Tukey's post-test correction. ns not significant, ****p<0.0001. The blot image shows a single independent experiment and is representative of 2 independent experiments.

4.2.9 Diethylsuccinate increases MMP-1 and MMP-9 secretion and gene expression in CoMTB-stimulated NHBEs

In addition to the role of glycolysis, I was interested in the effect of the TCA cycle intermediate, succinate, on MMPs in TB, succinate accumulation has been shown to mediate the Warburg effect via HIF-1α (296). I investigated whether diethylsuccinate, the cell-permeable form of succinate, is a modulator of MMPs in TB. Diethylsuccinate upregulated MMP-1 and -9 secretion in a dose-dependent manner in CoMTB-stimulated NHBEs at 72 hours. MMP-1 secretion increased 3.8-fold from 4121 ± 724 pg/ml to 15733 ± 1330 pg/ml ($p<0.0001$) (Figure 38A), while MMP-9 secretion increased 3.2-fold from 52809 ± 8204 pg/ml to 169060 ± 21063 pg/ml ($p<0.0001$) (Figure 38B). Although the fold changes were similar, MMP-9 is secreted in much greater concentrations in NHBEs upon CoMTB stimulation. This pattern of secretion was reflected at the level of gene expression; diethylsuccinate upregulated MMP-1 2.2-fold ($p<0.0001$) (Figure 38C) and MMP-9 1.6-fold ($p<0.001$) (Figure 38D) in CoMTB-stimulated NHBEs at 24 hours.

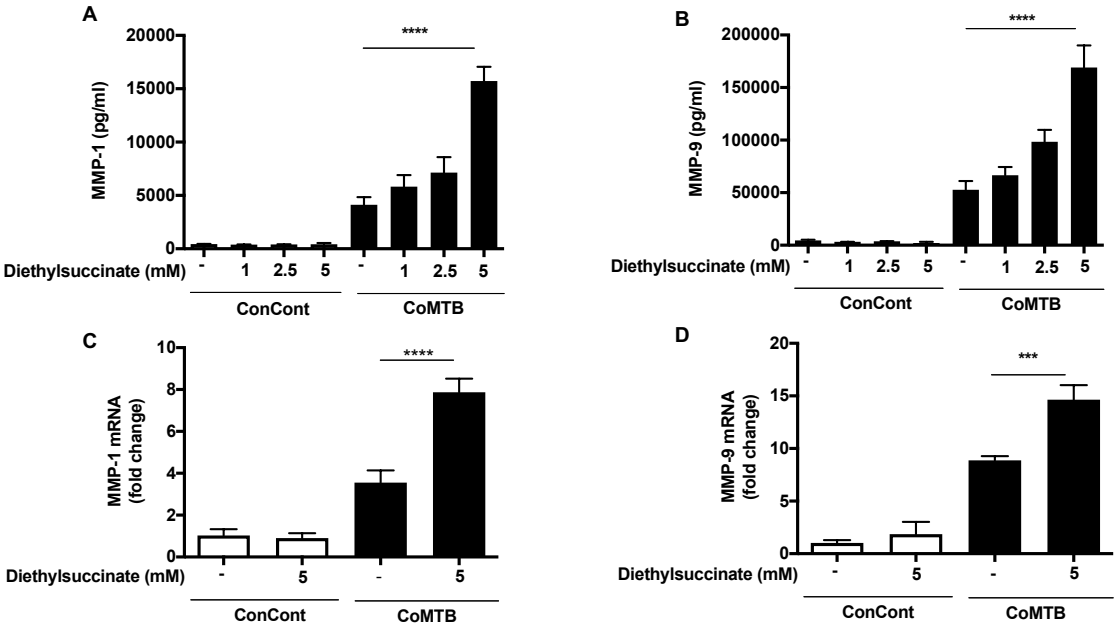


Figure 38: Diethylsuccinate upregulates MMP-1 and MMP-9 secretion and gene expression in CoMTB-stimulated NHBEs. NHBEs were stimulated with CoMTB or ConCont, with or without pre-treatment with diethylsuccinate for 2 hours. MMP-1 was detected by (A, B) ELISA or (C, D) RT-PCR. Diethylsuccinate significantly upregulated (A) MMP-1 and (B) MMP-9 secretion in a dose-dependent manner in CoMTB-stimulated NHBEs at 72 hours. Diethylsuccinate significantly upregulated (C) MMP-1 and (D) MMP-9 gene expression in CoMTB-stimulated NHBEs at 24 hours Bars show mean ± SD of 3 technical replicates of a single independent experiment and are representative of 3 independent experiments. Statistical analysis was performed using an ordinary one-way ANOVA with Tukey's post-test correction. ***p<0.001 ****p<0.0001.

4.2.10 Diethylsuccinate downregulates MMP-3 but upregulates MMP-10 secretion in CoMTB-stimulated NHBEs

I then ascertained the breadth of diethylsuccinate MMP regulation in TB by performing a Luminex assay. Diethylsuccinate decreased MMP-3 secretion 2-fold, from 1608 ± 58.7 pg/ml to 792 ± 44.5pg/ml ($p<0.0001$) (Figure 39B) and increased MMP-10 secretion 1.3-fold, from 8133 ± 290.1 pg/ml to 10267 ± 564.4 pg/ml in CoMTB-stimulated NHBEs ($p<0.01$) (Figure 39D). However, it had no effect on MMP-2 (Figure 39A) and MMP-8 (Figure 39B) secretion.

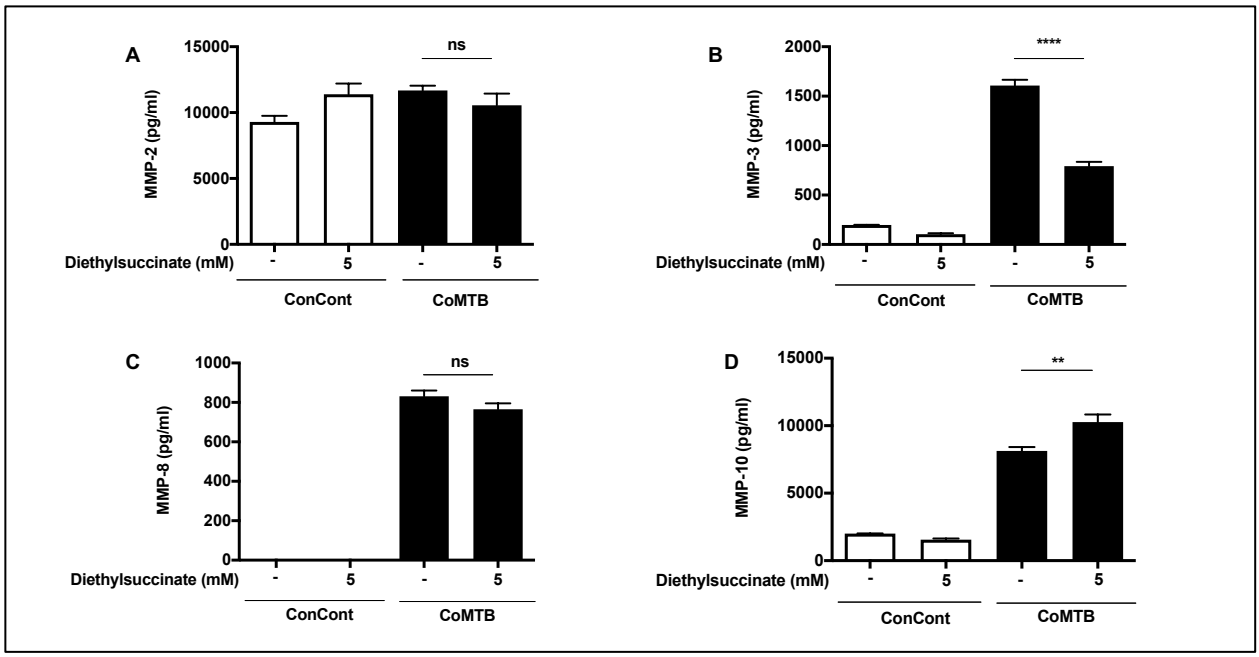


Figure 39: Diethylsuccinate regulates MMP-3 and MMP-10 secretion in CoMTB-stimulated NHBEs. NHBEs were stimulated with CoMTB or ConCont, with or without pre-treatment with diethylsuccinate for 2 hours. MMPs were detected by Luminex array. In CoMTB-stimulated NHBEs, diethlysuccinate (B) significantly downregulated MMP-3 secretion and (D) significantly upregulated MMP-10 secretion, but had no effect on (A) MMP-2 secretion or (C) MMP-8 secretion in CoMTB-stimulated NHBEs at 72 hours. Bars show mean ± SD of 3 technical replicates of a single independent experiment and are representative of 3 independent experiments. Statistical analysis was performed using an ordinary one-way ANOVA with Tukey's multiple comparison test. ns not significant, **$p<0.01$, ****$p<0.0001$.

4.2.11 Diethylsuccinate does not regulate TIMP secretion in CoMTB-stimulated NHBEs

I then went on to evaluate the role of diethylsuccinate in regulating TIMP secretion. TIMP-2 secretion was increased 9-fold from baseline by *M.tb* infection ($p<0.001$) (Figure 40B), but diethylsuccinate had no effect on secretion of TIMP-1 (Figure 40A) or TIMP-2 (Figure 40B).

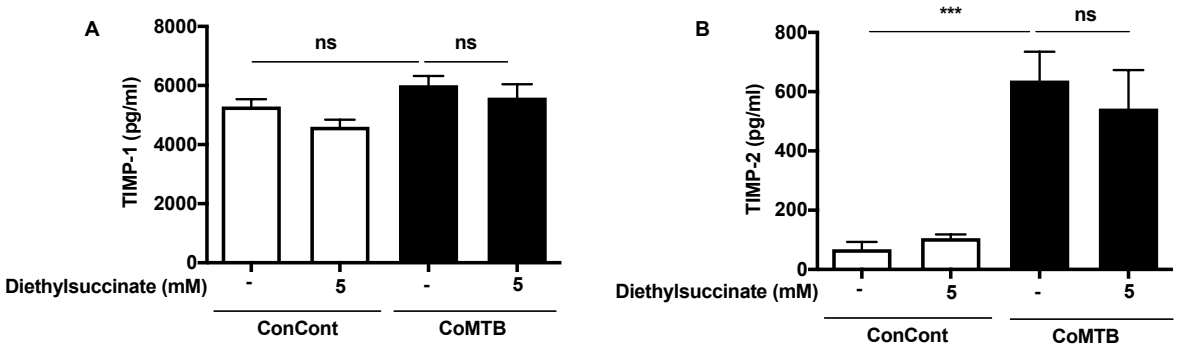


Figure 40: Diethylsuccinate does not regulate TIMP secretion in CoMTB-stimulated NHBEs. NHBEs were stimulated with CoMTB or ConCont, with or without pre-treatment with diethylsuccinate for 2 hours. TIMP-1 and -2 were detected by ELISA. (A) There was no significant difference in TIMP-1 secretion in NHBEs stimulated with CoMTB or ConCont. Diethylsuccinate did not affect TIMP-1 concentrations. (B) There was significant upregulation of TIMP-2 secretion in CoMTB-stimulated NHBEs, but diethylsuccinate did not affect TIMP-2 concentrations. Bars show mean ± SD of 3 technical replicates of a single independent experiment and are representative of 3 independent experiments. Statistical analysis was performed using an ordinary one-way ANOVA with Tukey's post-test correction. ns not significant ***$p<0.001$.

4.2.12 Diethylsuccinate upregulates a functional increase in collagenase and gelatinase activity in CoMTB-stimulated NHBEs

In order to assess the functional effect of diethylsuccinate, I then investigated if supernatants from CoMTB-stimulated NHBEs degraded fluorescent-labelled Type 1 DQ collagen and DQ gelatin following diethylsuccinate treatment. There was a significant upregulation of both Type 1 collagenase and gelatinase activity with diethylsuccinate. Active collagenase was increased 1.4-fold from 70097 ± 2570 RFU to 96283 ± 7363 RFU ($p<0.001$) (Figure 41A), while active gelatinase was increased 1.7-fold, from 128294 ± 9444 RFU to 216945 ± 6276 RFU (Figure 41B). This is consistent with the secretory pattern for MMP-1 and MMP-9 respectively.

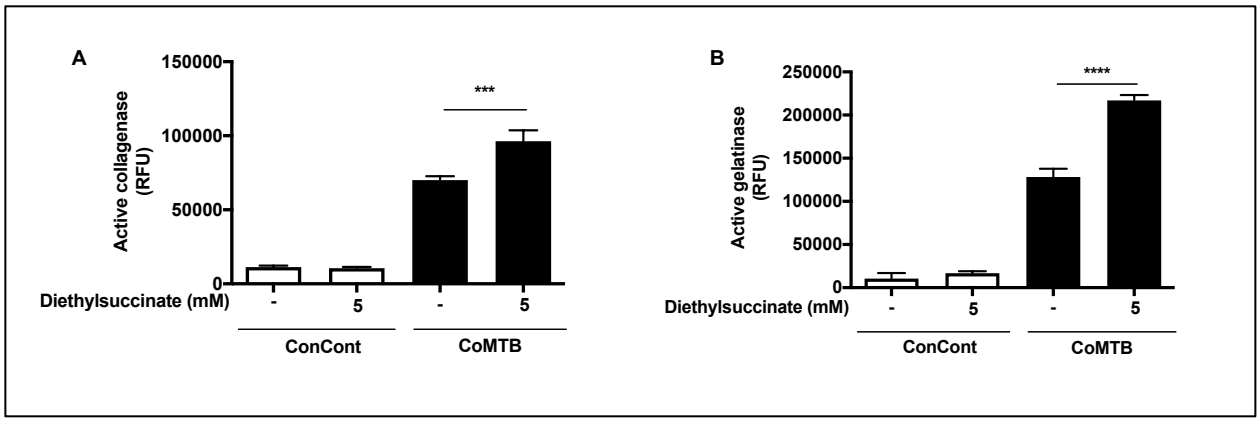


Figure 41: Diethylsuccinate upregulates functional collagenase and gelatinase activity in CoMTB-stimulated NHBEs. NHBEs were stimulated with CoMTB or ConCont, with or without pre-treatment with diethylsuccinate for 2 hours. Type 1 collagenase and gelatinase activity was detected by fluorescent degradation of DQ collagen and DQ gelatin respectively and quantified in relative fluorescent units (RFU). Diethylsuccinate upregulates (A) Type 1 collagenase activity and (B) gelatinase activity in CoMTB-stimulated NHBEs. Bars show mean ± SD of 3 technical replicates of a single independent experiment and are representative of 3 independent experiments. Statistical analysis was performed using an ordinary one-way ANOVA with Tukey's post-test correction. ***$p<0.001$ ****$p<0.0001$.

4.2.13 Diethylsuccinate upregulates HIF-1α *expression* in CoMTB-stimulated NHBEs

I then examined the expression of HIF-1α, the pivotal transcription factor in cellular metabolic reprogramming of macrophages, as I was interested to see if it was also upregulated in AECs (296). In addition, HIF-1α has also been shown to regulate MMP secretion in TB in both normoxia and hypoxia (259). CoMTB upregulated the expression of HIF-1α at 8 hours in NHBEs. HIF-1α expression was further stabilised at 4, 8 and 24 hours following diethylsuccinate treatment of CoMTB-stimulated NHBEs (Figure 42).

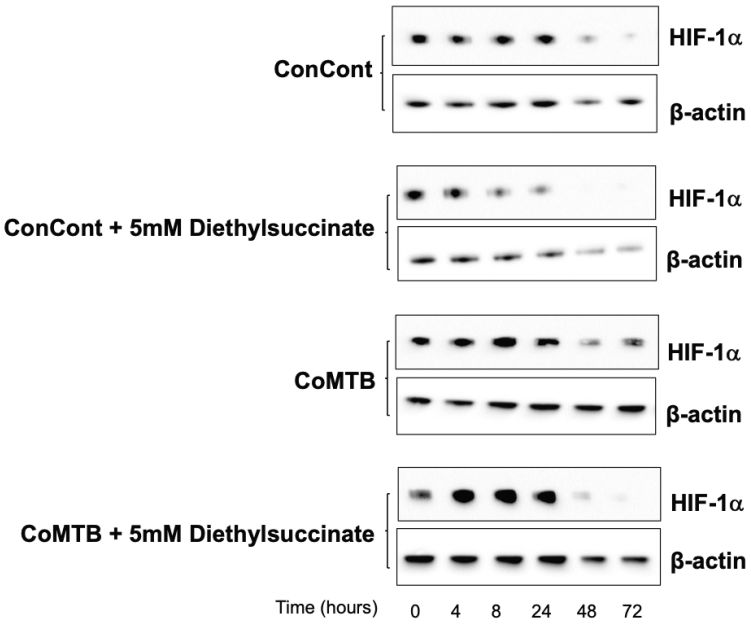


Figure 42: Diethylsuccinate stabilises HIF-1α expression in CoMTB-stimulated NHBEs. NHBEs were stimulated with CoMTB or ConCont, with or without pre-treatment with diethylsuccinate for 0, 4, 8, 24, 48 and 72 hours. Cell lysates were collected and HIF-1α and β-actin protein detected by Western blot. CoMTB alone upregulated HIF-1 expression at 8 hours. HIF-1α expression was further stabilised by diethylsuccinate at 4, 8 and 24 hours in CoMTB-stimulated NHBEs. The blot image shows a single independent experiment and is representative of 2 independent experiments.

4.2.14 AMPK upregulates MMP-1 and MMP-9 secretion and gene expression in CoMTB-stimulated NHBEs

Next, I assessed the role of the master metabolic regulator, AMPK in MMP regulation in CoMTB-stimulated NHBEs. Inhibition of AMPK with the specific chemical inhibitor, Compound C, downregulated MMP-1 and -9 secretion in a dose-dependent manner in CoMTB-stimulated NHBEs at 72 hours, with a particularly dramatic effect on MMP-9. MMP-1 secretion fell 1.6-fold from 16343 ± 635.7 pg/ml with CoMTB alone to 10537±1001 pg/ml with CoMTB stimulation and 10μM of Compound C ($p<0.0001$) (Figure 43A). MMP-9 secretion decreased 11-fold from 46025 ± 6833 pg/ml with CoMTB alone to 4259 ± 796.1 pg/ml with CoMTB stimulation and 10μM of Compound C ($p<0.0001$) (Figure 43B). This was reflected intracellularly at the level of gene expression, with a 4.6-fold and 65-fold decrease in MMP-1 ($p<0.0001$) (Figure 43C) and MMP-9 ($p<0.01$) (Figure 43D) mRNA respectively, with 10μM of Compound C in the presence of CoMTB compared to CoMTB stimulation alone. Hence, AMPK upregulates MMP-1 and -9 secretion and gene expression in TB.

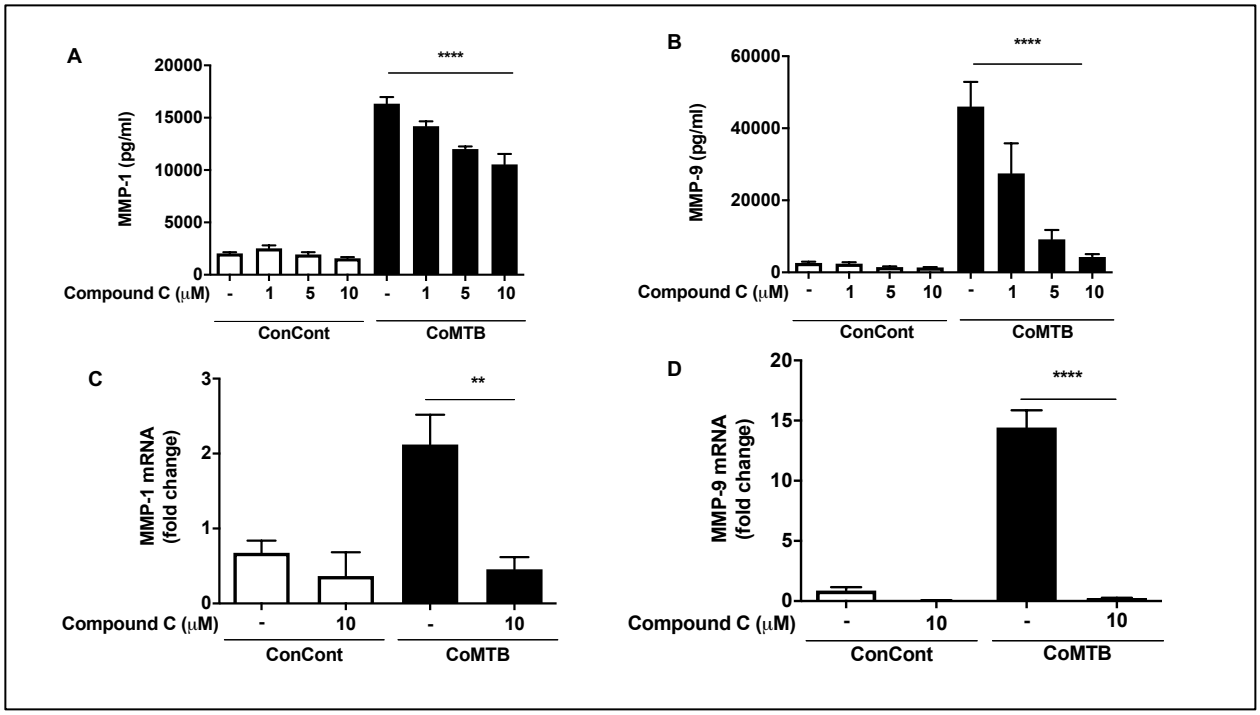


Figure 43: AMPK upregulates MMP-1 and MMP-9 gene expression and secretion in CoMTB-stimulated NHBEs. NHBEs were stimulated with CoMTB or ConCont, with or without pre-treatment with Compound C for 2 hours. MMP-1 was detected by (A, B) ELISA or (C, D) RT-PCR. Compound C significantly downregulated (A) MMP-1 and (B) MMP-9 secretion in a dose-dependent manner in CoMTB-stimulated NHBE at 72 hours. Compound C significantly downregulated (C) MMP-1 and (D) MMP-9 gene expression in CoMTB-stimulated NHBE at 24 hours. Bars show mean ± SD of 3 technical replicates of a single independent experiment and are representative of 3 independent experiments. Statistical analysis was performed using an ordinary one-way ANOVA with Tukey's post-test correction. **p<0.01 ****p<0.0001

4.2.15 AMPK upregulates MMP-3 and MMP-10 secretion in CoMTB-stimulated NHBEs

The effect of Compound C on MMP-3 and -10 secretion was assessed using a Luminex assay. Compound C downregulated MMP-3 and -10 in CoMTB-stimulated NHBEs. MMP-3 secretion was reduced 3-fold from 5067 ± 319.8 pg/ml to 1670 ± 204.1 pg/ml ($P<0.0001$) (Figure 44A) and MMP-10 secretion was reduced 6.9-fold from 16316 ± 2355 pg/ml to 2355 ± 164.5 pg/ml ($p<0.0001$) (Figure 44B) by Compound C in the presence of CoMTB compared to with CoMTB alone. Hence, AMPK upregulates MMP-3 and -10 secretion in TB. As Compound C caused a global downregulation of MMP secretion, an LDH release assay with a vehicular DMSO control was performed to exclude cytotoxicity. This demonstrated that the viability of NHBEs in all conditions was >90% compared to unstimulated control cells (Figure 44C).

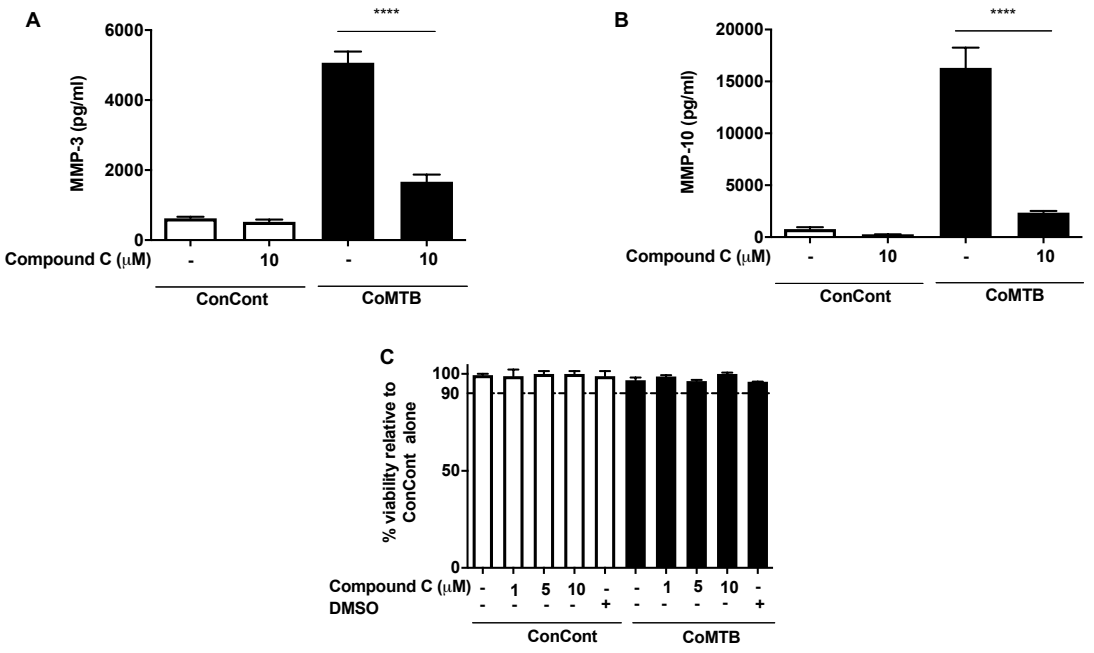


Figure 44: AMPK upregulates MMP-3 and MMP-10 secretion in CoMTB-stimulated NHBEs. NHBEs were stimulated with CoMTB or ConCont, with or without pre-treatment with Compound C for 2 hours. MMPs were detected by Luminex array. In CoMTB-stimulated NHBEs, Compound C significantly downregulated (A) MMP-3 secretion and (B) MMP-10 secretion at 72 hours. (C) LDH cytotoxicity assay shows that cell viability was >90% relative to unstimulated cells in all experimental conditions and in a DMSO control at 72 hours. Bars show mean ± SD of 3 technical replicates of a single independent experiment and are representative of 3 independent experiments. Statistical analysis was performed using an ordinary one-way ANOVA with Tukey's post-test correction. ****$p<0.001$.

4.2.16 AMPK upregulates a functional increase in collagenase and gelatinase activity in CoMTB-stimulated NHBEs

The pattern of MMP-1 and -9 secretion was mirrored at a functional level in a fluorescent matrix degradation assay. There was a 3-fold decrease in active collagenase breakdown of DQ collagen from 97422 ± 5848 RFU to 32915 ± 931.5 RFU with Compound C and CoMTB stimulation compared to CoMTB stimulation alone. The Compound C-induced 7-fold decrease in active gelatinase breakdown of DQ gelatin, from 143854 ± 11592 RFU ($p<0.0001$) (Figure 45A) to 206.23 ± 1494 RFU ($p<0.0001$) (Figure 45B) was much more pronounced. Hence, AMPK upregulated functional tissue destruction in CoMTB-stimulated NHBEs.

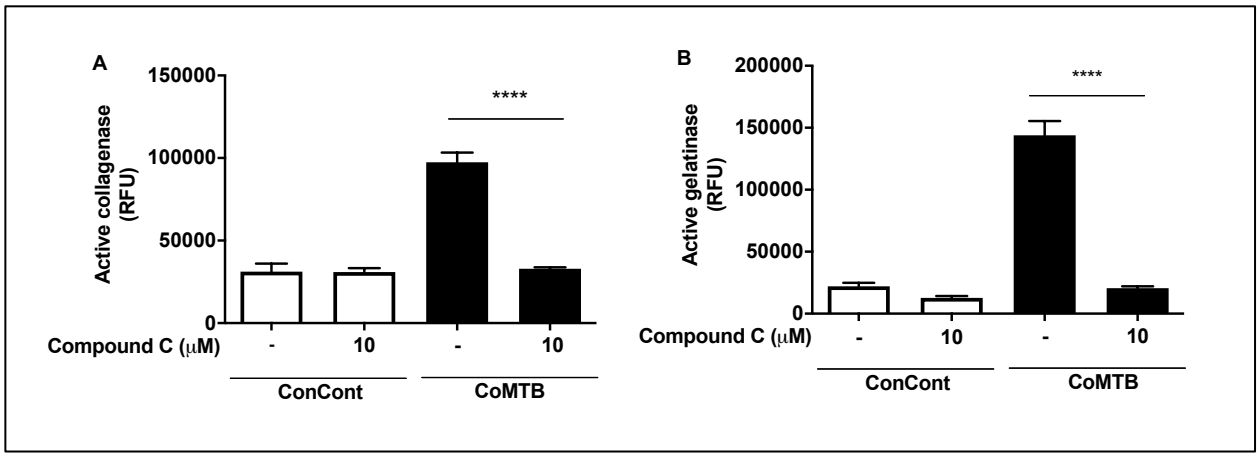


Figure 45: AMPK upregulates functional collagenase and gelatinase activity in CoMTB-stimulated NHBEs. NHBEs were stimulated with CoMTB or ConCont, with or without pre-treatment with Compound C for 2 hours. Type 1 collagenase and gelatinase activity was detected by fluorescent degradation of DQ collagen and DQ gelatin respectively and quantified in relative fluorescent units (RFU). AMPK upregulates (A) Type 1 collagenase activity and (B) gelatinase activity in CoMTB-stimulated NHBEs. Bars show mean ± SD of 3 technical replicates of a single independent experiment and are representative of 3 independent experiments. Statistical analysis was performed using an ordinary one-way ANOVA with Tukey's post-test correction. ****$p<0.0001$.

4.2.17 Metformin upregulates MMP-1 and MMP-9 secretion in CoMTB-stimulated NHBEs

Metformin is a commonly used antidiabetic drug with a known safety profile. Metformin is currently of interest as a potential adjuvant therapy for TB and human and murine data have shown that it reduces lung bacillary burden and improves clinical outcomes in TB (367). It is an AMPK activator and its mechanism of action in antituberculous drugs is thought to be the AMPK-mediated stimulation of anti-inflammatory, catabolic pathways (371). Given the recent promising studies, I was interested to ascertain whether metformin modulated the secretion of MMPs in TB. Interestingly, metformin significantly and dose-dependently increased the secretion of MMP-1 and -9 in CoMTB-stimulated NHBEs. MMP-1 secretion rose 1.7-fold from 4971 ± 96.7 pg/ml with CoMTB alone to 8279 ± 19.53 pg/ml following metformin treatment (Figure 46A), while MMP-9 secretion rose 1.4-fold from 238017 ± 31409 pg/ml with CoMTB alone to 327433 ± 17537 pg/ml with CoMTB and metformin (Figure 46B). Although the fold changes were similar for MMP-1 (Figure 46C) and MMP-9 (Figure 46D), MMP-9 was secreted in much greater concentrations.

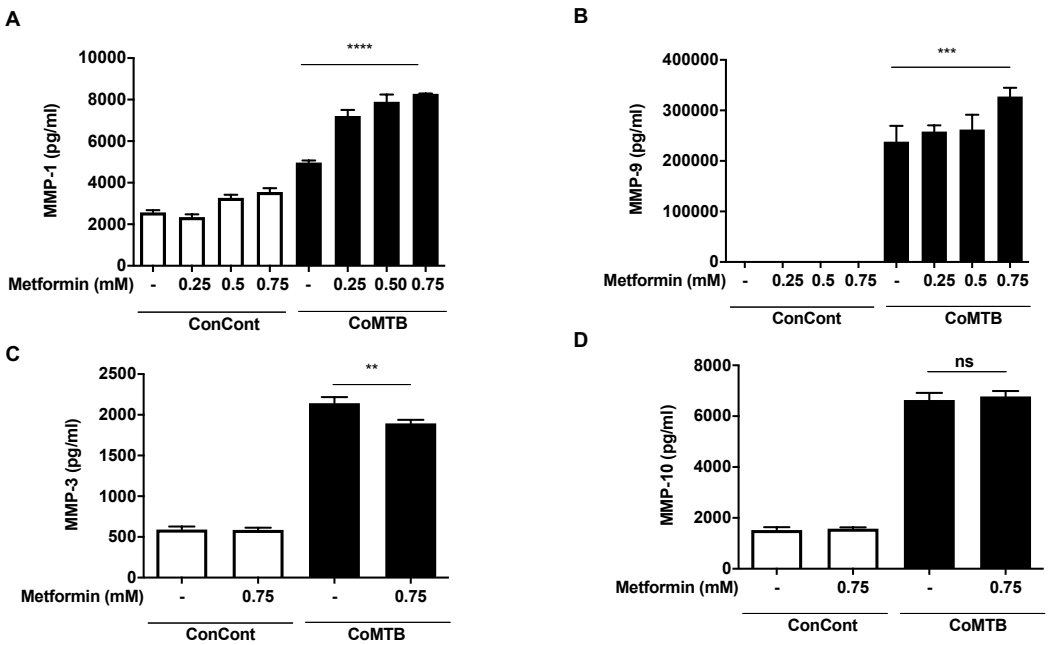


Figure 46: Metformin upregulates MMP-1 and MMP-9 secretion and gene expression in CoMTB-stimulated NHBEs. NHBEs were stimulated with CoMTB or ConCont, with or without pre-treatment with metformin for 2 hours. MMPs were detected by (A, B) ELISA or (C, D) Luminex array. Metformin significantly upregulated (A) MMP-1 secretion and (B) MMP-9 secretion in a dose-dependent manner in CoMTB-stimulated NHBEs at 72 hours. Metformin (C) significantly decreased MMP-3 secretion but (D) did not affect MMP-10 secretion in CoMTB-stimulated NHBEs at 72 hours. Bars show mean ± SD of 3 technical replicates of a single independent experiment and are representative of 3 independent experiments. Statistical analysis was performed using an ordinary one-way ANOVA with Tukey's post-test correction. ns not significant **p<0.01 ***p<0.0001 ****p<0.0001.

4.2.18 The Pi3-kinase-Akt-mTORC1 pathway downregulates MMP-1 and MMP-9 secretion in CoMTB-stimulated NHBEs

I then proceeded to examine the role of the Pi3-kinase/Akt/mTORC1 pathway in MMP secretion, with particular emphasis on its functional effect on ECM degradation and tissue damage in TB. The Pi3-kinase pathway has a central role in the bioenergetic shift to glycolysis in pro-inflammatory innate immune cells (357,374) and has been shown have a regulatory effect on MMPs (248,258). I analysed the 3 main components of this pathway using the following chemical inhibitors: LY294002, which inhibits the p110 subunit of Pi3-kinase; VIII, which inhibits Akt; and rapamycin, which inhibits the mTORC1 complex of mTOR. In preparation for examining the role of the Pi3-kinase/Akt/mTOR pathway in matrix breakdown, I assessed the effect of inhibition of this pathway on secretion of the key collagenase, MMP-1 and the important gelatinase, MMP-9 in CoMTB-stimulated NHBEs. Both MMP-1 and -9 were significantly upregulated in a dose-dependent manner in CoMTB-stimulated NHBEs with inhibition of all 3 signalling mediators in this pathway. LY294002 upregulated MMP-1 secretion 2.4-fold from 158748 ± 15041 pg/ml to 382354 ± 11789 pg/ml ($p<0.0001$) (Figure 47A) and MMP-9 2-fold increase from 96933 ± 7641 pg/ml to 193000 ± 8162 pg/ml ($p<0.0001$) (Figure 47B). VIII increased MMP-1 secretion 0.7-fold from 12397 ± 1102 pg/ml to 16840 ± 781.2 pg/ml ($p<0.0001$) (Figure 47C) and MMP-9 secretion 0.8-fold from 149611 ± 3557 pg/ml to 176100 ± 13447 pg/ml ($p<0.05$) (Figure 47D). Rapamycin upregulated MMP-1 secretion 0.6-fold from 17892 ± 2469 to 28558 ± 760 ($p<0.001$) (Figure 47E) and MMP-9 0.7-fold increase from 126667 ± 8717 to 193983 ± 13040 ($p<0.0001$) (Figure 47F). Hence, it appears that MMP-1 and -9 secretion is negatively regulated by this signal transduction pathway at all points.

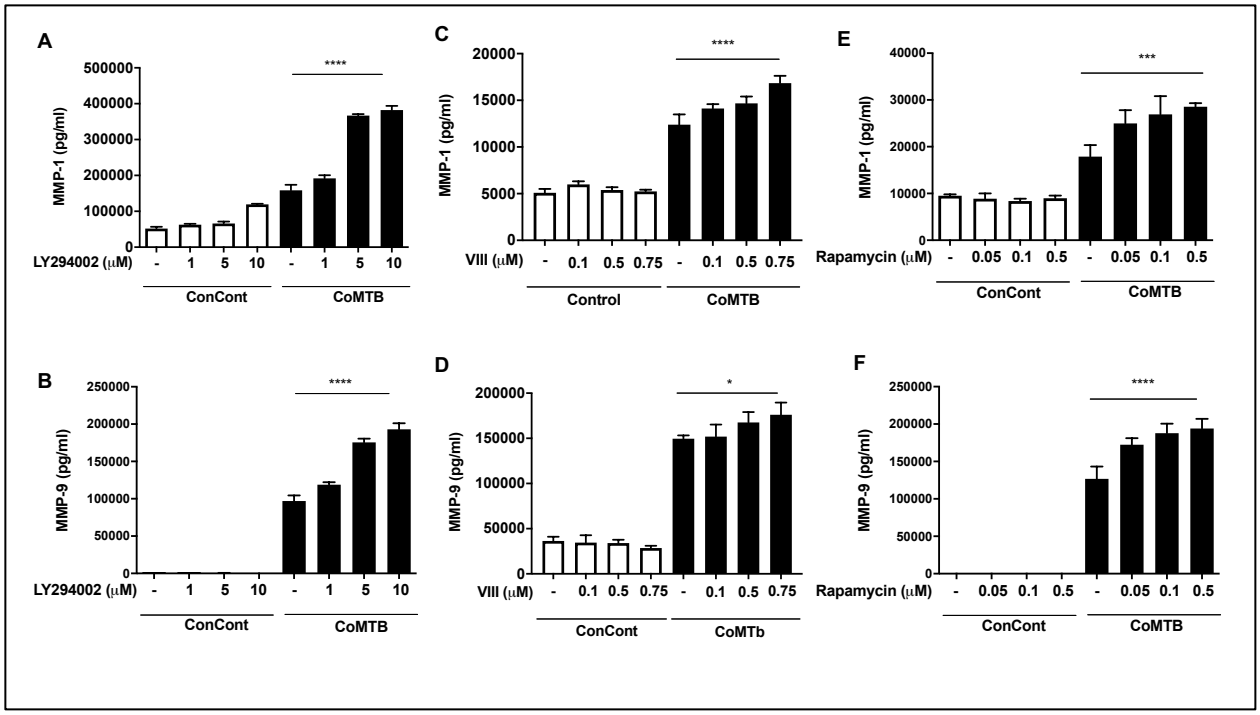


Figure 47: The Pi3-kinase-Akt-mTORC1 pathway downregulates MMP-1 and MMP-9 secretion in CoMTB-stimulated NHBEs. NHBEs were stimulated with CoMTB or ConCont, with or without pre-treatment with (A, B) LY294002, (C, D) VIII or (E, F) rapamycin for 2 hours. MMP-1 and -9 were detected by ELISA. LY294002 significantly upregulated (A) MMP-1 and (B) MMP-9 secretion in CoMTB-stimulated NHBEs at 72 hours. VIII significantly upregulated (C) MMP-1 and (D) MMP-9 secretion in CoMTB-stimulated NHBEs at 72 hours. Rapamycin significantly upregulated (E) MMP-1 and (F) MMP-9 secretion in CoMTB-stimulated NHBEs at 72 hours. Bars show mean ± SD of 3 technical replicates of a single independent experiment and are representative of 3 independent experiments. Statistical analysis was performed using an ordinary one-way ANOVA with Tukey's post-test correction. *p<0.05 ***p<0.0001 ****p<0.0001.

4.2.19 The Pi3-kinase-Akt-mTORC1 pathway upregulates MMP-3 and MMP-10 secretion in CoMTB-stimulated NHBEs

I was also interested to assess the role of the Pi3-kinase/Akt/mTORC1 pathway in the regulation of the stromelysins MMP-3 and -10 using a Luminex assay. In contrast to the effect on MMP-1 and -9, MMP-3 and -10 was generally significantly downregulated by this pathway. Following treatment with LY924002, MMP-3 fell 1.8-fold from 7682 ± 294.1 pg/ml to 4185 ± 473.4 pg/ml ($p<0.0001$) (Figure 48A) in CoMTB-stimulated NHBEs, though there was no effect on MMP-10 secretion (Figure 48B). VIII reduced MMP-3 secretion 1.3-fold from 6127 ± 89.6 to 4657 ± 359.1 ($p<0.0004$) (Figure 48C) and MMP-10 secretion 1.4-fold from 11798 ± 199.4 to 8576 ± 455.4 ($p<0.0001$) (Figure 48D) in CoMTB-stimulated NHBEs. Rapamycin treatment decreased MMP-3 1.4-fold from 2201 ± 88.9 with CoMTB alone to 608.3 ± 87.5 with rapamycin and CoMTB ($p<0.0001$) (Figure 48E) and MMP-10 2.5-fold from 20718 ± 399 pg/ml with CoMTB alone to 8210 ± 122.9 pg/ml ($p<0.001$) (Figure 48F) with both rapamycin and CoMTB stimulation.

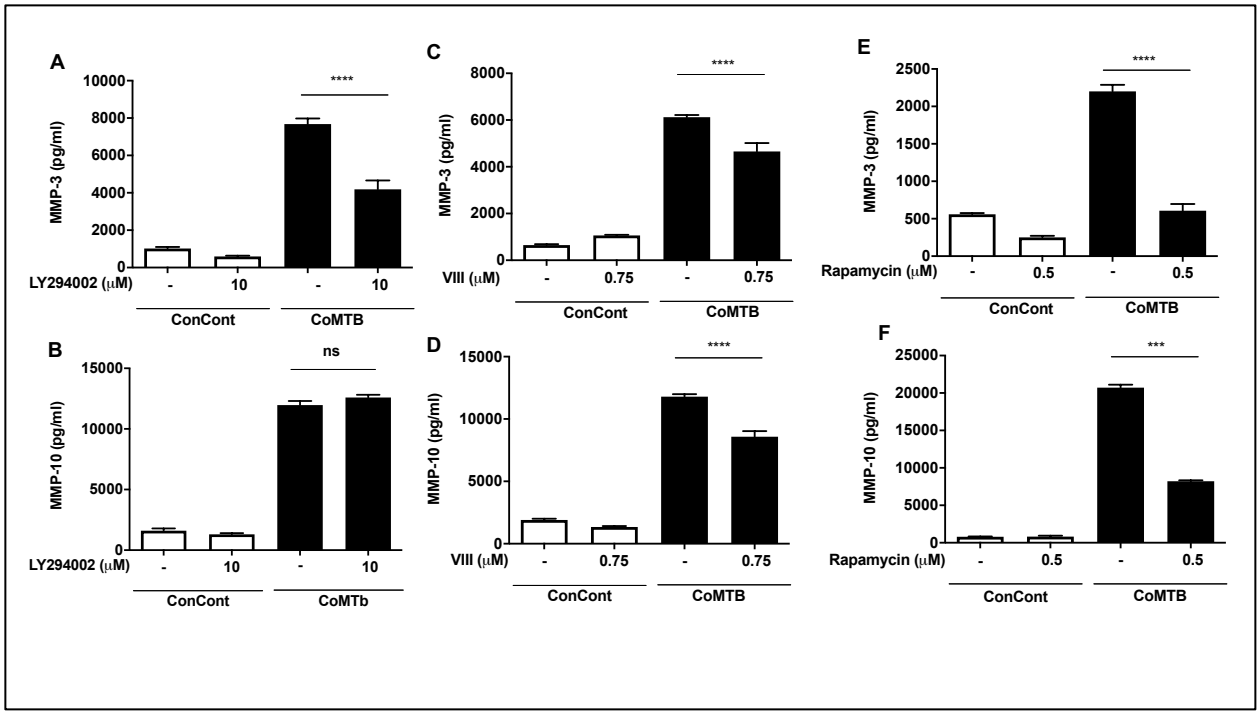


Figure 48: The Pi3-kinase-Akt-mTORC1 pathway upregulates MMP-3 and MMP-10 secretion and gene expression in CoMTB-stimulated NHBEs. NHBEs were stimulated with CoMTB or ConCont, with or without pre-treatment with (A, B) LY294002, (C, D) VIII or (E, F) rapamycin for 2 hours. MMP-3 and -10 were detected by Luminex array. LY294002 (A) decreased MMP-3 secretion in CoMTB-stimulated NHBEs at 72 hours, but (B) had no effect on MMP-10. VIII decreased (C) MMP-3 and (D) MMP-10 secretion in CoMTB-stimulated NHBEs at 72 hours. Rapamycin decreased (E) MMP-3 and (F) MMP-10 secretion in CoMTB-stimulated NHBEs at 72 hours. Bars show mean ± SD of 3 technical replicates of a single independent experiment and are representative of 3 independent experiments. Statistical analysis was performed using an ordinary one-way ANOVA with Tukey's post-test correction. ns not significant ***p<0.0001 ****p<0.0001.

4.2.20 The Pi3-kinase-Akt-mTORC1 pathway downregulates a functional increase in collagenase and gelatinase activity in CoMTB-stimulated NHBEs

I then performed a DQ collagen and DQ gelatin matrix degradation assay to ascertain whether the functional regulation of the collagenase MMP-1 and the gelatinase MMP-9 by the Pi3-kinase/Akt/mTORC1 pathway reflected their secretory patterns. This proved to be the case, as both active Type 1 collagenase and active gelatinase matrix breakdown was significantly downregulated, most potently by Pi3-kinase, in CoMTB-stimulated NHBEs. Treatment with LY294002 resulted in a 3.3-fold increase in collagenase activity from 46789 ± 3483 RFU with CoMTB alone to 127099 ± 14366 RFU ($p<0.0001$) (Figure 49A), while gelatinase activity rose 2.7-fold from 37705 ± 4476 RFU to 126303 ± 20346 RFU ($p<0.0001$) (Figure 49B). VIII resulted in a 1.7-fold increase in collagenase activity from 71364 ± 2408 RFU in CoMTB-stimulated NHBEs alone to 115533 ± 8829 RFU ($P<0.001$) (Figure 49C), while gelatinase activity rose 1.7-fold from 72220 ± 2589 RFU with CoMTB alone to 122357 ± 11534 RFU with both VIII and CoMTB ($p<0.001$) (Figure 49D). Rapamycin induced a 1.3-fold increase in collagenase activity from 59682 ± 6424 RFU with CoMTB alone to 78856 ± 5615 RFU ($p<0.05$) (Figure 49E) and also a 1.3-fold increase in gelatinase activity from 103419 ± 4909 RFU with CoMTB alone to 131309 ± 16552 RFU with both rapamycin and CoMTB ($p<0.05$) (Figure 49F).

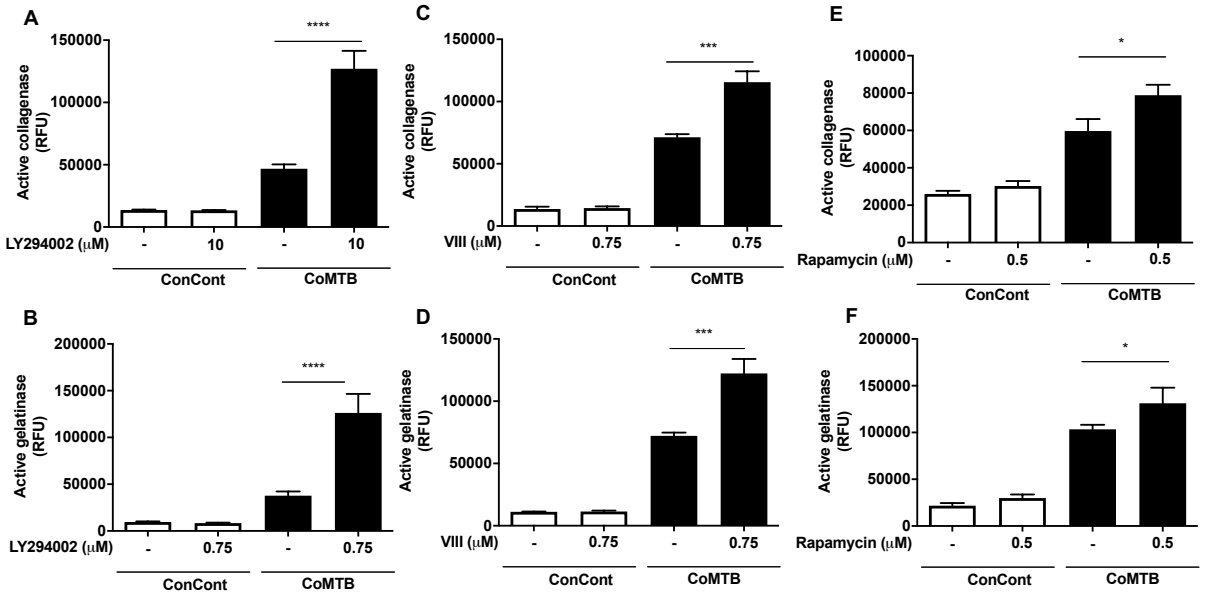


Figure 49: The Pi3-kinase-Akt-mTORC1 pathway downregulates functional collagenase and gelatinase activity in CoMTB-stimulated NHBEs. NHBEs were stimulated with CoMTB or ConCont, with or without pre-treatment with (A, B) LY294002, (C, D) VIII or (E, F) rapamycin for 2 hours. Type 1 collagenase and gelatinase activity was detected by fluorescent degradation of DQ collagen and DQ gelatin respectively and quantified in relative fluorescent units (RFU). LY294002 significantly upregulated (A) Type 1 collagenase activity and (B) gelatinase activity in CoMTB-stimulated NHBEs at 72 hours. VIII significantly upregulated (C) Type 1 collagenase activity and (D) gelatinase activity in CoMTB-stimulated NHBEs at 72 hours. Rapamycin significantly upregulated (E) Type 1 collagenase activity and (F) gelatinase activity in CoMTB-stimulated NHBEs at 72 hours. Bars show mean ± SD of 3 technical replicates of a single independent experiment and are representative of 3 independent experiments. Statistical analysis was performed using an ordinary one-way ANOVA with Tukey's post-test correction. *$p<0.05$ ***$p<0.001$ ****$p<0.0001$.

I also performed confocal imaging in DQ collagen and DQ gelatin coated plates to further evaluate functional tissue destruction by Pi3-kinase. DQ collagen and DQ gelatin, fluorescein conjugate, were used to pre-coat 8-well glass chamber μ slides at 150ng/ml for 2 hours. NHBEs were then seeded into wells at 25,000/cm^2 and incubated at 37°C / 5% v/v CO_2 for 4 hours to adhere to the plate. The cells were then incubated with Cell Tracker™ Deep Red Dye at a concentration of 10μM for 30 minutes. NHBEs were pre-treated with the Pi3-kinase inhibitor LY294002 for 2 hours, then stimulated with CoMTB or ConCont just prior to confocal imaging. Live-cell, time-lapse confocal imaging was then performed over a period of 72 hours, with images obtained every 30 minutes, using a Nikon A1R confocal microscope. There was increased fluorescence of DQ gelatin with LY294002 and CoMTB stimulation compared to CoMTB alone (Figure 50), but the DQ collagen plate showed no significant changes. Hence, Pi3-kinase downregulates functional gelatinase activity in CoMTB-stimulated NHBEs.

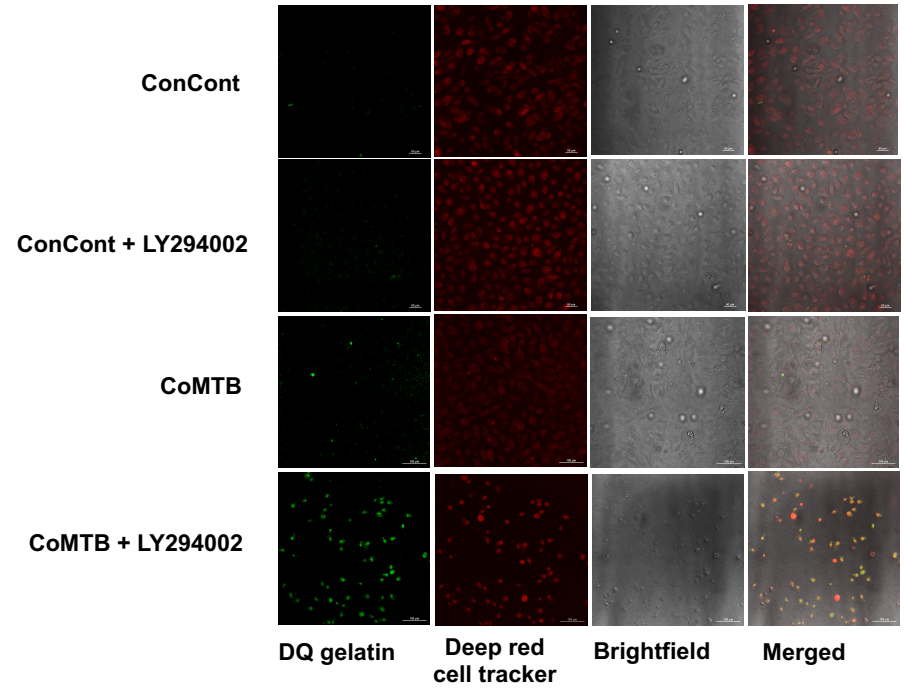


Figure 50: Pi3-kinase downregulates gelatinase activity in live-cell, time-lapse confocal imaging of CoMTB-stimulated NHBEs: DQ gelatin, fluorescein conjugate, was used to pre-coat 8 well glass chamber μ slides for 2 hours. NHBEs were seeded into wells, left to adhere for 4 hours, then incubated with Cell Tracker™ Deep Red Dye for 30 minutes. NHBEs were then stimulated with CoMTB or ConCont, with or without pre-treatment with LY294002 for 2 hours. Live-cell, time-lapse confocal imaging was then performed over a period of 72 hours, with images obtained every 30 minutes. There was increased fluorescence of DQ gelatin with LY294002 and CoMTB stimulation compared to CoMTB alone. The images show a single independent experiment and is representative of 2 independent experiments.

4.3 Discussion

AECs are crucial immune cells in TB and represent an important source of MMPs in response to monocyte-dependent cytokine networks. To date, there has been no investigation in AECs of the role of cellular energy metabolism on the regulation of MMPs in TB. For this aspect of my project, I used a murine model of pulmonary TB, as well as *in vitro* analysis of primary CoMTB-stimulated NHBEs to investigate MMP regulation by metabolic pathways. The key findings from the cellular experiments are summarized in Figure 51.

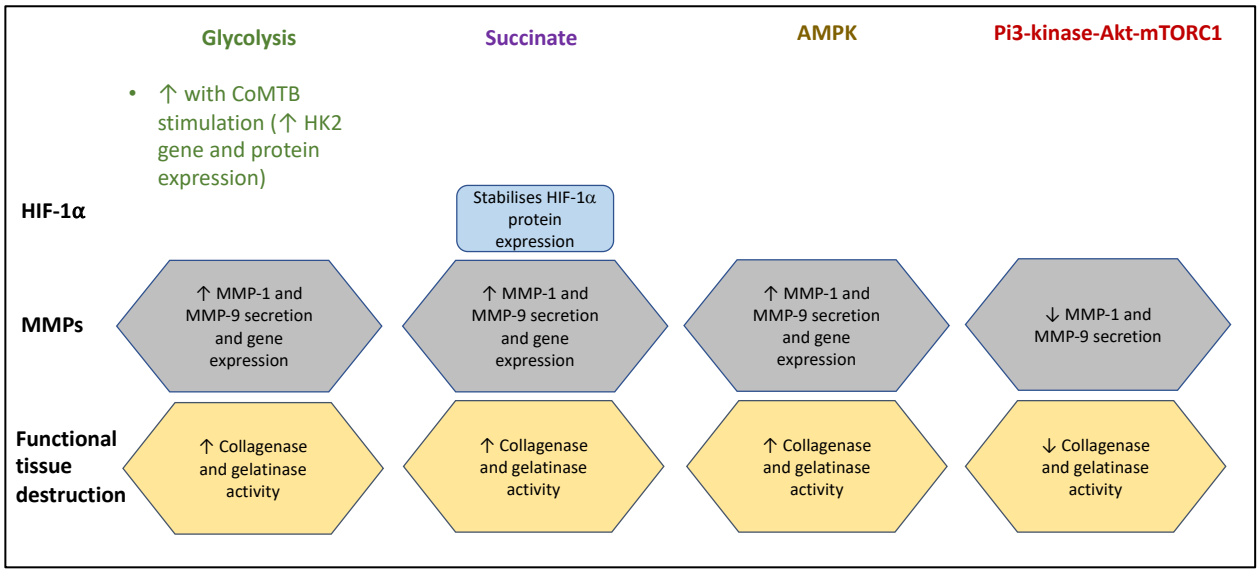


Figure 51: Summary of key findings from the *in vitro* metabolic signalling experiments in CoMTB-stimulated NHBEs

I first demonstrated that expression of the HK2 isoform of the first glycolytic enzyme was upregulated in in a murine model of pulmonary TB. Although mice do not form caseating necrotic granulomas, there was concentrated HK2 immunostaining at the site of inflammation, associated with characteristic foamy macrophages. In addition, there was loss of the normal alveolar

architecture and destruction of their walls, which can result in the clinical TB symptom of haemoptysis. Clear HK2 immunostaining was also detected in bronchial epithelial cells, suggesting that glycolysis is upregulated in *M.tb* infection.

I then investigated the presence of HK2 in primary CoMTB-stimulated NHBEs. There was a significant upregulation of HK2 gene and protein expression, suggesting enhanced glycolytic metabolism. This reflects the findings from a recent study in which AECs infected with human metapneumovirus underwent metabolic reprogramming from OXPHOS to aerobic glycolysis, with upregulation of HK2, PKM2 and LDHA (391). Interestingly, HK2 was upregulated to a greater extent in MDMs than in AECs, suggesting that MDMs are a more glycolytically active cell. In order to more fully characterise the bioenergetic profile of AECs in TB, it would be beneficial to perform transcriptomic and metabolomic studies and Seahorse analysis in AECs in future.

I then proceeded to analyse the relationship between glycolysis and MMPs *in vitro*, first by chemical inhibition of HK with 2DG. Glycolysis significantly upregulated gene expression and secretion of the key collagenase, MMP-1 and gelatinase, MMP-9, in CoMTB-stimulated NHBEs; MMP-9 levels were considerably higher than MMP-1. I also showed by gelatin zymography that glycolysis increases the amount of functionally active MMP-9 in CoMTB-stimulated NHBEs.

2DG is in widespread use as a glycolysis inhibitor; however, there have been reports of off-target effects, including Pi3-kinase activation. Hence, I performed siRNA knockdown of HK2 in CoMTB-stimulated NHBEs to confirm selected 2DG-induced data. Curiously, despite significant HK2 gene and protein knockdown with siRNA treatment, there was a decrease in MMP-9, but not MMP-1 gene expression. It might be possible that global HK inhibition is required to downregulate MMP-1 gene expression and HK2 isoform inhibition alone is insufficient. Transcriptomic studies have demonstrated that the HK3 isoform is also highly upregulated in TB mouse lungs (322) and perhaps compensates for the loss of HK2 in this siRNA model.

I then evaluated the regulation of MMPs by the TCA cycle intermediate, succinate. Cell-permeable diethylsuccinate induced a significant and dose-dependent increase in MMP-1 and -9 secretion in CoMTB-stimulated NHBEs. This was reflected intracellularly at the level of gene expression. Diethylsuccinate had divergent effects on the secretion of other MMPs; MMP-3 is decreased, MMP-10 increased and MMP-2 and -8 unaffected. MMP-10 is secreted at a much greater concentration than MMP-3, hence its regulatory effect on MMP-1 may predominate. Diethylsuccinate did not regulate secretion of TIMP-1 or TIMP-2. Diethylsuccinate treatment also upregulated the expression of HIF-1α. This is consistent with findings in LPS-stimulated murine macrophages, in which succinate accumulation inhibits PHDs to stabilise HIF-1α and induce pro-inflammatory IL-1β secretion (296). In this cellular model, I did not measure cytokine secretion, as CoMTB itself contains numerous cytokines (Table 2), which would have confounded the analysis. Of note, succinate-mediated HIF-1α activation in LPS-stimulated murine macrophages is regulated by PKM2 (350). I attempted to chemically manipulate PKM2 in CoMTB-stimulated NHBEs with an inhibitor, shikonin, and activator, Tepp-46, but the results were inconclusive.

I was then interested in measuring the effect of the signal transduction pathways AMPK and Pi3-kinase-Akt-mTOR. Interestingly, AMPK upregulated MMP-1 and -9 expression This finding is in keeping with a recent study where AMPKα2 deficient mice had decreased MMP-2 and were found to be resistant to developing abdominal aneurysms, a process which was demonstrated to be MMP-dependent (393). However, the Pi3-kinase-Akt-mTORC1 pathway had a negative regulatory effect on MMP-1 and -9 secretion in CoMTB-stimulated NHBEs. Interestingly, there was an increase in regulatory MMP-3 and -10 in this model. Of note, this partially diverges from previous NHBEs findings from our group (248), although functional matrix destruction was not measured in that study. However, it is consistent with the effect of the Pi3-kinase-Akt-mTORC1 pathway in *M.tb*-infected MDMs, both in my experiments and in previous studies from our group (258). This may be attributable to differences in NHBEs or CoMTB batches; the latter, in particular

contains numerous cytokines. AMPK and mTORC1 are known to have reciprocal effects, which is reflected in these findings. However, these data go against the conventional paradigm of anti-inflammatory AMPK and pro-inflammatory mTORC1 regulation (357). This may reflect the immunometabolic milieu of the cells in which the cross-talk between AMPK and mTORC1 is dynamic and continually responsive. These interactions are an interesting avenue for further research.

In order to investigate the impact of cellular metabolic pathways on matrix degradation in CoMTB-stimulated NHBEs, I performed functional assays of collagenase and gelatinase activity. The protease activity of MMP-1 and -9 reflected the secretory pattern, with an upregulation of collagen and gelatin degradation respectively with glycolysis, succinate and AMPK. This suggests for the first time that these metabolic signalling pathways promote a tissue-destructive phenotype in CoMTB-stimulated NHBEs. Conversely, all components of the Pi3-kinase-Akt-mTOR pathway downregulated collagen and gelatin degradation. Live-cell, time-lapse confocal imaging of CoMTB-stimulated NHBEs treated with LY294002 was undertaken to confirm the effect of Pi3-kinase signalling on ECM destruction. Increased fluorescence with LY294002 treatment in CoMTB-stimulated NHBEs confirmed that Pi3-kinase reduced tissue breakdown. ECM degradation in TB is strongly correlated with pulmonary cavitation, transmission, treatment failure and resistance, with profound implications for TB morbidity and mortality (197,240). Hence, metabolic regulation of tissue destruction has potential implications for innovative therapeutic strategies to improve TB outcomes.

Hence, the findings show that NHBEs have an essential immunometabolic role in TB pathogenesis, with novel evidence linking cellular metabolic signalling to MMP regulation and ECM destruction in TB.

Chapter 5: Conclusions and future perspectives

5.1 Summary of findings

In this project, I studied the effect of metabolic signalling on the innate inflammatory response in TB using primary human MDM and NHBE experiments, as well as immunohistochemical analysis of murine and human TB models.

The concept of TB-induced bioenergetic rewiring to aerobic glycolysis was supported by upregulation of HK2 gene and protein expression in both MDMs and NHBEs. This was further corroborated in MDMs by an increase in extracellular lactate secretion. Glycolysis also impaired intracellular survival of *M.tb* in MDMs.

Table 8 compares the main immunometabolic effects of glycolysis and succinate shown in *M.tb*-infected MDMs and CoMTB-stimulated NHBEs. I demonstrated for the first time that glycolysis regulates MMP gene expression and secretion in both cellular models of TB. In CoMTB-stimulated NHBEs, the upregulation of MMP-1 and -9 with glycolysis and succinate was reflected in functional ECM degradation, suggesting that cellular metabolism is a crucial driver of tissue destruction and pulmonary cavitation in TB. Glycolysis stabilised the key transcription factor HIF-1α in *M.tb*-infected MDMs, while pro-inflammatory cytokine IL-1β secretion was enhanced by both glycolysis and succinate. Succinate also stabilised HIF-1α in CoMTB-stimulated NHBEs. These findings are consistent with studies showing that succinate accumulates in murine TB lungs (326) and that HIF-1α is pivotal for metabolic reprogramming and bacterial containment in TB *in vitro* and *in vivo* (335). Glycolysis also increased secretion of the MMP inducer EMMPRIN, which regulates lactate MCTs, from *M.tb*-infected MDMs.

I also showed potent HK2 expression in areas of central granulomatous necrosis and tissue remodelling in murine pulmonary TB and human TB lymph nodes. HK2 immunostaining was

prominent in characteristic foamy and epithelioid macrophages and Langhans cells in both models; in addition, HK2 was expressed in bronchial epithelial cells in murine lung.

		***M.tb*-infected MDMs**	**CoMTB-stimulated NHBEs**
Glycolysis	HK2	-	-
	HIF-1α	Stabilises HIF-1α protein expression	-
	Cytokines	↑ IL1-β and IL-10, ↓ TNF-α secretion	-
	MMPs	↑ MMP-1 secretion and gene expression	↑ MMP-1 and -9 secretion and gene expression
	Functional tissue destruction	-	↑ Collagenase and gelatinase activity
Succinate	HK2	-	-
	HIF-1α	-	Stabilises HIF-1α protein expression
	Cytokines	↑ IL1-β, ↓ TNF-α and IL-10 secretion	-
	MMPs	Does not affect MMP-1 secretion	↑ MMP-1 and -9 secretion and gene expression
	Functional tissue destruction	-	↑ Collagenase and gelatinase activity

Table 8: Comparison of the key immunometabolic effects of glycolysis and succinate shown in *M.tb*-infected MDMs and CoMTB-stimulated NHBEs

Furthermore, I demonstrated that the master metabolic regulator AMPK and the key Pi3-kinase-Akt-mTORC1 signal transduction pathway have reciprocal roles in MMP and cytokine regulation. Protein expression of pAMPK was decreased in *M.tb*-infected macrophages, while that of $p70^{S6K}$, a downstream target of mTORC1, was increased.

Table 9 compares the salient immunometabolic effects of AMPK and the Pi3-kinase-Akt-mTOR pathway shown in *M.tb*-infected MDMs and CoMTB-stimulated NHBEs. AMPK was shown for the first time to upregulate MMP-1 secretion and gene expression in both MDM and NHBE models of TB. AMPK also stabilised HK2 and HIF-1α protein expression and enhanced secretion of the pro-inflammatory cytokines IL-1β and TNF-α in *M.tb*-infected MDMs. Metformin upregulated MMP-1 and -9 secretion in CoMTB-stimulated NHBEs, but had variable effects on MMP-1 and cytokine secretion in *M.tb*-infected MDMs. This might reflect the complex mechanisms of metformin action, which are both AMPK-dependent and AMPK-independent. The Pi3-kinase-Akt-mTORC1 pathway had a biphasic effect on MMP-1 secretion in MDMs, with an early upregulation at 24 hours, followed by a downregulation at 72 hours. This pathway also downregulated secretion of the proinflammatory cytokines IL-1β and TNF-α at 24 hours and 72 hours, but had a biphasic effect on IL-10 secretion, with an initial rise and later fall. The AMPK-induced upregulation and Pi3-kinase-Akt-mTORC1-induced downregulation of MMP-1 and -9 secretion were reflected in their functional effects on ECM destruction in CoMTB-stimulated NHBEs.

Interestingly the broadly pro-inflammatory effects of AMPK and broadly anti-inflammatory effects of the Pi3-kinase-Akt-mTOR diverge from the conventional paradigm in the literature (357). One explanation is that reciprocal interactions between AMPK and mTORC1 are highly dynamic and reflect the phase of infection, activation status and bioenergetic profile of immune cells. The balance of these communications is likely to be a crucial immunometabolic pivot for modulation of cellular innate host defence in TB (357).

Together, these findings strongly support my stated hypothesis that metabolic pathways regulate the gene expression and secretion of MMPs to drive immunopathology in TB. I will now summarise the therapeutic advances in targeting metabolic signalling mediators in inflammatory

diseases such as TB, followed by a discussion of intriguing avenues for further research in TB immunometabolism.

		***M.tb*-infected MDMs**	**CoMTB-stimulated NHBEs**
AMPK	HK2	Stabilises HK2 protein expression	-
	HIF-1α	Stabilises HIF-1α protein expression	-
	Cytokines	↑ IL1-β, TNF-α and IL-10 secretion	-
	MMPs	↑ MMP-1 secretion and gene expression	↑ MMP-1 and -9 secretion and gene expression
	Functional tissue destruction	-	↑ Collagenase and gelatinase activity
Pi3-kinase-Akt-mTORC1	HK2	-	-
	HIF-1α	-	-
	Cytokines	↓ IL1-β and TNF-α, but biphasic effect on IL-10 secretion (↑ at 24 hours and ↓ at 72 hours)	-
	MMPs	Biphasic effect on MMP-1 secretion (↑ at 24 hours and ↓ at 72 hours)	↓ MMP-1 and -9 secretion
	Functional tissue destruction	-	↓ Collagenase and gelatinase activity

Table 9: Comparison of the key immunometabolic effects of AMPK and the Pi3-kinase-Akt-mTORC1 pathway shown in *M.tb*-infected MDMs and CoMTB-stimulated NHBEs

5.2 Therapeutic implications

There is increasing evidence for targeting specific metabolic switch points as a host-directed strategy to limit inflammation and, hence, tissue destruction. The reprogramming of immune cells towards a less inflamed phenotype by metabolic manipulation with small molecules is emerging as an intriguing therapeutic concept (394). Effector and regulatory immune cell populations have differential metabolic requirements; hence, selective targeting of cells with high metabolic demands might reduce undesirable side effects, in contrast to an approach of global immunosuppression (394). This can facilitate enhanced host immune responses to *M.tb* infection, resulting in effective clearance, while minimising damage to host tissues.

Several small molecules used clinically in inflammatory and autoimmune conditions also target metabolic processes in immune cells. These agents include metformin, rapamycin, methotrexate and dimethyl fumarate (DMF). Metformin, commonly prescribed in type 2 diabetes, has been proposed as a supplementary TB treatment. It acts via multiple AMPK-dependent and AMPK-independent mechanisms, including mitochondrial ROS generation (371). In epidemiological studies, metformin is associated with lower TB mortality rates (367,368), enhanced treatment success (369) and higher sputum culture conversion (369,370). In a murine model of TB, metformin treatment also decreases lung bacillary load, ameliorates inflammation and tissue destruction and enhances the efficacy of conventional antituberculous drugs (367). Rapamycin (sirolimus), which inhibits mTORC1, resulted in clinical improvement in disease activity in patients with clinically active SLE over a period of 12 months in a phase 1/2 trial (395). Low-dose methotrexate, used in the treatment of rheumatoid arthritis, may act by upregulating intracellular AICAR, an activator of AMPK, to promote adenosine signalling (396). DMF is used to treat multiple

sclerosis and psoriasis and regulation of the PPP and fatty acid metabolism contribute to its anti-inflammatory effects, though the exact mechanisms are undefined (394).

The enzymes and intermediates of glycolysis and the TCA cycle can also be targeted for therapeutic purposes. 2DG shows promise in inhibiting glycolysis in experimental murine models of inflammatory disorders such as systemic lupus erythematosus (SLE) (397), rheumatoid arthritis (398) and experimental autoimmune neuritis (EAN) (399). In cancer patients, phase 1 clinical trials of 2DG suggest that it is well-tolerated at low doses, with favourable early outcomes (400). Modulation of succinate, itaconate and citrate is also being studied for potential therapeutic benefit (394).

Further research into TB host-pathogen interactions is essential to understand how targeting metabolism can be harnessed to optimise TB immune responses.

5.3 Future work

Several avenues of further research would help to elucidate the intricate metabolic signalling mechanisms governing immune responses and tissue destruction in TB.

It would be interesting to establish a co-culture model to better define the relationship between primary MDMs and NHBEs. Triple co-culture models, also including dendritic cells, have been used to simulate the human respiratory tract and assess the complex interplay of these cells in virosome studies (401). Co-culture models of monocytes and platelets have also been used to study MMP-mediated tissue destruction in TB (253). These models could be adapted and optimised for specific immunometabolism studies in TB. It would also be revealing to analyse AMs both alone and in a co-culture system. The first immune cells to interact with *M.tb* following inhalation, the reliance of AMs on fatty acid oxidation provide a metabolic advantage to bacteria

(331) and are key to determining the subsequent host response (34). The cross-talk between *M.tb*-infected AMs and uninfected AECs is also thought to be important in amplification of the TB immune response (38).

The cellular experiments in this project were performed mostly with chemical inhibitors; however, these can lack specificity or cause off-target effects. In order to support the 2DG findings, I performed siRNA knockdown of HK2 in NHBEs, though was unable to replicate this in MDMs. It would be helpful to extend this confirmation to all my *in vitro* studies with metabolic inhibitors. Hence, I would like to undertake further siRNA transfection or CRISPR-Cas9 gene editing to gain specific and robust data on metabolic signalling in TB. Successful HK2 (386), HIF-1α (402), AMPK α1/α2 (388) and mTORC1 (403) CRISPR-Cas9 gene knockouts have been reported in human cancer cell lines and these techniques can be applied to future TB research. Quantification of 3D ECM remodelling in TB under different metabolic conditions could also be performed by second harmonic generalisation (SHG) alongside multiphoton microscopy (MPM) techniques (404). This would allow a more nuanced understanding of the metabolic control of tissue destruction in TB.

Of note, HK inhibition also limits the glycolytic intermediates used in cellular anabolic processes, resulting in downstream effects on metabolism. Targeting of LDH has been proposed as an alternative to selectively decrease glycolytic flux without decreasing the availability of these intermediates (405). In this project, I attempted chemical inhibition of LDH in cellular models using sodium oxamate, but the results were inconclusive. However, another group has shown LDHA-deficient RAW264.7 murine cells to have impaired control of *M.tb* infection (406) and this approach might be worth assessing in human cells.

Macrophage polarisation, associated with cellular metabolic profile and immune effector functions, operates on a highly dynamic spectrum. Recently developed single-cell RNA sequencing techniques may help to characterise macrophage ontogeny and phenotype in TB

beyond the M1/M2 designation (407). It would also be useful to further investigate the glycolysis-induced increase in *M.tb* killing in macrophages seen here and in previous studies (154,322,331). Binding and phagocytosis of bacteria, as well as phagosome maturation and intracellular replication can be effectively analysed by flow cytometry or confocal microscopy using GFP-expressing *M.tb* (264,408); however, use of these techniques is limited by their need to be performed in a Category 3 setting.

Seahorse analysis could be performed in NHBEs to characterise their metabolic profile, as this has not been done in the context of TB. Several bioenergetic studies in *M.tb*-infected macrophages have shown metabolic reprogramming towards glycolysis (154,324,335), using the extracellular acidification rate (ECAR) as a measure of glycolysis. It has been postulated that the glycolytic proton efflux rate (glycoPER) is a more accurate indicator of glycolysis than ECAR (409) and it would be helpful to compare these outputs in future studies. In addition, it has been argued that the enhanced glucose uptake and lactate production seen in aerobic glycolysis can also occur in hypoxia (410). Hence, it is important to measure oxygen availability in order to define the Warburg effect as a separate phenomenon for modulation by HDTs (405). Human TB granulomas have been shown to be hypoxic (259) and it would be useful to assess this using PET imaging in future *in vivo* studies. Of interest, a set of experimental guidelines to investigate the Warburg effect in TB has recently been proposed to try and address some of these experimental challenges (405).

There is increasing evidence that the TCA cycle is pivotal for the generation of immunoregulatory metabolites. I would like to further assess the roles of the TCA cycle intermediates, succinate and itaconate, on tissue destruction in TB. In LPS-stimulated murine macrophages, succinate accumulates and, mediated by PKM2, signals through HIF-1α to increase IL-1β production (296,350). Succinate also accumulates in *M.tb*-infected murine lungs (326) and HIF-1α has been

shown to be essential for metabolic reprogramming and bacterial containment in *M.tb*-infected human macrophages (335). My data show that succinate stabilises HIF-1α and upregulates MMP-1 and -9 in CoMTB-stimulated NHBEs, but further studies are needed to delineate the precise mechanisms of action. Succinate also binds to a G-protein coupled receptor known as SUNCNR1, which contributes to determining macrophage phenotype in inflammation (411), but its role in TB is yet to be established. IRG1, which produces itaconate (315), is essential for host survival in murine TB, with *M.tb*-infected IRG1 knockout mice exhibiting excess inflammation and a higher bacterial burden (338). It has been postulated that succinate-driven pro-inflammatory mechanisms and itaconate-driven resolving mechanisms attempt to clear *M.tb* infection while minimising host damage (412). In line with this, recent metabolomics of *M.tb*-infected mouse lungs noted an increase in succinate 4 weeks post-infection which was dramatically reduced at 9 weeks, while itaconate steadily accumulated throughout this time course (328).

My *in vitro* experiments were conducted in primary cells using virulent *M.tb* H37Rv to maximise clinical relevance. However, it would be interesting to replicate these studies using immune cells from TB patients to ascertain the effect of metabolic manipulation on MMP and cytokine responses. TB patient cellular responses could be compared to healthy controls to obtain further insight into patterns of immunometabolic regulation.

Several additional aspects of TB immunometabolism present novel research opportunities (412). First, *M.tb* uses host fatty acids as its preferred energy source; numerous lipid-rich foamy macrophages are present in TB granulomas (413). It has been suggested that *M.tb*-induced metabolic reprogramming may promote lipid droplet production and aid immune evasion (332). *M.tb* inhibition of PFK-1, a rate-limiting enzyme in glycolysis, may increase flux through the PPP to boost fatty acid synthesis (332). Secondly, two amino acids, tryptophan and arginine, are also implicated in *M.tb* infection. Indoleamine 2,3-dioxygenase 1 (IDO1), which catalyses tryptophan

catabolism, is significantly increased in the *M.tb* granuloma in a non-human primate model (414); IDO1 inhibition improves mycobacterial containment (415). Arginine can be metabolised into RNS, which can act as antimicrobial effectors against *M.tb* and induce metabolic reprogramming in response to infection by stabilising HIF-1α (416). Thirdly, the host microbiome is an additional source of metabolites that may influence the host immune response and *M.tb* survival. Indole-3-propionic acid (IPA), a metabolite produced by the gut microbiome, inhibits *M.tb* growth *in vitro* and lowers splenic *M.tb* burden in a murine TB model (417). These interactions all remain poorly defined and are interesting avenues for more detailed studies.

Finally, development of an appropriate animal model would be highly beneficial in enhancing our understanding of metabolism in TB immunopathogenesis. Knockout animal models would allow *in vivo* assessment of the regulation of tissue destruction and bacterial replication in TB by targeted metabolic inhibition. In addition, therapeutic studies of immunoregulatory small molecules could be performed in experimental animal models of TB. My immunohistochemical studies showed that areas of TB inflammation strongly express HK2 in Balb/C mouse lungs. However, a limitation of C57BL/6 and Balb/C mouse strains is the lack of TB granuloma formation and tissue destruction analogous to human disease (263). Interestingly, it has been shown that C57BL/6 transgenic mice expressing MMP-1 under control of the scavenger receptor A promoter-enhancer can develop caseous necrosis (264). In addition, newer mouse strains such as C3HeB/FeJ and CBA/J, which produce cavities in response to *M.tb* infection, could be utilised in future research (418). Guinea pigs form TB granulomas without cavitation (267), while rabbits, which are naturally resistant to TB, develop cavitating disease (419). Hence, no animal model entirely replicates human TB immunopathology (261), but valuable data can be obtained from a variety of existing models. This is an essential step in the translation of *in vitro* research into the improvement of clinical outcomes in TB.

5.4 Final conclusions

Metabolism has emerged as a new frontier in TB immunopathogenesis. In this project, I have shown for the first time that cellular metabolic signalling functionally regulates MMPs and tissue destruction in TB. I have also demonstrated that metabolic pathways regulate cytokine profiles, the transcription factor HIF-1α and intracellular bacterial killing in TB. The findings in primary human MDMs and NHBEs, crucial to the TB immune response, suggest that their metabolic profile is closely coupled to their immune effector functions in TB. TB remains a major global health challenge and further elucidation of TB immunometabolism is key to developing novel host-directed therapeutics in future.

References

1. WHO. WHO | Global tuberculosis report 2019. World Health Organization. 2020.

2. M Cristina G, Brisse S, Brosch R, Fabre M, Omaïs B, Marmiesse M, et al. Ancient origin and gene mosaicism of the progenitor of Mycobacterium tuberculosis. PLoS Pathog. 2005;1(1):e5.

3. Comas I, Coscolla M, Luo T, Borrell S, Holt KE, Kato-Maeda M, et al. Out-of-Africa migration and Neolithic coexpansion of Mycobacterium tuberculosis with modern humans. Nat Genet. 2013;45(10):1176–82.

4. Murray JF. A century of tuberculosis. Am J Respir Crit Care Med. 2004;169(11):1181–6.

5. Daniel TM. The history of tuberculosis. Respir Med. 2006;100(11):1862–70.

6. CALMETTE A, GUERIN C, NEGRE L, BOQUET A. Immunization of the Newly Born against Tuberculosis. Premunition des Nouv Cent la Tuberc par le vaccin BCG (1921 a 1926). 1926;40:89–133.

7. Keshavjee S, Farmer PE. Tuberculosis, drug resistance, and the history of modern medicine. N Engl J Med. 2012;367(10):931–6.

8. Hmama Z, Peña-Díaz S, Joseph S, Av-Gay Y. Immunoevasion and immunosuppression of the macrophage by Mycobacterium tuberculosis. Immunol Rev. 2015;264(1):220–32.

9. Houben RMGJ, Dodd PJ. The Global Burden of Latent Tuberculosis Infection: A Re-estimation Using Mathematical Modelling. PLoS Med. 2016;13(10):e1002152.

10. Foster N, Vassall A, Cleary S, Cunnama L, Churchyard G, Sinanovic E. The economic burden of TB diagnosis and treatment in South Africa. Soc Sci Med. 2015;130:42–50.

11. O'Garra A, Redford PS, McNab FW, Bloom CI, Wilkinson RJ, Berry MPR. The Immune Response in Tuberculosis. Annu Rev Immunol. 2013;31(1):475–527.

12. Ai JW, Ruan QL, Liu QH, Zhang WH. Updates on the risk factors for latent tuberculosis

reactivation and their managements. Emerg Microbes Infect. 2016;5(2):e10.

13. Brändli O. The clinical presentation of tuberculosis. Respiration. 1998;65(2):97–105.

14. Tiemersma EW, van der Werf MJ, Borgdorff MW, Williams BG, Nagelkerke NJD. Natural history of tuberculosis: Duration and fatality of untreated pulmonary tuberculosis in HIV negative patients: A systematic review. PLoS One. 2011;6(4):e17601.

15. Richeldi L. An update on the diagnosis of tuberculosis infection. Am J Respir Crit Care Med. 2006;174:736–42.

16. Evenden P, Roche A, Karo B, Balasegaram S, Anderson CS. Presentation and healthcare delays among people with tuberculosis in London, and the impact on treatment outcome. BMJ Open Respir Res. 2019;6(1):e000468.

17. Millen SJ, Uys PW, Hargrove J, van Helden PD, Williams BG. The effect of diagnostic delays on the drop-out rate and the total delay to diagnosis of tuberculosis. PLoS One. 2008;3(4):e1933.

18. Bhalla AS, Goyal A, Guleria R, Gupta AK. Chest tuberculosis: Radiological review and imaging recommendations. Indian J Radiol Imaging. 2015;25(3):213–25.

19. Steingart KR, Henry M, Ng V, Hopewell PC, Ramsay A, Cunningham J, et al. Fluorescence versus conventional sputum smear microscopy for tuberculosis: a systematic review. Lancet Infect Dis. 2006;6(9):570–81.

20. Rageade F, Picot N, Blanc-Michaud A, Chatellier S, Mirande C, Fortin E, et al. Performance of solid and liquid culture media for the detection of Mycobacterium tuberculosis in clinical materials: Meta-analysis of recent studies. Eur J Clin Microbiol Infect Dis. 2014;33:867–70.

21. Pfyffer GE. Mycobacterium: General Characteristics, Laboratory Detection, and Staining Procedures*. In: Manual of Clinical Microbiology, 11th Edition. 2015. p. 536–69.

22. Opota O, Mazza-Stalder J, Greub G, Jaton K. The rapid molecular test Xpert MTB/RIF ultra: towards improved tuberculosis diagnosis and rifampicin resistance detection. Clin Microbiol Infect. 2019;25:1370–6.

23. Martin C, Aguilo N, Marinova D, Gonzalo-Asensio J. Update on TB vaccine pipeline. Appl

Sci. 2020;10(7):2632.

24. Mangtani P, Abubakar I, Ariti C, Beynon R, Pimpin L, Fine PEM, et al. Protection by BCG vaccine against tuberculosis: A systematic review of randomized controlled trials. Clin Infect Dis. 2014;

25. McShane H. Insights and challenges in tuberculosis vaccine development. The Lancet Respiratory Medicine. 2019.

26. Saukkonen JJ, Cohn DL, Jasmer RM, Schenker S, Jereb JA, Nolan CM, et al. An official ATS statement: Hepatotoxicity of antituberculosis therapy. Am J Respir Crit Care Med. 2006;174(8):935–52.

27. Velásquez GE, Becerra MC, Gelmanova IY, Pasechnikov AD, Yedilbayev A, Shin SS, et al. Improving outcomes for multidrug-resistant tuberculosis: Aggressive regimens prevent treatment failure and death. Clin Infect Dis. 2014;59(1):9–15.

28. Velayati AA, Farnia P, Hoffner S. Drug-resistant Mycobacterium tuberculosis: Epidemiology and role of morphological alterations. J Glob Antimicrob Resist. 2018;12:192–6.

29. Kiran D, Podell BK, Chambers M, Basaraba RJ. Host-directed therapy targeting the Mycobacterium tuberculosis granuloma: a review. Semin Immunopathol. 2016;38:167–83.

30. Tsenova L, Singhal A. Effects of host-directed therapies on the pathology of tuberculosis. J Pathol. 2020;250:636–46.

31. Young C, Walzl G, Du Plessis N. Therapeutic host-directed strategies to improve outcome in tuberculosis. Mucosal Immunol. 2020;13:190–204.

32. Zumla A, Maeurer M, Chakaya J, Hoelscher M, Ntoumi F, Rustomjee R, et al. Towards host-directed therapies for tuberculosis. Nat Rev Drug Discov. 2015;14(8):511–2.

33. Rothchild AC, Olson GS, Nemeth J, Amon LM, Mai D, Gold ES, et al. Alveolar macrophages generate a noncanonical NRF2-driven transcriptional response to Mycobacterium tuberculosis in vivo. Sci Immunol. 2019;4(37):eaaw6693.

34. Cohen SB, Gern BH, Delahaye JL, Adams KN, Plumlee CR, Winkler JK, et al. Alveolar

Macrophages Provide an Early Mycobacterium tuberculosis Niche and Initiate Dissemination. Cell Host Microbe. 2018;24(3):439-446.e4.

35. Wolf AJ, Linas B, Trevejo-Nuñez GJ, Kincaid E, Tamura T, Takatsu K, et al. Mycobacterium tuberculosis Infects Dendritic Cells with High Frequency and Impairs Their Function In Vivo. J Immunol. 2007;179(4):2509–19.

36. Sturgill-Koszycki S, Schlesinger PH, Chakraborty P, Haddix PL, Collins HL, Fok AK, et al. Lack of acidification in Mycobacterium phagosomes produced by exclusion of the vesicular proton-ATPase. Science (80-). 1994;263(5147):678–81.

37. Ryndak MB, Laal S. Mycobacterium tuberculosis Primary Infection and Dissemination: A Critical Role for Alveolar Epithelial Cells. Front Cell Infect Microbiol. 2019;9:299.

38. Reuschl AK, Edwards MR, Parker R, Connell DW, Hoang L, Halliday A, et al. Innate activation of human primary epithelial cells broadens the host response to Mycobacterium tuberculosis in the airways. PLoS Pathog. 2017;13(9):e1006577.

39. Nguyen L, Pieters J. The Trojan horse: Survival tactics of pathogenic mycobacteria in macrophages. Trends Cell Biol. 2005;15(5):269–76.

40. Norris BA, Ernst JD. Mononuclear cell dynamics in M. tuberculosis infection provide opportunities for therapeutic intervention. PLoS Pathog. 2018;14(10):e1007154.

41. Corleis B, Dorhoi A. Early dynamics of innate immunity during pulmonary tuberculosis. Immunol Lett. 2020;221:56–60.

42. Jasenosky LD, Scriba TJ, Hanekom WA, Goldfeld AE. T cells and adaptive immunity to Mycobacterium tuberculosis in humans. Immunol Rev. 2015;

43. Ramakrishnan L. Revisiting the role of the granuloma in tuberculosis. Nat Rev Immunol. 2012;12:352–66.

44. Volkman HE, Pozos TC, Zheng J, Davis JM, Rawls JF, Ramakrishnan L. Tuberculous granuloma induction via interaction of a bacterial secreted protein with host epithelium. Science (80-). 2010;327(5694):466–9.

45. Rubin EJ. The granuloma in tuberculosis - Friend or foe? N Engl J Med.

2009;360(23):2471.

46. Bold TD, Ernst JD. CD4 + T Cell-Dependent IFN-γ Production by CD8 + Effector T Cells in Mycobacterium tuberculosis Infection. J Immunol. 2012;189(5):2530–6.

47. Ulrichs T, Kaufmann SHE. New insights into the function of granulomas in human tuberculosis. J Pathol. 2006;208:261–9.

48. Cronan MR, Beerman RW, Rosenberg AF, Saelens JW, Johnson MG, Oehlers SH, et al. Macrophage Epithelial Reprogramming Underlies Mycobacterial Granuloma Formation and Promotes Infection. Immunity. 2016;45(4):861–76.

49. Martin CJ, Carey AF, Fortune SM. A bug's life in the granuloma. Semin Immunopathol. 2016;38(2):213–20.

50. Davis JM, Ramakrishnan L. The Role of the Granuloma in Expansion and Dissemination of Early Tuberculous Infection. Cell. 2009;136(1):37–49.

51. Guirado E, Schlesinger LS. Modeling the Mycobacterium tuberculosis granuloma - the critical battlefield in host immunity and disease. Front Immunol. 2013;4:98.

52. Kaplan G, Post FA, Moreira AL, Wainwright H, Kreiswirth BN, Tanverdi M, et al. Mycobacterium tuberculosis Growth at the Cavity Surface: A Microenvironment with Failed Immunity. Infect Immun. 2003;71(12):7099–108.

53. Lillebaek T, Dirksen A, Vynnycky E, Baess I, Thomsen VØ, Andersen ÅB. Stability of DNA Patterns and Evidence of Mycobacterium tuberculosis Reactivation Occurring Decades after the Initial Infection. J Infect Dis. 2003;188(7):1032–9.

54. CANETTI G. Dynamic aspects of the pathology and bacteriology of tuberculous lesions. Am Rev Tuberc. 1956;74(2 Part 2):13–21.

55. Dannenberg, Jr. AM, Cook JL. :Pathogenesis of Human Pulmonary Tuberculosis: Insights from the Rabbit Model. Clin Infect Dis. 2007;44(9):1257–8.

56. Lenaerts A, Barry CE, Dartois V. Heterogeneity in tuberculosis pathology, microenvironments and therapeutic responses. Immunol Rev. 2015;264(1):288–307.

57. Lin PL, Rodgers M, Smith L, Bigbee M, Myers A, Bigbee C, et al. Quantitative comparison of active and latent tuberculosis in the cynomolgus macaque model. Infect Immun. 2009;77(10):4631–42.

58. Gideon HP, Phuah JY, Myers AJ, Bryson BD, Rodgers MA, Coleman MT, et al. Variability in Tuberculosis Granuloma T Cell Responses Exists, but a Balance of Pro- and Anti-inflammatory Cytokines Is Associated with Sterilization. PLoS Pathog. 2015;11(1):1–28.

59. Gupta N, Kumar R, Agrawal B. New players in immunity to tuberculosis: The host microbiome, lung epithelium, and innate immune cells. Front Immunol. 2018;9:709.

60. Cadena AM, Flynn JL, Fortune SM. The importance of first impressions: Early events in mycobacterium tuberculosis infection influence outcome. MBio. 2016;7(2):e00342-16.

61. Dorhoi A, Reece ST, Kaufmann SHE. For better or for worse: The immune response against Mycobacterium tuberculosis balances pathology and protection. Immunol Rev. 2011;240(1):235–51.

62. Schorey JS, Schlesinger LS. Innate Immune Responses to Tuberculosis. Microbiol Spectr. 2016;4(6):TBTB2-0010–2016.

63. Verrall AJ, G. Netea M, Alisjahbana B, Hill PC, van Crevel R. Early clearance of Mycobacterium tuberculosis: A new frontier in prevention. Immunology. 2014;141(4):506–13.

64. Morrison J, Pai M, Hopewell PC. Tuberculosis and latent tuberculosis infection in close contacts of people with pulmonary tuberculosis in low-income and middle-income countries: a systematic review and meta-analysis. Lancet Infect Dis. 2008;8(6):359–68.

65. Kaufmann SHE, Dorhoi A. Inflammation in tuberculosis: Interactions, imbalances and interventions. Curr Opin Immunol. 2013;25(4):441–9.

66. Flynn JL, Chan J, Lin PL. Macrophages and control of granulomatous inflammation in tuberculosis. Mucosal Immunol. 2011;4(3):271–8.

67. Murray PJ. Macrophage Polarization. Annu Rev Physiol. 2017;79:541–66.

68. Galván-Peña S, O'Neill LAJ. Metabolic reprogramming in macrophage polarization. Front

Immunol. 2014;5.

69. Shi L, Jiang Q, Bushkin Y, Subbian S, Tyagi S. Biphasic dynamics of macrophage immunometabolism during Mycobacterium tuberculosis infection. MBio. 2019;10(2):e02550-18.

70. Schäfer G, Jacobs M, Wilkinson RJ, Brown GD. Non-opsonic recognition of mycobacterium tuberculosis by phagocytes. J Innate Immun. 2009;1(3):231–43.

71. Killick KE, Ní Cheallaigh C, O'Farrelly C, Hokamp K, Machugh DE, Harris J. Receptor-mediated recognition of mycobacterial pathogens. Cell Microbiol. 2013;15(9):1484–95.

72. Cywes L, Hoppe HC, Daffé M, Ehlers MRW. Nonopsonic binding of Mycobacterium tuberculosis to complement receptor type 3 is mediated by capsular polysaccharides and is strain dependent. Infect Immun. 1997;65(10):4258–66.

73. Mortaz E. Role of pattern recognition receptors in Mycobacterium tuberculosis infection. Int J Mycobacteriology. 2015;35(1):1–10.

74. Sasindran SJ, Torrelles JB. Mycobacterium tuberculosis infection and inflammation: What is beneficial for the host and for the bacterium? Front Microbiol. 2011;2:2.

75. Kleinnijenhuis J, Joosten LAB, van de Veerdonk FL, Savage N, van Crevel R, Kullberg BJ, et al. Transcriptional and inflammasome-mediated pathways for the induction of IL-1β production by Mycobacterium tuberculosis. Eur J Immunol. 2009;39(7):1914–22.

76. Fremond CM, Togbe D, Doz E, Rose S, Vasseur V, Maillet I, et al. IL-1 Receptor-Mediated Signal Is an Essential Component of MyD88-Dependent Innate Response to Mycobacterium tuberculosis Infection. J Immunol. 2007;179(2):1178–89.

77. Scanga CA, Bafica A, Feng CG, Cheever AW, Hieny S, Sher A. MyD88-Deficient Mice Display A Profound Loss in Resistance to Mycobacterium tuberculosis Associated with Partially Impaired Th1 Cytokine and Nitric Oxide Synthase 2 Expression. Infect Immun. 2004;72(4):2400–4.

78. Underhill DM, Ozinsky A, Smith KD, Aderem A. Toll-like receptor-2 mediates mycobacteria-induced proinflammatory signaling in macrophages. Proc Natl Acad Sci U S A.

1999;96(25):14459–63.

79. Drennan MB, Nicolle D, Quesniaux VJF, Jacobs M, Allie N, Mpagi J, et al. Toll-Like Receptor 2-Deficient Mice Succumb to Mycobacterium tuberculosis Infection. Am J Pathol. 2004;164(1):49–67.

80. Means TK, Jones BW, Schromm AB, Shurtleff BA, Smith JA, Keane J, et al. Differential Effects of a Toll-Like Receptor Antagonist on Mycobacterium tuberculosis -Induced Macrophage Responses. J Immunol. 2001;166(6):4074–82.

81. Reiling N, Hölscher C, Fehrenbach A, Kröger S, Kirschning CJ, Goyert S, et al. Cutting Edge: Toll-Like Receptor (TLR)2- and TLR4-Mediated Pathogen Recognition in Resistance to Airborne Infection with Mycobacterium tuberculosis. J Immunol. 2002;169(7):3480–4.

82. Abel B, Thieblemont N, Quesniaux VJF, Brown N, Mpagi J, Miyake K, et al. Toll-Like Receptor 4 Expression Is Required to Control Chronic Mycobacterium tuberculosis Infection in Mice. J Immunol. 2002;169(6):3155–62.

83. Bafica A, Scanga CA, Feng CG, Leifer C, Cheever A, Sher A. TLR9 regulates Th1 responses and cooperates with TLR2 in mediating optimal resistance to Mycobacterium tuberculosis. J Exp Med. 2005;202(12):1715–24.

84. Armstrong JA, Hart D. Response of cultured macrophages to Mycobacterium Tuberculosis, with observations on fusion of lysosomes with phagosomes. J Exp Med. 1971;134(3):713–40.

85. Kang PB, Azad AK, Torrelles JB, Kaufman TM, Beharka A, Tibesar E, et al. The human macrophage mannose receptor directs Mycobacterium tuberculosis lipoarabinomannan-mediated phagosome biogenesis. J Exp Med. 2005;202(7):987–99.

86. Bach H, Papavinasasundaram KG, Wong D, Hmama Z, Av-Gay Y. Mycobacterium tuberculosis Virulence Is Mediated by PtpA Dephosphorylation of Human Vacuolar Protein Sorting 33B. Cell Host Microbe. 2008;3(5):316–22.

87. Vergne I, Chua J, Lee HH, Lucas M, Belisle J, Deretic V. Mechanism of phagolysosome biogenesis block by viable Mycobacterium tuberculosis. Proc Natl Acad Sci U S A. 2005;102(11):4033–8.

88. Wong D, Bach H, Sun J, Hmama Z, Av-Gay Y. Mycobacterium tuberculosis protein tyrosine phosphatase (PtpA) excludes host vacuolar-H +-ATPase to inhibit phagosome acidification. Proc Natl Acad Sci U S A. 2011;108(48):19371–6.

89. Behar SM, Martin CJ, Booty MG, Nishimura T, Zhao X, Gan HX, et al. Apoptosis is an innate defense function of macrophages against Mycobacterium tuberculosis. Mucosal Immunol. 2011;4(3):279–87.

90. Martin CJ, Booty MG, Rosebrock TR, Nunes-Alves C, Desjardins DM, Keren I, et al. Efferocytosis is an innate antibacterial mechanism. Cell Host Microbe. 2012;12(3):289–300.

91. Luciw PA, Oslund KL, Yang XW, Adamson L, Ravindran R, Canfield DR, et al. Stereological analysis of bacterial load and lung lesions in nonhuman primates (rhesus macaques) experimentally infected with Mycobacterium tuberculosis. Am J Physiol - Lung Cell Mol Physiol. 2011;301(5):L731-738.

92. Keane J, Remold HG, Kornfeld H. Virulent Mycobacterium tuberculosis Strains Evade Apoptosis of Infected Alveolar Macrophages. J Immunol. 2000;164(4):2016–20.

93. Chen M, Gan H, Remold HG. A Mechanism of Virulence: Virulent Mycobacterium tuberculosis Strain H37Rv, but Not Attenuated H37Ra, Causes Significant Mitochondrial Inner Membrane Disruption in Macrophages Leading to Necrosis. J Immunol. 2006;176(6):3707–16.

94. Saquib NM, Jamwal S, Midha MK, Verma HN, Manivel V. Quantitative Proteomics and Lipidomics Analysis of Endoplasmic Reticulum of Macrophage Infected with Mycobacterium tuberculosis. Int J Proteomics. 2015;2015:270438.

95. Balcewicz-Sablinska MK, Keane J, Kornfeld H, Remold HG. Pathogenic Mycobacterium tuberculosis evades apoptosis of host macrophages by release of TNF-R2, resulting in inactivation of TNF-alpha. J Immunol. 1998;161(5):2636–41.

96. Lam A, Prabhu R, Gross CM, Riesenberg LA, Singh V, Aggarwal S. Role of apoptosis and autophagy in tuberculosis. Am J Physiol - Lung Cell Mol Physiol. 2017;313(2):L218–29.

97. Gutierrez MG, Master SS, Singh SB, Taylor GA, Colombo MI, Deretic V. Autophagy is a

defense mechanism inhibiting BCG and Mycobacterium tuberculosis survival in infected macrophages. Cell. 2004;119(6):753–66.

98. Sakowski ET, Koster S, Portal Celhay C, Park HS, Shrestha E, Hetzenecker SE, et al. Ubiquilin 1 Promotes IFN-γ-Induced Xenophagy of Mycobacterium tuberculosis. PLoS Pathog. 2015;11(7):e1005076.

99. Li F, Gao B, Xu W, Chen L, Xiong S. The defect in autophagy induction by clinical isolates of mycobacterium tuberculosis is correlated with poor tuberculosis outcomes. PLoS One. 2016;11(1):e0147810.

100. Dutta RK, Kathania M, Raje M, Majumdar S. IL-6 inhibits IFN-γ induced autophagy in Mycobacterium tuberculosis H37Rv infected macrophages. Int J Biochem Cell Biol. 2012;44(6):942–54.

101. Kim YS, Lee H-M, Kim JK, Yang C-S, Kim TS, Jung M, et al. PPAR-α Activation Mediates Innate Host Defense through Induction of TFEB and Lipid Catabolism. J Immunol. 2017;198(8):3283–95.

102. Russell RC, Yuan HX, Guan KL. Autophagy regulation by nutrient signaling. Cell Res. 2014;24(1):42–57.

103. Shin DM, Jeon BY, Lee HM, Jin HS, Yuk JM, Song CH, et al. Mycobacterium tuberculosis eis regulates autophagy, inflammation, and cell death through redox-dependent signaling. PLoS Pathog. 2010;

104. Duan L, Yi M, Chen J, Li S, Chen W. Mycobacterium tuberculosis EIS gene inhibits macrophage autophagy through up-regulation of IL-10 by increasing the acetylation of histone H3. Biochem Biophys Res Commun. 2016;473(4):1229–34.

105. Chandra P, Ghanwat S, Matta SK, Yadav SS, Mehta M, Siddiqui Z, et al. Mycobacterium tuberculosis Inhibits RAB7 Recruitment to Selectively Modulate Autophagy Flux in Macrophages. Sci Rep. 2015;5:16320.

106. Ouimet M, Koster S, Sakowski E, Ramkhelawon B, Van Solingen C, Oldebeken S, et al. Mycobacterium tuberculosis induces the MIR-33 locus to reprogram autophagy and host lipid metabolism. Nat Immunol. 2016;17(6):677–86.

107. Voskuil MI, Bartek IL, Visconti K, Schoolnik GK. The response of Mycobacterium tuberculosis to reactive oxygen and nitrogen species. Front Microbiol. 2011;2:105.

108. Jamaati H, Mortaz E, Pajouhi Z, Folkerts G, Movassaghi M, Moloudizargari M, et al. Nitric oxide in the pathogenesis and treatment of tuberculosis. Front Microbiol. 2017;8:2008.

109. Cooper AM, Segal BH, Frank AA, Holland SM, Orme IM. Transient loss of resistance to pulmonary tuberculosis in p47(phox-/-) mice. Infect Immun. 2000;68(3):1231–4.

110. Deffert C, Cachat J, Krause KH. Phagocyte NADPH oxidase, chronic granulomatous disease and mycobacterial infections. Cell Microbiol. 2014;16(8):1168–78.

111. Bustamante J, Aksu G, Vogt G, de Beaucoudrey L, Genel F, Chapgier A, et al. BCG-osis and tuberculosis in a child with chronic granulomatous disease. J Allergy Clin Immunol. 2007;120(1):32–8.

112. Flynn JL, Chan J. I MMUNOLOGY OF T UBERCULOSIS. Annu Rev Immunol. 2001;19(1):93–129.

113. Ehrt S, Schnappinger D. Mycobacterial survival strategies in the phagosome: Defence against host stresses. Cell Microbiol. 2009;11(8):1170–8.

114. Saini V, Cumming BM, Guidry L, Lamprecht DA, Adamson JH, Reddy VP, et al. Ergothioneine Maintains Redox and Bioenergetic Homeostasis Essential for Drug Susceptibility and Virulence of Mycobacterium tuberculosis. Cell Rep. 2016;14(3):572–85.

115. Sareen D, Newton GL, Fahey RC, Buchmeier NA. Mycothiol Is Essential for Growth of Mycobacterium tuberculosis Erdman. J Bacteriol. 2003;185(22):6736–40.

116. Lanoix JP, Lenaerts AJ, Nuermberger EL. Heterogeneous disease progression and treatment response in a C3HeB/FeJ mouse model of tuberculosis. DMM Dis Model Mech. 2015;8(6):603–10.

117. Hiemstra PS, McCray PB, Bals R. The innate immune function of airway epithelial cells in inflammatory lung disease. Eur Respir J. 2015;45(4):1150–62.

118. Whitsett JA, Alenghat T. Respiratory epithelial cells orchestrate pulmonary innate immunity. Nat Immunol. 2015;16(1):27–35.

119. Bermudez LE, Goodman J. Mycobacterium tuberculosis invades and replicates within type II alveolar cells. Infect Immun. 1996;64(4):1400–6.

120. Dobos KM, Spotts EA, Quinn FD, King CH. Necrosis of lung epithelial cells during infection with Mycobacterium tuberculosis is preceded by cell permeation. Infect Immun. 2000;68(11):6300–10.

121. Sato K, Tomioka H, Shimizu T, Gonda T, Ota F, Sano C. Type II Alveolar Cells Play Roles in Macrophage-Mediated Host Innate Resistance to Pulmonary Mycobacterial Infections by Producing Proinflammatory Cytokines. J Infect Dis. 2002;185(8):1139–47.

122. Castro-Garza J, King CH, Swords WE, Quinn FD. Demonstration of spread by Mycobacterium tuberculosis bacilli in A549 epithelial cell monolayers. FEMS Microbiol Lett. 2002;212(2):145–9.

123. Vir P, Gupta D, Agarwal R, Verma I. Immunomodulation of alveolar epithelial cells by Mycobacterium tuberculosis phosphatidylinositol mannosides results in apoptosis. APMIS. 2014;122(4):268–82.

124. Scordo JM, Knoell DL, Torrelles JB. Alveolar Epithelial Cells in Mycobacterium tuberculosis Infection: Active Players or Innocent Bystanders? J Innate Immun. 2016;8(1):3–14.

125. Fine KL, Metcalfe MG, White E, Virji M, Karls RK, Quinn FD. Involvement of the autophagy pathway in trafficking of Mycobacterium tuberculosis bacilli through cultured human type II epithelial cells. Cell Microbiol. 2012;14(9):1402–4.

126. Kinhikar AG, Verma I, Chandra D, Singh KK, Weldingh K, Andersen P, et al. Potential role for ESAT6 in dissemination of M. tuberculosis via human lung epithelial cells. Mol Microbiol. 2010;75(1):92–106.

127. Ferguson JS, Schlesinger LS. Pulmonary surfactant in innate immunity and the pathogenesis of tuberculosis. Tuber Lung Dis. 2000;80(4–5):173–84.

128. Li Y, Wang Y, Liu X. The role of airway epithelial cells in response to mycobacteria infection. Clin Dev Immunol. 2012;2012:791392.

129. Thomas LH, Wickremasinghe MIY, Friedland JS. IL-1β stimulates divergent upper and

lower airway epithelial cell CCL5 secretion. Clin Immunol. 2007;122:229–38.

130. Sonawane A, Santos JC, Mishra BB, Jena P, Progida C, Sorensen OE, et al. Cathelicidin is involved in the intracellular killing of mycobacteria in macrophages. Cell Microbiol. 2011;13(10):1601–17.

131. Méndez-Samperio P, Miranda E, Trejo A. Expression and secretion of cathelicidin LL-37 in human epithelial cells after infection by Mycobacterium bovis bacillus Calmette-Guérin. Clin Vaccine Immunol. 2008;15(9):1450–5.

132. Rivas-Santiago B, Hernandez-Pando R, Carranza C, Juarez E, Contreras JL, Aguilar-Leon D, et al. Expression of cathelicidin LL-37 during Mycobacterium tuberculosis infection in human alveolar macrophages, monocytes, neutrophils, and epithelial cells. Infect Immun. 2008;76(3):935–41.

133. Rivas-Santiago B, Schwander SK, Sarabia C, Diamond G, Klein-Patel ME, Hernandez-Pando R, et al. Human β-defensin 2 is expressed and associated with Mycobacterium tuberculosis during infection of human alveolar epithelial cells. Infect Immun. 2005;73(8):4505–11.

134. Rivas-Santiago B, Sada E, Tsutsumi V, Aguilar-León D, Contreras JL, Hernández-Pando R. β-Defensin Gene Expression during the Course of Experimental Tuberculosis Infection. J Infect Dis. 2006;194(5):697–701.

135. Rodriguez-Carlos A, Valdez-Miramontes C, Marin-Luevano P, González-Curiel I, Enciso-Moreno JA, Rivas-Santiago B. Metformin promotes Mycobacterium tuberculosis killing and increases the production of human β-defensins in lung epithelial cells and macrophages. Microbes Infect. 2020;22(3):111–8.

136. Cakir E, Torun E, Gedik AH, Umutoglu T, Aktas EC, Topuz U, et al. Cathelicidin and human β-defensin 2 in bronchoalveolar lavage fluid of children with pulmonary tuberculosis. Int J Tuberc Lung Dis. 2014;18(6):671–5.

137. Bongiovanni B, Marín-Luevano S, D'Attilio L, Díaz A, Fernández R del V, Santucci N, et al. Evidence that changes in antimicrobial peptides during tuberculosis are related to disease severity, clinical presentation, specific therapy and levels of immune-endocrine mediators. Cytokine. 2020;126:154913.

138. Sow FB, Nandakumar S, Velu V, Kellar KL, Schlesinger LS, Amara RR, et al. Mycobacterium tuberculosis components stimulate production of the antimicrobial peptide hepcidin. Tuberculosis. 2011;91(4):314–21.

139. Minchella PA, Armitage AE, Darboe B, Jallow MW, Drakesmith H, Jaye A, et al. Elevated hepcidin at HIV diagnosis is associated with incident tuberculosis in a retrospective cohort study. Int J Tuberc Lung Dis. 2014;18(11):1337–9.

140. Kerkhoff AD, Meintjes G, Burton R, Vogt M, Wood R, Lawn SD. Relationship between blood concentrations of hepcidin and anemia severity, mycobacterial burden, and mortality among patients with HIV-associated tuberculosis. J Infect Dis. 2016;213(1):61–70.

141. Harrington-Kandt R, Stylianou E, Eddowes LA, Lim PJ, Stockdale L, Pinpathomrat N, et al. Hepcidin deficiency and iron deficiency do not alter tuberculosis susceptibility in a murine M. tb infection model. PLoS One. 2018;13(1):e0191038.

142. Stefanova D, Raychev A, Arezes J, Ruchala P, Gabayan V, Skurnik M, et al. Endogenous hepcidin and its agonist mediate resistance to selected infections by clearing non–transferrin-bound iron. Blood. 2017;130(3):245–57.

143. Hsieh M-H, Ou C-Y, Hsieh W-Y, Kao H-F, Lee S-W, Wang J-Y, et al. Functional Analysis of Genetic Variations in Surfactant Protein D in Mycobacterial Infection and Their Association With Tuberculosis. Front Immunol. 2018;9:1543.

144. Nayak A, Dodagatta-Marri E, Tsolaki AG, Kishore U. An insight into the diverse roles of surfactant proteins, SP-A and SP-D in innate and adaptive immunity. Front Immunol. 2012;3:131.

145. Matucci A, Maggi E, Vultaggio A. Cellular and humoral immune responses during tuberculosis infection: Useful knowledge in the era of biological agents. J Rheumatol. 2014;91:17–23.

146. Cooper AM, Khader SA. The role of cytokines in the initiation, expansion, and control of cellular immunity to tuberculosis. Immunol Rev. 2008;226:191–204.

147. Domingo-Gonzalez R, Prince O, Cooper A, Khader SA. Cytokines and Chemokines in Mycobacterium tuberculosis Infection. Microbiol Spectr. 2016;4(5):10.1128.

148. Schenk M, Fabri M, Krutzik SR, Lee DJ, Vu DM, Sieling PA, et al. Interleukin-1β triggers the differentiation of macrophages with enhanced capacity to present mycobacterial antigen to T cells. Immunology. 2014;141(2):174–80.

149. Mayer-Barber KD, Barber DL, Shenderov K, White SD, Wilson MS, Cheever A, et al. Cutting Edge: Caspase-1 Independent IL-1β Production Is Critical for Host Resistance to Mycobacterium tuberculosis and Does Not Require TLR Signaling In Vivo. J Immunol. 2010;184(7):3326–30.

150. Yamada H, Mizumo S, Horai R, Iwakura Y, Sugawara I. Protective role of interleukin-1 in mycobacterial infection in IL-1 α/β double-knockout mice. Lab Investig. 2000;80(5):759–67.

151. Juffermans NP, Florquin S, Camoglio L, Verbon A, Kolk AH, Speelman P, et al. Interleukin-1 Signaling Is Essential for Host Defense during Murine Pulmonary Tuberculosis. J Infect Dis. 2000;182(3):902–8.

152. Sugawara I, Yamada H, Hua S, Mizuno S. Role of interleukin (IL)-1 type 1 receptor in mycobacterial infection. Microbiol Immunol. 2001;45(11):743–50.

153. Di Paolo NC, Shafiani S, Day T, Papayannopoulou T, Russell DW, Iwakura Y, et al. Interdependence between Interleukin-1 and Tumor Necrosis Factor Regulates TNF-Dependent Control of Mycobacterium tuberculosis Infection. Immunity. 2015;43(6):1125–36.

154. Gleeson LE, Sheedy FJ, Palsson-McDermott EM, Triglia D, O'Leary SM, O'Sullivan MP, et al. Cutting Edge: Mycobacterium tuberculosis Induces Aerobic Glycolysis in Human Alveolar Macrophages That Is Required for Control of Intracellular Bacillary Replication. J Immunol. 2016;196(6):2444–9.

155. Mayer-Barber KD, Andrade BB, Oland SD, Amaral EP, Barber DL, Gonzales J, et al. Host-directed therapy of tuberculosis based on interleukin-1 and type i interferon crosstalk. Nature. 2014;511(7507):99–103.

156. Novikov A, Cardone M, Thompson R, Shenderov K, Kirschman KD, Mayer-Barber KD, et al. Mycobacterium tuberculosis Triggers Host Type I IFN Signaling To Regulate IL-1β Production in Human Macrophages. J Immunol. 2011;187(5):2540–7.

157. Mayer-Barber KD, Andrade BB, Barber DL, Hieny S, Feng CG, Caspar P, et al. Innate and Adaptive Interferons Suppress IL-1α and IL-1β Production by Distinct Pulmonary Myeloid Subsets during Mycobacterium tuberculosis Infection. Immunity. 2011;35(6):1023–34.

158. Franchi L, Eigenbrod T, Muñoz-Planillo R, Nuñez G. The inflammasome: A caspase-1-activation platform that regulates immune responses and disease pathogenesis. Nat Immunol. 2009;10(3):241–7.

159. Briken V, Ahlbrand SE, Shah S. Mycobacterium tuberculosis and the host cell inflammasome: A complex relationship. Front Cell Infect Microbiol. 2013;3:62.

160. Mayer-Barber KD, Yan B. Clash of the Cytokine Titans: Counter-regulation of interleukin-1 and type i interferon-mediated inflammatory responses. Cell Mol Immunol. 2017;14(1):22–35.

161. Netea MG, Simon A, Van De Veerdonk F, Kullberg BJ, Van Der Meer JWM, Joosten LAB. IL-1β processing in host defense: Beyond the inflammasomes. PLoS Pathog. 2010;6(2):e1000661.

162. Wilkinson RJ, Patel P, Llewelyn M, Hirsch CS, Pasvol G, Snounou G, et al. Influence of polymorphism in the genes for the interleukin (IL)-1 receptor antagonist and IL-1β on tuberculosis. J Exp Med. 1999;189(12):1863–974.

163. Flynn JAL, Goldstein MM, Chan J, Triebold KJ, Pfeffer K, Lowenstein CJ, et al. Tumor necrosis factor-α is required in the protective immune response against mycobacterium tuberculosis in mice. Immunity. 1995;2(6):561–72.

164. Bean A, Roach D, Briscoe H, France M, Korner H. Structural Deficiencies in Granuloma Formation in TNF Gene-Targeted Mice Underlie the Heightened …. J Immunol. 1999;162(6):3504–11.

165. Scott Algood HM, Lin PL, Flynn JL. Tumor Necrosis Factor and Chemokine Interactions in the Formation and Maintenance of Granulomas in Tuberculosis. Clin Infect Dis. 2005;41(Suppl 3):S189-93.

166. Roach DR, Bean AGD, Demangel C, France MP, Briscoe H, Britton WJ. TNF Regulates Chemokine Induction Essential for Cell Recruitment, Granuloma Formation, and Clearance

of Mycobacterial Infection. J Immunol. 2002;168(9):4620–7.

167. Kaneko H, Yamada H, Mizuno S, Udagawa T, Kazumi Y, Sekikawa K, et al. Role of tumor necrosis factor-α in Mycobacterium-induced granuloma formation in tumor necrosis factor-α-deficient mice. Lab Investig. 1999;79(4):379–86.

168. Clay H, Volkman HE, Ramakrishnan L. Tumor Necrosis Factor Signaling Mediates Resistance to Mycobacteria by Inhibiting Bacterial Growth and Macrophage Death. Immunity. 2008;29(2):283–94.

169. Mohan VP, Scanga CA, Yu K, Scott HM, Tanaka KE, Tsang E, et al. Effects of tumor necrosis factor alpha on host immune response in chronic persistent tuberculosis: Possible role for limiting pathology. Infect Immun. 2001;69(3):1847–55.

170. Keane J, Balcewicz-Sablinska MK, Remold HG, Chupp GL, Meek BB, Fenton MJ, et al. Infection by Mycobacterium tuberculosis promotes human alveolar macrophage apoptosis. Infect Immun. 1997;65(1):298–304.

171. Orvedahl A, McAllaster MR, Sansone A, Dunlap BF, Desai C, Wang YT, et al. Autophagy genes in myeloid cells counteract IFNγ-induced TNF-mediated cell death and fatal TNF-induced shock. Proc Natl Acad Sci U S A. 2019;116(33):16497–506.

172. Ramirez GML, Rom WN, Ciotoli C, Talbot A, Martiniuk F, Cronstein B, et al. Mycobacterium tuberculosis alters expression of adhesion molecules on monocytic cells. Infect Immun. 1994;62(6):2515–20.

173. Roca FJ, Whitworth LJ, Redmond S, Jones AA, Ramakrishnan L. TNF Induces Pathogenic Programmed Macrophage Necrosis in Tuberculosis through a Mitochondrial-Lysosomal-Endoplasmic Reticulum Circuit. Cell. 2019;178(6):1344–61.

174. Harris J, Hope JC, Keane J. Tumor Necrosis Factor Blockers Influence Macrophage Responses to Mycobacterium tuberculosis. J Infect Dis. 2008;198(12):1842–50.

175. Keane J, Gershon S, Wise RP, Mirabile-Levens E, Kasznica J, Schwieterman WD, et al. Tuberculosis associated with infliximab, a tumor necrosis factor α-neutralizing agent. N Engl J Med. 2001;345(15):1098–104.

176. Gardam MA, Keystone EC, Menzies R, Manners S, Skamene E, Long R, et al. Anti-tumour necrosis factor agents and tuberculosis risk: Mechanisms of action and clinical management. Lancet Infect Dis. 2003;3(3):148–55.

177. Harris J, Keane J. How tumour necrosis factor blockers interfere with tuberculosis immunity. Clin Exp Immunol. 2010;161(1):1–9.

178. Botha T, Ryffel B. Reactivation of Latent Tuberculosis Infection in TNF-Deficient Mice. J Immunol. 2003;171(6):3110–8.

179. Abdalla AE, Lambert N, Duan X, Xie J. Interleukin-10 family and tuberculosis: An old story renewed. Int J Biol Sci. 2016;12(6):710–7.

180. Ke Z, Yuan L, Ma J, Zhang X, Guo Y, Xiong H. IL-10 polymorphisms and tuberculosis susceptibility: An updated meta-analysis. Yonsei Med J. 2015;56(5):1274–87.

181. Kumar NP, Moideen K, Banurekha V V., Nair D, Sridhar R, Nutman TB, et al. Il-27 and tgfb mediated expansion of th1 and adaptive regulatory t cells expressing il-10 correlates with bacterial burden and disease severity in pulmonary tuberculosis. Immun Inflamm Dis. 2015;3(3):289–99.

182. Eum SY, Jeon BY, Min JH, Kim SC, Cho S, Park SK, et al. Tumor necrosis factor-alpha and interleukin-10 in whole blood is associated with disease progression in pulmonary mulitdrug-resistant tuberculosis patients. Respiration. 2008;76(3):331–7.

183. Lago PM, Boéchat N, Migueis DP, Almeida AS, Lazzarini LC, Saldanha MM, et al. Interleukin-10 and interferon-gamma patterns during tuberculosis treatment: Possible association with recurrence. Int J Tuberc Lung Dis. 2012;16(5):656–9.

184. O'Leary S, O'Sullivan MP, Keane J. IL-10 blocks phagosome maturation in Mycobacterium tuberculosis-infected human macrophages. Am J Respir Cell Mol Biol. 2011;45(1):172–80.

185. Roach DR, Martin E, Bean AGD, Rennick DM, Briscoe H, Britton WJ. Endogenous inhibition of antimycobacterial immunity by IL-10 varies between mycobacterial species. Scand J Immunol. 2001;54(1–2):163–70.

186. Redford PS, Boonstra A, Read S, Pitt J, Graham C, Stavropoulos E, et al. Enhanced

protection to Mycobacterium tuberculosis infection in IL-10-deficient mice is accompanied by early and enhanced Th1 responses in the lung. Eur J Immunol. 2010;40(8):2200–10.

187. North RJ. Mice incapable of making IL-4 or IL-10 display normal resistance to infection with Mycobacterium tuberculosis. Clin Exp Immunol. 1998;113(1):55–8.

188. Jung YJ, Ryan L, Lacourse R, North RJ. Increased interleukin-10 expression is not responsible for failure of T helper 1 immunity to resolve airborne Mycobacterium tuberculosis infection in mice. Immunology. 2003;109(2):295–9.

189. Higgins DM, Sanchez-Campillo J, Rosas-Taraco AG, Lee EJ, Orme IM, Gonzalez-Juarrero M. Lack of IL-10 alters inflammatory and immune responses during pulmonary Mycobacterium tuberculosis infection. Tuberculosis. 2009;89(2):149–57.

190. Elkington P, Shiomi T, Breen R, Nuttall RK, Ugarte-Gil CA, Walker NF, et al. MMP-1 drives immunopathology in human tuberculosis and transgenic mice. J Clin Invest. 2011;121(5):1827–33.

191. Palaci M, Dietze R, Hadad DJ, Ribeiro FKC, Peres RL, Vinhas SA, et al. Cavitary disease and quantitative sputum bacillary load in cases of pulmonary tuberculosis. J Clin Microbiol. 2007;45(12):4064–6.

192. Kübler A, Luna B, Larsson C, Ammerman NC, Andrade BB, Orandle M, et al. Mycobacterium tuberculosis dysregulates MMP/TIMP balance to drive rapid cavitation and unrestrained bacterial proliferation. J Pathol. 2015;235(3):431–44.

193. Dheda K, Booth H, Huggett JF, Johnson MA, Zumla A, Rook GAW. Lung Remodeling in Pulmonary Tuberculosis. J Infect Dis. 2005;192(7):1201–9.

194. Davidson JM. Biochemistry and turnover of lung interstitium. Eur Respir J. 1990;3(9):1048–63.

195. Russell DG, VanderVen BC, Lee W, Abramovitch RB, Kim MJ, Homolka S, et al. Mycobacterium tuberculosis wears what it eats. Cell Host Microbe. 2010;19(5):291–304.

196. Elkington PT, D'Armiento JM, Friedland JS. Tuberculosis immunopathology: The neglected role of extracellular matrix destruction. Sci Transl Med. 2011;3(71):71ps6.

197. Elkington PT, Ugarte-Gil CA, Friedland JS. Matrix metalloproteinases in tuberculosis. Eur Respir J. 2011;

198. Sternlicht MD, Werb Z. How Matrix Metalloproteinases Regulate Cell Behavior. Annu Rev Cell Dev Biol. 2001;17(1):463–516.

199. GROSS J, LAPIERE CM. Collagenolytic activity in amphibian tissues: a tissue culture assay. Proc Natl Acad Sci U S A. 1962;48:1014–22.

200. Rohlwink UK, Walker NF, Ordonez AA, Li YJ, Tucker EW, Elkington PT, et al. Matrix metalloproteinases in pulmonary and central nervous system tuberculosis—A review. Int J Mol Sci. 2019;20(6):1350.

201. Klein T, Bischoff R. Physiology and pathophysiology of matrix metalloproteases. Amino Acids. 2011;41(2):271–90.

202. Tokito A, Jougasaki M. Matrix metalloproteinases in non-neoplastic disorders. Int J Mol Sci. 2016;17(7):1178.

203. Nagase H. Activation mechanisms of matrix metalloproteinases. Biol Chem. 1997;378(3–4):151–60.

204. Bode W. A helping hand for collagenases: the haemopexin-like domain. Structure. 1995;3(6):527–30.

205. Nagase H, Visse R, Murphy G. Structure and function of matrix metalloproteinases and TIMPs. Cardiovasc Res. 2006;69(3):562–73.

206. Lopez-Avila V, Spencer J V. Methods for Detection of Matrix Metalloproteinases as Biomarkers in Cardiovascular Disease. Clin Med Cardiol. 2008;2:75–87.

207. Brkic M, Balusu S, Libert C, Vandenbroucke RE. Friends or Foes: Matrix Metalloproteinases and Their Multifaceted Roles in Neurodegenerative Diseases. Mediators Inflamm. 2015;2015:620581.

208. Parks WC, Wilson CL, López-Boado YS. Matrix metalloproteinases as modulators of inflammation and innate immunity. Nat Rev Immunol. 2004;4(8):617–29.

209. Visse R, Nagase H. Matrix metalloproteinases and tissue inhibitors of metalloproteinases: Structure, function, and biochemistry. Circ Res. 2003;92(8):827–39.

210. Loffek S, Schilling O, Franzke C-W. Biological role of matrix metalloproteinases: a critical balance. Eur Respir J. 2011;38(1):191–208.

211. Khokha R, Murthy A, Weiss A. Metalloproteinases and their natural inhibitors in inflammation and immunity. Nat Rev Immunol. 2013;13(9):649–65.

212. Mittal R, Patel AP, Debs LH, Nguyen D, Patel K, Grati M, et al. Intricate Functions of Matrix Metalloproteinases in Physiological and Pathological Conditions. J Cell Physiol. 2016;23(12):2599–621.

213. Pilcher BK, Dumin JA, Sudbeck BD, Krane SM, Welgus HG, Parks WC. The activity of collagenase-1 is required for keratinocyte migration on a type I collagen matrix. J Cell Biol. 1997;137(6):1445–57.

214. Dunsmore SE, Saarialho-Kere UK, Roby JD, Wilson CL, Matrisian LM, Welgus HG, et al. Matrilysin expression and function in airway epithelium. J Clin Invest. 1998;102(7):1321–31.

215. Malemud CJ. Matrix metalloproteinases (MMPs) in health and disease: An overview. Front Biosci. 2006;1(11):1696–701.

216. Nissinen L, Kähäri VM. Matrix metalloproteinases in inflammation. Biochim Biophys Acta - Gen Subj. 2014;1840(8):2571–80.

217. Ito A, Mukaiyama A, Itoh Y, Nagase H, Thøgersen IB, Enghild JJ, et al. Degradation of interleukin 1β by matrix metalloproteinases. J Biol Chem. 1996;271(25):14657–60.

218. Schönbeck U, Mach F, Libby P. Generation of biologically active IL-1 beta by matrix metalloproteinases: a novel caspase-1-independent pathway of IL-1 beta processing. J Immunol. 1998;161(7):3340–6.

219. Van Lint P, Libert C. Chemokine and cytokine processing by matrix metalloproteinases and its effect on leukocyte migration and inflammation. J Leukoc Biol. 2007;82(6):1375–81.

220. Corry DB, Kiss A, Song L-Z, Song L, Xu J, Lee S-H, et al. Overlapping and independent

contributions of MMP2 and MMP9 to lung allergic inflammatory cell egression through decreased CC chemokines. FASEB J. 2004;18(9):995–7.

221. McQuibban GA, Gong JH, Tam EM, McCulloch CAG, Clark-Lewis I, Overall CM. Inflammation dampened by gelatinase a cleavage of monocyte chemoattractant protein-3. Science (80-). 2000;289(5482):1202–6.

222. Ra HJ, Parks WC. Control of matrix metalloproteinase catalytic activity. Matrix Biol. 2007;26(8):587–96.

223. Fanjul-Fernández M, Folgueras AR, Cabrera S, López-Otín C. Matrix metalloproteinases: Evolution, gene regulation and functional analysis in mouse models. Biochim Biophys Acta - Mol Cell Res. 2010;1803(1):3–19.

224. Mancini A, Di Battista JA. Transcriptional regulation of matrix metalloprotease gene expression in health and disease. Front Biosci. 2006;11:423–6.

225. Vincenti MP, Brinckerhoff CE. Signal transduction and cell-type specific regulation of matrix metalloproteinase gene expression: Can MMPs be good for you? J Cell Physiol. 2007;213(2):355–64.

226. Chernov A V., Strongin AY. Epigenetic regulation of matrix metalloproteinases and their collagen substrates in cancer. Biomol Concepts. 2011;2(3):135–47.

227. Jiang Y, Muschel RJ. Regulation of matrix metalloproteinase-9 (MMP-9) by translational efficiency in murine prostate carcinoma cells. Cancer Res. 2002;

228. Van Wart HE, Birkedal-Hansen H. The cysteine switch: A principle of regulation of metalloproteinase activity with potential applicability to the entire matrix metalloproteinase gene family. Proc Natl Acad Sci U S A. 1990;87(14):5578–82.

229. Springman EB, Angleton EL, Birkedal-Hansen H, Van Wart HE. Multiple modes of activation of latent human fibroblast collagenase: Evidence for the role of a Cys73 active-site zinc complex in latency and a “cysteine switch” mechanism for activation. Proc Natl Acad Sci U S A. 1990;87(1):364–8.

230. Knäuper V, Murphy G, Tschesche H. Activation of human neutrophil procollagenase by

stromelysin 2. Eur J Biochem. 1996;235(1–2):187–91.

231. Nakamura H, Fujii Y, Ohuchi E, Yamamoto E, Okada Y. Activation of the precursor of human stromelysin 2 and its interactions with other matrix metalloproteinases. Eur J Biochem. 1998;253(1):67–75.

232. Ogata Y, Enghild JJ, Nagase H. Matrix metalloproteinase 3 (stromelysin) activates the precursor for the human matrix metalloproteinase 9. J Biol Chem. 1992;267(6):3581–4.

233. Suzuki K, Morodomi T, Nagase H, Enghild JJ, Salvesen G. Mechanisms of Activation of Tissue Procollagenase by Matrix Metalloproteinase 3 (Stromelysin). Biochemistry. 1990;29(44):10261–70.

234. Tocchi A, Parks WC. Functional interactions between matrix metalloproteinases and glycosaminoglycans. FEBS J. 2013;280(10):2332–41.

235. Murphy G. Tissue inhibitors of metalloproteinases. Genome Biol. 2011;12(11):233.

236. Lee MH, Atkinson S, Murphy G. Identification of the Extracellular Matrix (ECM) binding motifs of tissue inhibitor of metalloproteinases (TIMP)-3 and effective transfer to TIMP-1. J Biol Chem. 2007;282(9):6887–98.

237. Brew K, Nagase H. The tissue inhibitors of metalloproteinases (TIMPs): An ancient family with structural and functional diversity. Biochim Biophys Acta - Mol Cell Res. 2010;1803(1):55–71.

238. Hernandez-Barrantes S, Toth M, Bernardo MM, Yurkova M, Gervasi DC, Raz Y, et al. Binding of active (57 kDa) membrane type 1-matrix metalloproteinase (MT1-MMP) to tissue inhibitor of metalloproteinase (TIMP)-2 regulates MT1-MMP processing and pro-MMP-2 activation. J Biol Chem. 2000;275(16):12080–9.

239. Wang Z, Juttermann R, Soloway PD. TIMP-2 is required for efficient activation of proMMP-2 in vivo. J Biol Chem. 2000;275(34):26411–5.

240. Ong CWM, Elkington PT, Friedland JS. Tuberculosis, pulmonary cavitation, and matrix metalloproteinases. Am J Respir Crit Care Med. 2014;190(1):9–18.

241. Price NM, Farrar J, Chau TTH, Mai NTH, Hien TT, Friedland JS. Identification of a Matrix-

Degrading Phenotype in Human Tuberculosis In Vitro and In Vivo. J Immunol. 2001;166(6):4223–30.

242. Price NM, Gilman RH, Uddin J, Recavarren S, Friedland JS. Unopposed Matrix Metalloproteinase-9 Expression in Human Tuberculous Granuloma and the Role of TNF-α-Dependent Monocyte Networks. J Immunol. 2003;171(10):5579–86.

243. Elkington PTG, Nuttall RK, Boyle JJ, O'Kane CM, Horncastle DE, Edwards DR, et al. Mycobacterium tuberculosis, but not vaccine BCG, specifically upregulates matrix metalloproteinase-1. Am J Respir Crit Care Med. 2005;172(12):1596–604.

244. Brilha S, Sathyamoorthy T, Stuttaford LH, Walker NF, Wilkinson RJ, Singh S, et al. Early secretory antigenic target-6 drives matrix metalloproteinase-10 gene expression and secretion in tuberculosis. Am J Respir Cell Mol Biol. 2017;56(2):223–32.

245. London IC, Diseases I. The Role of Matrix Metalloproteinases in Leukocyte Migration and Collagen Degradation in Tuberculosis Tarangini Sathyamoorthy. Imperial College London; 2013.

246. Elkington PTG, Emerson JE, Lopez-Pascua LDC, O'Kane CM, Horncastle DE, Boyle JJ, et al. Mycobacterium tuberculosis Up-Regulates Matrix Metalloproteinase-1 Secretion from Human Airway Epithelial Cells via a p38 MAPK Switch. J Immunol. 2005;175(8):5333–40.

247. Elkington PT, Green JA, Emerson JE, Lopez-Pascua LD, Boyle JJ, O'Kane CM, et al. Synergistic up-regulation of epithelial cell matrix metalloprotemase-9 secretion in tuberculosis. Am J Respir Cell Mol Biol. 2007;37(4):431–7.

248. Singh S, Saraiva L, Elkington PTG, Friedland JS. Regulation of matrix metalloproteinase-1, -3, and -9 in Mycobacterium tuberculosis-dependent respiratory networks by the rapamycin-sensitive PI3K/p70S6K cascade. FASEB J. 2014;28(1):85–93.

249. Green JA, Elkington PT, Pennington CJ, Roncaroli F, Dholakia S, Moores RC, et al. Mycobacterium tuberculosis Upregulates Microglial Matrix Metalloproteinase-1 and -3 Expression and Secretion via NF-κB– and Activator Protein-1–Dependent Monocyte Networks. J Immunol. 2010;184(11):6492–503.

250. Green JA, Dholakia S, Janczar K, Ong CWM, Moores R, Fry J, et al. Mycobacterium

tuberculosis-infected human monocytes down-regulate microglial MMP-2 secretion in CNS tuberculosis via TNFα, NFκB, p38 and caspase 8 dependent pathways. J Neuroinflammation. 2011;8:46.

251. O'Kane CM, Elkington PT, Jones MD, Caviedes L, Tovar M, Gilman RH, et al. STAT3, p38 MAPK, and NF-κB drive unopposed monocyte-dependent fibroblast MMP-1 secretion in tuberculosis. Am J Respir Cell Mol Biol. 2010;43(4):465–74.

252. Harris JE, Nuttall RK, Elkington PT, Green JA, Horncastle DE, Graeber MB, et al. Monocyte-Astrocyte Networks Regulate Matrix Metalloproteinase Gene Expression and Secretion in Central Nervous System Tuberculosis In Vitro and In Vivo. J Immunol. 2007;178(2):1199–207.

253. Fox KA, Kirwan DE, Whittington AM, Krishnan N, Robertson BD, Gilman RH, et al. Platelets regulate pulmonary inflammation and tissue destruction in tuberculosis. Am J Respir Crit Care Med. 2018;198(2):245–55.

254. Sathyamoorthy T, Tezera LB, Walker NF, Brilha S, Saraiva L, Mauri FA, et al. Membrane Type 1 Matrix Metalloproteinase Regulates Monocyte Migration and Collagen Destruction in Tuberculosis. J Immunol. 2015;195(3):882–91.

255. Ong CWM, Elkington PT, Brilha S, Ugarte-Gil C, Tome-Esteban MT, Tezera LB, et al. Neutrophil-Derived MMP-8 Drives AMPK-Dependent Matrix Destruction in Human Pulmonary Tuberculosis. PLoS Pathog. 2015;11(5):e1004917.

256. Ong CWM, Pabisiak PJ, Brilha S, Singh P, Roncaroli F, Elkington PT, et al. Complex regulation of neutrophil-derived MMP-9 secretion in central nervous system tuberculosis. J Neuroinflammation. 2017;14(1):31.

257. Rand L, Green JA, Saraiva L, Friedland JS, Elkington PTG. Matrix Metalloproteinase-1 Is Regulated in Tuberculosis by a p38 MAPK-Dependent, p -Aminosalicylic Acid-Sensitive Signaling Cascade. J Immunol. 2009;182(9):5865–72.

258. Brace PT, Tezera LB, Bielecka MK, Mellows T, Garay D, Tian S, et al. Mycobacterium tuberculosis subverts negative regulatory pathways in human macrophages to drive immunopathology. PLoS Pathog. 2017;13(6):e1006367.

259. Belton M, Brilha S, Manavaki R, Mauri F, Nijran K, Hong YT, et al. Hypoxia and tissue destruction in pulmonary TB. Thorax. 2016;71(12):1145–53.

260. Ong CWM, Fox K, Ettorre A, Elkington PT, Friedland JS. Hypoxia increases neutrophil-driven matrix destruction after exposure to Mycobacterium tuberculosis. Sci Rep. 2018;8(1):11475.

261. Dharmadhikari AS, Nardell EA. What animal models teach humans about tuberculosis. Am J Respir Cell Mol Biol. 2008;39(5):503–8.

262. Parks WC, Shapiro SD. Matrix metalloproteinases in lung biology. Respir Res. 2001;2(1):10–9.

263. Young D. Animal models of tuberculosis. Eur J Immunol. 2009;39(8):2011–4.

264. Al Shammari B, Shiomi T, Tezera L, Bielecka MK, Workman V, Sathyamoorthy T, et al. The Extracellular Matrix Regulates Granuloma Necrosis in Tuberculosis. J Infect Dis. 2015;212(3):463–73.

265. Taylor JL, Hattle JM, Dreitz SA, Troudt JLM, Izzo LS, Basaraba RJ, et al. Role for matrix metalloproteinase 9 in granuloma formation during pulmonary Mycobacterium tuberculosis infection. Infect Immun. 2006;74(11):6135–44.

266. Majeed S, Radotra BD, Sharma S. Adjunctive role of MMP-9 inhibition along with conventional anti-tubercular drugs against experimental tuberculous meningitis. Int J Exp Pathol. 2016;97(3):230–7.

267. Elkington PTG, Friedland JS. Matrix metalloproteinases in destructive pulmonary pathology. Thorax. 2006;61(3):259–66.

268. Walker NF, Clark SO, Oni T, Andreu N, Tezera L, Singh S, et al. Doxycycline and HIV infection suppress tuberculosis-induced matrix metalloproteinases. Am J Respir Crit Care Med. 2012;85(9):989–97.

269. Subbian S, Tsenova L, O'Brien P, Yang G, Koo MS, Peixoto B, et al. Phosphodiesterase-4 inhibition combined with isoniazid treatment of rabbits with pulmonary tuberculosis reduces macrophage activation and lung pathology. Am J Pathol. 2011;179(1):289–301.

270. Mehra S, Pahar B, Dutta NK, Conerly CN, Philippi-Falkenstein K, Alvarez X, et al. Transcriptional reprogramming in nonhuman primate (Rhesus Macaque) tuberculosis granulomas. PLoS One. 2010;

271. Ugarte-Gil CA, Elkington P, Gilman RH, Coronel J, Tezera LB, Bernabe-Ortiz A, et al. Induced Sputum MMP-1, -3 & -8 Concentrations during Treatment of Tuberculosis. PLoS One. 2013;8(4):e61333.

272. Seddon J, Kasprowicz V, Walker NF, Yuen HM, Sunpath H, Tezera L, et al. Procollagen iii n-terminal propeptide and desmosine are released by matrix destruction in pulmonary tuberculosis. J Infect Dis. 2013;208(10):1571–8.

273. Sundararajan S, Babu S, Das SD. Comparison of localized versus systemic levels of Matrix metalloproteinases (MMPs), its tissue inhibitors (TIMPs) and cytokines in tuberculous and non-tuberculous pleuritis patients. Hum Immunol. 2012;73(10):985–91.

274. Kuo HP, Wang YM, Wang CH, He CC, Lin SM, Lin HC, et al. Matrix metalloproteinase-1 polymorphism in Taiwanese patients with endobronchial tuberculosis. Tuberculosis. 2008;88(3):262–7.

275. Wang CH, Lin HC, Lin SM, Huang CD, Liu CY, Huang KH, et al. MMP-1(-1607G) polymorphism as a risk factor for fi brosis after pulmonary tuberculosis in Taiwan. Int J Tuberc Lung Dis. 2010;14(5):627–34.

276. Ganachari M, Ruiz-Morales JA, Gomez De La Torre Pretell JC, Dinh J, Granados J, Flores-Villanueva PO. Joint effect of MCP-1 genotype GG and MMP-1 genotype 2G/2G increases the likelihood of developing pulmonary tuberculosis in BCG-vaccinated individuals. PLoS One. 2010;5(1):e8881.

277. Lee SH, Han SK, Shim YS, Yim JJ. Effect of matrix metalloproteinase-9 -1562C/T gene polymorphism on manifestations of pulmonary tuberculosis. Tuberculosis. 2009;89(1):68–70.

278. Thwaites GE, Bang ND, Dung NH, Quy HT, Oanh DTT, Thoa NTC, et al. Dexamethasone for the treatment of tuberculous meningitis in adolescents and adults. N Engl J Med. 2004;351(17):1741–51.

279. Green JA, Tran CTH, Farrar JJ, Nguyen MTH, Nguyen PH, Dinh SX, et al. Dexamethasone, cerebrospinal fluid matrix metalloproteinase concentrations and clinical outcomes in tuberculous meningitis. PLoS One. 2009;4(9):e7277.

280. Gapski R, Hasturk H, Van Dyke TE, Oringer RJ, Wang S, Braun TM, et al. Systemic MMP inhibition for periodontal wound repair: Results of a multi-centre randomized-controlled clinical trial. J Clin Periodontol. 2009;36(2):149–56.

281. Bhattacharyya P, Paul R, Bhattacharjee P, Ghosh A, Dey R, Ghosh M, et al. Long-term use of doxycycline can improve chronic asthma and possibly remodeling: The result of a pilot observation. J Asthma Allergy. 2012;5:33–7.

282. Dalvi PS, Singh A, Trivedi HR, Ghanchi FD, Parmar DM, Mistry SD. Effect of doxycycline in patients of moderate to severe chronic obstructive pulmonary disease with stable symptoms. Ann Thorac Med. 2011;6(4):221–6.

283. Winer A, Adams S, Mignatti P. Matrix metalloproteinase inhibitors in cancer therapy: Turning past failures into future successes. Mol Cancer Ther. 2018;17(6):1147–55.

284. Lewis EJ, Bishop J, Bottomley KMK, Bradshaw D, Brewster M, Broadhurst MJ, et al. Ro 32-3555, an orally active collagenase inhibitor, prevents cartilage breakdown in vitro and in vivo. Br J Pharmacol. 1997;121(3):540–6.

285. Xu Y, Wang L, Zimmerman MD, Chen KY, Huang L, Fu DJ, et al. Matrix metalloproteinase inhibitors enhance the efficacy of frontline drugs against Mycobacterium tuberculosis. PLoS Pathog. 2018;14(4):e1006974.

286. Ordonez AA, Pokkali S, Kim S, Carr B, Klunk MH, Tong L, et al. Adjunct antibody administration with standard treatment reduces relapse rates in a murine tuberculosis model of necrotic granulomas. PLoS One. 2018;13(5):e0197474.

287. Phelan JJ, Basdeo SA, Tazoll SC, McGivern S, Saborido JR, Keane J. Modulating iron for metabolic support of TB host defense. Front Immunol. 2018;9:2296.

288. Warburg O, Wind F, Negelein E. The metabolism of tumors in the body. J Gen Physiol. 1927;8(6):519–30.

289. Palsson-Mcdermott EM, O'Neill LAJ. The Warburg effect then and now: From cancer to inflammatory diseases. BioEssays. 2013;35(11):965–73.

290. Escoll P, Song OR, Viana F, Steiner B, Lagache T, Olivo-Marin JC, et al. Legionella pneumophila Modulates Mitochondrial Dynamics to Trigger Metabolic Repurposing of Infected Macrophages. Cell Host Microbe. 2017;22(3):302–16.

291. Gillmaier N, Götz A, Schulz A, Eisenreich W, Goebel W. Metabolic Responses of Primary and Transformed Cells to Intracellular Listeria monocytogenes. PLoS One. 2012;7(12):e52378.

292. Telser J, Volani C, Hilbe R, Seifert M, Brigo N, Paglia G, et al. Metabolic reprogramming of Salmonella infected macrophages and its modulation by iron availability and the mTOR pathway. Microb Cell. 2019;6(12):531–43.

293. Prusinkiewicz MA, Tu J, Dodge MJ, MacNeil KM, Radko-Juettner S, Fonseca GJ, et al. Differential Effects of Human Adenovirus E1A Protein Isoforms on Aerobic Glycolysis in A549 Human Lung Epithelial Cells. Viruses. 2020;12(6):E610.

294. Xu ZP, Chang H, Ni YY, Li C, Chen L, Hou M, et al. Schistosoma japonicum infection causes a reprogramming of glycolipid metabolism in the liver. Parasites and Vectors. 2019;12(1):388.

295. Rodríguez-Prados J-C, Través PG, Cuenca J, Rico D, Aragonés J, Martín-Sanz P, et al. Substrate Fate in Activated Macrophages: A Comparison between Innate, Classic, and Alternative Activation. J Immunol. 2010;185(1):605–14.

296. Tannahill GM, Curtis AM, Adamik J, Palsson-Mcdermott EM, McGettrick AF, Goel G, et al. Succinate is an inflammatory signal that induces IL-1β through HIF-1α. Nature. 2013;496:238–42.

297. Krawczyk CM, Holowka T, Sun J, Blagih J, Amiel E, DeBerardinis RJ, et al. Toll-like receptor-induced changes in glycolytic metabolism regulate dendritic cell activation. Blood. 2010;115(23):4742–9.

298. Jha AK, Huang SCC, Sergushichev A, Lampropoulou V, Ivanova Y, Loginicheva E, et al. Network integration of parallel metabolic and transcriptional data reveals metabolic

modules that regulate macrophage polarization. Immunity. 2015;42(3):419–30.

299. Shi L, Eugenin EA, Subbian S. Immunometabolism in tuberculosis. Front Immunol. 2016;7:150.

300. Van den Bossche J, O'Neill LA, Menon D. Macrophage Immunometabolism: Where Are We (Going)? Trends Immunol. 2017;38:395–406.

301. Wang T, Liu H, Lian G, Zhang SY, Wang X, Jiang C. HIF1 α -Induced Glycolysis Metabolism Is Essential to the Activation of Inflammatory Macrophages. Mediators Inflamm. 2017;2017:9029327.

302. Byles V, Covarrubias AJ, Ben-Sahra I, Lamming DW, Sabatini DM, Manning BD, et al. The TSC-mTOR pathway regulates macrophage polarization. Nat Commun. 2013;4:2834.

303. West AP, Shadel GS, Ghosh S. Mitochondria in innate immune responses. Nat Rev Immunol. 2011;11:389–402.

304. Sag D, Carling D, Stout RD, Suttles J. Adenosine 5′-Monophosphate-Activated Protein Kinase Promotes Macrophage Polarization to an Anti-Inflammatory Functional Phenotype. J Immunol. 2008;181(12):8633–41.

305. Tan HY, Wang N, Li S, Hong M, Wang X, Feng Y. The Reactive Oxygen Species in Macrophage Polarization: Reflecting Its Dual Role in Progression and Treatment of Human Diseases. Oxid Med Cell Longev. 2016;2016:2795090.

306. Atri C, Guerfali FZ, Laouini D. Role of human macrophage polarization in inflammation during infectious diseases. Int J Mol Sci. 2018;19(6):1801.

307. Xu F, Kang Y, Zhang H, Piao Z, Yin H, Diao R, et al. Akt1-mediated regulation of macrophage polarization in a murine model of staphylococcus aureus pulmonary infection. J Infect Dis. 2013;208(528–538).

308. Ryan DG, O'Neill LAJ. Krebs Cycle Reborn in Macrophage Immunometabolism. Annu Rev Immunol. 2020;38:289–313.

309. O'Neill LAJ. A Broken Krebs Cycle in Macrophages. Immunity. 2015;42(3):393–4.

310. Kolliputi N, Rollin Cox Jr R, Mannam P, Srivastava A. Warburg revisited: lessons for innate immunity and sepsis A Commentary on mTOR-and HIF-1 -mediated aerobic glycolysis as metabolic basis for trained immunity. Front Physiol Physiol. 2015;

311. Liu PS, Wang H, Li X, Chao T, Teav T, Christen S, et al. α-ketoglutarate orchestrates macrophage activation through metabolic and epigenetic reprogramming. Nat Immunol. 2017;18(9):985–94.

312. Infantino V, Iacobazzi V, Palmieri F, Menga A. ATP-citrate lyase is essential for macrophage inflammatory response. Biochem Biophys Res Commun. 2013;440(1):105–11.

313. Carroll RG, Zasłona Z, Galván-Peña S, Koppe EL, Sévin DC, Angiari S, et al. An unexpected link between fatty acid synthase and cholesterol synthesis in proinflammatory macrophage activation. J Biol Chem. 2018;293(15):5509–21.

314. Meiser J, Krämer L, Sapcariu SC, Battello N, Ghelfi J, D'Herouel AF, et al. Pro-inflammatory macrophages sustain pyruvate oxidation through pyruvate dehydrogenase for the synthesis of itaconate and to enable cytokine expression. J Biol Chem. 2016;291(8):3932–46.

315. Michelucci A, Cordes T, Ghelfi J, Pailot A, Reiling N, Goldmann O, et al. Immune-responsive gene 1 protein links metabolism to immunity by catalyzing itaconic acid production. Proc Natl Acad Sci U S A. 2013;110(19):7820–5.

316. Lampropoulou V, Sergushichev A, Bambouskova M, Nair S, Vincent EE, Loginicheva E, et al. Itaconate Links Inhibition of Succinate Dehydrogenase with Macrophage Metabolic Remodeling and Regulation of Inflammation. Cell Metab. 2016;24(1):158–66.

317. Mills EL, Kelly B, Logan A, Costa ASH, Varma M, Bryant CE, et al. Succinate Dehydrogenase Supports Metabolic Repurposing of Mitochondria to Drive Inflammatory Macrophages. Cell. 2016;167(2):457–70.

318. Mills EL, Ryan DG, Prag HA, Dikovskaya D, Menon D, Zaslona Z, et al. Itaconate is an anti-inflammatory metabolite that activates Nrf2 via alkylation of KEAP1. Nature. 2018;556(7699):113–7.

319. Bambouskova M, Gorvel L, Lampropoulou V, Sergushichev A, Loginicheva E, Johnson K, et al. Electrophilic properties of itaconate and derivatives regulate the IκBζ-ATF3 inflammatory axis. Nature. 2018;556(7702):501–4.

320. Qin W, Qin K, Zhang Y, Jia W, Chen Y, Cheng B, et al. S-glycosylation-based cysteine profiling reveals regulation of glycolysis by itaconate. Nat Chem Biol. 2019;15:983–91.

321. Kumar R, Singh P, Kolloli A, Shi L, Bushkin Y, Tyagi S, et al. Immunometabolism of Phagocytes During Mycobacterium tuberculosis Infection. Front Mol Biosci. 2019;6:105.

322. Shi L, Salamon H, Eugenin EA, Pine R, Cooper A, Gennaro ML. Infection with Mycobacterium tuberculosis induces the Warburg effect in mouse lungs. Sci Rep. 2015;5:18176.

323. Subbian S, Tsenova L, Kim MJ, Wainwright HC, Visser A, Bandyopadhyay N, et al. Lesion-specific immune response in granulomas of patients with pulmonary tuberculosis: A pilot study. PLoS One. 2015;10(7):e0132249.

324. Lachmandas E, Beigier-Bompadre M, Cheng SC, Kumar V, van Laarhoven A, Wang X, et al. Rewiring cellular metabolism via the AKT/mTOR pathway contributes to host defence against Mycobacterium tuberculosis in human and murine cells. Eur J Immunol. 2016;46(11):2574–86.

325. Vrieling F, Kostidis S, Spaink HP, Haks MC, Mayboroda OA, Ottenhoff THM, et al. Analyzing the impact of Mycobacterium tuberculosis infection on primary human macrophages by combined exploratory and targeted metabolomics. Sci Rep. 2020;10:7085.

326. Shin JH, Yang JY, Jeon BY, Yoon YJ, Cho SN, Kang YH, et al. 1H NMR-based metabolomic profiling in mice infected with Mycobacterium tuberculosis. J Proteome Res. 2011;10(5):2238–47.

327. Somashekar BS, Amin AG, Rithner CD, Troudt J, Basaraba R, Izzo A, et al. Metabolic profiling of lung granuloma in Mycobacterium tuberculosis infected guinea pigs: Ex vivo 1H magic angle spinning NMR studies. J Proteome Res. 2011;10(9):4186–95.

328. Fernández-García M, Rey-Stolle F, Boccard J, Reddy VP, García A, Cumming BM, et al.

Comprehensive Examination of the Mouse Lung Metabolome following Mycobacterium tuberculosis Infection Using a Multiplatform Mass Spectrometry Approach. J Proteome Res. 2020;19(5):2053–70.

329. Billig S, Schneefeld M, Huber C, Grassl GA, Eisenreich W, Bange FC. Lactate oxidation facilitates growth of Mycobacterium tuberculosis in human macrophages. Sci Rep. 2017;7:6484.

330. Kirk P, Wilson MC, Heddle C, Brown MH, Barclay AN, Halestrap AP. CD147 is tightly associated with lactate transporters MCT1 and MCT4 and facilitates their cell surface expression. EMBO J. 2000;19(15):3896–904.

331. Huang L, Nazarova E V., Tan S, Liu Y, Russell DG. Growth of Mycobacterium tuberculosis in vivo segregates with host macrophage metabolism and ontogeny. J Exp Med. 2018;215(4):1135–52.

332. Hackett EE, Charles-Messance H, O'Leary SM, Gleeson LE, Muñoz-Wolf N, Case S, et al. Mycobacterium tuberculosis Limits Host Glycolysis and IL-1β by Restriction of PFK-M via MicroRNA-21. Cell Rep. 2020;30(1):124–36.

333. Phelan JJ, McQuaid K, Kenny C, Gogan KM, Cox DJ, Basdeo SA, et al. Desferrioxamine Supports Metabolic Function in Primary Human Macrophages Infected With Mycobacterium tuberculosis. Front Immunol. 2020;11:836.

334. Lachmandas E, Boutens L, Ratter JM, Hijmans A, Hooiveld GJ, Joosten LAB, et al. Microbial stimulation of different Toll-like receptor signalling pathways induces diverse metabolic programmes in human monocytes. Nat Microbiol. 2016;2:16246.

335. Braverman J, Sogi KM, Benjamin D, Nomura DK, Stanley SA. HIF-1α Is an Essential Mediator of IFN-γ–Dependent Immunity to Mycobacterium tuberculosis. J Immunol. 2016;197(4):1287–97.

336. Nazarova E V., Montague CR, La T, Wilburn KM, Sukumar N, Lee W, et al. Rv3723/LucA coordinates fatty acid and cholesterol uptake in Mycobacterium tuberculosis. Elife. 2017;6:e26969.

337. Huang Z, Luo Q, Guo Y, Chen J, Xiong G, Peng Y, et al. Mycobacterium tuberculosis-

induced polarization of human macrophage orchestrates the formation and development of tuberculous granulomas in vitro. PLoS One. 2015;10(6):e0129744.

338. Nair S, Huynh JP, Lampropoulou V, Loginicheva E, Esaulova E, Gounder AP, et al. Irg1 expression in myeloid cells prevents immunopathology during M. tuberculosis infection. J Exp Med. 2015;215(4):1035–45.

339. Semenza GL. HIF-1 and mechanisms of hypoxia sensing. Curr Opin Cell Biol. 2001;13(2):167–71.

340. Huang LE, Gu J, Schau M, Bunn HF. Regulation of hypoxia-inducible factor 1α is mediated by an O2-dependent degradation domain via the ubiquitin-proteasome pathway. Proc Natl Acad Sci U S A. 1998;95(14):7987–92.

341. Corcoran SE, O'Neill LAJ. HIF1α and metabolic reprogramming in inflammation. J Clin Invest. 2016;126(10):3699–707.

342. Blouin CC, Pagé EL, Soucy GM, Richard DE. Hypoxic gene activation by lipopolysaccharide in macrophages: Implication of hypoxia-inducible factor 1α. Blood. 2004;103(3):1124–30.

343. Jantsch J, Chakravortty D, Turza N, Prechtel AT, Buchholz B, Gerlach RG, et al. Hypoxia and Hypoxia-Inducible Factor-1α Modulate Lipopolysaccharide-Induced Dendritic Cell Activation and Function. J Immunol. 2008;180(7):4697–705.

344. Peyssonnaux C, Cejudo-Martin P, Doedens A, Zinkernagel AS, Johnson RS, Nizet V. Cutting Edge: Essential Role of Hypoxia Inducible Factor-1α in Development of Lipopolysaccharide-Induced Sepsis. J Immunol. 2007;178(12):7516–9.

345. Cramer T, Yamanishi Y, Clausen BE, Förster I, Pawlinski R, Mackman N, et al. HIF-1α is essential for myeloid cell-mediated inflammation. Cell. 2003;112(5):645–57.

346. Peyssonnaux C, Datta V, Cramer T, Doedens A, Theodorakis EA, Gallo RL, et al. HIF-1α expression regulates the bactericidal capacity of phagocytes. J Clin Invest. 2005;115(7):1806–15.

347. Anand RJ, Gribar SC, Li J, Kohler JW, Branca MF, Dubowski T, et al. Hypoxia causes an

increase in phagocytosis by macrophages in a HIF-1α-dependent manner. J Leukoc Biol. 2007;82(5):1257–65.

348. Rius J, Guma M, Schachtrup C, Akassoglou K, Zinkernagel AS, Nizet V, et al. NF-κB links innate immunity to the hypoxic response through transcriptional regulation of HIF-1α. Nature. 2008;453(7196):807–11.

349. Nizet V, Johnson RS. Interdependence of hypoxic and innate immune responses. Nat Rev Immunol. 2009;9(9):609–17.

350. Palsson-McDermott EM, Palsson-McDermott EM, Curtis AM, Curtis AM, Goel G, Goel G, et al. Pyruvate Kinase M2 Regulates Hif-1α Activity and IL-1β Induction and Is a Critical Determinant of the Warburg Effect in LPS-Activated Macrophages. Cell Metab. 2015;21(1):65–80.

351. Luo W, Hu H, Chang R, Zhong J, Knabel M, O'Meally R, et al. Pyruvate kinase M2 is a PHD3-stimulated coactivator for hypoxia-inducible factor 1. Cell. 2011;145(5):732–44.

352. Olson N, Van Der Vliet A. Interactions between nitric oxide and hypoxia-inducible factor signaling pathways in inflammatory disease. Nitric Oxide - Biol Chem. 2011;25(2):125–37.

353. Kietzmann T, Görlach A. Reactive oxygen species in the control of hypoxia-inducible factor-mediated gene expression. Semin Cell Dev Biol. 2005;16(4–5):474–86.

354. Subbian S, Tsenova L, Yang G, O'Brien P, Parsons S, Peixoto B, et al. Chronic pulmonary cavitary tuberculosis in rabbits: A failed host immune response. Open Biol. 2011;1(4):110016.

355. Elks PM, Brizee S, van der Vaart M, Walmsley SR, van Eeden FJ, Renshaw SA, et al. Hypoxia Inducible Factor Signaling Modulates Susceptibility to Mycobacterial Infection via a Nitric Oxide Dependent Mechanism. PLoS Pathog. 2013;9(12):1–16.

356. Baay-Guzman GJ, Duran-Padilla MA, Rangel-Santiago J, Tirado-Rodriguez B, Antonio-Andres G, Barrios-Payan J, et al. Dual role of hypoxia-inducible factor 1 α in experimental pulmonary tuberculosis: Its implication as a new therapeutic target. Future Microbiol. 2018;13(7):785–98.

357. Jo EK, Silwal P, Yuk JM. AMPK-targeted effector networks in mycobacterial infection. Front Microbiol. 2019;10:520.

358. O'Neill LAJ, Grahame Hardie D. Metabolism of inflammation limited by AMPK and pseudo-starvation. Nature. 2013;493(7432):346–55.

359. O'Neill LAJ, Pearce EJ. Immunometabolism governs dendritic cell and macrophage function. J Exp Med. 2016;213(1):15–23.

360. Carroll KC, Viollet B, Suttles J. AMPKα1 deficiency amplifies proinflammatory myeloid APC activity and CD40 signaling. J Leukoc Biol. 2013;94(6):1113–21.

361. Yang CS, Kim JJ, Lee HM, Jin HS, Lee SH, Park JH, et al. The AMPK-PPARGC1A pathway is required for antimicrobial host defense through activation of autophagy. Autophagy. 2014;

362. Kim SY, Yang CS, Lee HM, Kim JK, Kim YS, Kim YR, et al. ESRRA (estrogen-related receptor α) is a key coordinator of transcriptional and post-translational activation of autophagy to promote innate host defense. Autophagy. 2018;14(1):152–68.

363. Grabacka M, Pierzchalska M, Dean M, Reiss K. Regulation of ketone body metabolism and the role of PPARα. Int J Mol Sci. 2016;17(12):2093.

364. Chauhan S, Mandell MA, Deretic V. IRGM governs the core autophagy machinery to conduct antimicrobial defense. Mol Cell. 2015;58(3):507–21.

365. Jeon CY, Murray MB. Diabetes mellitus increases the risk of active tuberculosis: A systematic review of 13 observational studies. PLoS Med. 2008;5(7):e152.

366. Baker MA, Harries AD, Jeon CY, Hart JE, Kapur A, Lönnroth K, et al. The impact of diabetes on tuberculosis treatment outcomes: A systematic review. BMC Med. 2011;9:81.

367. Singhal A, Jie L, Kumar P, Hong GS, Leow MKS, Paleja B, et al. Metformin as adjunct antituberculosis therapy. Sci Transl Med. 2014;6(263):263ra159.

368. Degner NR, Wang JY, Golub JE, Karakousis PC. Metformin Use Reverses the Increased Mortality Associated with Diabetes Mellitus during Tuberculosis Treatment. Clin Infect Dis. 2018;66(2):198–205.

369. Ma Y, Pang Y, Shu W, Liu YH, Ge QP, Du J, et al. Metformin reduces the relapse rate of tuberculosis patients with diabetes mellitus: experiences from 3-year follow-up. Eur J Clin Microbiol Infect Dis. 2018;37(7):1259–63.

370. Lee MC, Chiang CY, Lee CH, Ho CM, Chang CH, Wang JY, et al. Metformin use is associated with a low risk of tuberculosis among newly diagnosed diabetes mellitus patients with normal renal function: A nationwide cohort study with validated diagnostic criteria. PLoS One. 2018;13(10):e0205807.

371. Lachmandas E, Eckold C, Böhme J, Koeken VACM, Marzuki MB, Blok B, et al. Metformin Alters Human Host Responses to Mycobacterium tuberculosis in Healthy Subjects. J Infect Dis. 2019;220(1):139–50.

372. Dutta NK, Pinn ML, Karakousis PC. Metformin adjunctive therapy does not improve the sterilizing activity of the first-line antitubercular regimen in mice. Antimicrob Agents Chemother. 2017;61(8):e00652-17.

373. Kodiha M, Rassi JG, Brown CM, Stochaj U. Localization of AMP kinase is regulated by stress, cell density, and signaling through the MEK→ERK1/2 pathway. Am J Physiol - Cell Physiol. 2007;293(5):C1427-1436.

374. Weichhart T, Hengstschläger M, Linke M. Regulation of innate immune cell function by mTOR. Nat Rev Immunol. 2015;15(10):599–614.

375. Moon JS, Hisata S, Park MA, DeNicola GM, Ryter SW, Nakahira K, et al. MTORC1-Induced HK1-Dependent Glycolysis Regulates NLRP3 Inflammasome Activation. Cell Rep. 2015;12(1):102–15.

376. Yang CS, Song CH, Lee JS, Jung SB, Oh JH, Park J, et al. Intracellular network of phosphatidylinositol 3-kinase, mammalian target of the rapamycin/70 kDa ribosomal S6 kinase 1, and mitogen-activated protein kinases pathways for regulating mycobacteria-induced IL-23 expression in human macrophages. Cell Microbiol. 2006;8(7):1158–71.

377. Sun Q, Chen X, Ma J, Peng H, Wang F, Zha X, et al. Mammalian target of rapamycin up-regulation of pyruvate kinase isoenzyme type M2 is critical for aerobic glycolysis and tumor growth. Proc Natl Acad Sci U S A. 2011;108(10):4129–34.

378. Elkington PTG, Green JA, Friedland JS. Filter sterilization of highly infectious samples to prevent false negative analysis of matrix metalloproteinase activity. J Immunol Methods. 2006;309(1–2):115–9.

379. Ong CWM. Neutrophils and the regulation of matrix metalloproteinases in tuberculosis. Imperial College London; 2013.

380. Pfaffl MW. A new mathematical model for relative quantification in real-time RT-PCR. Nucleic Acids Res. 2001;29(9):45e – 45.

381. Kirwan DE, Ugarte-Gil C, Gilman RH, Hasan Rizvi SM, Cerrillo G, Cok J, et al. Histological examination in obtaining a diagnosis in patients with lymphadenopathy in Lima, Peru. Am J Trop Med Hyg. 2017;97(4):1271–6.

382. Handa N, Takagi T, Saijo S, Kishishita S, Takaya D, Toyama M, et al. Structural basis for compound C inhibition of the human AMP-activated protein kinase α2 subunit kinase domain. Acta Crystallogr Sect D Biol Crystallogr. 2011;67:480–7.

383. Ong C, Elkington P, Ugarte-Gil C, Roncaroli F, Friedland J. Neutrophil MMP-8/-9 is increased in tuberculosis: Evidence from in vitro studies and patients with pulmonary disease. Clin Microbiol Infect. 2012;

384. Mills EL, O'Neill LA. Reprogramming mitochondrial metabolism in macrophages as an anti-inflammatory signal. Eur J Immunol. 2016;46(1):13–21.

385. Zhong D, Xiong L, Liu T, Liu X, Liu X, Chen J, et al. The glycolytic inhibitor 2-deoxyglucose activates multiple prosurvival pathways through IGF1R. J Biol Chem. 2009;284(35):23225–33.

386. Blakeway D, Karakoula K, Morris M, Rowther F, Ashton K, Dawson T, et al. PATH-33. HEXOKINASE 2 KNOCKOUT VIA CRISPR REDUCES DOWNSTREAM GENE EXPRESSION, IMPLICATING A REDUCTION IN CELL PROLIFERATION AND DRUG RESISTANCE. Neuro Oncol. 2018;20(S6):vi165–6.

387. Dite TA, Langendorf CG, Hoque A, Galic S, Rebello RJ, Ovens AJ, et al. AMP-activated protein kinase selectively inhibited by the type II inhibitor SBI-0206965. J Biol Chem. 2018;293:8874–85.

388. Grenier A, Sujobert P, Olivier S, Guermouche H, Mondésir J, Kosmider O, et al. Knockdown of human AMPK using the CRISPR/Cas9 genome-editing system. Methods Mol Biol. 2018;1732:171–94.

389. Zhao C, Chen J, Cheng L, Xu K, Yang Y, Su X. Deficiency of HIF-1α enhances influenza A virus replication by promoting autophagy in alveolar type II epithelial cells. Emerg Microbes Infect. 2020;9(1):691–706.

390. Martín-Vicente M, González-Riaño C, Barbas C, Jiménez-Sousa MÁ, Brochado-Kith O, Resino S, et al. Metabolic changes during respiratory syncytial virus infection of epithelial cells. PLoS One. 2020;15(3):e0230844.

391. Zhao Y, Chahar HS, Komaravelli N, Dossumekova A, Casola A. Human metapneumovirus infection of airway epithelial cells is associated with changes in core metabolic pathways. Virology. 2019;531:183–91.

392. Maurice NM, Bedi B, Yuan Z, Goldberg JB, Koval M, Hart CM, et al. Pseudomonas aeruginosa Induced Host Epithelial Cell Mitochondrial Dysfunction. Sci Rep. 2019;9(1):11929.

393. Wang S, Zhang C, Zhang M, Liang B, Zhu H, Lee J, et al. Activation of AMP-activated protein kinase α2 by nicotine instigates formation of abdominal aortic aneurysms in mice in vivo. Nat Med. 2012;18(6):902–10.

394. Pålsson-McDermott EM, O'Neill LAJ. Targeting immunometabolism as an anti-inflammatory strategy. Cell Res. 2020;30:300–14.

395. Lai ZW, Kelly R, Winans T, Marchena I, Shadakshari A, Yu J, et al. Sirolimus in patients with clinically active systemic lupus erythematosus resistant to, or intolerant of, conventional medications: a single-arm, open-label, phase 1/2 trial. Lancet. 2018;391:1186–96.

396. Friedman B, Cronstein B. Methotrexate mechanism in treatment of rheumatoid arthritis. Jt Bone Spine. 2019;86:301–7.

397. Yin Y, Choi SC, Xu Z, Perry DJ, Seay H, Croker BP, et al. Normalization of CD4+ T cell metabolism reverses lupus. Sci Transl Med. 2015;7:274ra18.

398. Abboud G, Choi SC, Kanda N, Zeumer-Spataro L, Roopenian DC, Morel L. Inhibition of glycolysis reduces disease severity in an autoimmune model of rheumatoid arthritis. Front Immunol. 2018;9:1973.

399. Liu RT, Zhang M, Yang CL, Zhang P, Zhang N, Du T, et al. Enhanced glycolysis contributes to the pathogenesis of experimental autoimmune neuritis. J Neuroinflammation. 2018;15:51.

400. Raez LE, Papadopoulos K, Ricart AD, Chiorean EG, Dipaola RS, Stein MN, et al. A phase i dose-escalation trial of 2-deoxy-d-glucose alone or combined with docetaxel in patients with advanced solid tumors. Cancer Chemother Pharmacol. 2013;71:523–30.

401. Blom RAM, Erni ST, Krempaská K, Schaerer O, Van Dijk RM, Amacker M, et al. A triple co-culture model of the human respiratory tract to study immune-modulatory effects of liposomes and virosomes. PLoS One. 2016;11(9):e0163539.

402. Liu Q, Fan D, Adah D, Wu Z, Liu R, Yan QT, et al. CRISPR/Cas9-mediated hypoxia inducible factor-1a knockout enhances the antitumor effect of transarterial embolization in hepatocellular carcinoma. Oncol Rep. 2018;40(5):2547–57.

403. Woodcock H V., Eley JD, Guillotin D, Platé M, Nanthakumar CB, Martufi M, et al. The mTORC1/4E-BP1 axis represents a critical signaling node during fibrogenesis. Nat Commun. 2019;10:6.

404. Robinson BK, Cortes E, Rice AJ, Sarper M, Hernañdez ADR. Quantitative analysis of 3D extracellular matrix remodelling by pancreatic stellate cells. Biol Open. 2016;5:875–82.

405. Cumming BM, Pacl HT, Steyn AJC. Relevance of the Warburg Effect in Tuberculosis for Host-Directed Therapy. Front Cell Infect Microbiol. 2020;10:576596.

406. Osada-Oka M, Goda N, Saiga H, Yamamoto M, Takeda K, Ozeki Y, et al. Metabolic adaptation to glycolysis is a basic defense mechanism of macrophages for Mycobacterium tuberculosis infection. Int Immunol. 2019;31(12):781–93.

407. Wang Z, Koenig AL, Lavine KJ, Apte RS. Macrophage Plasticity and Function in the Eye and Heart. Trends Immunol. 2019;40(9):825–41.

408. Johansson J, Karlsson A, Bylund J, Welin A. Phagocyte interactions with Mycobacterium tuberculosis - Simultaneous analysis of phagocytosis, phagosome maturation and intracellular replication by imaging flow cytometry. J Immunol Methods. 2015;427:73–84.

409. Mookerjee SA, Brand MD. Measurement and analysis of extracellular acid production to determine glycolytic rate. J Vis Exp. 2015;12(106):e53464.

410. DeBerardinis RJ, Chandel NS. We need to talk about the Warburg effect. Nat Metab. 2020;2:127–9.

411. Keiran N, Ceperuelo-Mallafré V, Calvo E, Hernández-Alvarez MI, Ejarque M, Núñez-Roa C, et al. SUCNR1 controls an anti-inflammatory program in macrophages to regulate the metabolic response to obesity. Nat Immunol. 2019;20:581–92.

412. Hackett EE, Sheedy FJ. An Army Marches on Its Stomach: Metabolic Intermediates as Antimicrobial Mediators in Mycobacterium tuberculosis Infection. Front Cell Infect Microbiol. 2020;10:446.

413. Peyron P, Vaubourgeix J, Poquet Y, Levillain F, Botanch C, Bardou F, et al. Foamy macrophages from tuberculous patients' granulomas constitute a nutrient-rich reservoir for M. tuberculosis persistence. PLoS Pathog. 2008;4:e1000204.

414. Mehra S, Alvarez X, Didier PJ, Doyle LA, Blanchard JL, Lackner AA, et al. Granuloma correlates of protection against tuberculosis and mechanisms of immune modulation by Mycobacterium tuberculosis. J Infect Dis. 2013;207:1115–27.

415. Gautam US, Foreman TW, Bucsan AN, Veatch A V., Alvarez X, Adekambi T, et al. In vivo inhibition of tryptophan catabolism reorganizes the tuberculoma and augments immune-mediated control of Mycobacterium tuberculosis. Proc Natl Acad Sci U S A. 2018;115:E62–71.

416. Braverman J, Stanley SA. Nitric Oxide Modulates Macrophage Responses to Mycobacterium tuberculosis Infection through Activation of HIF-1α and Repression of NF-κB. J Immunol. 2017;199:1805–16.

417. Negatu DA, Liu JJJ, Zimmerman M, Kaya F, Dartois V, Aldrich CC, et al. Whole-cell screen of fragment library identifies gut microbiota metabolite indole propionic acid as

antitubercular. Antimicrob Agents Chemother. 2018;62:3.

418. Kramnik I, Beamer G. Mouse models of human TB pathology: roles in the analysis of necrosis and the development of host-directed therapies. Semin Immunopathol. 2016;38(2):221–37.

419. Subbian S, Tsenova L, O'Brien P, Yang G, Koo MS, Peixoto B, et al. Phosphodiesterase-4 inhibition alters gene expression and improves isoniazid - mediated clearance of mycobacterium tuberculosis in rabbit lungs. PLoS Pathog. 2011;

Appendix 1: List of abbreviations

ADP	Adenosine diphosphate
AEC	Airway epithelial cell
AM	Alveolar macrophage
AMP	Adenosine monophosphate
AMPK	AMP-activated protein kinase
ATP	Adenosine triphosphate
BALF	Bronchoalveolar lavage fluid
BCG	Bacille Calmette-Guérin
BEGM	Bronchial epithelial growth medium
BSA	Bovine serum albumin
CFU	Colony-forming units
CL3	Category level 3
CNS	Central nervous system
CoMTB	Conditioned medium from *M.tb*-infected monocytes
ConCont	Conditioned medium from control monocytes

COX	Cyclooxygenase
CSF	Cerebrospinal fluid
DC	Dendritic cell
DTT	Dithiothreitol
ECM	Extracellular matrix
ESAT-6	Early Secretory Antigenic Target 6 kDA
EMMPRIN	Extracellular Matrix Metalloproteinase Inducer
ERK	Extracellular Signal Related Kinase
ESX-1	ESAT-6 secretion system 1
FCS	Foetal calf serum
GM-CSF	Granulocyte Macrophage Colony Stimulating Factor
HBSS	Hanks Balanced Salt Solution
HIV	Human Immunodeficiency Virus
HIF-1α	Hypoxia Inducible Factor - 1α
HK	Hexokinase
HK2	Hexokinase 2
HRE	Hypoxia response element

IFN-γ	Interferon-γ
IHC	Immunohistochemistry
IL-1β	Interleukin-1β
IL-10	Interleukin-10
IGRA	Interferon-γ Release Assay
IM	Interstitial macrophage
iNOS	Inducible Nitric Oxide Synthase
LDH	Lactate Dehydrogenase
LAM	Lipoarabinomannan
LDH	Lactate dehydrogenase
M-CSF	Macrophage Colony Stimulating Factor
MAPK	Mitogen-activated Protein Kinase
MCT	Monocarboxylate Transporter
MDM	Monocyte-derived Macrophage
MDR-TB	Multi-drug resistant tuberculosis
MMP	Matrix Metalloproteinase
M.tb	*Mycobacterium tuberculosis*

mTOR	Mammalian Target of Rapamycin
mTORC1	Mammalian Target of Rapamycin Complex 1
MYD88	Myeloid Differentiation Response Gene – 88
OD	Optical density
OXPHOS	Oxidative phosphorylation
PBMC	Peripheral Blood Mononuclear Cells
PHD	Prolyl Hydroxylase
NF-κB	Nuclear factor kappa B
NHBE	Normal Human Bronchial Epithelial Cell
RT-PCR	Reverse Transcriptase - Polymerase Chain Reaction
PRR	Pattern Recognition Receptor
Pi3-kinase	Phosphatidylinsositol-3-kinase
PIIINP	Procollagen III N-terminal Peptide
RNS	Reactive Nitrogen Species
ROS	Reactive Oxygen Species
RPMI	Roswell Park Memorial Institute
siRNA	Small Interfering Ribonucleic Acid

TCA cycle	Tricarboxylic Acid Cycle
TB	Tuberculosis
TLR	Toll-like Receptor
TNF-α	Tumour Necrosis Factor - α
TIMP	Tissue Inhibitor of Metalloproteinases
TST	Tuberculin Skin Test
XDR-TB	Extensively Drug Resistant Tuberculosis
% v/v	Percentage volume/volume
WT	Wild-type
% w/v	Percentage weight/volume

Appendix 2: Conference proceedings

Inhibition of metabolic signalling pathways controls inflammatory tissue destruction in tuberculosis (Poster). Asher R and Friedland JS. 30th European Congress of Clinical Microbiology and Infectious Diseases, 18-21 April 2020, Paris, France. Abstract accepted, but conference subsequently cancelled due to the Covid-19 pandemic.

Pi3-kinase, AMPK and metabolic control of inflammatory tissue destruction in tuberculosis (Poster). Asher R and Friedland JS. British Society for Immunology Congress, 2-5 December 2019, Liverpool, UK.

Metabolic change and the regulation of tissue destruction in tuberculosis: a potential target for host-directed therapies (Oral). Asher R and Friedland JS. 29th European Congress of Clinical Microbiology and Infectious Diseases, 13-16 April 2019, Amsterdam, The Netherlands.

Investigating metabolic mechanisms regulating collagen breakdown in tuberculosis (Poster). Asher R and Friedland JS. 5th European Congress of Immunology, 2-5 September 2018, Amsterdam, The Netherlands. Awarded Best Poster Prize in Session. Funded by a British Society for Immunology Travel Bursary.